IL
NUOVO CIMENTO
ORGANO DELLA SOCIETÀ ITALIANA DI FISICA
SOTTO GLI AUSPICI DEL CONSIGLIO NAZIONALE DELLE RICERCHE

VOL. IV, N. 1 *Serie decima* 1° Luglio 1956

Anti-Proton Annihilation.

H. A. BETHE (*) and J. HAMILTON
Cavendish Laboratory - Cambridge (England)

(ricevuto il 16 Marzo 1956)

Summary. — It is shown how simple experiments on the annihilation of the anti-proton in various materials may be used to determine the nature of the annihilation process in nuclear matter, and to get information on nucleon-anti-nucleon forces. The annihilation of anti-protons from atomic states is examined in detail, and corrections are made for specifically nuclear effects.

1. – Introduction.

The discovery of the anti-proton [1] should make it possible to obtain information about nucleon-pion forces which is quite distinct from that obtained from nucleon-nucleon and nucleon-pion scattering. Some of this new information is contained in the matrix element for nucleon-anti-nucleon annihilation which determines the lifetime of the anti-nucleon in nuclear matter, and a virtual analogue of this matrix element which contributes to nucleon-anti-nucleon scattering. This latter term might be determined from the deformation of an anti-proton wave function by a nucleus. A further range of phenomena should be shown by the details of the annihilation process. It is to be expected that the release of 2 GeV energy will often lead to multiple pion production in the annihilation event [2]; also if annihilation occurs in

(*) On leave of absence from Cornell University, Ithaca, N. Y.

(1) O. CHAMBERLAIN, E. SEGRE, C. WIEGAND and T. YPSILANTIS: *Phys. Rev.*, **100**, 947 (1955).

(2) For evidence on multiple pion production at the energies considered see L. EISBERG *et al.*: *Phys. Rev.*, **97**, 797 (1955); G. MAENCHEN *et al.*: *Phys. Rev.*, **99**, 1619 (1955).

a large nucleus, some fast pions will produce other pions on passing through the nucleus ([3]). However it is expected that annihilation into two pions should also occur sometimes, and that in favourable circumstances such events should be observed. The distribution of charge in the three-pion events occurring in light nuclei may perhaps be of use in deciding which of the several matrix elements for three-pion annihilation of a nucleon and an anti-nucleon is important, but it is chiefly to the two-pion annihilation events that we must look for information about the annihilation process.

The aim of this paper is to show how essentially simple experiments on the annihilation of anti-protons in various materials (preferably gaseous materials) may be used to obtain information about the annihilation process and about the forces between anti-nucleons and nucleons. Information on the strength of the annihilation interaction can be deduced from a knowledge of the *atomic* states in which a *stopped* anti-proton is annihilated. The angular momentum of the *atomic* states in which a stopped anti-proton is annihilated may be deduced from the charge distribution of the two-pion events on comparing the annihilation in various materials. Knowing the angular momentum of these atomic states, the lifetime for annihilation may be found; in the same way the strength of the annihilation interaction and its dependence on isotopic spin and other variables may be determined. The annihilation of anti-protons which are stopped in hydrogen has been studied theoretically by BROWN and PESHKIN ([4]), who make an assumption very different from ours; they suggest that for states of the « protonic atom » whose decay into two-pion states is forbidden, annihilation into two γ-rays may be comparable with multi-pion annihilation. The possibility of the annihilation of a proton and an anti-proton leading to a pair of K-mesons ([5]) has been considered by REGGE, OKUBO and MARSHAK ([6]). Annihilation may also lead to a single pion and a γ-ray as was noted by MICHEL ([7]). In this paper only annihilation leading to pions will be discussed.

In Sect. 2 the selection rules based on charge independence, charge conjugation, angular momentum and parity are given, and in the Appendix the relation between charge conjugation and isotopic spin is put into a suitable simple form. Sect. 3 contains a detailed discussion of the annihilation mecha-

([3]) The cross section for inelastic events (production of one or more pions) for 1.5 GeV pions in H is at least 20 mb. [cf. ref. ([2])].

([4]) L. M. BROWN and M. PESHKIN: *Northwest University Preprint*; see also L. M. BROWN, I. HARRIS and M. PERSHKIN: *Bull. Amer. Phys. Soc.*, **1**, no. 1, 52 (1956).

([5]) Assuming the anti-proton has zero « strangeness », and using the scheme of M. GELL-MANN (*Pisa Conference Report, Suppl. Nuovo Cimento*, 1956) it follows that an even number of K-mesons must be produced. A stopped anti-proton can produce only two K-mesons.

([6]) T. REGGE, S. OKUBO and R. MARSHAK: *Bull. Amer. Phys. Soc.*, **30**, no. 8, 26 (1955).

([7]) L. MICHEL: *Nuovo Cimento*, **10**, 319 (1953).

nism in a « protonic atom », based on using scaled down H-atom wave functions for the anti-proton; Sect. 4 and 5 discuss corrections to this naive picture. The effect of a possible attractive potential between the anti-proton and the nucleus is examined in Sect. 4 as well as the effect of an imaginary potential arising from the absorption of the anti-proton wave function in the nucleus. Sect. 5 discusses some of the ways in which nuclear effects may complicate the picture; in particular, estimates are given for the probability that the anti-proton jumps directly into the nucleus by ejecting an « Auger nucleon ».

2. – Selection Rules for Anti-Proton Annihilation.

The selection rules for the annihilation of anti-protons have been given by several authors ([8]). Besides angular momentum and parity, it is necessary to consider the charge conjugation operation ([9]) which changes the sign of all charges, and the charge symmetry operation ([9]) which exchanges protons with neutrons and anti-protons with anti-neutrons. Because we discuss annihilation into pions, and because in some cases we deal with short range forces between the anti-nucleon and the nucleus, it is simplest to assume that the annihilation interaction between pions, nucleons, and anti-nucleons is charge independent and use the concept of isotopic spin (cf. Appendix). In discussing the annihilation of an anti-proton which is moving in a Bohr orbit around a nucleus, the initial state is an eigenstate of T_3, but it may be a mixture of two eigenstates having different eigenvalues of T^2.

The isotopic spin of anti-nucleons is $\frac{1}{2}$, and the pair of state vectors $(u_{\bar{P}}, u_{\bar{N}})$ for anti-proton and anti-neutron respectively, is covariant, under rotations in isotopic space, with the pair $(u_N, -u_P)$ where N, P denote neutron and proton ([10]). A nucleon anti-nucleon pair form isotopic spin states $T = 0, 1$,

$$(1) \qquad \begin{cases} T = 0: \qquad 2^{-\frac{1}{2}}(u_P u_{\bar{P}} + u_N u_{\bar{N}}) \, ; \\ T = 1, \; T_3 = 1, \; 0, \; -1: \qquad u_P u_{\bar{N}}, \; 2^{-\frac{1}{2}}(u_N u_{\bar{N}} - u_P u_{\bar{P}}), \; -u_N u_{\bar{P}} \, . \end{cases}$$

Each of these states can be symmetrized and anti-symmetrized with respect to particle exchange, so that (1), gives, in all, 8 isotopic spin components. The notation $T = 0^s, 0^a; 1^s, 1^a$ may be used to distinguish these isotopic states.

([8]) See especially L. MICHEL, ref. ([7]); also D. AMATI and B. VITALE: *Nuovo Cimento*, **2**, 719 (1955).

([9]) A general discussion is given by A. PAIS and R. JOST: *Phys. Rev.*, **87**, 871 (1952); and L. WOLFENSTEIN and D. R. RAVENHALL: *Phys. Rev.*, **88**, 279 (1952).

([10]) See M. CINI and A. GAMBA: *Nuovo Cimento*, **10**, 1040 (1953), and J. HAMILTON: *Pisa Conference Report, Suppl. Nuovo Cimento* (1956).

Anti-proton annihilation is described by the isotopic states

$$(2) \qquad \begin{cases} |\bar{P}P\rangle = 2^{-\frac{1}{2}}|T=0\rangle - 2^{-\frac{1}{2}}|T=1,\ T_3=0\rangle \\ |\bar{P}N\rangle = -|T=1,\ T_3=-1\rangle\ . \end{cases}$$

Each of equations (2) can further be divided into symmetric and anti-symmetric components, and if we consider states formed by an anti-proton and one nucleon, the Pauli principle gives the classification of nucleon anti-nucleon pair states shown in Table I.

TABLE I.

$T=0^s$ or 1^s	$^1S_0$	$^3P_{0,1,2}$	$^1D_2$	$^3F_{2,3,4}$
$T=0^a$ or 1^a	$^3S_1$	$^1P_1$	$^3D_{1,2,3}$	$^1F_3$
Parity	−	+	−	+

In obtaining the last line of Table I it is assumed that the intrinsic parities of the anti-nucleon and the nucleon are opposite, as is the case for the positron and the electron. The only matrix elements which can describe the decay of an S-state of positronium into two photons of momenta $\boldsymbol{p}$, $-\boldsymbol{p}$ and polarization $\boldsymbol{e}_1$, $\boldsymbol{e}_2$, respectively, are the scalar $(\boldsymbol{e}_1\cdot\boldsymbol{e}_2)f(|\boldsymbol{p}|)$ and the pseudoscalar $(\boldsymbol{e}_1\cdot\boldsymbol{e}_2\times\boldsymbol{p})f(|\boldsymbol{p}|)$. The two photons emitted in the decay of the $^1S_0$ state of positronium have perpendicular polarization, indicating that the pseudo-scalar matrix element describes the decay and therefore that the positron and electron have opposite parities ([11]).

The charge conjugation operator C replaces the charged pion field $\varphi(\varphi^*)$ by $\varphi^*(\varphi)$ and leaves the neutral component φ_3 unaltered; also $C(u_p, u_N) = (u_{\bar{p}}, u_{\bar{N}})$ and $C(u_{\bar{p}}, u_{\bar{N}}) = (u_p, u_N)$. The charge symmetry operator T acting on nucleons gives $T(u_p, u_N) = (u_N, u_p)$ and $T(u_{\bar{p}}, u_{\bar{N}}) = (u_{\bar{N}}, u_{\bar{p}})$, and, if we assume charge independence, T replaces $\varphi(\varphi^*)$ by $\varphi^*(\varphi)$ and replaces φ_3 by $-\varphi_3$. The operation $W = C\cdot T$ formed by following T by C leaves φ and φ^* unaltered and changes the sign of φ_3; therefore a state containing n neutral pions is multiplied by $(-1)^n$ on applying W. Using $W(u_p, u_N) = (u_{\bar{N}}, u_{\bar{p}})$ etc., we see that applying W to the $T=0$ state of equation (1) gives the same state apart from an exchange of the two particles; therefore the $T=0^s(0^a)$ state has the eigenvalue $W'=+1(-1)$. The $T_3=0$, $T=1^s(1^a)$ state of (1) has the eigenvalue $W'=-1(+1)$. Further details are given in the Appendix

([11]) For a comprehensive discussion of positronium decay see S. DEBENEDETTI and H. C. CORBEN: *Annual Review of Nuclear Science*, **4** (1954).

where it is shown that it is only necessary to know W' for the $T_3 = 0$ state of any set of states with given T^2.

Two-Pion Annihilation. Two pions can combine to give isotopic spin $T = 0, 1, 2$. The states $T = 0, 2$ are symmetric in the two pions so they have even angular momentum J and even parity; their $T_3 = 0$ components must have an even number of π^0, so $W' = +1$. The state $T = 1$ is anti-symmetric for pion exchange and has odd angular momentum and odd parity; its $T_3 = 0$ component again has $W' = +1$. In annihilation of a nucleon anti-nucleon pair giving two-pion states, conservation of W' shows that only $T = 0^s, 1^a$ can occur. Comparing parity and angular momentum with Table I it is clear that 2-pion events with $T = 0$ can only arise from states ${}^3P_{0,2}$, ${}^3F_{2,4}$, ... and $T = 1$ events only from states ${}^3S_1$, ${}^3D_{1,3}$, ...: It should be noted that 2-pion events can only come from triplet states. In $T = 0$ states, the pair (π^+, π^-) occur on the average in $\frac{2}{3}$ of all events, while (π^0, π^0) occurs in the remaining $\frac{1}{3}$. All $T = 1$, $T_3 = 0$ are (π^+, π^-) and all $T = 1$, $T_3 = -1$ must of course be (π^0, π^-). From (2) we see that in the S, D, ... states, annihilation of an anti-proton, by a neutron is twice as probable as annihilation by a proton, and also that the P, F, ... states can gives proton, but not neutron, annihilation of the anti-proton.

Three-Pion Annihilation. Two pions (called 1 and 2 below) combine to give isotopic spin $T' = 0, 1, 2$ and the third pion can give resultant $T = 0, 1$ states in several ways.

(*a*) $T = 0$ can arise only from $T' = 1$. This isotopic state is completely anti-symmetric against pion exchange.

(*b*) $T = 1$, $T' = 0$ *or* 2. These states are symmetric against exchange of pions 1 and 2.

(*c*) $T = 1$, $T' = 1$. This state is anti-symmetric in the pions 1 and 2 and if $t(1, 2; 3)$ is the isotopic state vector it obeys the relation

$$t(1, 2; 3) + t(2, 3; 1) + t(3, 1; 2) = 0 .$$

In each case (*a*), (*b*), (*c*), the $T_3 = 0$ term contains an odd number of π^0, so $W' = -1$. Therefore 3-pion annihilation of a nucleon anti-nucleon pair can only occur in $T = 0^a$ or $T = 1^s$ states (Table I). Amongst the S and P states only ${}^3P_0$ is excluded by angular momentum and parity conservation. ${}^3P_0$ must lead to a state of even parity and zero angular momentum; allowing for the odd intrinsic parity of the three pions, we have to form a pseudoscalar out of the momenta $\boldsymbol{p}_1$, $\boldsymbol{p}_2$, $\boldsymbol{p}_3$ of the three pions. The only pseudoscalar is $(\boldsymbol{p}_1 \cdot \boldsymbol{p}_2 \times \boldsymbol{p}_3)$, and this vanishes because $\boldsymbol{p}_1 + \boldsymbol{p}_2 + \boldsymbol{p}_3 = 0$ in the centre of mass system.

The selection rules for two- and there-pion annihilation of a nucleon anti-nucleon pair are given in Table II. The distribution of charge in the 3-pion annihilation events is given in Table III.

TABLE II. – *Allowed Transitions.*

2-π annihilation	$T = 0^s$ $T = 1^a$	$^3P_{0,2}$ $^3S_1$	$^3F_{2,4}$ ... $^3D_{1,3}$ ...
3-π annihilation	$T = 0^a$ $T = 1^s$	$^3S_1$ $^1S_0$	$^1P_1$ ... $^3P_{1,2}$ ...

TABLE III.

Isotopic Type			*Relative Probabilities*	
T	T_3	T'	$(\pi^+ \pi^- \pi^-)$	$(\pi^- \pi^0 \pi^0)$
1	— 1	0	2/3	1/3
..	..	1	1/2	1/2
..	..	2	19/30	11/30
			$(\pi^+ \pi^0 \pi^-)$	$(\pi^0 \pi^0 \pi^0)$
1	0	0	2/3	1/3
..	..	1	1	—
..	..	2	11/15	4/15
0	—	—	1	—

3. – Annihilation in the Nucleus.

In the original observation of anti-protons ([1]) no attempt was made to examine the annihilation process. An experiment by BRABANT *et al.* ([12]) using a large Čerenkov counter has examined the energy of annihilation which goes into the production of π^0-mesons, and CHAMBERLAIN, AMALDI *et al.* ([13]) have observed an anti-proton star in a photographic emulsion exposed at the bevatron; these stars originate from stopped antiprotons.

BRABANT and collaborators state that their experiment indicates that the annihilation interaction for anti-protons of a few hundred MeV has a cross-section which is at least as large as the geometrical cross-section of the nuclei in the dense flint glass of their Čerenkov counter. Further evidence to support

([12]) J. M. BRABANT *et al.*: *Phys. Rev.*, **101**, 498 (1956).

([13]) O. CHAMBERLAIN, E. AMALDI *et al.*: *Nuovo Cimento*, **3**, 447 (1956); see also *Time Magazine* (New York, 1956), p. 46 and *Radiation Laboratory, Berkeley, Report* No. 3325 (1956).

this view has been obtained by SEGRÈ's group [14] who have examined the total cross-section for absorption and scattering (excluding shadow scattering) of anti-protons in targets of 68 gm·cm^{-2} copper, or 37.5 gm·cm^{-2} beryllium. The incident anti-protons have momentum about 1.2 GeV/c and the ordinary stopping power of the target cannot be important. The total cross-sections are about twice that for protons in the same material, and it is estimated that in about half of the events the anti-proton is annihilated. We understand [15] that further examination of emulsions exposed at the Bevatron shows that about half the annihilations occur while the anti-proton is still in flight. For anti-protons of about 1.2 GeV/c this again suggests that the annihilation cross-section is about equal to the geometrical cross-section of the annihilating nuclei. These results indicate that the annihilation interaction is very large, and the lifetime of the anti-proton in nuclear matter is very short—probably of the order of 10^{-23} s, this value being obtained by dividing the thickness of the nuclear surface ($\sim 10^{-13}$ cm) by the velocity of the anti-proton ($\sim 10^{10}$ cm/s).

It is difficult to examine more closely the information to be obtained from annihilation in flight. This is because we cannot make much useful analysis except for nuclei of high symmetry like D and He. Even for these nuclei several different angular momentum values would have to be allowed for, because of the large momentum of the anti-proton. Much more can be said about the annihilation of stopped anti-protons and we limit our discussion to that case.

An anti-proton of 0.5 GeV kinetic energy on passing through matter is slowed down by inelastic atomic collisions and occasional nuclear collisions; when it is almost at rest, it will be captured in an outer Bohr orbit of an atom. It will almost certainly be in a state of high angular momentum. Angular momentum and energy will be lost, at first by Auger transitions, and later by radiative transitions, until the anti-proton falls into an orbit whose overlap with the nucleus is sufficiently great for annihilation to occur. In this sequence of transitions to lower energy levels, radiative transitions will be predominant for jumps between orbits which are within the Bohr radius for the electrons of the atom; the states we will be interested in belong to this category.

As was pointed out in Sect. 1 above, it is likely that annihilation will frequently give rise to three or more pions. Although 2-pion annihilation may not be so common, it should occur; such events should be easily recognized by the energy of either of the pions, which is the maximum possible in any

[14] O. CHAMBERLAIN *et al.*: *Radiation Laboratory, Berkeley, Report* No. 3327 (1956).

[15] *Rochester Conference*, 1956. We are indebted to Dr. R. J. EDEN and Dr. A. SALAM for information on this point.

annihilation event ([16]). Whether the anti-proton annihilates when it is in an S, P or D state depends on the competition between the annihilation probability and the radiative transition probability; the stronger the annihilation interaction the larger is the orbital angular momentum of the state in which annihilation takes place. From Table II we see that (at least in hydrogen) 2π-annihilation in S, D, ... states is distinguished from that in P, F, ... states by the different isotopic spin of the process, and this difference will show up in the charge distribution of the two pions. It is also clear from Table II that such a distinction between orbital angular momenta does not occur in 3π-annihilation. (By observing 3π-annihilation events it may be possible, on the basis of the charge distribution gives in Table III, to get information about the isotopic spin of the most important matrix elements.) In the following discussion we confine ourselves to the 2π-annihilation process which is clearly the process most likely to give direct information about the annihilation probability.

Let τ be the lifetime of an anti-nucleon of given angular momentum when inside a nucleus. Then if n is the probability (calculated from the atomic wave function) that the anti-nucleon is within the nuclear radius, τ/n is its lifetime in an *atomic* state. τ is presumably larger than $\hbar/Mc^2$ ($M=$ proton mass), which would be $0.7\cdot10^{-24}$ s, and probably not smaller than $r/c=4\cdot10^{-24}$ s where r_0 is defined by $r_0A^{\frac{1}{3}}$ being the nuclear radius. The observed ([14]) large probability of annihilation in flight makes it likely that τ is close to this figure, let us say of the order of 10^{-23} s.

Originally, we had thought that the annihilation was an unlikely process, and τ considerably longer than 10^{-23} s. The reasons for this belief were that *virtual* pair processes seem to be strongly suppressed ([17]); this suppression hypothesis also brings the observed lifetime of the π^0 meson into agreement with theory ([18]); it also appears ([13]) that the production of anti-protons is a very rare process. In view of all these facts it is surprising that the annihilation seems to be highly probable ([19]).

For the moment n will be calculated on the assumption that the wave functions can be scaled down from those of the H-atom, and the necessary

([16]) The pion in the event $\pi+\gamma$ [cf. ref. ([7])] would have slightly greater energy. We do not consider this to be a likely annihilation process, because of the smallness of the fine structure constant.

([17]) K. A. Brueckner, M. Gell-Mann and M. Goldberger: *Phys. Rev.*, **90**, 476 (1953).

([18]) J. Iwadare and K. Nishijima: *Proc. Theor. Phys.*, **12**, 108 (1954).

([19]) There is no direct contradiction between the small anti-proton production cross-section and rapid annihilation, because the two processes are not inverse processes. In production only one pion is involved, whereas we understand that in annihilation on the average between 3 and 4 pions are produced.

corrections will be made in the next section. This approximation will only be reasonable when these atomic wave functions are mostly outside the nuclear radius. The series of radiative transitions will bring the anti-proton, which has been captured in an atom, into a state for which the lifetime for radiative transition to a lower energy level is of the same order as the annihilation lifetime τ/n for that state. Call this state the *critical* state. For example, for the $2p$ state we calculate a *critical time* τ_p such that if $\tau < \tau_p$ the anti-proton in general annihilates while still is the $2p$ state, but if $\tau > \tau_p$ it first drops to the $1s$ level, emitting a γ-ray. For any critical state we can similarly define a critical time; if the quantum number of the state in which annihilation occurs can be determined by observing the resulting pions, then this will in turn determine τ.

The radius of a nucleus of weight A is taken to be $R = 1.2 \cdot 10^{-13} A^{\frac{1}{3}}$ cm, and the Bohr orbit radius for an anti-proton in the Coulomb field of a nucleus of charge Z is $a = 2.9 \cdot 10^{-12} (A+1)/(AZ)$ cm. Therefore $R = a$ for $Z \simeq 9$; $R \simeq 2a$ for $Z \simeq 15$ and $R = 3a$ for $Z \simeq 21$. However the absorption experiments ([14]) indicate that it may be necessary to assume a somewhat larger nuclear radius λR $(\lambda \geqslant 1)$ for phenomena involving the anti-proton: we will in general assume $1.4 \geqslant \lambda \geqslant 1$, although for hydrogen we will allow the possibility that λ is as great as 2. To calculate τ_p we require

$$n = \int_0^{\lambda R} r^2 \psi_p^2 \, \mathrm{d}r \,,$$

where ([20])

$$r\psi_p = \frac{1}{2\sqrt{6a}} \left(\frac{r}{a}\right)^2 \exp\left[-r/2a\right].$$

Using the integral

$$\int_0^y \exp\left[-x\right] x^4 \, \mathrm{d}x = \frac{1}{5} y^5 \exp\left[-y\right] \left\{1 + \frac{1}{6} y + \frac{1}{6.7} y^2 + \ldots\right\},$$

gives

$$n = \frac{1}{120} \left(\frac{\lambda R}{a}\right)^5 \exp\left[-\lambda R/a\right] \left\{1 + \frac{1}{6} \left(\frac{\lambda R}{a}\right) + \ldots\right\}. \tag{3}$$

The lifetime of the $2p$ state for radiation is ([20]) $1.6 \cdot 10^{-9}/(M'Z^4)$ s where M' is the reduced mass of the anti-proton in units of the electron mass; this

([20]) H. A. BETHE: *Hand. der Phys.*, **24/1** (Berlin, 1933), p. 284.

gives $0.87 \cdot 10^{-12}(A+1)/(AZ^4)$ s. Equating this to τ_p/n gives

$$\tau_p = 0.9 \cdot 10^{-21} \lambda^5 \left(\frac{A}{A+1}\right)^4 A^{\frac{1}{3}} Z \exp\left[-\lambda R/a\right] \left\{1 + \frac{1}{6}\left(\frac{\lambda R}{a}\right) + \ldots\right\} \text{ s}. \tag{4}$$

In the same way we calculate the critical time τ_d which has the property that if $\tau < \tau_d$, annihilation takes place in the $3d$ state, while if $\tau > \tau_d$ the anti-proton drops to the $2p$ orbit by radiating a γ-ray. We use [20]

$$r\psi_d = \frac{4}{81\sqrt{30}a}\left(\frac{r}{a}\right)^3 \exp\left[-r/3a\right],$$

and for the lifetime for radiation take $0.85 \cdot 10^{-11}(A+1)/(AZ^4)$ s. This gives

$$\tau_d = 2.0 \cdot 10^{-26} \lambda^7 \left(\frac{A}{A+1}\right)^6 A^{\frac{7}{3}} Z^3 \exp\left[-\frac{2}{3}\lambda R/a\left\{1 + \frac{1}{8}\left(\frac{2}{3}\frac{\lambda R}{a}\right) + \ldots\right\}\right]. \tag{5}$$

For hydrogen τ_p equals $\lambda^5 \cdot 6 \cdot 10^{-23}$ s, and for heavier elements it increases rapidly. Therefore if, as we suggest, $10^{-24}\text{ s} < \tau < 10^{-22}$ s, it is probable that the anti-proton will annihilate from the $2p$ state even in hydrogen. (If τ is near the upper limit 10^{-22} s this is still true, provided that for hydrogen λ is larger than unity, which is very likely). For heavier materials annihilation will always occur in the $2p$ state before the anti-proton has time to jump into the $1s$ state by a radiative transition.

For hydrogen $\tau_d = \lambda^7 \cdot 3 \cdot 10^{-28}$ s, and even if we assume a large value of λ ($\lambda \simeq 2$), it is not possible for annihilation to occur in the $3d$ state, unless τ is much smaller than we expect. τ_d rises from $\lambda^7 \cdot 10^{-24}$ s for ${}_2^4\text{He}$ to $\lambda^7 \cdot 10^{-22}$ s for ${}_4^9\text{Be}$, so we might expect annihilation from the $3d$ state to set in somewhere in this range of nuclei. The critical time τ_f (for the transition $4f \rightarrow 3d$) is very small for light nuclei, and only reaches $6\lambda^9 \cdot 10^{-25}$ s for ${}_6^{12}\text{C}$.

We now discuss the information that should be obtained from annihilation events occurring in known nuclei. It is reasonable to assume that on annihilation a nucleon disappears without any appreciable transfer of energy or momentum to the rest of the nucleus. This means that the resulting pions are in isotopic states $T = 0$ or 1 only. Because correlations between the nuclear particles are unimportant, it is convenient to use the shell model to describe the nucleus. The anti-proton moves in an orbit about the centre of mass of the « protonic atom », and the nucleons move in orbits around the centre of mass of the nucleus; the change of parity between the protonic atom and the residual nucleus equals minus the product of the parities of the shell state of the annihilated nucleon and of the anti-proton state.

Annihilation in hydrogen is the simplest case. Assuming (as we do in this

section) that H-atom type wave functions are adequate to describe the anti-proton state, and assuming a *proton* radius of $1.2 \cdot 10^{-13}$ cm as above, the critical time for the $2p$ state is (by equation (4)) $\tau_c \sim \lambda^5 \cdot 6 \cdot 10^{-23}$ s; (we will discuss later the precise meaning of τ_c). As we have said above, annihilation almost certainly takes place from the $2p$ state. We discuss the consequences of this. Equation (2) shows that the isotopic spin of the initial state is a mixture of $T = 0, 1$. The matrix elements for annihilation may be written

$$(6) \qquad 2^{-\frac{1}{2}} \langle \bar{T} = 0 | H_{\text{int}} | T = 0 \rangle - 2^{-\frac{1}{2}} \langle \bar{T} = 1 | H_{\text{int}} | T = 1 \rangle ,$$

where $\bar{T} = 0, 1$ are the pion states. Further $|T = 0\rangle = 2^{-\frac{1}{2}} |T = 0^a\rangle + 2^{-\frac{1}{2}} |T = 0^s\rangle$ etc., so Table II gives the selection rules. The singlet states (both S and P) cannot give 2π-events, but the triplet states $^3S_1$, $^3P_0$ and $^3P_2$ can. Table II shows that the 2π-events have $T = 1$ if the initial state is ^3S but $T = 0$ if it is ^3P. In the very unlikely case that the antiproton annihilates in the S state, the pion wave function would be antisymmetric in the charge, so (π^0, π^0) could not occur. For $\tau \sim \lambda^5 \cdot 6 \cdot 10^{-23}$ s annihilation occurs in the P states of Table II and the pion pair is in the state $T = 0$. The isotopic state vector may be written,

$$(7) \qquad |T = 0\rangle = 3^{-\frac{1}{2}} (\pi_1^+ \pi_2^- + \pi_1^- \pi_2^+ - \pi_1^0 \pi_2^0)$$

and in this case the 2π-events include (π^0, π^0). Thus in hydrogen one might have to look for events in which *all* the energy is in γ-radiation, e.g. by an extension of the experiment of BRABANT *et al.* [12].

For nuclei heavier than ^{4}He, a complication arises because the nucleons in the nucleus (the « target nucleons ») may themselves have angular momentum different from zero. Now, by observing the charge distribution and other features of the 2π-annihilation events we can, at best, find the orbital angular momentum L of the nucleon anti-nucleon pair before annihilation. But in order to determine τ we must know the orbital angular momentum l of the anti-proton itself in the state from which its annihilation took place. For the lightest nuclei up to ^{4}He, the target nucleon has no orbital angular momentum, hence in this case $l = L$. But nuclei heavier than ^{4}He contain target nucleons in p states, therefore 2π-annihilation having the characteristics of an $L = 1$ state may be observed even if all the anti-protons are in fact in the $1s$ state before they are annihilated. This will be discussed in somewhat more detail below.

Next we discuss information to be obtained from nuclei like ^{2}D, ^{4}He, ^{12}C, ^{14}N, ^{16}O etc., whose ground states have zero isotopic spin, so that before annihilation the protonic atom has isotopic spin $T = \frac{1}{2}$, $T_3 = -\frac{1}{2}$. The residual nucleus (which may be in a highly excited state and may thus disintegrate

immediately) has isotopic spin values $T''=\frac{1}{2}$, $T''_3=\pm\frac{1}{2}$, because it has one nucleon less than the original $T=0$ nucleus (we assume nuclear Coulomb force effects may be ignored). The pions produced in the annihilation event have isotopic spin $\bar{T}=0$ or $\bar{T}=1$. The two residual nuclei $T''_3=\pm\frac{1}{2}$ should in some cases be distinguishable (from their disintegration products), and we will compare the matrix elements for the two cases.

Isotopic state vectors for $T''=\frac{1}{2}$, $\bar{T}=1$ can be combined to give total isotopic spin $T=\frac{1}{2}$ or $\frac{3}{2}$. The $T_3=-\frac{1}{2}$ components may be written

$$(8)\quad \begin{cases} |T''_3=\frac{1}{2},\ \bar{T}_3=-1\rangle = 3^{-\frac{1}{2}}|T=\frac{3}{2}(1),\ T_3=-\frac{1}{2}\rangle - (\frac{2}{3})^{\frac{1}{2}}|T=\frac{1}{2}(1),\ T_3=-\frac{1}{2}\rangle \\ |T''_3=-\frac{1}{2},\ \bar{T}_3=0\rangle = (\frac{2}{3})^{\frac{1}{2}}|T=\frac{3}{2}(1),\ T_3=-\frac{1}{2}\rangle + 3^{-\frac{1}{2}}|T=\frac{1}{2}(1),\ T_3=-\frac{1}{2}\rangle \end{cases}$$

$|T=\frac{3}{2}(1),\ T_3=-\frac{1}{2}\rangle$ is the $T_3=-\frac{1}{2}$ component of the $T=\frac{3}{2}$ set formed from $T''=\frac{1}{2}$, $\bar{T}=1$, etc. Because our initial state of anti-proton plus nucleus is $T=\frac{1}{2}$, the terms $|T=\frac{3}{2}(1),\ T_3=-\frac{1}{2}\rangle$ in (8) cannot give any contribution to the matrix elements.

Taking the nucleus ^{4}He as an example, we assume that it is sufficiently accurate to describe the residual «nuclei» ^{3}He and ^{3}H as components of the same isotopic spin. According as the pions produced are in states $T=0$ or 1 we have independent matrix elements $\langle T=\frac{1}{2}(0)|H_{\text{int}}|T=\frac{1}{2}\rangle$ or $\langle T=\frac{1}{2}(1)|H|T_{\text{int}}=\frac{1}{2}\rangle$. Using (8) this gives for pions in $\bar{T}=1$ the matrix elements

$$(9)\quad \begin{cases} {}^3\text{He},\ T=1,\ \bar{T}_3=1\ H_{\text{int}}\ {}^4\text{He},\ \bar{\text{P}} = -(\frac{2}{3})^{\frac{1}{2}}\ T=\frac{1}{2},\ (1)|H_{\text{int}}|T=\frac{1}{2} \\ \langle {}^3\text{H},\ \bar{T}=1,\ \bar{T}_3=0|H_{\text{int}}|{}^4\text{He},\ \bar{\text{P}}\rangle = 3^{-\frac{1}{2}}\langle T=\frac{1}{2},\ (1)|H_{\text{int}}|T=\frac{1}{2}\rangle\ . \end{cases}$$

For pions in $T=0$, we have

$$(10)\qquad \langle {}^3\text{H},\ \bar{T}=0|H_{\text{int}}|{}^4\text{He},\ \bar{\text{P}}\rangle = \langle T=\tfrac{1}{2},\ (0)|H_{\text{int}}|T=\tfrac{1}{2}\rangle\ .$$

In (9) and (10) the angular momentum dependence of the matrix elements is omitted for conciseness in writing. Formulae similar to (9) and (10) are obtained by replacing ^{4}He, ^{3}He, ^{3}H by D, P, N; ^{12}C, ^{11}C, ^{11}B; ^{14}N, ^{13}C, ^{13}C; ^{16}O, ^{15}O, ^{15}N respectively.

Consider further the annihilation in ^{4}He. For this nucleus $\tau_a \simeq \lambda\cdot 10^{-24}$ s, so we might expect annihilation to occur either in the $2p$-state or in the $3d$ state. For 2-pion annihilation the isotopic components of the matrix element are described uniquely by (9) and (10); therefore whatever the initial and

final angular momentum and spin values, the $\bar{T}=1$ process (if it exists) leads twice as often to final states with ^{3}He as to final states with ^{3}H, while $\bar{T}=0$ never gives ^{3}He. If the anti-proton is in a state of orbital angular momentum l, the parity of the annihilated pair is $(-1)^{l+1}$ because the annihilated nucleon is in the s-shell; hence if l is even the 2-pion events must be $T=1$, and if l is odd they must be $\bar{T}=0$. It should be possible to decide whether l is even or odd either by examining whether the nuclear fragment for 2π-events contains one or two protons, or by finding the ratio of π^- to π^+ in the 2π-events. For $T=0$ this ratio is unity (cf. equation (7)) while for $T=1$ it is 3:1 ($\bar{T}=1$ gives equal numbers of π^+ and π^- for $T_3=0$, and equal numbers of π^- and π^0 for $T_3=-1$; using (9) the ratio 3:1 follows).

We examine further the annihilation in other nuclei with zero isotopic spin. On the basis of the experiment of Chamberlain *et al.* [11] we shall use $\lambda=1.4$. Now suppose for example that $\tau\cong 10^{-22}$ s. Using (5) we see that $\tau\gtrsim\tau_n$ for the nucleus $^6_3$Li. Thus in H and He (and probably in the comparatively large nucleus D) we expect annihilation to occur in the $2p$ state, so that $\bar{T}=0$ type pion events should occur. For heavier nuclei ($A>4$) we expect annihilation to occur mostly when the anti-proton is in the $3d$ state. In these nuclei the p-shell contains nucleons, so if a p-shell nucleon is annihilated we expect $\bar{T}=0$ type 2π-events, while if the annihilation involves an s-shell nucleon the events are $\bar{T}=1$. Because the wave function of the anti-proton in a $3d$ state is greater near the surface of the nucleus than inside it, there is a preference for the annihilation of a p-shell nucleon (other factors being equal). The heavier the nuclei the more marked should be this preference. Formulae (9) and (10) still hold whether the annihilated nucleon is in the s-shell or the p-shell (these cases are distinguished by the angular momentum quantum numbers which we have not written down explicitly); thus, for example, we expect the $\bar{T}=1$ process in ^{12}C to lead to ^{11}C twice as often as to ^{11}B, while $\bar{T}=0$ only leads to ^{11}B.

From Table III the ratio of the total numbers of π^- to π^+ occurring in 3-pion events from the annihilation of an anti-proton by a neutron is seen to lie between $\frac{5}{2}$ and $\frac{3}{1}$. For $T=0$ type events there must of course be equal numbers of π^- and π^+ in 3-pion events. Using (2) and Table III it is easy to see that, in general, the π^-/π^+ ratio in 3-pion annihilation events of the type $T=1$ occuring in a nucleus is between $(5A-4Z)/(2A-Z)$ and $(3A-2Z)/A$; for light nuclei the ratio is therefore about $\frac{2}{1}$. The $\bar{T}=0$ process gives $(\pi^+\pi^0\pi^-)$ in each 3-pion event. It is clear from the selection rules given in Table II that it is not possible to relate the parity change to the isotopic spin of the 3-pion events in a unique way, but if the three-pion events can be observed, the ratio of the number of π^- to π^+ will give a measure of the relative size of the $\bar{T}=0$ and $\bar{T}=1$ matrix elements for 3-pion annihilation.

4. – Nuclear Effects.

The interaction between an anti-nucleon and a nucleon may be somewhat smaller in magnitude than that between two nucleons ([21]). The interactions are not identical, as can be seen from the simple graphs in Fig. 1, describing scattering under a pseudo-scalar interaction. For two nucleons both (*a*) and (*b*) are possible. (*c*) is the anti-nucleon nucleon scattering corresponding to (*a*) while (*d*) corresponds to (*b*). Using the charge conjugation property for fermion operators the values of (*a*) and (*c*) are seen to be equal, but the dependence of (*d*) on the energy momentum variables is different from that of (*b*). A higher order graph similar to (*d*) is (*e*) which can be divided into two parts ([22]) —« real » and « virtual »—according as both the boson lines do, or do not, have the energy and momentum values of real pions. The *real* part describes the 2-pion annihilation of the nucleon p and anti-nucleon q and the subsequent production of a nucleon anti-nucleon pair q, p by the two pions; the *virtual* part describes the scattering of p and q. We have assumed the real annihilation matrix elements are somewhat smaller than the size of the coupling constant would indicate; it is probable that virtual processes like (*d*) and the virtual part of (*e*) are also small.

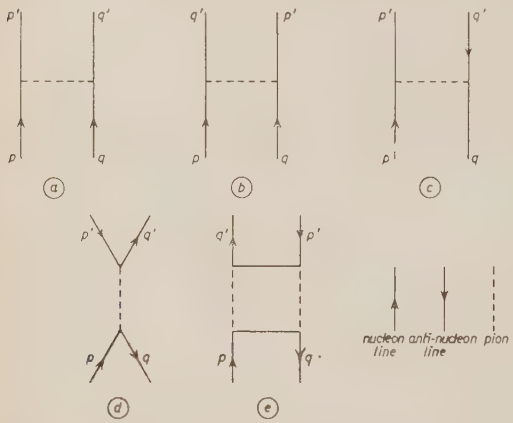

Fig. 1. – Nucleon-nucleon graphs (*a*), (*b*); anti-nucleon-nucleon graphs (*c*), (*d*), (*e*).

It seems reasonable to assume that a fairly strong attractive potential is provided by graph (*c*), and that therefore the interaction between an anti-proton and a complex nucleus will be represented by a rather deep potential well. The depth of the well is assumed to be about 40 MeV and the radius is $R = \lambda \cdot 1.2 \cdot 10^{-13} A^{\frac{1}{3}}$ cm. The effect of this attraction on the anti-proton wave function has to be estimated.

([21]) This is opposite to the suggestion of DUERR and TELLER [*Phys. Rev.*, **101**, 494 (1956)] that the interaction between anti-nucleon and nucleon is extremely strong, corresponding to a potential of about 1000 MeV.

([22]) J. HAMILTON: *Proc. Camb. Phil. Soc.*, **48**, 640 (1952).

The change in the $1s$ H-atom type state due to the nuclear potential may be considerable; in addition, because we have assumed that a deep potential well exists, there may be nuclear states (of low angular momentum) in which the anti-proton is almost entirely inside the nucleus. These states which we denote by $1s_N$, $2s_N$, ...; $1p_N$, $2p_N$, ... etc., are similar to the shell model states and we assume they have energies and wave forms similar to the shell model states. The unperturbed H-atom type state has energy $-2.6(Z/10)^2$ MeV and a radial spread of the order of a. Such a function is shown schematically in Fig. $2a$.

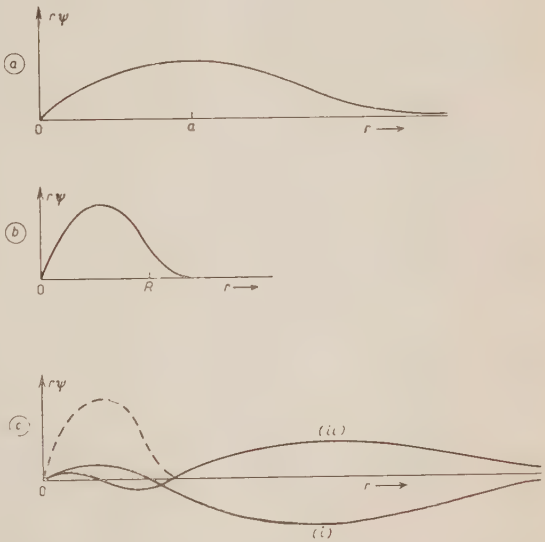

Fig. 2. – Anti-Proton S Wave Functions: (a) $1s$ H atom wave function; (b) $1s$: nuclear state; (c) wave functions (i) and (ii) mainly outside the nuclear potential well.

Consider now the solutions of the wave equation when the strong potential well is included. Inside the potential well the nuclear interaction predominates. If it is strong enough there will be a state $1s_N$ as shown in Fig. $2b$ which is almost entirely inside the well and is very little influenced by Coulomb forces. For a somewhat higher energy, the wave function in the same potential will have greater curvature; it will cut the axis as shown in curve (i) of Fig. $2c$, and will then, outside the well, be subject merely to the Coulomb attraction. If $a \gg R$, the start of the wave function at small r will have little influence on its behaviour outside the nuclear well, therefore the shape of curve (i) Fig. $2c$, for $r > a$ will not differ greatly from that of the pure Coulomb function Fig. $2a$. If the nuclear potential increases in strength, a second nuclear state $2s_N$ will be bound, and then the Coulomb type function will have two nodes inside or near the nucleus as shown in curve (ii) Fig. $2c$.

The change in energy levels is not great for the H-atom $2p$, $3d$, ... states of nuclei with $Z < 10$ (we do not consider heavier nuclei above). These states are almost entirely outside the nucleus, and a perturbation estimate of the correction should be adequate. For $Z = 10$ the factor u for the $2p$-state (equ. (3) above) is less than 1/300, so the change in energy due to the 40 MeV well is

appreciably smaller than the Bohr energy of the $2p$-state, $-0.6(Z/10)^2$ MeV; for $Z < 10$ the relative effect of the well is smaller still.

Although the energies and general form of these $2p$, $3d$, ... states is not much changed, we do expect that the part of their wave functions which is inside the nucleus is altered. We estimate that, with the potential well stated, the anti-proton density inside the nucleus may be altered by a factor between 2 and 5 in either direction. The estimates in Sect. 3 are therefore probably only correct to this order of magnitude. We expect that the error is least important for light nuclei, especially for hydrogen.

For states, such as the Coulomb state $1s$, which are appreciable inside the nucleus another phenomenon occurs: because of the possible annihilation of the anti-proton inside the nucleus, its wave function may not penetrate very far inside the nucleus, and this results in a suppression of that part of the wave function which is inside the nucleus. An imaginary term added to the potential describes this ([23]); the probability of the anti-proton being in volume element $\mathrm{d}V$, obeys the relation

$$\frac{\partial}{\partial t}(\psi^*\psi)\,\mathrm{d}V = -\frac{1}{\hbar}\,\psi^* W \psi\,, \tag{11}$$

when $W = \hbar/T$, and T (which may be a function of position) is the lifetime of the anti-proton. The modified Schrödinger equation that gives (11) is

$$i\hbar\,\frac{\partial\psi}{\partial t} = H\psi \qquad \text{with} \qquad H = Mc^2 + \frac{p^2}{2M} + V - \frac{i}{2}\,W\,. \tag{12}$$

We assume that the imaginary part of the energy is small compared with Mc^2, although the imaginary potential W need not be small inside the nucleus: this is equivalent to assuming that the lifetime of the states we consider is long compared with $\hbar/Mc^2 = 0.7 \cdot 10^{-24}$ s. It is now possible to solve the eigenvalue equation

$$H\psi = E'\psi$$

in which the imaginary part of E' is ignored. Then substituting for H from (12) gives the equation for $f = r\psi$ for an s-state

$$\frac{\mathrm{d}^2 f}{\mathrm{d}r^2} + \frac{2M}{\hbar^2}\left\{E - V(r) + \frac{i}{2}\,W(r)\right\} f = 0\,, \tag{13}$$

([23]) See, for example, H. A. BETHE: *Phys. Rev.*, **57**, 1125 (1940), and H. FESHBACH, C. E. PORTER and V. F. WEISSKOPF: *Phys. Rev.*, **96**, 448 (1954).

(E is the non-relativistic energy). $W(r)$ is taken to be proportional to the density of nucleons, such that $W = \hbar/\tau$ inside the nucleus.

A convenient approximate solution to (13) is obtained by writing $f = f_0 \exp[\omega/\hbar]$, where f_0 is a solution of

$$\frac{\mathrm{d}^2 f_0}{\mathrm{d}r^2} + \frac{2M}{\hbar^2}\{E - V(r)\} f_0 = 0 \,, \tag{14}$$

such that $f_0 \to 0$ as $r \to \infty$. Substituting in (13) gives

$$2f_0'\omega'/\hbar + f_0(\omega''/\hbar + \omega'^2/\hbar^2) = -\frac{iM}{\hbar^2} W(r) f_0 \,. \tag{15}$$

Neglecting the term in ω'' gives the solution

$$f(r) = C \exp\left[\int_{\infty}^{r} \left\{ (f_0'/f_0)^2 - \frac{iMW(r)}{\hbar^2} \right\}^{\frac{1}{2}} \mathrm{d}r \right] , \tag{16}$$

where C is a normalization constant. For small W the departure of E from an eigenvalue of (14) may be neglected. Neglecting ω'' in (15) is a good approximation for large $W(r)$, provided it does not change rapidly.

For H-atom type wave functions the order of magnitude of the correction in (16) is seen by examining

$$Ma^2 W/\hbar^2 = \left(\frac{A+1}{AZ} \right)^2 \cdot \frac{1.3 \cdot 10^{-20}\ \mathrm{s}}{\tau} \,, \tag{17}$$

where $W = \hbar/\tau$. In the $2p$-state

$$f_0'/f_0 = [2 - (r/2a)]/r \,,$$

so that the value of $(f_0'/f_0)^2$ in the nucleus is nearly $4/r^2$. The second term inside the square root sign in (16) is therefore less than the first provided $MWr^2/\hbar^2 < 4$. For light nuclei the condition for this second term to be negligible is $MWR^2/\hbar^2 < 4/\lambda^2$, or $\tau \gtrsim 6\lambda^2 A^{\frac{2}{3}} \cdot 10^{-21}$ s. We cannot assume that τ satisfies this condition, therefore it is to be expected that the $2p$ state wave function inside the nucleus is distorted in such a way as to reduce the probability of the anti-proton being inside the nucleus. This will have two main effects: the time the anti-proton spends in the $2p$ state will be somewhat longer that the estimates given above, and also, when annihilation occurs in an atomic orbit, the distortion of the wave function will favour the annihilation of an outer shell nucleon. The size of both effects will depend

markedely on the value of r. For the $3d$ state

$$f_0'/f_0 = [3 - (r/a)]/r$$

and the condition for the distortion effect to be important is much the same as for the $2p$ state. Wave functions which are large inside the nucleus will suffer appreciable distortion due to this effect, and their binding energy may be considerably reduced because of the increased probability for the anti-proton to be outside or near the surface of the nucleus.

5. – The Nuclear Auger Effect.

So far we have assumed that the anti-proton jumps from one atomic orbit to a lower one until it reaches an atomic orbit in which it is annihilated; now we consider whether the anti-proton can jump into the nucleus before it is annihilated ([24]). The obvious ways in which such a transition could occur are by the ejection of a nucleon from the nucleus, by the excitation of the nucleus, or possibly by radiation.

Since we do not know the depth of the potential well attracting the anti-proton to a nucleus or the depth and range of the interaction between the anti-proton and a nucleon, it is not possible to discuss these processes quantitatively; we confine ourselves to a few general arguments.

It is not necessary to consider an anti-proton in an s type atomic state because we expect the anti-proton to be annihilated in the $2p$ state or a higher state. In such an atomic state the binding energy of the anti-proton will be 1 MeV or less for *light* nuclei ($Z \leqslant 10$). If the anti-proton is attracted to the nucleus by a potential well which is much the same as that for a proton, then there will be bound shell-type states in which the anti-proton can be inside the nucleus. Because the exclusion principle does not forbid it, the anti-proton can fall into *any* of these states.

A priori it is unlikely that the discrete energy levels of the compound nucleus (formed by adding an anti-proton to a light nucleus) are accidently so situated that they coincide with the energy level of a protonic atom. This is because for light nuclei the width of discrete levels is very small compared with their separation (by discrete levels we mean those which can only decay by radiation and not by particle emission). Therefore we expect that capture of the anti-proton by the nucleus without the ejection of a nucleon is unlikely. We shall only consider the Auger type of capture in which a nucleon is ejected.

([24]) We are indebted to Professor R. E. PEIERLS for a discussion on the importance of this effect.

If the nuclear potential well for an anti-proton is no deeper than that for a proton, this type of capture cannot occur in nuclei up to ^{4}He because there is not sufficient energy available to eject an s-shell nucleon. For nuclei heavier than ^{4}He an outer shell nucleon can be ejected even if the anti-proton potential well is somewhat less deep than that for the proton. If the potential well is very deep (as suggested by DUERR and TELLER ([21])) the Auger type capture becomes very important in all nuclei. For definiteness we assume in what follows that the anti-proton nuclear potential well is not markedly different from that for the proton.

Auger capture upsets the considerations of Sect. 3 above, because it breaks the chain of deduction from the observed charge distribution of the disintegration products to the radiative lifetime of the atomic state in which annihilation occurs. However if we know (from experiment) that Auger capture occurs, we can give a lower bound for the annihilation lifetime τ. This is because the probability for Auger capture from an atomic orbit (of low angular momentum) must be approximately proportional to the probability n that the anti-proton in this state is inside the nuclear radius λR. Thus the lifetime for Auger capture is τ_A/n where τ_A is a time constant. The occurrence of Auger capture would prove that τ is greater than τ_A.

Now we give an estimate of τ_A. We assume that in light nuclei the anti-proton can drop into an s state having binding energy of about 30 MeV and that it can eject a p shell nucleon with a kinetic energy of about 10 MeV. We also assume that the interaction between anti-proton and nucleon is about the same as between two nucleons. Then the transfer of energy from the anti-proton to the nucleon will be similar to that from an incident nucleon to a nucleon in the target nucleus, provided the same amount of energy is available, i.e. about 30 MeV. This means we should compare our process with that of an incident nucleon of about 20 MeV kinetic energy: such a nucleon can go into a bound state of about 10 MeV without violating the exclusion principle so that 30 MeV can be transferred to the target nucleon. The probability of this transfer is given by the imaginary part W of the complex potential $V+iW$ by FESHBACH *et al.* ([23]) which is experimentally found to be ([25]) of the order of 10 MeV at 20 MeV kinetic energy, and smaller at other energies. We shall therefore assume that the same probability also applies to the Auger capture of the anti-proton which gives

$$\tau_A = \hbar/W = 6\cdot 10^{-23}\ \mathrm{s}\,. \tag{18}$$

This estimate assumes that all nucleons are available for the Auger effect;

([25]) A. M. LANE and C. F. WANDEL: *Phys. Rev.*, **99**, 647 (1955).

actually only the $(A-4)$ nucleons in the p shell are available, and therefore (18) should be multiplied by $(A-4)/A$.

We consider the estimate (18) more reliable than an estimate from perturbation theory which gives $\tau_A \simeq 10^{-23}$ s. It is well known that perturbation theory is apt to overestimate the probability of nuclear reactions ([26]) because it does not take into account correlations between the nucleons. In any case, the time given by (18) is close to the time required by a nucleon of 10 MeV kinetic energy to travel the average distance between two nucleons, i.e. about $2r_0$.

The result (18) is at the upper limit of the range (10^{-24} to 10^{-22} s) we estimated for the lifetime τ for annihilation. Therefore it is likely that annihilation will take place before the Auger effect, although it cannot be excluded that the two processes are of comparable probability.

If the latter is true, (i.e. if annihilation is relatively slow), and if in addition the interaction between anti-proton and nucleon is *greater* than between two nucleons, then Auger effect will occur sometimes in the lightest nuclei, up to ^{4}He, and the annihilation will then have the character of an initial S rather than a P state. Such a result would be interesting mainly because it would indicate a large attraction between anti-nucleon and nucleon.

If the Auger effect occurs, at least one nucleon is ejected, and therefore the nucleus is no longer the original one, and is in general not konwn. The remarks made in Sect. 4 about nuclei of high symmetry like ^{4}He can then no longer be applied. Auger capture from the $3d$ state can lead to ejection of a p-shell nucleon into a p-state. The capture probability is now more strongly dependent on the wave number of the ejected nucleon. For $k\lambda R \sim 1$ the time τ_A is somewhat longer than that given by (18).

Finally, we have to consider whether it is possible to have *radiative* transitions of the anti-proton from atomic orbits directly into nuclear states. The lifetime for such transitions must be approximately proportional to n, the probability that the anti-proton (in an atomic orbit) is inside the nucleus: we write the lifetime as τ_R/n. Because of the small value of the fine structure constant, we expect this *radiative* lifetime τ_R to be longer than the Auger lifetime τ_A, unless there is not sufficient energy available for the Auger effect to occur. In the latter case, it is clear that annihilation should occur before a radiative transition into the nucleus, because, for the same general reasons, we expect the radiative lifetime τ_R to be longer than the annihilation lifetime τ.

([26]) A. M. LANE, R. G. THOMAS and E. P. WIGNER: *Phis. Rev.*, **98**, 693 (1955).

Appendix

We discuss briefly a useful form of the relation between charge conjugation and isotopic spin. Proton and neutron states are represented by the components u_P, u_N of the binary vector (u_P, u_N), and anti-protons and anti-neutrons by the components of $(u_{\bar{P}}, u_{\bar{N}})$. Rotations in isotopic space are represented by unitary transformations of (u_P, u_N) ([27]); such transformations leave invariant $u_P^* u_P + u_N^* u_N$ ([28]). It is known ([29]) that $(u_P, u_{\bar{N}})$ transforms like (u_P^*, u_N^*). The (complex) charged pion field variables Φ, Φ^* ([30]) and the (real) neutral pion field Φ_3 transform like $u_P^* u_N$, $-u_P u_N^*$ and $u_P^* u_P$, $-u_N^* u_N$ respectively ([31]).

Charge conjugation C is the transformation

$$\Phi' = \exp[2i\alpha]\Phi^*, \quad \Phi^{*\prime} = \exp[-2i\alpha]\Phi, \quad \Phi_3' = \Phi_3 \qquad (\alpha, \text{ real}).$$

This is described by a reflection in any plane through O_3 in the 3-dimensional isotopic space; the related binary vector transformation is

$$u_P' = \exp[-i\beta]u_P^*, \quad u_N' = \exp[i\beta]u_N^*, \quad u_P^{*\prime} = \exp[i\beta]u_P, \quad u_N^{*\prime} = \exp[-i\beta]u_N,$$

where $\beta = \alpha + \frac{1}{2}\pi$. Assuming invariance of the Hamiltonian under C, and under the charge symmetry operator T which gives ([32])

$$\Phi' = \Phi^*, \qquad \Phi^{*\prime} = \Phi, \qquad \Phi_3' = -\Phi_3,$$

it is obvious (omitting unimportant phase factors, by putting $\alpha = 0$) that the operation ([33]) $W = C \cdot T$ describes reflection in the O_{12} plane in 3-dimensional isotopic space. $W^2 = 1$, and W commutes with T_3 the generator of infinitesimal rotations about the O_3 axis. States having the same T_3 eigenvalue may be combined to give eigenstates of W, but of such states, only those describing equal numbers of nucleons and anti-nucleons are important. W anti-commutes with T_1 and T_2 the generators of infinitesimal rotations about the O_1 and O_2 axes, so W commutes with T^2. Operating on eigenstates of T_3 with $(T_1 \pm iT_2)$ raises or lowers the T_3 eigenvalue by unity; because W anti-commutes with $(T_1 \pm iT_2)$, applying either of these operators to an eigenstate of W changes the sign of the eigenvalue of W (which must in any case be ± 1). Therefore

([27]) See B. L. van der Waerden: *Gruppentheoretische Methode in der Quantenmechanik* (Berlin, 1932), p. 16.

([28]) u^* is the complex conjugate of u.

([29]) See ref. ([10]).

([30]) $\varphi = \varphi_1 + i\varphi_2$ where $(\varphi_1, \varphi_2, \varphi_3)$ is a 3-vector in isotopic space.

([31]) See ref. ([9]).

([32]) See the first reference in footnote ([9]).

([33]) See the second reference in footnote ([8]).

all information given by W for a set of eigenstates of T^2 is contained in the eigenvalue of W for the $T_3 = 0$ eigenstate.

The binary representation of W is

$$(A.1) \quad u'_P = \exp[i\gamma] u^*_N, \; u'_N = \exp[i\gamma] u^*_P, \; u^{*\prime}_P = \exp[-i\gamma] u_N, \; u^{*\prime}_N = \exp[-i\gamma] u_P .$$

If superscripts (1) and (2) refer to particles (1) and (2), letting W act on the $T_3 = 0$ eigenstate [cf. equation (1)] gives

$$W(u^{(1)}_P u^{(2)}_{\bar{P}} + u^{(1)}_N u^{(2)}_{\bar{N}}) = u^{(1)}_{\bar{N}} u^{(2)}_N + u^{(1)}_{\bar{P}} u^{(2)}_P .$$

The $T = 0$ eigenstates may be separated into the symmetric $T = 0^s$ and the anti-symmetric $T = 0^a$,

$$\tfrac{1}{2}\{u^{(1)}_P u^{(2)}_{\bar{P}} \pm u^{(1)}_{\bar{P}} u^{(2)}_P + u^{(1)}_N u^{(2)}_{\bar{N}} \pm u^{(1)}_{\bar{N}} u^{(2)}_N\} ,$$

the upper (lower) sign giving $0^s(0^a)$. 0^s has the eigenvalue $W' = -1$ and 0^a has $W' = -1$. Similarly for $T_3 = 0$, $T = 1^s$ (1^a) have eigenvalues $W' = -1(+1)$. The permutation character appears because of the exchange of particles in (A.1). The eigenvalue of W for a pion state which has n neutral pions is $(-1)^n$.

RIASSUNTO (*)

Si mostra come semplici esperimenti sull'annichilamento dell'antiprotone in materiali diversi possano essere usati per determinare la natura del processo di annichilamento nella materia nucleare e per ottenere informazioni sulle forze nucleone-antinucleone. Si esamina in dettaglio l'annichilamento degli antiprotoni derivanti da stati atomici e si danno correzioni per effetti nucleari specifici.

(*) *Traduzione a cura della Redazione.*

On the Energy Loss and Specific Ionization of a Relativistic Particle in a Polarizable Medium - I.

P. Budini

Istituto di Fisica dell'Università - Trieste

L. Taffara

Istituto di Fisica dell'Università - Padova
Istituto Nazionale di Fisica Nucleare - Sezione di Padova

(ricevuto il 3 Aprile 1956)

Summary. - The average total energy loss of a particle on passing through a polarizable medium has been calculated by introducing into the theory of Fermi an expression for the dielectric constant which is apt to represent both the dispersive and absorptive properties of the medium. The average total energy may then be divided into the average energy lost as excitation, Čerenkov radiation and primary ionization of the atoms of the medium. The effect has been calculated of the polarizability of the medium on the number of ions generated by the ionizing particle per unit length and on the number of events in which an atomic electron has been emitted with energy greater than a certain threshold energy. These numbers show a logarithmic increase at relativistic energies and a subsequent saturation caused by the polarizability of the medium, both dependent on the threshold energy.

Introduction.

The influence of the polarizability of the medium on the energy loss to which a charged particle is subject on passing through it, has been given by Fermi ([1,2]). He found that, due to the effect of the polarizability, the well known logarithmic increase of energy loss postulated by the classical theory

([1]) E. Fermi: *Phys. Rev.*, **56**, 1242 (1939).
([2]) E. Fermi: *Phys. Rev.*, **57**, 485 (1940).

of BETHE ([3,4]), BLOCH ([5,6]), WILLIAMS ([7]) and BOHR ([8]) is reduced at high energy. Fermi's work has been subsequently extended especially by the introduction of a more correct expression for the characteristic dielectric constant of the medium ([9-14]): these extensions have not changed either the theoretical scheme nor the qualitative results of the original theory.

Fermi's theory is suitable for describing the average total energy loss of a ionizing particle and, for this problem, it is in satisfactory accord with the experimental results. Difficulties arise when the theory of energy loss is invoked to explain phenomena such as the formation of tracks in cloud chambers or in nuclear emulsions, in which the experimental information is represented by the number of droplets or grains formed per unit length of tracks. In this case at least three sort of difficulties have to be considered: the first concerns the relation between the number of ions generated by the ionizing particle and the number of droplets found in the cloud chamber tracks or the number of grains in emulsion tracks. It is usually avoided with the help of one of the parameters which appear in Fermi's formula: the average ionization energy. This generally serves as a normalization parameter for the theoretical curve with respect to the experimental one. The second is connected with the maximum energy transferable in close collisions, which in the problem of the total energy loss gives rise to the well known problem of fluctuations treated by LANDAU ([15,16]), and introduces instead, into the ionization problem, a parameter which is usually fixed more or less arbitrarily. The third difficulty derives from the fact that one does not know which part of the total loss contributes to the ionization of the atoms of the medium and which part contributes to excitation and Čerenkov radiation; this problem has been treated in various theoretical works, but with various results ([17-20]).

([3]) H. BETHE: *Ann. der Phys.*, **5**, 293 (1930).
([4]) H. BETHE: *Zeits. f. Phys.*, **76**, 326 (1932).
([5]) F. BLOCH: *Zeits. f. Phys.*, **81**, 363 (1932).
([6]) F. BLOCH: *Ann. der Phys.*, **16**, 285 (1933).
([7]) E. J. WILLIAMS: *Proc. Roy. Soc.*, A **139**, 163 (1933).
([8]) N. BOHR: *Det. Kgl. Dans. Vid. Sels.*, **18**, 9 (1948).
([9]) G. C. WICK: *Ric. Scient.*, **11**, 273 (1940).
([10]) G. C. WICK: *Ric. Scient.*, **12**, 858 (1941).
([11]) G. C. WICK: *Nuovo Cimento*, **1**, 302 (1943).
([12]) O. HALPERN and H. HALL: *Phys. Rev.*, **73**, 477 (1948).
([13]) R. M. STERNHEIMER: *Phys. Rev.*, **91**, 256 (1953).
([14]) G. N. FOWLER and G. M. B. D. JONES: *Proc. Phys. Soc.*, **66**, 597 (1953).
([15]) L. LANDAU: *Journ. Phys.* (*USRR*), **8**, 201 (1944).
([16]) K. R. SYMON: *Thesis, Harvard University* (1948) (unpublished).
([17]) M. SCHÖNBERG: *Nuovo Cimento*, **8**, 159 (1951).
([18]) M. SCHÖNBERG: *Nuovo Cimento*, **9**, 372 (1952).
([19]) M. HUYBRECHTS and M. SCHÖNBERG: *Nuovo Cimento*, **9**, 764 (1952).
([20]) P. BUDINI: *Zeits. f. Naturforsch.*, **72**, 722 (1952).

In the course of the discussions on this last problem, which followed the discovery of relativistic increase in ionization ([21-23]), it has clearly resulted that it is not possible to interpret the experimental results by means of Fermi's theory, if one takes into account the dielectric properties of the medium by an $\varepsilon(\omega)$ which represents the dispersive properties of the medium and ignores the absorptive ones. In fact, in this way, one obtains a relativistic increase due only to the dispersive properties of the medium i.e. due solely to Čerenkov radiation ([17]).

In this paper we will try to recast the theory by introducing, from the very beginning, an $\varepsilon(\omega)$ which represents both the dispersive and absorptive properties of the medium (Sect. 1). In this way one can see that the separation of the energy loss into that due to ionization, excitation and Čerenkov radiation may be obtained from the theory rather easily and without ambiguity (Sect. 2-5). Even in a more correct theory such as this, the energy loss by ionization is not, as far as we can see, the most suitable one for comparison with the experimental results for the number of ions. The average energy lost by ionization depends critically on two parameters: the mean energy of ionization of the atoms of the medium and the maximum energy which can be transfered to an electron in close collisions. These parameters can only be theoretically calculated with great difficulty and therefore usually one does not attempt their theoretical determination but uses them as normalization parameters. However, it is clear that, of these two parameters, the second one (the maximum transferable energy), while important in the computation of the energy loss, should not influence the mean number of ions produced per unit length since collisions in which the energy transfer is very large are extremly rare. For the purposes of obtaining a more suitable expression for comparison with the experimental data, we have calculated the direct influence of the polarization on the specific primary ionization (Sect. 6). As was to be expected, the final formula, which predicts a logarithmic increase of the number of ions followed by a saturation as indicated by experimental results, does not depend in a critical manner on the maximum transferable energy.

It is to think ([21-25]) that the specific number of grains observed in emulsions depends on a critical minimum energy necessary for the formation of a grain, which in turn depends on the type of emulsion and on the degree of development. We have adapted our theory to take account of this effect, and have

([21]) L. Voyvodic and E. Pickup: *Phys. Rev.*, **80**, 89 (1950).
([22]) L. Voyvodic: *Bristol Conference* (1951).
([23]) S. G. Gosh, G. M. D. B. Jones and J. G. W. Wilson: *Proc. Phys. Soc.*, **65**, 68 (1952).
([24]) L. M. Brown: *Phys. Rev.*, **90**, 95 (1953).
([25]) B. T. Price: *Report of Progress in Physics*, **18**, 52 (1955).

discussed the possible qualitative consequences of such hypothesis. Quantitative computations will be given in the second part of this work. These previsions are susceptible of experimental verification.

1. – Total Energy Loss.

The total energy loss per unit length suffered by a particle of charge e in collisions at impact parameters larger than ϱ can be calculated, following FERMI [2], by means of the flux of the Poynting vector coming out from a cylinder having its axis on the particle trajectory, and radius ϱ i.e.:

$$\frac{\partial W_\varrho}{\partial z} = \frac{4ne^4}{mv^2} \operatorname{Re} \int_0^\infty \left[\frac{1}{\varepsilon(\omega)} - \beta^2 \right] \chi^* \cdot K_1(\chi^*) K_0(\chi) i\omega \, \mathrm{d}\omega \,, \tag{1}$$

where

$$\chi = \frac{\omega \varrho}{v} \sqrt{1 - \beta^2 \varepsilon(\omega)} \,, \tag{2}$$

K_1, K_0 are the modified Hankel functions, n is the number of electrons per cm^3 and the other symbols have the usual meaning. In (1) and (2), as in the following, the frequencies are measured in units of $\sqrt{4\pi ne^2/m}$.

If $\varrho \approx \varrho_0$ atomic radius, the asymptotic expressions of the Hankel functions for $|\chi| \ll 1$ can be inserted in (1) which then becomes:

$$\frac{\partial W_{\varrho_0}}{\partial z} = \frac{4ne^4}{mv^2} \operatorname{Re} \int_0^\infty \left[\frac{1}{\varepsilon(\omega)} - \beta^2 \right] \log \frac{A}{\omega^2 [1 - \beta^2 \varepsilon(\omega)]} \, i\omega \, \mathrm{d}\omega \,, \tag{1'}$$

where

$$A = \frac{mv^2}{\pi n \gamma^2 \varrho_0^2 e^2} \qquad \text{and} \qquad \log \gamma = 0.577 \ldots . \tag{3}$$

In order that (1') should give the energy lost by Čerenkov radiation, excitation and ionization, we have to introduce for $\varepsilon(\omega)$ an expression which represents the dispersive as well as the absorptive properties of the medium. As an example we adopt for $\varepsilon(\omega)$ the following expression:

$$\varepsilon(\omega) = 1 + \sum_{i=1}^{z} \frac{f_i}{\omega_i^2 - \omega^2 + i g_i \omega} + \frac{mc}{2\pi^2 e^2} \sum_{k=1}^{z} \int_0^\infty \frac{\sigma_k(\omega') \theta(\omega' - \omega_k) \mathrm{d}\omega'}{\omega'^2 - \omega^2 + i g \omega} \,, \tag{4}$$

with

$$\theta(\omega' - \omega_k) = \begin{cases} 0\,, & \text{for } \omega' < \omega_k\,, \\ 1\,, & \text{for } \omega' \geqslant \omega_k\,, \end{cases}$$

$\sigma_k(\omega')$ = photoelectric cross-section of the atoms of the medium and Z atomic number.

The real and imaginary parts of $\varepsilon(\omega)$ can also be written in the following form [26].

$$\text{(5)} \qquad \operatorname{Re}\varepsilon(\omega) = 1 + \sum_{i=1}^{n} \frac{f_i(\omega_i^2 - \omega^2)}{(\omega_i^2 - \omega^2)^2 + g_i^2\omega^2} + \\ + \frac{mc}{2\pi^2 e^2} \sum_{k=1}^{z} \int_0^{\infty} \frac{\sigma_k(\omega')(\omega'^2 - \omega^2),\, \theta(\omega' - \omega_k)}{(\omega'^2 - \omega^2)^2 + g^2\omega^2}\, \mathrm{d}\omega'\,,$$

$$\text{(6)} \qquad \operatorname{Im}\varepsilon(\omega) = \sum_{i=1}^{n} \frac{f_i g_i \cdot \omega}{(\omega_i^2 - \omega^2)^2 + g_i^2\omega^4} + \frac{mc}{4\pi e^2 \omega} \sum_{k=1}^{z} \sigma_k(\omega)\,.$$

With $\varepsilon(\omega)$ given by (4), (1′) can be integrated in the complex plane on the same line of Halpern-Hall calculus [12] i.e. from zero to $i \cdot a$, where the frequency a is the single positive root of the equation

$$\text{(7)} \qquad 1 - \beta^2 \cdot \varepsilon(iy) = 0\,,$$

and then from $i \cdot a$ to $i \cdot r$ (with r very large), and from $i \cdot r$ to r through a quarter of a circle of radius r and center at the origin. One thus obtains

$$\text{(8)} \qquad \frac{\partial W_{\varrho_0}}{\partial z} = \frac{2\pi e^4 n}{mv^2}\left[\log\frac{A}{1-\beta^2} + a(1-\beta^2) - \beta^2 + 2J\right],$$

with

$$\text{(9)} \qquad \begin{cases} J = \displaystyle\int_a^r y\,\mathrm{d}y\left[1 - \frac{1}{\varepsilon(iy)}\right] - \log r = \\ = \displaystyle\sum_{i=1}^{n} f_i \int_a^r \frac{y\,\mathrm{d}y}{\omega_i^2 + y^2} \frac{}{g_i y} + \frac{mc}{2\pi^2 e^2} \sum_{k=1}^{z} \int_{\omega_k}^{\infty} \sigma_k(\omega')\,\mathrm{d}\omega' \int_a^r \frac{y\,\mathrm{d}y}{\omega'^2 + y^2} \frac{}{gy} - \log r = \\ = -\log\left[(\omega_1^2 + a^2)^{f_1/2} \cdot (\omega_2^2 + a^2)^{f_2/2} \ldots (\omega_n^2 + a^2)^{f_n/2}\right] - \\ \qquad - \frac{1}{2}\,\frac{mc}{2\pi^2 e^2} \sum_{k=1}^{z} \int_{\omega_k}^{\infty} \sigma_k(\omega') \log\left[\omega'^2 + a^2\right] \mathrm{d}\omega'\,. \end{cases}$$

[26] A. H. Compton and S. K. Allison: *X-Rays in Theory and Experiment* (1948).

The integral on the right hand side of (9) can be calculated exactly when the analytical expressions of $\sigma_k(\omega')$ are known; however, in general, one can write:

$$J = -\log\left[(\omega_1^2 + a^2)^{f_{1/2}} \cdot (\omega_2^2 - a^2)^{f_{2/2}} \dots (\omega_n^2 + a^2)^{f_{n/2}}\right] - \tag{10}$$
$$- \log\left[(\bar{\omega}_1^2 + a^2)^{\bar{f}_{1/2}} \dots (\bar{\omega}_z^2 + a^2)^{\bar{f}_{z/2}}\right],$$

where ω_k represents a weighted mean value which, in general, is very near to the frequencies of ionization, ω_k and $\bar{f}_k$ are given by

$$\bar{f}_k = \frac{mc}{2\pi^2 e^2} \int_{\omega_k}^{\infty} \sigma_k(\omega')\, \mathrm{d}\omega' . \tag{11}$$

Putting:

$$\begin{cases} \omega_1^{*\delta_1} = (\omega_1^2 + a^2)^{f_{1/2}} \cdot (\omega_2^2 + a^2)^{f_{2/2}} \dots (\omega_n^2 + a^2)^{f_{n/2}} \\ \omega_2^{*\delta_2} = (\bar{\omega}_1^2 + a^2)^{\bar{f}_{1/2}} \cdot (\bar{\omega}_2^2 + a^2)^{\bar{f}_{2/2}} \dots (\bar{\omega}_z^2 + a^2)^{\bar{f}_{z/2}} , \end{cases} \tag{12}$$

and:

$$\sum_{i=1}^{n} f_i = \delta_1; \qquad \sum_{k=1}^{z} \bar{f}_k = \delta_2 , \tag{13}$$

one gets:

$$\frac{\partial W_{\varrho_0}}{\partial z} = \frac{2\pi e^4 n}{mv^2} \left[\log \frac{1}{(\omega_1^{*\delta_1} \cdot \omega_2^{*\delta_2})^2 (1 \quad \beta)^2} - a^2(1 - \beta)^2 \quad - \beta^2 \right] . \tag{14}$$

Further taking into account that:

$$\delta_1 + \delta_2 = 1 , \tag{13'}$$

the limiting value for $\beta^2 \to 1$ $(a \to \infty)$ is given by:

$$\frac{\partial W_{\varrho_0}}{\partial z}\,(v = c) = \frac{2\pi e^4 n}{mc^2} \log \frac{mc^2}{\pi n \gamma^2 \varrho_0^2 e^2} , \tag{15}$$

that is, it is independent of $\varepsilon(\omega)$, in agreement with the result of Fermi. In this way one obtains an expression very similar to that obtained by Halpern-Hall but in which the frequencies ω_1^* and ω_2^*, referring respectively to the discrete spectrum (principally responsible for dispersion and Cerenkov radiation) and to the continuous (principally responsible for ionization) of the atoms of the medium, are separated. Already in this formula one can separate two

contributions proportional to δ_1 and δ_2 referring respectively to the discrete and continuous spectrum.

As is known, the total energy loss (1) contributes both to the Čerenkov radiation and to the excitation and ionization of the atoms of the medium: we now procede to the separation of these contributions.

2. – Čerenkov Radiation.

The Čerenkov radiation is, by definition, formed by energy sent at large distances from the path of the primary particle; thus, choosing $\varrho = \varrho_1 \gg \varrho_0$, and inserting in (1) the asymptotic expressions of the Hankel functions for large arguments, one obtains for it

$$\frac{\partial W_{\varrho_1}}{\partial z}\,(\text{Čer.}) = \tag{16}$$

$$\frac{4\pi e^4 n}{m v^2}\int_{\text{Čerenkov}}\left[\exp\left(-\sqrt{\frac{4\pi e^2 n}{m}}\,\frac{\omega}{v}\,\beta^2\,\mathrm{Im}\,\varepsilon(\omega)\varrho_1\right)\right]\left[\beta^2\,\frac{\mathrm{Re}\,\varepsilon(\omega)}{|\varepsilon(\omega)|^2}\right]\omega\,\mathrm{d}\omega\,,$$

where the integration must be made over those frequencies which satisfy the condition

$$\beta^2\,\mathrm{Re}\,\varepsilon(\omega) - 1 > 0\,. \tag{17}$$

It is more convenient, for our purpose, to separate the integration over the frequencies $\omega < \omega_0$ from the integration over the frequencies $\omega > \omega_0$ with ω_0 = lowest frequency of ionization and therefore, taking account of (6), (16) can also be written

$$\frac{\partial W_{\varrho_1}}{\partial z}\,(\text{Cer.}) = \tag{16'}$$

$$= -\frac{4\pi e^4 n}{m v^2}\int_{\text{Čerenkov}\,<\omega_0}\left[\exp\left(-\sqrt{\frac{4\pi e^2 n}{m}}\,\frac{\omega}{v}\,\beta^2\,\mathrm{Im}_{\text{ecc}}\,\varepsilon(\omega)\varrho_1\right)\right]\left[\beta^2 - \frac{\mathrm{Re}\,\varepsilon(\omega)}{|\varepsilon(\omega)|^2}\right]\omega\,\mathrm{d}\omega +$$

$$+\frac{4\pi e^4 n}{m v^2}\int_{\text{Čerenkov}\,>\omega_0}\left[\exp\left(-\sqrt{\frac{4\pi e^2 n}{m}}\,\frac{\omega}{v}\,\beta^2\,\mathrm{Im}\,\varepsilon(\omega)\varrho_1\right)\right]\left[\beta^2 - \frac{\mathrm{Re}\,\varepsilon(\omega)}{|\varepsilon(\omega)|^2}\right]\omega\,\mathrm{d}\omega\,,$$

where $\mathrm{Im}_{\text{ecc}}\,\varepsilon(\omega)$ represents only the first term of (6).

Clearly, because of the dependence of (16) on ϱ_1, it is impossible to define, in a general way, the Čerenkov radiation observed at distances greater than ϱ_1 without specifing the particular experimental situation. On the other hand,

(16) would be independent of ϱ_1 only if the medium were rigorously non-absorbing [$\operatorname{Im} \varepsilon(\omega) = 0$]. Now, if the ideal condition of a rigorously non-absorbing medium can be approximated in reality in the region of discrete spectrum (low density, temperature, ...) where dispersion is the characteristic feature of $\varepsilon(\omega)$, this is not possible in the region of continuous spectrum where absorption characterizes in an essential way the dielectric behaviour of the medium. This means that it is admissible to put $g_i = 0$ but we must leave in the integral part of the dielectric constant $g \neq 0$; in this way, while in the first term of (16′) the exponential reduces to one, in the second term it is unchanged. Therefore, in the limit $\varrho_1 \to \infty$ and with $g_i = 0$ in (16′), we obtain the following expression for the maximum energy sent as Čerenkov radiation at very large distances from the path:

$$\frac{\partial W}{\partial z}_{(\text{Čer. max.})} = \frac{4\pi e^4 n}{m v^2} \int_{\text{Čerenkov} < \omega_0} \left[\beta^2 - \frac{1}{\varepsilon(\omega)}\right] \omega \, \mathrm{d}\omega \,. \tag{18}$$

3. – Excitation and Ionization.

As shown in a previous work [27] one can quite generally separate from the total energy loss (1) the energy spent in primary excitation and ionization of the atoms of the medium:

$$\frac{\partial W_{\varrho_0}}{\partial z}(\text{exc.} + \text{ion.}) = \frac{4e^4 n}{m v^2} \int_0^\infty \omega \, \frac{\operatorname{Im} \varepsilon(\omega)}{|\varepsilon(\omega)|^2} \left[\log \frac{A}{\omega^2 |1 - \beta^2 \varepsilon(\omega)|} - \beta^2 \operatorname{Re} \varepsilon(\omega)\right] . \tag{19}$$

In order to integrate (19) it is more convenient to put it into the form:

$$\frac{\partial W_{\varrho_0}}{\partial z}(\text{exc.} + \text{ion.}) = \frac{4e^4 n}{m v^2} [P_1 + P_2 + Q] , \tag{20}$$

with:

$$P_1 = \tfrac{1}{2} \operatorname{Re} \int_0^\infty \frac{i\omega \, \mathrm{d}\omega}{\varepsilon(\omega)} \log \frac{A}{\omega^2 [1 - \beta^2 \varepsilon(\omega)]} , \tag{21}$$

$$P_2 = \tfrac{1}{2} \operatorname{Re} \int_0^\infty \frac{i\omega \, \mathrm{d}\omega}{\varepsilon(\omega)} \log \frac{A}{\omega^2 [1 - \beta^2 \varepsilon^*(\omega)]} \tag{21′}$$

$$Q = -\beta^2 \operatorname{Re} \int_0^\infty \frac{i\omega \operatorname{Re} \varepsilon(\omega) \, \mathrm{d}\omega}{\varepsilon(\omega)} , \tag{21″}$$

(27) P. BUDINI: *Nuovo Cimento*, **9**, 236 (1953).

and to procede separately to the integration of the single terms.

3·1. *Integration of P_1 and P_2.* – For this purpose we observe that:

1) The singularities of $[\varepsilon(\omega)]^{-1}$ lay on the upper half of the complex plane. These singularities, as will be shown, are simple poles.

2) In the lower half of the complex plane there is, at most, one singularity of $\log(\omega^2[1-\beta^2\varepsilon(\omega)])$ and this falls on the immaginary axis for $\omega = -i\cdot a$ with a defined by:

$$1-\beta^2\varepsilon(-ia)=0\,. \tag{22}$$

3) Noting that:

$$1-\beta^2\varepsilon(iy)=1-\beta^2\varepsilon^*(-iy)\,, \tag{23}$$

it follows from 2) that the only possible singularity of $\log(\omega^2[1-\beta^2\varepsilon^*(\omega)])$ in the upper half of the complex plane lays on the immaginary axis at $\omega=-i\cdot a$. Therefore it is convenient to calculate P_1 integrating first on the immaginary axis from zero to $-i\cdot a$ and from $-i\cdot a$ to $-i\cdot r$ (later r will go to infinity) and then on a quarter of circle from $-i\cdot r$ to r. P_2 is to be integrated symmetrically to P_1 on the upper half of the complex plane i.e. from zero to $i\cdot a$, from $i\cdot a$ to $i\cdot r$ and from $i\cdot r$ to r; owing to 1) the residua of the integrand at the poles of $[\varepsilon(\omega)]^{-1}$ will contribute to P_2.

We have then:

$$P_1 = P_1' + P_1'' + P_1'''\,, \tag{24}$$

where:

$$P_1' = \tfrac{1}{2}\,\mathrm{Re}\int_0^{-ia}\frac{i\omega\,\mathrm{d}\omega}{\varepsilon(\omega)}\log\frac{A}{\omega^2[1-\beta^2\varepsilon(\omega)]}\,, \tag{25}$$

$$P_1'' = \tfrac{1}{2}\,\mathrm{Re}\int_{-ia}^{-ir}\frac{i\omega\,\mathrm{d}\omega}{\varepsilon(\omega)}\log\frac{A}{\omega^2[1-\beta^2\varepsilon(\omega)]}\,, \tag{25'}$$

$$P_1''' = \tfrac{1}{2}\,\mathrm{Re}\oint_{-ir}^{r}\frac{i\omega\,\mathrm{d}\omega}{\varepsilon(\omega)}\log\frac{A}{\omega^2[1-\beta^2\varepsilon(\omega)]}\,, \tag{25''}$$

and

$$P_2 = P_2' + P_2'' + P_2''' + \tfrac{1}{2}\,\mathrm{Re}\sum_i\left[\mathrm{Residua}\left(\frac{i\omega}{\varepsilon(\omega)}\log\frac{A}{\omega^2[1-\beta^2\varepsilon^*(\omega)]}\right)\right]\,, \tag{26}$$

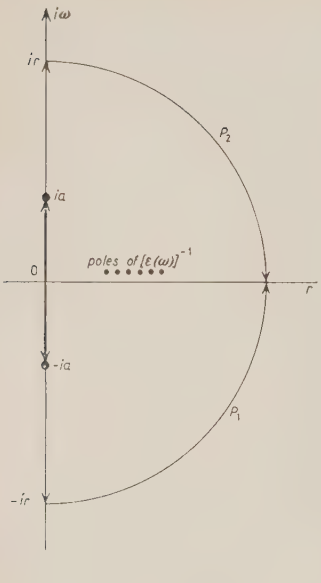

where:

$$(27)\qquad P_2' = \tfrac{1}{2}\,\mathrm{Re}\int_0^{ia}\frac{i\omega\,\mathrm{d}\omega}{\varepsilon(\omega)}\log\frac{A}{\omega^2[1-\beta^2\varepsilon^*(\omega)]}\,,$$

$$(27')\qquad P_2'' = \tfrac{1}{2}\,\mathrm{Re}\int_{ia}^{ir}\frac{i\omega\,\mathrm{d}\omega}{\varepsilon(\omega)}\log\frac{A}{\omega^2[1-\beta^2\varepsilon^*(\omega)]}\,,$$

$$(27'')\qquad P_2''' = \tfrac{1}{2}\,\mathrm{Re}\oint_{ir}^{r}\frac{i\omega\,\mathrm{d}\omega}{\varepsilon(\omega)}\log\frac{A}{\omega^2[1-\beta^2\varepsilon^*(\omega)]}\,.$$

Now, as one can easily verify, $P_1' = P_2' = 0$ because the integrands are immaginary inside the interval of integration.

$P_1'' + P_2''$ is a monotonically decreasing function of a; its maximum value, obtainedf or $a = 0$, is given by:

$$(28)\qquad (P_1'' + P_2'')_{\max} = \frac{\pi^2}{4}\left\{\sum_{i=1}^{n}\frac{f_i g_i}{\omega_i} + g\sum_{k=1}^{z}\int_{\omega_k}^{\infty}\frac{f_k(\omega')\,\mathrm{d}\omega'}{\omega'}\right\},$$

while it vanishes for $a \to \infty$. Therefore, owing to the very small values of g_i and g, it is possible to neglect $P_1'' + P_2''$ without appreciable error.

In $P_1''' + P_2'''$ we put $\omega = r\exp[i\varphi]$ and obtain:

$$P_1''' + P_2''' = -\int_{\pi/2}^{0}\mathrm{d}\varphi\,\frac{r^2\exp[2i\varphi]}{\varepsilon(r,\varphi)}\log\frac{A}{r^2\exp[2i\varphi][1-\beta^2\varepsilon(r,\varphi)]}$$

$$-\int_{\pi/2}^{0}\mathrm{d}\varphi\,\frac{r^2\exp[2i\varphi]}{\varepsilon(r,\varphi)}\log\frac{A}{r^2\exp[2i\varphi][1-\beta^2\varepsilon^*(r,\varphi)]} =$$

$$= \int_0^{\pi}\mathrm{d}\varphi\left\{\frac{r^2\exp[2i\varphi]}{\varepsilon(r,\varphi)}\log\frac{A}{r^2\exp[2i\varphi][1-\beta^2\varepsilon^*(r,\varphi)]}\right.$$

$$\left.-\frac{r^2\exp[-2i\varphi]}{\varepsilon(r,-\varphi)}\log\frac{A}{r^2\exp[-2i\varphi][1-\beta^2\varepsilon(r,-\varphi)]}\right\},$$

now since r is very large we have

$$\text{Re } \varepsilon(r, \varphi) = \text{Re } \varepsilon(r, -\varphi) = \text{Re } \varepsilon^*(r, \varphi) ,$$

$$\text{Im } \varepsilon(r, \varphi) = \text{Im } \varepsilon^*(r, \varphi) \quad = -\text{Im } \varepsilon(r, -\varphi) .$$

Then the two terms of the integrand are complex conjugate to each other and

$$\text{Re } (P_1''' + P_2''') = 0 .$$

In conclusion:

$$P_1 + P_2 = \tfrac{1}{2} \text{ Re } \sum \left[\text{Residua} \left(\begin{matrix} i\omega \\ \varepsilon(\omega) \end{matrix} \log \frac{A}{[1 - \beta^2 \varepsilon^*(\omega)]} \right) \right] . \tag{29}$$

3·2. *Integration of Q.* – In this case we must take into account that the singularities of the integrand are the poles of $[\varepsilon(\omega)]^{-1}$ which lie, as already mentioned, in the upper half of the complex plane and the poles of Re $\varepsilon(\omega)$ corresponding to $\omega_i^2 - \omega^2 - ig\omega = 0$ which obviously lie in the lower half. For this reason it is convenient to integrate (21″) in the same way as for P_2. Then one can easily demonstrate that all the contributions of the integration on the immaginary axis and on the circle vanish identically and therefore only the residua of the integrand function remain which are at the poles of $[\varepsilon(\omega)]^{-1}$ in the upper half of the complex plane i.e.:

$$Q = -\beta^2 \text{ Re } \sum \left[\text{ Residua} \left(\frac{i\omega \text{ Re } \varepsilon(\omega)}{\varepsilon(\omega)} \right) \right] . \tag{30}$$

Taking into account (29) one finds the following expression for the energy loss for primary excitation and ionization:

$$-\frac{\partial W_{e_0}}{\partial z} \text{ (exc. + ion.)} = \tag{31}$$

$$= \frac{2e^4 n}{mv^2} \text{ Re } \sum \left[\text{Residua} \left\{ \frac{i\omega}{\varepsilon(\omega)} \left| \log \frac{A}{\omega^2 [1 - \beta^2 \varepsilon^*(\omega)]} - 2\beta^2 \text{ Re } \varepsilon(\omega) \right| \right\} \right] .$$

In order to calculate (31) explicitely it is necessary to localize the zeros of $\varepsilon(\omega)$. We make the simplifying assumption:

$$g_i = g = g_0 ,$$

it can be shown that this hypothesis is not essential and that the following arguments can be extended to the general case $g_i \neq g_0$. In order to unify

the calculations for the discrete and continuous spectrum, and considering that $f_k(\omega')$ are wellbehaved functions, we put

$$\varepsilon(\omega) = 1 + \sum_{\nu} \frac{f_\nu \Delta\omega_\nu}{\omega_\nu^2 - \omega^2 + i g_0 \omega} , \tag{32}$$

with $\Delta\omega_\nu = 1$ for the discrete and $f_\nu \Delta\omega_\nu \to f_k(\omega')\,\mathrm{d}\omega' = (mc/2\pi^2 e^2)\sigma_k(\omega')\,\mathrm{d}\omega'$ as $\Delta\omega_\nu$ tends to zero, for the continuous.

Then one can easy see that, in each band of the complex plane parallel to the immaginary axis and delimited by the frequencies ω_ν and $\omega_{\nu+1}$ there is a simple zero of $\varepsilon(\omega)$ at the point

$$\bar{\omega}_\nu = x_\nu + \frac{i}{2} g_0 , \tag{33}$$

with x_ν with good approximation only depending on ω_ν, f_ν and given by

$$x_\nu^2 = \omega_\nu^2 - \frac{g_0^2}{4} + f_\nu \Delta\omega_\nu \quad (*) . \tag{34}$$

The residua which appear in (31) can be then easily calculated: one finds on taking into account that $\mathrm{Re}\,\varepsilon(\bar{\omega}_\nu) = \frac{1}{2}\varepsilon^*(\bar{\omega}_\nu)$

$$\begin{aligned} (35)\quad \frac{\partial W_{\varrho_0}}{\partial z}(\mathrm{exc.}+\mathrm{ion.}) &= \frac{2e^4 n}{mv^2}\,\mathrm{Re}\sum_\nu \frac{2\pi\bar{\omega}_\nu}{(\mathrm{d}\varepsilon/\mathrm{d}\omega)_{\omega=\bar{\omega}_\nu}}\left[\log\frac{A}{\bar{\omega}_{\nu\lfloor}^2 1 - \beta^2\varepsilon^*(\bar{\omega}_\nu)]} - \beta^2\varepsilon^*(\bar{\omega}_\nu)\right] - \\ &= \frac{2\pi e^4 n}{mv^2}\,\mathrm{Re}\sum_\nu \sum_i f_i \Delta\omega_i/(\omega_i^2 \quad \frac{1}{\bar{\omega}_\nu^2 \quad f_\nu \Delta\omega_i)^2}\left[\log\frac{A}{\bar{\omega}_{\nu\lfloor}^2 1 \quad \beta^2\varepsilon^*(\bar{\omega}_\nu)]} \quad \beta^2\varepsilon^*(\bar{\omega}_\nu)\right] = \\ &= \frac{2\pi e^4 n}{mv^2}\,\mathrm{Re}\sum_\nu f_\nu \Delta\omega_\nu\left[\log\frac{A}{\bar{\omega}_{\nu\lfloor}^2 1 - \beta^2\varepsilon^*(\bar{\omega}_\nu)]} \quad \beta^2\varepsilon^*(\bar{\omega}_\nu)\right] . \end{aligned}$$

The last step is a good approximation for the discrete spectrum and is exact for the continuous which is of interest for the present work. Going to the limit for $\Delta\omega_\nu \to 0$ in (35) and separating the residua in the discrete spectrum from those in the continuous, one finally obtains:

$$\begin{aligned} (36)\quad \frac{\partial W_{\varrho_0}}{\partial z}(\mathrm{exc.}+\mathrm{ion.}) &= \frac{2\pi e^4 n}{mv^2}\,\mathrm{Re}\sum_{i=1}^{n} f_i\left[\log\frac{A}{\bar{\omega}_{i\lfloor}^2 1 \quad \beta^2\varepsilon^*(\bar{\omega}_i)]} - \beta^2\varepsilon^*(\bar{\omega}_i)\right] + \\ &+ \frac{2\pi e^4 n}{mv^2}\,\mathrm{Re}\sum_{k=1}^{z}\int_{\omega_k}^{\infty} f_k(\omega')\,\mathrm{d}\omega'\left[\log\frac{A}{\omega'^2\lfloor 1 - \beta^2\varepsilon^*(\bar{\omega}')]} - \beta^2\varepsilon^*(\bar{\omega}')\right] . \end{aligned}$$

(*) A further approximation brings about a factor $(1+\Sigma_\nu')^{-1}$ with Σ_ν' given by (39) to multiply $f_\nu \Delta_\nu$ in (34) (see also note on page 38).

Clearly the first term on the right hand side represents the energy spent in excitation, and the second term in ionization. For a more detailed study we will discuss the two parts of (37) separately.

4. – Excitation.

From (36) we see that the behaviour of the energy loss in excitation as well as in ionization at relativistic energy depends critically on the values of $\varepsilon^*(\omega)$ at the points $\bar{\omega}_i$ where $\varepsilon(\omega)$ vanishes. From the discrete part of the spectrum one can easily get, inserting (33) in $\varepsilon^*(\omega)$:

$$\varepsilon^*(\bar{\omega}_i) = \frac{\theta_i^2(1+\Sigma_i')^3}{1+\theta_i^2(1+\Sigma_i')^2} + i\,\frac{\theta_i(1+\Sigma_i')^2}{1+\theta_i(1+\Sigma_i')^2}\,, \tag{37}$$

with

$$\theta_i = \frac{2g_0\omega_i}{f_i} \quad (*)\,, \tag{38}$$

and

$$\Sigma_\nu' = \sum_{j\neq\nu} \frac{f_j \Delta\omega_j}{\omega_j^2 - \omega_\nu^2}\,, \tag{39}$$

which are of the same form as (41) and (46) of reference [27] (+).

The energy spent in excitation is then given by

$$\frac{\partial W_{e_0}}{\partial z}\,(\text{exc.}) = -\frac{2\pi e^4 n}{mv^2}\cdot\sum_i f_i \left[\log \frac{A}{\omega_i^2\left\{\left[1-\dfrac{\beta^2\theta_i^2}{1+\theta_i^2}(1+\Sigma_i')\right]^2+\left[\dfrac{\beta^2\theta_i}{1+\theta_i^2}(1+\Sigma_i')\right]^2\right\}^{\frac{1}{2}}} - \beta^2\frac{\theta_i^2(1+\Sigma_i')^3}{1+\theta_i^2(1+\Sigma_i')^2} + \frac{g}{2}\frac{1}{x_i}\,\mathrm{tg}^{-1}\frac{\beta^2\theta_i(1+\Sigma_i')}{1+\theta_i^2+(1+\Sigma_i')\beta^2\theta_i^2}\right]. \tag{41}$$

(*) In the general case ($g_i \neq g_0$) one would have obtained

$$\theta_i = \frac{2g_i\omega_i}{p_i}\,. \tag{40}$$

(+) Actually the θ_i in (38) differ from the corresponding of reference [27] by a factor 2. This depends on the method developed for the calculation in [27]. In fact this method consisted in evaluating the integral (34) with the mean value theorem and taking the integral function in square brackets of (34) at the maxima of $\sigma_i/|\varepsilon|^2$. Now, in this evaluation the errors are of the order of g_i/ω_i as one can see, for example, on comparing (40) of [27] with (33) of this paper. This gives the factor $\frac{1}{2}$ in the θ_i as compared with the exact calculation followed here. In any case this factor is unimportant in the general discussion and in the final formula it would imply a factor 2 in the arguments of the logarithm in (53) of [27].

The important difference between (41) and the corresponding expression of reference ([27]) lays in the fact that in (41) $\sum_{i=1}^{n} f_i < 1$; that is in (41) proper account is taken of the fact that excitation refers to the discrete spectrum of the atoms. The term in $\tan^{-1}$ in (41) is very small and can be dropped.

For the discussion on the energy spent in excitation it then follows, as in Sect. 4 of reference ([27]), that the relativistic increase of this energy is in competition with the energy spent in Čerenkov radiation and depends on the ratio θ_i (which contains g_i/density of the medium); for $\theta_i \ll 1$ one has no relativistic increase in excitation and (41) becomes

$$\frac{\partial W_{\varrho_0}}{\partial z}\,(\text{exc.}) = \frac{2\pi e^4 n}{mv^2} \sum_{i=1}^{n} f_i \log \frac{mv^2}{\pi n \omega_i^2 \varrho_0^2 e^2}\,. \tag{42}$$

5. – Ionization.

For the continuous one obtains for $\varepsilon^*(\omega')$ appearing in (37), dropping terms of the order g^2/ω^2 with respect to 1,

$$\varepsilon^*(\overline{\omega}') = 1 + \Sigma''(\omega') + \sum_{k=1}^{z} \int_{\omega_k}^{\infty} \frac{f_k(\omega)\,\mathrm{d}\omega}{\omega^2 - \omega'^2 - 2ig\omega'}\,, \tag{43}$$

where

$$\Sigma''(\omega') = \sum_i \frac{f_i}{\omega_i^2 - \omega'^2}\,, \tag{44}$$

and therefore for $\omega' - \omega_k \gg g$ (which is the only important case in applications):

$$|1 - \beta^2 \varepsilon^*(\overline{\omega}')| = \{[1 - \beta^2\,\mathrm{Re}\,\varepsilon(\omega')]^2 + [\beta^2\,\mathrm{Im}\,\varepsilon(\omega')]^2\} = |1 - \beta^2 \varepsilon(\omega')|\,. \tag{45}$$

We get also the following formula for the ionization loss:

$$\frac{\partial W_{\varrho_0}}{\partial z}\,(\text{ion. prim.}) = \tag{46}$$

$$= \frac{2\pi e^4 n}{mv^2} \sum_{k=1}^{z} \int_{\omega_k}^{\infty} f(\omega')\,\mathrm{d}\omega' \left| \log \frac{A}{\omega'^2 |1 - \beta^2 \varepsilon^*(\overline{\omega}')|} - \beta^2\,\mathrm{Re}\,\varepsilon^*(\omega') \right|,$$

with $|1 - \beta^2 \varepsilon^*(\overline{\omega}')|$ given by (45).

Considering that the integrand of (46) is a wellbehaved function of ω' and

that $f_k(\omega')$ is rapidly decreasing in the interval of integration, one can apply the mean value theorem and so obtains, taking account of (45),

$$(47) \qquad \frac{\partial W_{\varrho_0}}{\partial z}\,(\text{ion. prim.}) = \frac{2\pi e^4 n}{mv^2}\sum_{k=1}^{z} f_k \left[\log \frac{A}{\tilde{\omega}_k\,|1-\beta^2\varepsilon(\tilde{\omega}_k)|} - \beta^2\,\mathrm{Re}\,\varepsilon(\tilde{\omega}_k)\right],$$

where $\tilde{\omega}_k$ is an opportune mean value.

The saturation limit for $\beta^2 = 1$ is given by

$$(47') \qquad \frac{\partial W_{\varrho_0}}{\partial z}\,(\text{ion. prim.})\,(\beta^2=1) = \frac{2\pi e^4 n}{mv^2}\sum_{k=1}^{z} f_k \left[\log \frac{A}{\tilde{\omega}_k\,|1-\varepsilon(\tilde{\omega}_k)|} - \mathrm{Re}\,\varepsilon(\tilde{\omega}_k)\right].$$

We can conclude then that, in the case of ionization loss there always exists a relativistic increase whose maximum value depends essentially on $|1-\varepsilon(\tilde{\omega}_k)|$ which, in the general case, is very different from 1.

The analytical integration of (46) (or exact calculation of $\tilde{\omega}_k$) is difficult in the general case owing to the complicated form of the integrand. An attempt to integrate (46) for the simplest cases and numerical results will be given in a future paper.

6. – Connection with Energy Loss for Close Collisions.

The preceeding considerations, based on the statistical description of the medium, are valid for ϱ_0 (collision parameter) larger than the radius of the atoms of the medium. For smaller collision parameters one can ignore the polarizability of the medium and then the energy loss with energy transfers smaller than T is given by ([8])

$$(48) \qquad \frac{\partial W}{\partial z}\Big|_{<\varrho_0} = \frac{2\pi e^4 n}{mv^2}\log\frac{mT\varrho_0^2\gamma^2}{2\hbar^2}.$$

This can be added to (14) giving rise to the total energy loss suffered by a relativistic ionizing particle in a medium, i.e.:

$$(49) \qquad \frac{\partial W}{\partial z} = \frac{2\pi e^4 n}{mv^2}\left[\log\frac{B\cdot T}{(\omega_1^{*\delta_1}\cdot\omega_2^{*\delta_2})^2(1-\beta^2)} + a^2(1-\beta^2) - \beta^2\right],$$

where

$$(50) \qquad B = \frac{m^2v^2}{2\pi m e^2\hbar^2}.$$

Now, from the formulas of the preceeding paragraphs one has that, as far

as the dependence of the energy loss on ϱ_0 is concerned, we can write (*)

$$(51) \qquad \left.\frac{\partial W}{\partial z}\right|_{>\varrho_0} (\text{exc.}) = \frac{2\pi e^4 n}{mv^2}\,\delta_1 \log \varrho_0^2 + \text{terms independent of } \varrho_0\,,$$

$$(52) \qquad \left.\frac{\partial W}{\partial z}\right|_{>\varrho_0} (\text{ion. prim.}) = \frac{2\pi e^4 n}{mv^2}\,\delta_2 \log \varrho_0^2 + \text{terms independent of } \varrho_0\,.$$

If we sum (48) with (51) and (52) and remember (13′), the terms containing ϱ_0 eliminate and we obtain that the energy totally spent in excitation and ionization in collisions with any collision parameter does not depend on ϱ_0 as is to be expected and as results from (49) taking into account that the Čerenkov energy loss does not depends on ϱ_0.

Summing (36) and (48) we thus obtain

$$(53) \qquad \frac{\partial W}{\partial z}(\text{exc.} + \text{ion.}) = \frac{2\pi e^4 n}{mv^2}\,\text{Re}\sum_{i=1}^{n} f_i \left[\log \frac{BT}{\bar{\omega}_i^2[1 - \beta^2\varepsilon^*(\bar{\omega}_i)]} - \beta^2\varepsilon^*(\bar{\omega}_i)\right] +$$

$$+ \frac{2\pi e^4 n}{mv^2}\,\text{Re}\sum_{k=1}^{z}\int_{\omega_k}^{\infty} f_n(\omega')\,\mathrm{d}\omega' \left[\log \frac{BT}{\omega'^2[1 - \beta^2\varepsilon^*(\bar{\omega}_i')]} - \beta^2\varepsilon^*(\bar{\omega}')\right].$$

In order to separate the contributions of excitation and ionization from this expression let us also multiply and divide the arguments of the logarithms

---

(*) If one takes account of the correction referred in the note at p. 34 then in place of δ_1 and δ_2 in (51) and (52) should appear:

$$\delta_1' = \sum_{i=1}^{n} \frac{f_i}{(1 + \Sigma_i')^2} \qquad \text{and} \qquad \delta_2' = \sum_{k=1}^{z}\int_{\omega_k}^{\infty} \frac{f(\omega')\,\mathrm{d}\omega'}{[1 + \Sigma_k'(\omega')]^2}\,.$$

Now, it can be easily seen that Σ' are small and of alternate signs such that the property $\delta_1' + \delta_2' = 1$ is maintained with good approximation. Thus, the sum of (51) and (52) joins continuously with (48) for small ϱ_0. On the other hand, the energy spent at small ϱ_0 in excitation and ionization or in excitation of a single line has a ϱ_0-dependence which, at first sight, should be not expected from the theory of Bohr (for $\varrho_0 <$ radius of the atoms of the medium) where the polarizability of the medium is not taken into account. In fact, the energy absorbed from the atoms at small distances is independent of ϱ_0 but there are grounds to expect that the subsequent repartition of this energy in excitation of a single line and ionization, does depend on the polarizability of the medium ([20]). This is still an open problem.

in each term of the first sum in (53) by I_k, the ionization of the electron to which the f_i refers (*).

We obtain

$$(54)\qquad \frac{\partial W}{\partial z}(\text{exc.} + \text{ion.}) = -\frac{2\pi e^4 n}{mv^2}\,\mathrm{Re}\sum_{i=1}^{n} f_i\left[\log\frac{B\cdot I_k}{\omega_i^2[1-\beta^2\varepsilon^*(\bar\omega_i)]} - \beta^2\varepsilon^*(\omega_i)\right] -$$

$$+\frac{2\pi e^4 n}{mv^2}\sum_{i=1}^{n} f_i\log\frac{T}{I_k} + \frac{2\pi e^4 n}{mv^2}\,\mathrm{Re}\sum_{k=1}^{z}\int_{\omega_k}^{\infty} f_k(\omega')\,\mathrm{d}\omega'\left[\log\frac{BT}{\omega'^2[1-\beta^2\varepsilon^*(\bar\omega')]} - \beta^2\varepsilon^*(\bar\omega')\right].$$

Clearly then, only the first term is to be interpreted as energy spent in excitation as it implies collisions with energy transfers smaller than the ionization energies of the various shells. The second sum contributes to ionization so long as $T > I_k$, as it implies collisions with energy transfers larger than the ionization energy (+).

We obtain thus for energy spent in excitation

$$(55)\qquad \frac{\partial W}{\partial z}(\text{exc.}) = \frac{2\pi e^4 n}{mv^2}\sum_{i=1}^{n} f_i\left[\log\frac{B\cdot I_k}{\omega_i^2|1-\beta^2\varepsilon^*(\bar\omega_i)|} - \beta^2\,\mathrm{Re}\,\varepsilon^*(\bar\omega_i)\right],$$

where $\varepsilon^*(\bar\omega_i)$ is given by (39).

The energy spent in ionization with energy transfers smaller than T is given by:

$$(56)\qquad \frac{\partial W}{\partial z}(\text{ion. prim.}) = \frac{2\pi e^4 n}{mv^2}\sum_{i=1}^{n} f_i\log\frac{T}{I_k} +$$

$$-\frac{2\pi e^4 n}{mv^2}\sum_{k=1}^{z}\int_{\omega_k}^{\infty} f(\omega')\,\mathrm{d}\omega'\left[\log\frac{BT}{\omega'^2|1-\beta^2\varepsilon^*(\omega')|} - \beta^2\,\mathrm{Re}\,\varepsilon^*(\bar\omega')\right] -$$

$$=\frac{2\pi e^4 n}{mv^2}\left\{\log\frac{T}{\bar I_0} + \sum_{k=1}^{z}\int_{\omega_k}^{\infty} f(\omega')\,\mathrm{d}\omega'\left[\log\frac{BI_k}{\omega'^2|1-\beta^2\varepsilon^*(\bar\omega')|} - \beta^2\,\mathrm{Re}\,\varepsilon^*(\omega')\right]\right\},$$

where $\varepsilon^*(\bar\omega')$ is given by (43) and $\bar I_0$ by

$$(57)\qquad \bar I_0 = I_1^{\bar f_1}\cdot I_2^{\bar f_2}\ldots I_z^{\bar f_z},$$

(*) Rigorously f_i as well as ω_i should carry two indices i.e. f_{ik} and ω_{ik}, the one referring to the various absorption lines of a single electron and the other referring to the various electrons. In order to avoid this formal complication we keep a single index for f_i and ω_i but one should take account of the fact that the indices k of I_k vary only when f_i and ω_i in the sum refer to different electrons.

(+) If $T < I_k$ it would contribute negatively to excitation but in the following we will consider only the case $T > I_k$.

where

$$\bar{f}'_k = \bar{f}_k + f_{k_1} + f_{k_2} + \ldots + f_{k_z}, \tag{58}$$

and $f_{k1}, f_{k2}, f_{k3}, \ldots f_{kz}$ are the oscillator strength of the absorption lines referring to the K^{th} electron. Clearly then:

$$\sum_k \bar{f}'_k = \delta_1 + \delta_2 = 1 . \tag{59}$$

In applications one may be interested in the energy lost in collisions in which the electrons come out from the ionized atom with energy larger than a minimum energy τ. One has than simply to substitute $I_k + \tau$ for the ionization energy I_k and thus obtains

$$\frac{\partial W}{\partial z}\,(\text{ion. prim.}) = \frac{2\pi e^4 n}{mv^2} \log \frac{T}{(\overline{I_0 + \tau})} + \tag{60}$$

$$+ \frac{2\pi e^4 n}{mv^2} \sum_{k=1}^{z} \int_{\omega_k + \tau/\hbar}^{\infty} f(\omega')\,\mathrm{d}\omega' \left[\log \frac{B(I_k + \tau)}{\omega'^2 \left| 1 - \beta^2 \varepsilon^*(\overline{\omega}') \right|} - \beta^2 \operatorname{Re} \varepsilon^*(\overline{\omega}') \right],$$

where

$$\overline{I_0 + \tau} = (I_1 + \tau)^{\bar{f}'_1} (I_2 + \tau)^{\bar{f}'_2} \ldots (I_z + \tau)^{\bar{f}'_z} . \tag{61}$$

7. – Calculation of the Number of Ions.

Until now we have only treated the problem of the energy loss of the ionizing particle. The formulas of the energy loss are, however, not the most convenient for comparison with experimental results where the number of ions is the most important datum. In fact, one can easily verify that the maximum transferable energy T plays in (56) a critical role especially for those elements for which $\delta_1 \ll \delta_2$, that is for all but the lightest ones. Now, if it is to be expected that the rare collisions with large energy transfer T play an important role in the problem of the total energy loss and give rise to the well known problem of fluctuations ([15]), these collisions are certainly not determinant for the problem of the number of ions, and so that parameter T should not enter critically in the formula to be compared with specific ionization.

We will therefore try to give a method to be applied directly to the calculation of the number of ions. With this aim in view we start from the following expression

$$\frac{\partial N_{e_0}}{\partial z}\,(\text{ion.} + \text{exc.}) = \frac{4e^4 n}{mv^2\hbar} \operatorname{Re} \int_0^{\infty} \frac{i\,\mathrm{d}\omega}{\varepsilon(\omega)} \left[\log \frac{A}{\omega^2 \left| 1 - \beta^2 \varepsilon(\omega) \right|} - \beta^2 \operatorname{Re} \varepsilon(\omega) \right], \tag{62}$$

obtained by dividing the integrand of (19) by $\hbar\omega$, and which gives the number of events (ionization + excitation) produced by a relativistic particle in collisions with collision-parameter larger than ϱ_0. Putting (62) in the form:

$$\frac{\partial N_{\varrho_0}}{\partial z}\,(\text{ion.} + \text{exc.}) = \frac{4e^4 n}{mv^2\hbar}\,[P_1 + P_2 + Q]\,, \tag{63}$$

with:

$$P_1 = \tfrac{1}{2}\,\mathrm{Re}\int_0^\infty \frac{i\,\mathrm{d}\omega}{\varepsilon(\omega)}\log\frac{A}{\omega^2[1-\beta^2\varepsilon(\omega)]}\,, \tag{64}$$

$$P_2 = \tfrac{1}{2}\,\mathrm{Re}\int_0^\infty \frac{i\,\mathrm{d}\omega}{\varepsilon(\omega)}\log\frac{A}{\omega^2[1-\beta^2\varepsilon^*(\omega)]}\,, \tag{64'}$$

$$Q = -\beta^2\,\mathrm{Re}\int_0^\infty \frac{i\,\mathrm{Re}\,\varepsilon(\omega)\,\mathrm{d}\omega}{\varepsilon(\omega)}\,. \tag{64''}$$

We proceed separately to the integration in the complex plane of the single terms (64) on the same line as for the energy loss: this is possible because the integrands of (64) present the same poles as the integrands of (21). In this way, maintaining the same meaning for the symbols as in the integration of energy loss, we can also in this case write

$$\begin{cases} P_1 = P_1' + P_1'' + P_1'''\,, \\ P_2 = P_2' + P_2'' + P_2''' + \tfrac{1}{2}\,\mathrm{Re}\sum_i\left[\text{Residua}\left(\frac{i}{\varepsilon(\omega)}\log\frac{A}{\omega^2[1-\beta^2\varepsilon^*(\omega)]}\right)\right]. \end{cases} \tag{65}$$

One obtains

$$\begin{aligned} P_1' + P_2' + P_1'' + P_2'' = \\ = \sum_{i=1}^{n} f_i \int_0^r \frac{g_i y\,\mathrm{d}y}{(\omega_i^2 + y^2) - g_i^2 y^2}\log\frac{A}{|y^2[1-\beta^2\varepsilon^*(iy)]|} + \\ + \sum_{k=1}^{z}\int_{\omega_k}^\infty f_k(\omega_j)\,\mathrm{d}\omega_j \int_0^r \mathrm{d}y\,\frac{gy\log\left(A/|y^2[1-\beta^2\varepsilon^*(iy)]|\right)}{(\omega_j^2 + y^2)^2 - g^2y^2}\,. \end{aligned} \tag{66}$$

In order to calculate the order of magnitude of these terms, we will sim-

plify the expression for $\varepsilon^*(y)$ by putting it in the following form:

$$\varepsilon^*(iy) = 1 + \frac{\varepsilon^*(0) - 1}{1 + y^2} . \tag{67}$$

In this way, taking into account that the integrand function has poles for $1 - \beta^2\varepsilon^*(iy) = 0$ i.e. at the point

$$a = \left[\frac{\beta^2\varepsilon^*(0) - 1}{A - \beta^2}\right]^{\frac{1}{2}} ,$$

(66) becomes

$$P_1' + P_2' + P_1'' + P_2'' = \tfrac{1}{2}\sum_{i=1}^{n} f_i \frac{g_i}{\omega_i^2}\left[\log\frac{A}{\beta^2\varepsilon^*(0) - 1} - \frac{\omega_i^2}{\omega_i^2 + a^2}\log\frac{\omega_i^2}{a^2}\right] + \tag{68}$$

$$+ \tfrac{1}{2}\sum_{k=1}^{z} g \int_{\omega_k}^{\infty} \frac{f_k(\omega_j)\,\mathrm{d}\omega_j}{\omega_j^2}\left[\log\frac{A}{\beta^2\varepsilon^*(0) - 1} - \frac{\omega_j^2}{\omega_j^2 + a^2}\log\frac{\omega_j^2}{a^2}\right] .$$

It will result obvious later that this term is to be neglected with respect to the other because the smallness of the constants g_i and g.

We find further

$$P_1''' + P_2''' = 0 , \tag{69}$$

and

$$Q = -\beta^2 \operatorname{Re}\sum_i \left[\text{Residua}\left(\frac{i \operatorname{Re}\varepsilon(\omega)}{\varepsilon(\omega)}\right)\right] , \tag{70}$$

thus

$$\frac{\partial N_{\varrho_0}}{\partial z}\,(\text{ion.} + \text{exc.}) = \tag{71}$$

$$- \frac{2e^4 n}{mv^2\hbar} \operatorname{Re}\sum_i \left[\text{Residua}\left\{\frac{i}{\varepsilon(\omega)}\left(\log\frac{A}{\omega^2[1 - \beta^2\varepsilon^*(\omega)]} - 2\beta^2 \operatorname{Re}\varepsilon(\omega)\right)\right\}\right] .$$

Taking into account (33) and (34), (71) becomes:

$$\frac{\partial N_{\varrho_0}}{\partial z}\,(\text{exc.} + \text{ion.}) = -\frac{2\pi e^4 n}{mv^2\hbar}\sum_{i=1}^{n}\frac{f_i}{\omega_i} \cdot \tag{72}$$

$$\cdot\left[\log\frac{A}{\omega_i^2\sqrt{(1 - \beta^2(\theta_i^2/1 + \theta_i^2)(1 + \Sigma_i')^2)^2 + (\beta^2(\theta_i/1 + \theta_i^2)(1 + \Sigma_i'))^2}} - \beta^2\frac{\theta_i^2(1 + \Sigma_i')^3}{1 + \theta_i^2(1 + \Sigma_i')^2}\right] -$$

$$- \frac{2\pi e^4 n}{mv^2\hbar}\sum_{k=1}^{z}\int_{\omega_k}^{\infty}\frac{f(\omega')\,\mathrm{d}\omega'}{\omega'}\left[\log\frac{A}{\omega'^2\,|1 - \beta^2\varepsilon^*(\overline{\omega}')|} - \beta^2 \operatorname{Re}\varepsilon^*(\overline{\omega}')\right] ,$$

where $\varepsilon^*(\overline{\omega}')$ is given by (43).

Clearly the first term on the right hand side represents the number of excitated atoms and the second term the number of ions produced per unit length by the primary particle at a distance larger than ϱ_0 from its trajectory. The second term is of importance for comparison with experimental data on ionization and therefore we will concentrate our attention on it in the following.

Here also we have to connect formula (72) with the number of events generated by the particle at close distances. For this purpose we differentiate (48) with respect to T and obtain:

$$\mathrm{d}\left(\frac{\partial W}{\partial z}\bigg|_{<\varrho_0}\right) = \frac{2\pi e^4 n}{mv^2}\,\frac{1}{T}\,\mathrm{d}T\,. \tag{73}$$

This is the well known formula (5) representing the mean energy loss per cm per interval $\mathrm{d}T$ of the transfered energy T for large values of T (so long as the energy of the ionizing particle $\gg T$). In order to re-obtain (48), we have to integrate (73) between the limits T_0 and T with:

$$T_0 = \frac{2\hbar^2}{m\varrho_0^2\gamma^2}\,. \tag{74}$$

We thus obtain a relation between ϱ_0 and T_0. Remembering that T_0 is the minimum transferable energy in close collisions we can take for T_0 the mean ionization energy of the atom, or better still for each electron its ionization energy.

In order to obtain the number of ions created in collisions at close distances ($< \varrho_0$) we have only to divide (73) by T and to integrate it between T_0 and T:

$$\frac{\partial N}{\partial z}_{<\varrho_0} = \frac{2\pi e^4 n}{mv^2}\int_{T_0}^{T}\frac{\mathrm{d}T}{T^2} = \frac{2\pi e^4 n}{mv^2}\left(\frac{1}{T_0}-\frac{1}{T}\right), \tag{75}$$

ϱ_0 can now be eliminated also from (72) with the substitution (74). Summing with (75) the formula obtained in this way, and putting in each term of the sum $T_0 = I_k$, ionization energy of the corresponding electron (correspondingly we must substitute $\sum_k \bar{f}_k'/I_k$ for $1/T_0$ in (75)), we obtain:

$$\frac{\partial N}{\partial z}\,(\text{ion.}) = \frac{2\pi e^4 n}{mv^2}\sum_{k=1}^{z}\left\{\frac{\bar{f}_k'}{I_k}-\frac{1}{T}+\right. \tag{76}$$

$$\left.+\int_{\omega_k'}^{\infty}\frac{f(\omega')\,\mathrm{d}\omega'}{\hbar\omega'}\left[\log\frac{BI_k}{\omega'^2\,|1-\beta^2\varepsilon^*(\bar{\omega}')|}-\beta^2\,\mathrm{Re}\,\varepsilon^*(\bar{\omega}')\right]\right\}.$$

In general, $T \gg I_k$ and therefore the number of ions will be independent of the maximum transferable energy T as is to be expected.

In particular cases the integral appearing in (76) can be explicitely integrated; in general the mean value theorem can be applied and one obtains:

$$(77) \qquad \frac{\partial N}{\partial z}\,(\text{ion.}) = \frac{2\pi e^4 n}{m v^2} \sum_{k=1}^{z} \left\{ \frac{\bar{f}'_k}{I_k} - \frac{1}{T} + \right.$$

$$\left. + \frac{\bar{f}_k}{\hbar\tilde{\omega}_k}\left[\log \frac{B \cdot I_k}{\tilde{\omega}_k^2 \,|\, 1 - \beta^2 \varepsilon(\tilde{\omega}_k)|} - \beta^2 \,\mathrm{Re}\, \varepsilon(\tilde{\omega}_k)\right]\right\}.$$

This formula shows that the number of ions presents a logarithmic increase and a subsequent saturation because of the polarizability of the medium.

In this case also one may be interested in the number of ions in which the electron comes out with energy larger than a minimum energy τ. One has then simply to substitute in the preceeding formula the ionization energy I_k by $I_k + \tau$:

$$(78) \qquad \left.\frac{\partial N}{\partial z}\,(\text{ion.})\right|_{>\tau} = \frac{2\pi e^4 n}{m v^2} \sum_{k=1}^{z} \left\{ \frac{\bar{f}'_k}{I_k + \tau} - \frac{1}{T} + \right.$$

$$\left. + \int_{\omega_k + \tau/\hbar}^{\infty} \frac{f(\omega')\,\mathrm{d}\omega'}{\hbar\omega'}\left[\log \frac{B \cdot (I_k + \tau)}{\omega'^2 \,|\, 1 - \beta^2 \varepsilon^*(\bar{\omega}')|} - \beta^2 \,\mathrm{Re}\, \varepsilon^*(\bar{\omega}')\right]\right\}.$$

As τ increases, the terms with the integrals will, in general decrease faster than the corresponding terms in the sum since $f(\omega')$ behaves as ω'^{-n} where $n > 1$; on the other hand the $\varepsilon(\omega)$ inside the logarithm will be calculated for larger values of the argument ω at which $\varepsilon(\omega)$ will become very near to one; thus the integral term will present a more prolonged logarithmic increase as $\beta \to 1$. In other words with increasing τ the logarithmic increase should become flattened (predominance of the finite over the integral terms) but reach later saturation as $\beta > 1$. This behaviour will be illustrated in numerical applications in the next part of this work and could be tested, for example, by the dependence of the logarithmic increase on the degree of development in nuclear emulsion ([24,25,27]).

For τ very large the integral term vanishes and if $\tau \gg I_k$ we obtain because of (59):

$$(79) \qquad \left.\frac{\mathrm{d}N}{\mathrm{d}z}\,(\text{ion.})\right|_{>\tau} = \frac{2\pi e^4 n}{m v^2}\left(\frac{1}{\tau} - \frac{1}{T}\right),$$

that is the number of events presents no relativistic increase and they are generated only in close collisions.

RIASSUNTO

Si calcola la perdita di energia totale media che una particella subisce nell'attraversare un mezzo polarizzabile introducendo nella teoria di Fermi un'espressione della costante dielettrica che rappresenti correttamente sia le proprietà dispersive che quelle di assorbimento del mezzo. L'energia totale media si può così separare in energia media spesa in eccitazione, radiazione Čerenkov e ionizzazione primaria degli atomi del mezzo. Si calcola l'effetto della polarizzabilità del mezzo sul numero di ioni generati dalla particella ionizzante per unità di lunghezza e sul numero di eventi nei quali è stato emesso un elettrone atomico con energia maggiore di una certa data che potrebbe venir identificata come energia di soglia per la formazione di un granulo in emulsione nucleare. All'aumentare dell'energia della particella ionizzante questi numeri presentano un aumento logaritmico seguito da saturazione. Sia l'andamento dell'aumento che il valore raggiunto alla saturazione dipendono in modo critico dall'energia di soglia.

Observation of Electron Secondaries from V^0 Decays (*).

M. M. Block, E. M. Harth, M. E. Blevins and G. G. Slaughter

Department of Physics, Duke University - Durham, North Carolina

(ricevuto il 9 Aprile 1956)

Summary. — Three examples of V^0 particles having electron secondaries have been observed in a cloud chamber exposed to a 1.9 GeV π^- beam from the Cosmotron. The experimental evidence is suggestive of the decay scheme, $K^0_{e3} \to \pi^\pm + e^\mp + \nu$.

1. – Experiment.

Three (1) examples of V^0-particles, each having an electron (or positron) as one of its secondaries, were observed in a 20 atm, hydrogen-filled diffusion cloud chamber (2). The chamber, located in a magnetic field of 10 500 gauss, was exposed to a 1.9 GeV π^- beam of the Brookhaven Cosmotron. There were a total of 61 V^0-particles observed, all of which presumably originated in the stainless steel walls and floor of the cloud chamber.

Case 1. Event No. 11375, which is illustrated in Fig. 1, shows the decay of a V^0 into a positive track *a* and a negative track *b*. By comparison with neighboring beam tracks, the ionizations of both *a* and *b* were estimated to be minimum. Track *a*, whose momentum was measured to be $1\,240 \pm 200$ MeV/c, traveled close to the beam direction for 13 cm before leaving the sensitive region. The space angle between *a* and *b* was $43.5 \pm 1°$. Track *b*, which left the sensitive layer after 5 cm, had a very low momentum, 8.0 ± 0.1 MeV/c. Taking 1.5 as the upper limit for the specific ionization of *b*, we deduce from

(*) This work was supported by a joint ONR-AEC contract.

(1) Two of these have been presented in a preliminary report; M. M. Block, E. M. Harth and M. E. Blevins: *Phys. Rev*, **100**, 959 (1955).

(2) W. B. Fowler, R. P. Shutt, A. M. Thorndike and W. L. Whittemore: *Rev. Sci. Instr.*, **25**, 996 (1954).

the above momentum that the upper limit of rest mass of *b* is in the neighborhood of 10 MeV. In order to be as heavy as a muon, it would be necessary for *b* to have an ionization of 80 X minimum for the measured momentum, or conversely, a momentum of 100 MeV/c for the observed ionization. Both of these conditions are well outside our experimental uncertainties. The most reasonable assumption, therefore, is that *b* is a negative electron. Because of the high momentum of *a*, very little can be said about the identity of this particle.

Case 2. Event No. 08735, is pictured in Fig. 2. As in Case 1, both secondaries appear to have minimum ionization. The positive track *c* had a momentum of 43 ± 4 MeV/c, whereas the negative track *d* had a momentum of 228 ± 18 MeV/c. The angle included by *c* and *d* was $68 \pm 1°$.

From ionization and momentum, an upper limit of 50 MeV is found for the rest mass of *c*, and we conclude that it is a positron. Track *d* has an upper mass limit of 250 MeV, and we conclude that its mass is that of a pion or lighter.

Case 3. Event No. 12647, illustrated in Fig. 3, shows the decay of a V^0 into a positive particle *e* and a negative particle *f*, whose lengths in the sensitive region are 3.5 and 12 cm, respectively. The included angle between *e* and *f* is $46 \pm 1°$. Again, both tracks are estimated to have minimum ionization. The momentum of *e* could not be determined; a lower limit is 300 MeV/c. The momentum of *f* was 86 ± 1 MeV/c. Because of our inaccuracies in estimating ionization, it is not possible in this event to rule out the interpretation of *f* as a μ-meson (the specific ionization required for a μ-meson of this momentum is 1.9). However, the most probable interpretation, corresponding to our estimate of minimum ionization for *f*, is that *f* is a negative electron. Nothing can be said about the identity of track *e*.

2. – Interpretation.

An attempt was made to explain these events either as electron pair production in hydrogen or μ-e decays with the μ-meson moving opposite to the beam direction. Because of the large opening angle and the large energy disparity between the two particles, we can rule out the interpretation of our events as electron pairs from probability considerations. If they had indeed been electron pairs, we estimate that we should have expected to observe a total of approximately 10^8 electron pairs in the gas, whereas in fact less than a dozen events attributable to pair formation in hydrogen have been found. The other interpretation, μ-e decay, is ruled out in these 3 cases by the kinematics of this decay process. We thus conclude that cases 1 and 2 are clear

evidence for the existence of V^0-particles having electron secondaries, whereas Case 3 is supporting evidence.

COWAN [3] has reported on a cosmic ray V^0 event found in a cloud chamber, in which the negative secondary was identified as either an electron or a particle of nucleonic mass on the basis of drop count and momentum determination. The positive secondary was identified as a pion from its observed π-μ decay. More recently HARMON [4], using a cloud chamber containing eleven $\frac{1}{4}$ inch lead plates, triggered on cosmic ray showers, found a neutral V event in which one secondary produces an electron shower upon entering the first $\frac{1}{4}$ inch lead plate. The mass of the other secondary, on the basis of range, scattering, and ionization, was consistent with that of a light meson. Further, if a large angle scattering in one of the plates is interpreted as nuclear scattering, this particle is most likely to be a pion.

It is reasonable to assume that these two cosmic ray events, as well as our three Cosmotron observations, are examples of the β-decay of a neutral V particle. Of these five events, two require the other secondary to be a pion, one requires it to be a light meson, while the fourth and fifth cases give no information on this point. On the assumption that all five cases represent the same phenomenon we identify particles *a*, *d* and *e* in our events as pions, and compute the Q-values for the decay scheme $V^0 \to \pi^{\pm} + e^{\mp}$. The values thus found are $Q = 18 \pm 4$ MeV for Case 1 and $Q = 48 \pm 5$ MeV for Case 2. Case 3 yields only a minimum Q, which is 62 MeV. These values are to be compared with $Q = 225 \pm 20$ MeV found by COWAN under the assumption of this decay scheme, and $Q = 350$ MeV found by HARMON. (A lower limit of 223 MeV is also given.)

If we wish to attribute all five events to the decay of the same particle, they must be at least 3-body decays, with the charged secondaries being a pion and an electron. Under the assumptions that all hyperons are fermions and that baryons are conserved, we can rule out the interpretation that the V^0's here observed are hyperons undergoing 3-body decays. It therefore appears reasonable to identify them as K-particles. Further, if we require that the K-particle be a boson, the neutral secondary would have to be a neutrino. The proposed decay scheme is, therefore,

$$K^0_{e_3} \to \pi^{\pm} + e^{\mp} + \nu . \tag{1}$$

The two-body Q distribution for the pion and electron in (1) has been computed from phase space assuming a mass of 494 MeV for the $K^0_{e_3}$. The results

---

[3] E. W. COWAN: *Phys. Rev.*, **94**, 161 (9154).

[4] N. F. HARMON: *Ph. D. Dissertation, Washington University*, private communication (1955).

Fig. 1. – Event No. 11375. The negative track *b* of the V^0 is identified as an electron. The photograph has been retouched for clarity. Tracks *a* and *b* are estimated to have minimum ionization.

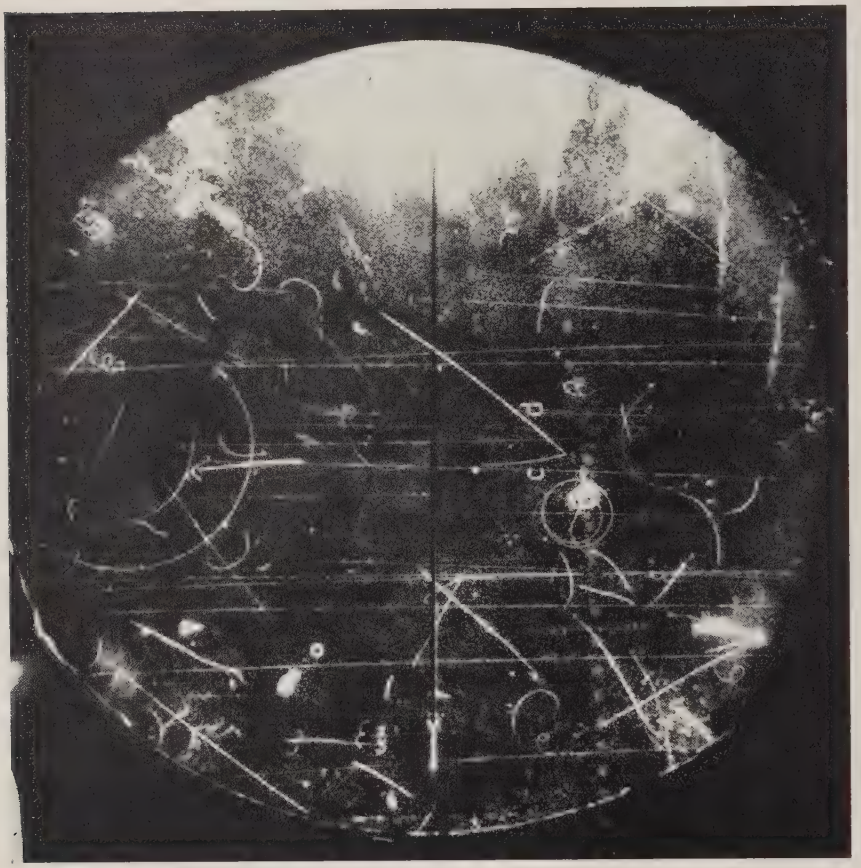

Fig. 2. – Event No. 08735. The positive track c of the V^0 is identified as a positron. The photograph has been retouched for clarity. Tracks c and d are estimated to have minimum ionization.

Fig. 3. – Event No. 12647. The negative track *f* of the V^0 is most probably an electron. The photograph has been retouched for clarity. Tracks *e* and *f* are estimated to have minimum ionization.

are shown in Fig. 4. All five observed Q-values are below the highest Q-value allowed in this interpretation. Since in our experiment only those electrons which have low laboratory momenta ($\lesssim 85$ MeV/c) can be distinguished from light mesons, there exists a strong bias toward low Q-values among our identified cases of the above decay scheme (1).

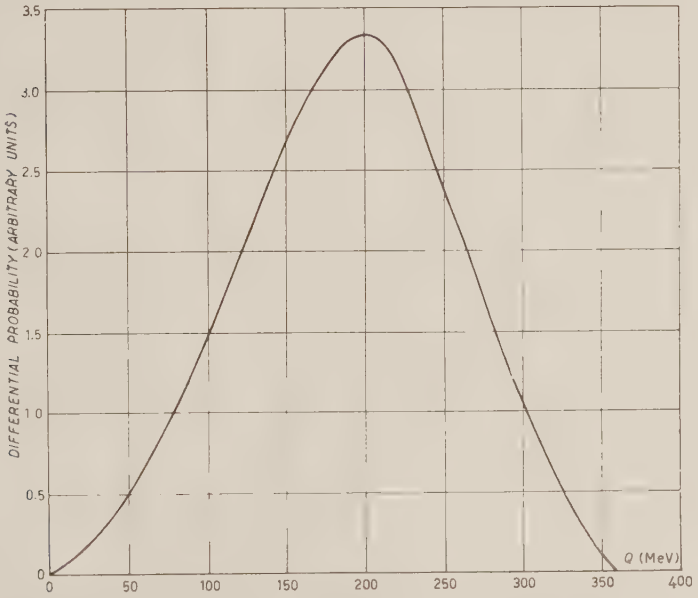

Fig. 4. – The relative probability for the Q between the pion and the electron to lie in the interval between Q and $Q + dQ$, as calculated from phase space for the 3-body decay scheme $K^0_{e3} \to \pi^{\pm} + e^{\mp} + \nu$. The K^0_{e3} rest mass was assumed to be 494 MeV.

The decay scheme $K^0_{e3} \to \pi^- + e^+ + \nu$ suggested here may be the neutral counterpart to the charged K_{e3} meson observed in nuclear emulsions where $K^{\pm}_{e3} \to e^{\pm} + ? + ?$. This then implies that the neutral decay products of the $K^{\mp}_{e3}$ are the neutrino and the π^0-meson and would insure the $K^{\pm}_{e3}$ being boson. In this connection it is interesting to note that the $K_{\mu 3}$ decay scheme has recently been determined (5) to be $K^+_{\mu 3} \to \mu^+ + \pi^0 + \nu$ if the $K^+_{\mu 3}$ is a boson. It is not clear from current evidence whether the K^0 undergoing electron decay is an alternate mode of the θ^0 (or perhaps the τ^0) or whether it is a new particle.

(5) T. F. Hoang, M. F. Kaplon and G. Yekutieli: *Bull. Am. Phys. Soc.*, **1**, Paper V4 (January 1956).

However, under the assumption that the K^0_{e3}, $K^{\pm}_{e3}$, and the $K^{\pm}_{\mu 3}$ are identical with those K-mesons which decay into two pions, the above decay schemes indicate that one of the pion secondaries may be replaced by either an e-ν or a μ-ν pair.

* * *

We would like to thank Drs. R. Shutt, A. Thorndike and W. Whittemore of the Brookhaven Cloud Chamber Group for kindly supplying us with the exposures and equipment for this experiment.

RIASSUNTO (*)

In una camera a nebbia esposta ad un fascio di mesoni π^- di 1.9 GeV del cosmotrone si sono osservati tre esempi di particelle V^0 dotate di elettroni secondari. I risultati sperimentali suggeriscono lo schema di decadimento $K^0_{e3} \to \pi^{\pm} + e^{\mp} + \nu$.

(*) *Traduzione a cura della Redazione.*

Mass and Spin-Parity Character of the τ-Meson.

H. H. Heckman, F. M. Smith and W. H. Barkas

Radiation Laboratory, University of California - Berkeley, California

(ricevuto l'11 Aprile 1956)

Summary. — In this paper we present analyses of 41 τ- and τ'-meson decay events. Since the emulsion density was accurately known, and an improved range-energy curve is available, a Q-value for the τ-decay was obtained which is more precise than that available heretofore. It is 75.08 ± 0.20 MeV. Analysis to determine the character of the τ-meson was made by comparing the experimental data with the 5 spin-parity combinations that lead to unique energy and angular distributions. It is found on employing a χ^2 test that there is a probability of 18% that the χ^2 for the (0, —) choice may exceed that observed, whereas the next most probable choice, (3, —), yields a probability of only 2.8%. The data could not distinguish between the (0, —) and (2, —) states of the τ-meson. The τ'/τ ratio observed is 0.25 ± 0.12, which is consistent with the hypothesis of charge independence. The energy distribution of the π^+-meson in the τ'-decay is consistent with a decay scheme $\tau' \to \pi^+ + 2\pi^0$, and an associated electron pair also confirms this supposed mode of decay.

1. – Introduction.

During the systematic scanning for K-particles in the K^+-meson mass experiment [1], $7.8 \pm 1.4\%$ of all stopping K-particles were identified as τ^+-mesons. The 28 τ^+ observed were easily recognized by their characteristic 3-pion, coplanar mode of decay. The details of the experimental arrangement are given in the paper referred to. The essential feature of the emulsion exposure was the use of a strong-focusing lens system at 90° to the 4.8 GeV proton beam. The momentum interval selected for this experiment was 340

[1] H. H. Heckman, F. M. Smith and W. H. Barkas: *Nuovo Cimento*, **3**, 85 (1956).

to 410 MeV/c. The proper flight time from the $\frac{1}{4}'' \times \frac{1}{2}''$ Ta target to the position of the emulsion stack was $1.2 \cdot 10^{-8}$ s.

While the number of events in this study is not large, a complete analysis of the τ-meson decay is valuable for two reasons. First, accurate measurements of the emulsion density and thickness were taken which, along with the experimentally determined range-energy relation of BARKAS *et al.* [2], permits us to make an improved evaluation of the Q-value of the τ-decay. Second, the method of « along the track » scanning employed throughout the K-mass experiment has given a virtually unbiased selection of τ-mesons. The energy and angular correlation data obtained from these events will, therefore, be useful to augment existing data that pertain to the spin and parity of the τ-meson.

2. – Q Value and Mass.

For « τ completes » (events where all 3 pions stop in the emulsion), the Q-value was determined by measuring the range of each pion, converting to kinetic energy, and taking the sum of the three energies for Q. The error in Q is primarily due to the inherent range straggling of the pions. In events where only two pions stopped in the stack, the Q-value was evaluated by measuring their ranges (i.e., momentum) and the included angle, and invoking momentum balance. In this latter case, the Q-value is determined with less precision, since the angle measured is generally between the lower-momentum pions (the high-momentum pions tend to leave the stack) and thus subject to error.

The principal sources of systematic errors that arise from the uncertainties in the emulsion density and the range-energy relation have been largely eliminated in this experiment. The measured ranges were normalized to an emulsion of specific density 3.815, the standard density chosen for the range-energy relation, assuming the difference in densities is due to different moisture contents. The relation between the observed range R in a medium of density ϱ and the range R_0 in a medium of density ϱ_0 (3.815 g/cm^3) is given in the first approximation by

$$R = R_0 \left[1 - \left(\frac{\varrho - \varrho_0}{\varrho_0 - 1} \right) \left(1 - \frac{\iota_W}{\iota} \right) \right],$$

where ι_W and ι are the rates of energy loss in water and emulsion, respectively. The specific gravity of the emulsion used for this experiment was

---

[2] W. H. BARKAS, P. H. BARRETT, P. CÜER, H. H. HECKMAN, F. M. SMITH and H. K. TICHO: *Phys. Rev.*, **102**, 583 (1955).

3.844 $\pm$ 0.003 and the correction applied to the measured ranges was + 0.4 to 0.6%. The emulsions were essentially free of shear-type distortions and no corrections were made for this effect. Also, the development of the emulsion was uniform, including the top few microns of the emulsion surface, which permitted the entrance and exit points to be easily located.

The distributions of Q are shown in Fig. 1. The weighted mean of Q from these measurements is 75.08 $\pm$ 0.20 MeV. The median value of Q, combining distributions *a*) and *b*), is 74.93 MeV and is, therefore, within the standard error of the mean. Using the mass values of 273.3 $\pm$ 0.2 m_e (P.E.) and 272.8 $\pm$ 0.3 m_e (P.E.) ([3]) for the π^+ and π^-, respectively, we find that the mass of the τ-meson (and its standard error) becomes 966.3 $\pm$ 0.7 m_e.

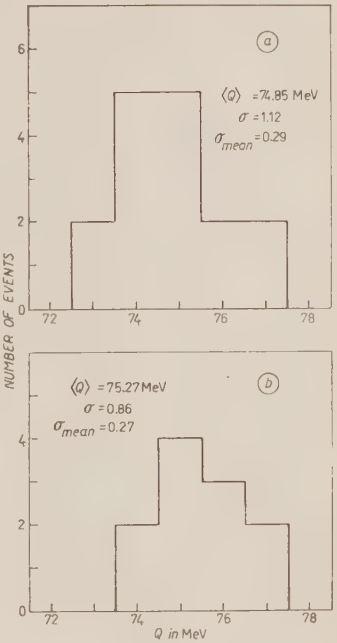

Fig. 1. – Distributions of the decay energies of the τ^+-meson. (*a*) Q value in MeV of the τ^+-decay evaluated from two pion ranges (i.e., momenta) and their included angle. (*b*) Q value of τ^+-decay where all pion ranges were measurable. The weighted mean of Q = 75.08 $\pm$ 0.20 MeV.

3. – Spin and Parity of the τ-Meson.

The theoretical investigations by DALITZ ([4,5]) and FABRI ([6]) have shown that an analysis of the decay configurations of the τ-meson provides a sensitive method for determining its spin and parity. In the decay events where all charges of the pions are known, the decay configuration can be completely described by specifying the kinetic energy of the unlike meson (π^-) and the angle θ between the relative momentum vector $\boldsymbol{q}$ of the like pions and the momentum vector $\boldsymbol{p}$ of the π^-, where $\cos\theta = (\boldsymbol{p}\cdot\boldsymbol{q})/|p_1||q|$. (See Fig. 2, which

([3]) W. H. BARKAS, W. BIRNBAUM and F. M. SMITH: *Phys. Rev.*, **101**, 778 (1956).
([4]) R. H. DALITZ: *Phil. Mag.*, **44**, 1068 (1953).
([5]) R. H. DALITZ: *Phys. Rev.*, **94**, 1046 (1954).
([6]) E. FABRI: *Nuovo Cimento*, **11**, 479 (1954).

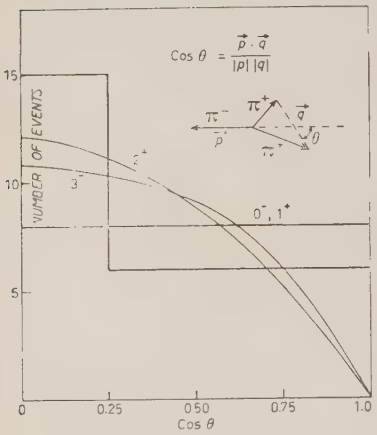

Fig. 2. – Correlation in angle between the relative momentum of the π^+'s and the momentum of the π^-. The theoretical curves are representatives of the several final state distributions that can be expressed by a unique decay amplitude.

gives the observed distribution of $\cos\theta$). Fig. 3 is the histogram of T/T_{max} (T_{max} = = 48.2 MeV) for the π^--meson in the τ^+-decay. Included in these data are the results of previous measurements on the τ-decay (7). The relevant theoretical distributions with which these are compared are the unique distributions obtained when only the minimum angular momenta are used in the matrix element describing the decay, and assuming that the momentum dependence is determined by the penetration of the centrifugal barrier. The spins and parities of the τ-meson that can be described by these single modes of decay are (0, —), (1, +), (1, —), (2, +), and (3, —) (4-6). Of these distributions, the over-all best fit (*) to the data is obtained from the (0, -) state of the τ-meson. The distributions for the (2, —) τ-meson (not shown) involve a linear combination of two equally probable matrix elements. While the (2, -) and (0, -) final-state distributions are not in detail alike, the experimental data cannot distinguish between them. In order that these data may be compiled with similar types of measurements on the τ-decay, Table I tabulates for each event the kinetic energies of the pions, Q of the decay, and $\cos\theta$.

It should be noted that there was no clear evidence for a radiative decay

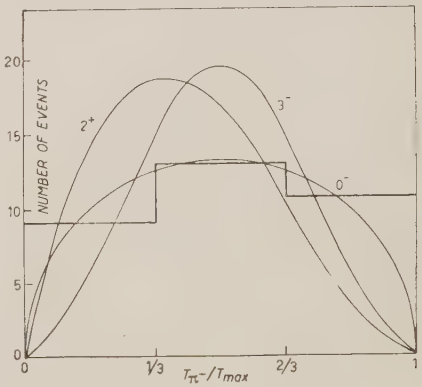

Fig. 3. – Energy distribution of the π^--meson from the τ^+-decay, $\tau^+ \to \pi^+ + \pi^+ + \pi^- + \pi^-$. Maximum kinetic energy (rel.) of π^- is 48.2 MeV.

(7) H. H. HECKMAN: *University of California Radiation Laboratory*, Report No. UCRL-3003 (1955).

(*) The χ^2 test in this case gives an 18% probability for χ^2 equal to or greater than that observed. This can be compared to a 2.8% probability for the (3, -) state, the next best fit for the unique distributions.

TABLE I. – *Tabulation of pion kinetic energies, the Q of the τ-decay in* MeV, *and* $\cos\theta = (\boldsymbol{p}\cdot\boldsymbol{q})/(|p||q|)$.

	T_1^+ (MeV)	T_2^+ (MeV)	T_3^- (MeV)	Q (MeV)	$\cos\theta$
τ_1	19.30	26.80	28.40	74.50	0.184
τ_2	16.39	16.80	43.37	76.56	0.021
τ_3	20.31	23.01	32.18	75.50	0.066
τ_4	9.71	39.02	25.28	74.01	0.727
τ_5	8.90	43.32	23.37	75.59	0.843
τ_6	27.32	29.70	18.05	75.07	0.064
τ_7	28.25	32.84	13.92	75.01	0.139
τ_8	4.83	28.22	42.73	75.78	0.786
τ_9	25.81	32.95	15.41	74.17	0.080
τ_{10}	13.00	32.02	29.91	74.93	0.468
τ_{11}	19.88	23.82	33.11	76.81	0.098
τ_{12}	16.10	(40.32)	18.45	74.87	0.632
τ_{13}	21.72	(42.68)	10.35	74.75	0.628
τ_{14}	20.52	(40.61)	10.53	71.66 (*)	0.661
τ_{15}	4.46	(42.82)	26.90	74.18	0.913
τ_{16}	4.47	24.61	(45.37)	74.45	0.886
τ_{17}	35.91	(36.83)	1.63	74.37	0.070
τ_{18}	(33.46)	33.51	9.47	76.44	0.003
τ_{19}	18.00	25.69	(31.10)	74.79	0.195
τ_{20}	25.92	(43.03)	7.82	76.77	0.619
τ_{21}	11.44	(42.34)	19.45	73.23	0.797
τ_{22}	(29.50)	37.62	8.11	75.23	0.296
τ_{23}	5.38	(39.04)	29.68	74.10	0.936
τ_{24}	15.11	15.62	(43.82)	74.55	0.021
τ_{25}	17.66	(25.82)	33.10	76.58	0.201
τ_{26}	12.47	23.36	(37.48)	73.31	0.232
τ_{27}	11.80	24.75	(37.40)	73.95	0.288
τ_{28}	(20.78)	38.22	16.98	75.98	0.466
τ_a	16.2	24.3	(34.0)	See (+)	0.215
τ_b	17.6	43.2	14.7	—	0.718
τ_c	17.3	19.6	(37.5)	—	0.066
τ_d	18.2	34.7	22.4	—	0.414
τ_e	18.3	37.4	19.2	—	0.498

Events τ_1 through τ_{11}: all pion ranges measured.

Events τ_{12} through τ_{28}: entries in parentheses evaluated by momentum balance.

Events τ_a through τ_e from UCRL-3003.

(*) Not included in the averaging of Q as deviation $\sim 3\,\sigma$ from mean of distribution. This may be an example of a radiative decay of the τ-meson.

(+) Q-values for τ_a to τ_e were not included in the evaluation of the mean Q as the emulsion density was not accurately measured.

of the τ-meson. One event (τ_{14}) appears to have an anomalously low Q value of 71.66 MeV, but the statistical expectation of this event is about twice as great as the probability for the emission of a photon of $k \geqslant \sim 3$ MeV in the τ-decay by an « internal bremsstrahlung » process ([8]). Among the 400 K^{τ}-particle endings observed, no radiative decays that could be classified as $\tau^{\tau} \rightarrow$ $\rightarrow \pi^{\tau} + \gamma$ were seen. Of course this γ-ray would have virtually no chance of being detected. A decay mode $\tau^{+} \rightarrow \pi^{\tau} + e^{\tau} + e^{-}$ (internal pair conversion) would have been readily observed and was not (+). These latter types of radiative decay of the τ would be expected to compete favorably with the 3π mode of decay for non zero spins of the τ ([8]). That none were observed gives some additional evidence that the τ is a particle of zero spin.

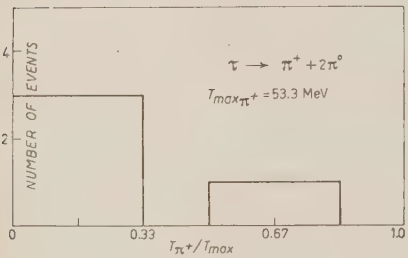

Fig. 4. – Energy distribution of the π^{+}-meson in the $\tau' \rightarrow \pi^{+} + 2\pi^{0}$ decay. $T_{max} = 53.3$ MeV.

4. – Alternative Decay Mode of the τ.

A small fraction, i.e., $1.9 \pm 0.8\%$, of the K-mesons that decay into a singly charged secondary give rise to a positive pion having a spectrum of energies up to ~ 50 MeV. This type of decay is interpreted as the alternate mode of the τ-decay, i.e., $\tau' \rightarrow$ $\rightarrow \pi^{+} + \pi^{0} + \pi^{0}$. Fig. 4 is the observed distribution of T/T_{max} for the π^{+}-meson, where $T_{max} = 53.3$ MeV. A tabulation of the range and kinetic energies of the π^{+} is given in Table II. Although the statistics are poor, the energy distribution of the π^{+}-meson in the τ'-decay appears to be unsymmetrical, in contrast to the π^{-} energy distribution from the τ-decay (Fig. 3). It is not believed that this difference can be accounted for by observational bias, as all K secondaries of grain density greater than that expected for the secondaries from $K_{\pi 2}$ and $K_{\mu 2}$ particles were followed to their termination. DALITZ ([5]) has pointed out, however, that these distributions are not in general expected to be unique.

The hypothesis of the conservation of isotopic spin gives no further information on the decay of the $\tau^{+} \rightarrow 2\pi^{+} + \pi^{-}$, but does lead to relations between

([8]) R. H. DALITZ: *Phys. Rev.*, **99**, 915 (1955).

(+) An electron pair of 60 ± 15 MeV was observed to accompany a π^{+}-meson from a decay interpreted as $\tau' \rightarrow \pi^{+} + \pi^{0} + (\pi^{0} \rightarrow \gamma + e^{+} + e^{-})$. This type of event is not confusable with $\tau^{+} \rightarrow \pi^{+} + e^{+} + e^{-}$. The energy of the π^{+} meson in τ' decay is always less than 53.3 MeV. Accompanying such a pion, the electron pair observed could not conserve momentum and energy.

TABLE II. – *Range and energy of the π^+-meson in the $\tau' \to \pi^+ + 2\pi^0$ decay.*

R (cm)	E (MeV)
2.206	37.5
1.541	29.7
0.515	15.8
0.418	14.0
0.352	12.5
0.084	5.7
0.047	4.1
0.039	3.7

the probabilities of the two modes of decay. The main consequence of the hypothesis (9) is a statement that the ratio

$$r = \frac{N(\tau' \to 2\pi^0 + \pi^+)}{N(\tau \to 2\pi^+ + \pi^-)},$$

must satisfy $\frac{1}{4} \leqslant r \leqslant 1$ for isotopic spin $T = 1$. The observed ratio is 0.25 ± 0.12, consistent with the hypothesis of charge independence.

* * *

The authors wish to express their thanks to Dr. E. J. LOFGREN and the Bevatron crew for their aid in making the exposure. Also, we appreciate the technical assistance given us by Mrs. N. FREED, Miss H. LOWE, Mrs. R. SPEER, Mr. J. DYER and Mr. J. GRAY, who performed much of the plate scanning.

This work was performed under the auspices of the U. S. Atomic Energy Commission.

(9) R. H. DALITZ: *Proc. Phys. Soc.* (*London*), A **66**, 710 (1953).

RIASSUNTO (*)

Nel presente lavoro esponiamo analisi di 41 decadimenti di mesoni τ e τ'. Poichè la densità dell'emulsione era esattamente nota, e disponiamo di una ottima curva range-energia, si è ottenuto per decadimento τ un valore di Q maggiormente preciso

(*) *Traduzione a cura della Redazione.*

di quello finora disponibile. È 75.08 $\pm$ 0.20 MeV. Confrontando i dati sperimentali con le 5 combinazioni spin-parità, che conducono alle uniche distribuzioni dell'energia e angolari, si sono eseguite analisi per determinare il carattere del mesone τ. Per mezzo di un testo χ^2 si trova che esiste una probabilità del 18% che il χ^2 per la scelta (0, —) superi il valor osservato, mentre la scelta immediatamente meno probabile (3, —) offre una probabilità di soltanto il 2.8%. I dati sperimentali non permettono di distinguere tra gli stati (0, —) e (2, —) del mesone τ. Il rapporto τ'/τ osservato è 0.25 $\pm$ 0.12 compatibile con l'ipotesi dell'indipendenza della carica. La distribuzione energetica del mesone π^+ nel decadimento τ' è compatibile con lo schema di decadimento $\tau' \rightarrow \pi^+ + 2\pi^0$ e una coppia di elettroni associati conferma a sua volta tale supposto modo di decadimento.

The Diffusion Parameters of Thermal Neutrons in Water.

A. Bracci and C. Coceva

Laboratori CISE - Milano

(ricevuto il 14 Aprile 1956)

Summary. — A measurement of the diffusion time of slow neutrons in water is presented. The neutrons are produced with a pulsed source using d+d reaction and slowed down and diffused in cylindrical tanks of different shape filled with distilled water. Neutron detectors situated on the surface of the tanks and connected with an eighty channel time analyser give a measure of the neutron flux as a function of time. Results obtained for the life time of neutrons in water and for the collision mean free path are discussed and compared with the known values.

1. – Introduction.

In the last few years methods were developed for the determination of the diffusion parameters of neutrons in various moderators, using pulsed neutron sources ([1,10-13]).

([1]) J. H. Manley, L. J. Haworth and E. A. Luebke: *Phys. Rev.*, **61**, 152 (1941).
([2]) B. W. J. Whitehouse and G. A. R. Graham: *Can. Journ. Res.*, A **25**, 261 (1947).
([3]) R. L. Walker: M.D.D.C. 414.
([4]) L. G. Schulz and M. Goldhaber: *Phys. Rev.*, **67**, 202 (1945).
([5]) E. Fermi: AECD 2644.
([6]) S. Glasstone and M. C. Edlund: *The elements of nuclear reactor theory* (New York, 1952).
([7]) D. J. Hughes: *Pile Neutron Research* (Cambridge Mass., 1953).
([8]) B. Hamermesh, G. R. Ringo and S. Wexler: *Phys. Rev.*, **90**, 603 (1953).
([9]) S. P. Harris, C. O. Muehlhause, D. Rose, H. P. Schroeder, G. E. Thomas jr. and S. Wexler: *Phys. Rev.*, **91**, 125 (1953).
([10]) F. R. Scott, D. B. Thomson and W. Wright: *Phys. Rev.*, **95**, 582 (1954).
([11]) G. F. Von Dardel: *Trans. Roy. Inst. Techn. Stockholm*, **75** (1954).
([12]) G. F. Von Dardel and M. Sjostrand: *Phys. Rev.*, **96**, 1245 (1954).
([13]) A. V. Antonov, A. I. Isakoff, I. D. Murin, B. A. Neupocoyev, J. M. Frank, F. L. Shapiro and I. V. Shtranich: *Geneva Conference* (5 July 1955).

With such methods the variation in the neutronic density inside the moderator versus time is measured. The advantage with respect to methods with stationary sources consists of greater simplicity and less need of slowing-down material.

2. – Theory.

A uniform medium of finite dimensions, is subjected to a flux from a source of fast neutrons. If the source is shut off, the neutron velocities, after a certain time, reach within the medium a stationary distribution provided the slowing-down time is sufficiently short with respect to the mean life of the neutrons in the moderator. When this stage is reached the density $n(\boldsymbol{r}, t)$ of the neutrons satisfies the relation

$$D\Delta n - \frac{n}{T_0} = \frac{\partial n}{\partial t}, \tag{1}$$

where D is the diffusion coefficient and T_0, the capture mean life, the latter, for a given velocity, being given by:

$$\frac{1}{T_0(v)} = v\,\Sigma_c(v).$$

If Σ_c (macroscopic capture cross-section) follows the $1/v$ law, $T_0(v) = T_0$ will not depend on the neutron velocity.

D on the other hand is given by

$$D(v) = \frac{\lambda_t v}{3},$$

and as the transport mean free path $\lambda_t(v)$ generally follows a different law from the proportionality with v [1], $D(v)$ will depend on the distribution of the neutron velocities.

The general solution of (1) may be put in the following form:

$$n(\boldsymbol{r}, t) \quad \sum_{l=1}^{\infty}\sum_{m=1}^{\infty}\sum_{n=1}^{\infty} a_{lmn} R_{lmn}(\boldsymbol{r}) \exp\left[-\left(\frac{t}{T_0} + B_{lmn}^2 \int_0^t D(t)\,\mathrm{d}t\right)\right]. \tag{2}$$

$R_{lmn}(\boldsymbol{r})$ and B_{lmn} are respectively the eigen-functions and the eigenvalues of the differential equation

$$\Delta R = -B^2 R, \tag{3}$$

with boundary conditions determined by $R(\boldsymbol{r})$ becoming equal to zero at the extrapolated boundaries of medium.

The coefficients a_{lmn} of the various terms of the expansion depend instead on the initial distribution of the fast neutrons and in the approximation of the « age theory » of Fermi, are proportional to $\exp[-B^2_{lmn}\tau]$, where τ is the age.

The term

$$\exp\left[-\left(B^2_{lmn}\int_0^t D(t)\,\mathrm{d}t\right)\right],$$

takes into account the neutron escape and $\exp[-t/T_0]$ the capture of the medium.

Each term of the expansion in series (2) decays exponentially with time with its own decay constant. If a sufficiently long time is allowed to pass after shutting off the source, the period depending both on the relative importance of the various harmonics, i.e. the factors a_{lmn} (and hence on the initial distribution of the fast neutrons) as on the relative importance of the eigenvalues B_{lmn}, the density of the neutrons, at a certain point, can be represented by only one term of the expansion (2) which is the one corresponding to the smallest B_{lmn} eigenvalue.

A certain time t' after shutting off the source of fast neutrons therefore, we have the equation

$$n(\boldsymbol{r}, t) = A(\boldsymbol{r}) \exp\left[-t\left(\frac{1}{T_0} + B_0^2\int_0^t D(t)\,\mathrm{d}t\right)\right], \qquad (t > t') \tag{4}$$

the smallest B_{lmn} eigenvalue having been represented by B_0.

It was put into evidence by Von Dardel [11] that the equilibrium value of the diffusion coefficient D does not only depend on the composition and temperature of the moderator but also on its geometry. In fact the number of neutrons with velocity v that escapes from a unit volume element of the moderator per unit time is given by:

$$-D(v)\Delta n = D(v)B_0^2 n\,,$$

and therefore from the behaviour of $\lambda_l(v)$ in the region of the equilibrium velocity at room temperature, a « leakage » is generally foreseen, which is greater, the greater the neutron velocity is.

As regards the equilibrium distribution in a infinite medium (Maxwellian velocity distribution) a relative diminution in the neutronic spectrum, by reason of the escape, takes place in the high velocity part of it. This means a lower average temperature and consequently a lower average value of D.

Besides this effect is greater the greater « buckling » B_0^2 is. The value of D can be expanded into a power series of B_0^2 and, as in practice the correction is small enough, it is possible to stop at the first order term

$$D = D_0(1 - CB_0^2)\,, \tag{5}$$

where D_0 is the diffusion coefficient corresponding to the infinite medium and C a constant related to the velocity at which the energy between the neutrons and the moderator is exchanged.

In the approximations shown, the mean life T of the neutrons is given by the relation:

$$\frac{1}{T} = \frac{1}{T_0} + B_0^2 D_0(1 - CB_0^2)\,. \qquad (t > t'). \tag{6}$$

The measurement of $1/T$ at various values of B_0 furnishes therefore the diffusion parameters T_0, D_0 and C. The diffusion length, which is the quantity directly measured in the stationary experiments, is deduced from the relation:

$$L^2 = D_0 T_0\,.$$

3. – Experimental Arrangements.

The reaction d(d, n)^{3}He was used as neutron source. The deutons were accelerated to a kinetic energy of about 300 000 eV with a Cockroft and Walton accelerator. The target consisted of heavy ice, cooled by liquid air. The peak intensity was a few 10^9 neutrons per second.

The ion source works with 15 μs pulses repeated about every 10 mean lives of the neutrons in the moderator, so as to eliminate overlapping.

Common water in cylindrical geometry is used as a slowing down medium. In this case formula (3) furnishes the value of B_0^2, thus:

$$B_0^2 = \left(\frac{2.405}{R}\right)^2 + \left(\frac{\pi}{H}\right)^2\,,$$

2.405 is the first zero of the cylindrical Bessel function of zero order; R and H are respectively the extrapolated radius and the extrapolated height of the cylinder, obtained by assuming the value of the extrapolation length as 0.32 cm. Containers of 12 and 18 cm diameters respectively and with a heigth ranging between 2 and 18 cm were used.

The containers were of aluminium, of 1 to 2 mm thickness, coated with a 0.2 mm sheet of cadmium and 10 mm layer of boron carbide to reduce the

effect of the reflections from the laboratory walls, which form an epithermal neutron source extending in the time after the neutron bursts. The detector was a scintillation counter having a mixture of ZnS and BN as phosphor. In view of the high capture cross-section for neutrons, the detector is placed in contact with the external surface of the aluminum container. In this way the characteristics of the medium are not disturbed and no deformations in the time spectrum due to the time of flight of the neutrons from the moderator to the detector take place.

The pulses are registered with a time analyzer of 80 channels. The time chosen for the channels was 0.5 or 5 μs interval according to the value of the mean life. The period of measurement lasted generally, from 3 to 5 mean lives, beginning 2 to 4 mean lives after the source had been shut off, according to the buckling value.

Great importance was given to the selection of the position of the neutron source and the detector so as to reduce to a minimum the time up to the moment when the neutronic density detected was represented practically by the fundamental harmonic mode alone.

Such selection of position was to make measurements with enough neutronic density and hence a sufficiently high counting speed.

As regards the source, the neutrons of the first collision must have a spacial distribution as near that of the fundamental harmonic mode as possible. The source-moderator solid angle should be as big as possible so that the time dispersal of the neutrons entering the moderator, due to the reflections on the laboratory walls, remain as little as possible. This was made possible by placing the heavy ice target on the axis of the cylinder of the moderator and at a distance of 5 cm from the surface of the water, as shown in Fig. 1.

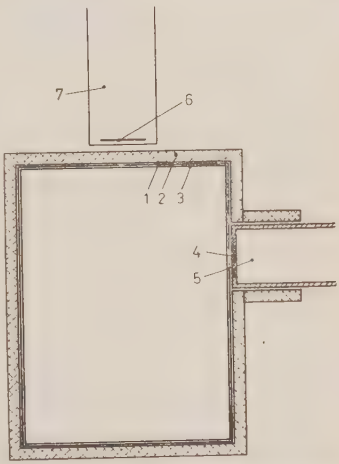

Fig. 1. - Experimental arrangement. 1) Cadmium sheet. 2) Boron layer. 3) Aluminium container. 4) Scintillator. 5) Phototube. 6) Heavy ice target. 7) Accelerator tube.

As far as concerns the detector, two cases are to be distinguished:

1) for small geometric bucklings the height of the cylinder is such that the maximum density of the fast neutrons is turned, with respect to the center of the moderator, towards the neutron source;

2) for big bucklings (low cylinders) instead, the density reaches equilibrium distributions along the axis very soon.

TA

Reference	T_0 (μs)	D_0 (cm² s⁻¹)	L (cm)	σ_a (barn)
(1)	197 ±10 (1)	—	—	0.345 (1)
(2)	—	—	—	0.313 ± 0.013
(3)	—	—	—	0.313 ± 0.010
(4)	—	—	—	0.363 ± 0.012
(5)	—	31 200	2.76 ± 0.03	—
(6)	—	—	2.88	—
(7)	—	31 240	2.85	0.330
(8)	—	—	—	0.329 ± 0.004
(9)	—	—	—	0.332 ± 0.007
(10)	213 ± 4	38 500 ± 800	2.85 ± 0.05	—
	(216 ± 4) (2)			
(12)	204.4 ± 2.0	36 340 ± 750	2.725 ± 0.003	0.333 ± 0.003
(13)	207 ± 6	35 000 ± 1 000	2.7 ± 0.1	(0.329 ± 0.010
present work	202 ± 6	34 850 ± 1 100	2.66 ± 0.11	0.337 ± 0.010

(1) T_0 and σ_a were calculated from the experimental data using the value $D_0 = 35\,000$ cm² s⁻¹. The Aut
(2) Correction calculated in ref (13).

In case 1 to have awaited the complete decay of harmonic modes superior to the fundamental mode would have slowed down the counting to the detriment of measurement statistics. We therefore placed the detector laterally in two positions (one of wich is indicated in Fig. 1) corresponding to the nodes of the third longitudinal harmonic mode which thus was eliminated. The second harmonic mode has two equal values in the two positions but of opposite sign (Fig. 2) its effect was cancelled by averaging the results obtained in the two positions. Harmonic modes higher than the third mode could be definitely ignored.

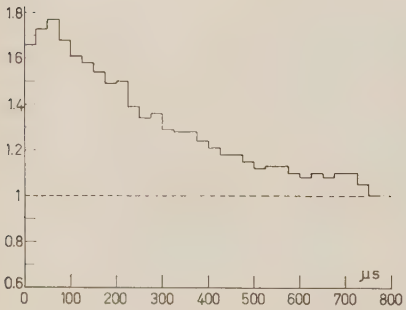

Fig. 2. – Ratio between the neutronic densities in the two positions of the detector corresponding to the nodes of the third longitudinal harmonic mode versus time. $B_0^2 = 0.093$ cm⁻².

In case 2 it was enough to place the detector on the axis in symmetrical position with respect to the neutron source.

The decay constant was corrected by less than 0.5% to take into account the neutrons scattered by the laboratory walls. Such correction was evaluated by changing the solid angle between the moderator and the source.

C (cm²)	Method
—	Pulsed source - infinite geometry
—	$\sigma_B/\sigma_H = 2\,270$ integration method
—	$\sigma_B/\sigma_H = 2\,270$
—	$\sigma_B/\sigma_H = 1\,955 \pm 24$
—	$\sigma_B/\sigma_H = 2\,292$; $\sigma_B = 755$ barn
—	$\sigma_B/\sigma_H = 2\,274$; $\sigma_B = 755$ barn
—	Pulsed - finite geometry B_0^2 ranging between $0.006 \div 0.018$ cm^{-2}
.20 ± 0.04	Pulsed - finite geometry B_0^2 ranging between $0.1 \div 0.7$ cm^{-2}
.11 ± 0.03	Pulsed - finite geometry B_0^2 ranging between $0.09 \div 0.93$ cm^{-2}
.090 ± 0.035	Pulsed - finite geometry B_0^2 ranging between $0.09 \div 0.96$ cm^{-2}

their paper $T_0 = 205 \pm 10$ μs and $\sigma_a = 345$ barn using the value $D_0 = 24000$ cm² s^{-1}.

4. – Results.

The measurements were made with fourteen different values of geometric buckling at a temperature of 22 °C. The bucklings used ranged from $B_2^0 = 0.09$ cm^{-2} to $B_0^2 = 0.96$ cm^{-2}. By means of the least squares method, the values of $1/T$ obtained (Fig. 3 (were adapted to equation (6). The results are

$$1/T_0 = 4.945 \pm 150 \text{ s}^{-1},$$
$$D_0 = 34.850 \pm 1.100 \text{ cm}^2 \text{ s}^{-1},$$
$$C = 0.090 \pm 0.035 \text{ cm}^2.$$

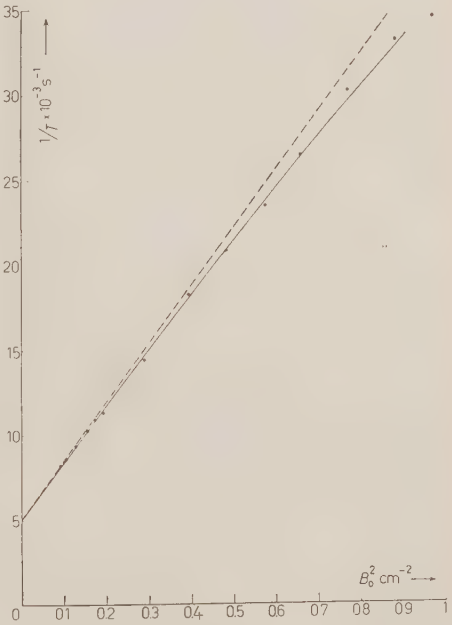

Fig. 3. – The curve represents the function $1/T = 4.945 + 34.850B_0^2 \cdot (1 - 0.090B_0^2)$. The dashed line represents the function $1/T = 4.945 + 34.850B_0^2$. The points are the experimental results.

The error was mostly due to the statistics and the uncertainty of the geometric buckling.

Considering that the oxygen does not affect the water absorption, the neutron proton thermal cross-section value:

$$\sigma_a = 0.337 \pm 0.010 \text{ barn} ,$$

is deduced from the measured value of $1/T_0$, while

$$L = 2.66 \pm 0.11 \text{ cm} .$$

The results of the various measurements of H_2O are set down in the table for comparison. The value of D_0 is in perfect agreement with that obtained from the Russian researchers, whereas it is rather low in comparison with that obtained by the Swedes.

The comparison of D_0 with the investigations based on static methods must be made using the diffusion length L which, being an indirect value here, shows a big error.

Our value of C is in good agreement with that obtained by the Russian researchers ([13]). VON DARDEL ([11,12]) computed theoretically the value of C as 0.059 cm^2 on the assumption that the moderator is a monoatomic gas of mass 18. The value of C however is still uncertain both because its experimental determination is affected by a considerable error and because its theoretical interpretation is not simple.

RIASSUNTO

Viene descritta una misura del tempo di diffusione di neutroni lenti in acqua. I neutroni vengono prodotti con un generatore impulsato per mezzo della reazione d+d e vengono rallentati e diffusi in recipienti cilindrici di varie dimensioni, riempiti con acqua distillata. Il flusso di neutroni alla superficie di tali cilindri viene misurato in funzione del tempo per mezzo di contatori a scintillazione. I risultati ottenuti e in particolare la vita media dei neutroni nell'acqua e il cammino libero medio vengono confrontati con i valori noti e discussi.

IL NUOVO CIMENTO Vol. IV, N. 1 1° Luglio 1956

A New Method of Measuring Asymmetries in Neutron Polarization Experiments.

P. Hillman, G. H. Stafford and C. Whitehead

Atomic Energy Research Establishment - Harwell, Berkshire, England

(ricevuto il 16 Aprile 1956)

Summary. — A solenoid has been constructed 11 feet in length and with a maximum rating of $1.14 \cdot 10^6$ ampere turns which enables the plane of polarization of a neutron beam to be turned through 90° in either direction. This enables asymmetry measurements to be made in neutron polarization experiments without moving the detecting apparatus. This is a great advantage in experiments in which polarization effects are small and false asymmetries, which can be introduced when the detector is moved, correspondingly very difficult to eliminate with sufficient accuracy. The method has been tested by using the partially polarized neutron beam produced with a beryllium target in the Harwell cyclotron. Asymmetry measurements were made by counting neutrons scattered at an angle of $\frac{1}{3}$° off a uranium scatterer. Four values of the solenoid current were used and the results obtained agree well with those expected theoretically..

1. – Introduction.

If $I(\theta, \varphi)$ is defined as the scattered intensity of a polarized beam at an angle θ and measured at an azimuthal angle φ with respect to the plane perpendicular to the direction of polarization then it may be shown [1] that the asymmetry is

$$\varepsilon = \frac{I(\theta, 0) - I(\theta, \pi)}{I(\theta, 0) + I(\theta, \pi)} = P_1 P_2 ,$$

where P_1 is the polarization of the incident neutron beam and P_2 is the pola-

[1] J. V. Lepore: *Phys. Rev.*, **79**, 137 (1950).

rization produced in the second scattering process. In polarization experiments reported in the literature so far the values of $I(\theta, 0)$ and $I(\theta, \pi)$ have been obtained either by rotation of the counter telescope about the line of the neutron beam or by moving the telescope on a calibrated arm from one side of the beam to the other. When the telescope is moved, false asymmetries can be introduced for a number of different reasons which have been discussed in some detail in a previous communication (2). These false asymmetries, though small, are particularly important in neutron polarization experiments because of the low initial polarization available (less than 15%). However, instead of counting in two directions q with respect to a fixed plane of polarization it is clearly equivalent to rotate the plane of polarization with respect to a fixed counting direction (3). It is possible to do this by the use of a magnetic field as will be discussed in the next section. This procedure has the considerable advantage that the counters are placed in a given position and not moved at all during an asymmetry measurement.

2. – Principle of the Method.

If a spinning magnetic moment is acted on by a uniform magnetic field it will precess in a direction normal to the plane containing the spin and the magnetic field vectors, the frequency of precession being given by

$$\nu_p = \hbar^{-1} g \mu_N H \,, \tag{1}$$

where h = Plank's constant.

g = gyromagnetic ratio,

μ_N = nuclear magneton,

H = magnetic field.

If v = velocity of the particle

and

l = path length of the particle in the magnetic field, then the field required to produce a precession of 90° is given relativistically by

$$H = \frac{vh}{4lg\mu_N(1-\beta^2)^{\frac{1}{2}}} \,. \tag{2}$$

With a spin direction perpendicular to the line of flight, the magnetic field

(2) P. HILLMAN and G. H. STAFFORD: *Nuovo Cimento*, **3**, 633 (1956).

(3) We are grateful to Prof. R. WILSON of Harvard University for pointing out this fact and some of its ramifications.

can be applied either at right angles to both the line of flight and the spin direction, using an electromagnet, or parallel to the line of flight using a long solenoid. If an electromagnet were used the procedure would be to place the detecting apparatus at a given angle in the horizontal plane and to make measurements with zero magnetic field and with a field of sufficient magnitude to precess the particles through 180 degrees. With a solenoid, on the other hand, a precession of only 90 degrees would be necessary, the field being reversed to produce a rotation of 180° of one spin direction relative to the other. The counting would then be carried out in a plane perpendicular to the plane of the first scattering. We have used a solenoid for this purpose. It was designed for use with neutrons of approximately 100 MeV energy which required a value of $lH = 1.33 \cdot 10^6$ gauss cm. This was obtained with a solenoid of 903 turns, approximately 11 feet long and a maximum current of 1 250 A. Detail and design features of the solenoid are given in the appendix.

3. – Experimental Check of the Method.

Recently Voss and Wilson [4] have measured the polarization of the neutron beam from the Harwell cyclotron using scattering off uranium at angles less than 1° where the interaction between the magnetic moment of the neutron and the Coulomb field of the uranium nucleus is important. At a scattering angle of $\frac{1}{2}$° the polarization produced by this process is high (75 %) and so it provides a relatively large asymmetry for testing the operation of the solenoid and the physical principles involved in the method.

In both this experiment and that of Voss and Wilson the polarized neutron beam was provided by a beryllium target inside the cyclotron, the angle between the incident protons and the neutron beam used being 26°. The uranium scatterer was 3.2 cm thick and the neutrons were detected with the same liquid scintillation counter as used by Voss and Wilson. The fundamental difference between the two experiments was that in the experiment of Voss and Wilson the second scattering was in the horizontal plane and asymmetry measurements were made by moving the counter, whereas in the solenoid experiment the second scattering was in the vertical plane and the counter was not moved. A full description of the experiment is given in the paper by Voss and Wilson [4].

In our experiment counting rates were determined for both directions of the solenoid field for currents of 500, 900, 1 030 and 1 200 A. The asymmetry is defined here as:

$$\varepsilon = \frac{\text{Counting rate with neutrons rotated anti-clockwise} - \text{Counting rate with neutrons rotated clockwise}}{\text{Counting rate with neutrons rotated anti-clockwise} + \text{Counting rate with neutrons rotated clockwise}} .$$

[4] R. G. P. Voss and R. Wilson: *Phil. Mag.*, **1**, 175 (1956).

In Fig. 1 the measured asymmetry has been plotted as a function of solenoid current.

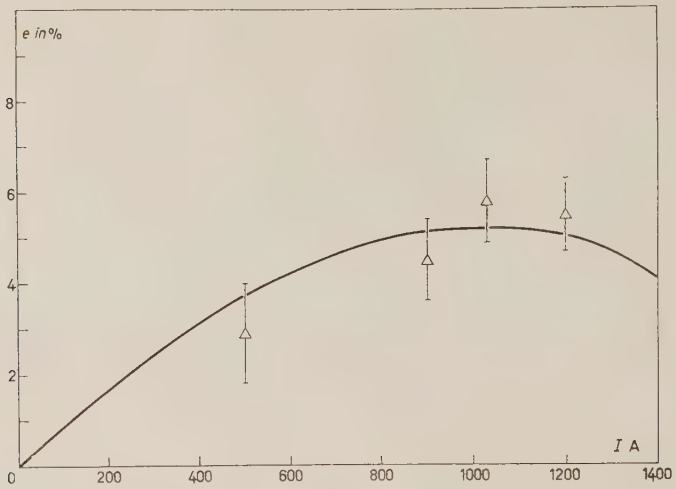

Fig. 1

The solid curve is the least squares fit to the experimental points of $e - e_0 \sin kI$; e_0 being the variable and k being calculated from the measured solenoid parameters. This value of k has an uncertainty of less than $\pm 2\%$ which would introduce an uncertainty of ± 0.0006 in the value of e_0. The value of e_0 obtained from this fit is -0.052 ± 0.005.

Using a calculated value of $P_2 = -0.75$ and making a correction for multiple scattering in the uranium and for a possible false asymmetry of -0.004 ± 0.002 (see Sect. 4) we finally obtain a value of 0.073 ± 0.008 for P_1 the polarization of the incident beam. The effective energy was 95 ± 2 MeV as calculated from a measurement of the attenuation of the beam by polythene. Some other measurements made at a higher bias corresponding to an effective energy of 99 ± 2 MeV gave a value of P_1 equal to 0.084 ± 0.020.

These values are to be compared with the value of 0.092 ± 0.013 obtained by Voss and Wilson at an effective energy of 97 ± 2 MeV.

Combining the results of Voss and Wilson with those obtained in the present experiment the best value for P_1 the neutron beam polarization at an energy of 98 ± 3 MeV as used in a previous experiment [2] is now believed to be 0.085 ± 0.006.

4. – Sources of Spurious Asymmetries.

It is very important to check if any false asymmetries are introduced by the use of the solenoid. A number of possible causes are considered below.

a) Movement of the coil in the cyclotron field on reversal of the solenoid current; no movement was observed.

b) Perturbation of the cyclotron magnetic field by the field of the solenoid. This field could be as high as 10 gauss at the cyclotron target and might have affected (i) the energy of the proton beam (ii) the direction of incidence of the protons on the Be target or (iii) the part of the target struck by the proton.

These effects would be small but in this experiment where scattering was at small angles and the neutron counter was biassed close to the maximum neutron energy these effects could be important. The following tests were therefore made as a result of which an upper limit of -0.004 ± 0.002 can be placed on any spurious asymmetry from these effects.

(i) The neutron counter was placed on the edge of the direct neutron beam where the counting rate was very sensitive to change in the position of the beam. Changing the direction of solenoid field produced a counting rate change which corresponded to a beam shift of $.03 \pm .03$ mm. This would have given rise to a false asymmetry of less than -0.00017.

(ii) The counter was also placed fully in the direct beam where it would be more sensitive to spectrum changes than to movement of the beam. Counting rate as a function of the direction of the solenoid field was again measured and from these measurements an asymmetry of -0.004 ± 0.002 was calculated. If it were assumed that there was no beam shift then the measurements in (i) above are an additional check on the possibility of spectrum changes. The asymmetry calculated from these measurements was -0.01 ± 0.01.

(iii) A BF_3 slow neutron counter situated approximately half way between the first and second scatterer was used as a monitor for the above experiments. Its performance was later compared with that of a three crystal coincidence telescope which detected high energy recoils from a 1 cm thick polythene scatterer placed in the direct neutron beam. The polythene scatterer was placed after the solenoid and so that the telescope counting rate should be independent of beam polarization it was placed in the horizontal plane.

Under these conditions a proton counting rate asymmetry of 0.0007 ± 0.003 was observed from which it is concluded that within the limits of measurement the BF_3 chamber is a reliable monitor.

c) Effect of the solenoid field on the neutron counter: the neutron counter was 13 m from the solenoid and at this distance the field is negligibly small.

d) Incorrect amount of precession of the neutrons:

(i) It is easily shown that the integrated field along any line parallel to the axis of the solenoid is exactly $H_0 l_0$ (see Appendix for definition of H_0 and l_0) so that the precession is independent of the path of the neutron through the solenoid.

(ii) The solenoid current was manually maintained constant to better than 0.5% so that the effect of current variations is entirely negligible.

(iii) In the experiment reported here the energy spread in the neutrons detected was from 85 MeV to 120 MeV. For a given solenoid field it is only possible to precess neutrons of one discrete energy by exactly 90°. For neutrons in the above energy range the precession angles extended from 96° to 79° but as it is the projected spin vector that is important this spread in angles is not serious. Moreover, if the effective neutron energy spectrum is known an exact correction can be made. This correction amounts to 0.5% of the value of the observed asymmetry at the correct solenoid current. At solenoid currents removed from the exact value for 90° precession the correction for spread in neutron energies is even smaller.

e) Effects of components of field not parallel to the axis of the solenoid: there will be a radial component of the field at the ends of the solenoid and also a component of the field not parallel to the axis of the solenoid because of the method of construction of the solenoid. These fields will rotate the spin vectors out of the plane normal to the line of flight but the estimated effect on the asymmetry is entirely negligible.

5. – Conclusion.

This method of measuring asymmetries has been found to work very well and no difficulties whatever have been experienced. It has also been used in some neutron-proton polarization experiments (to be published) where it was found to be much more satisfactory than the conventional method of asymmetry measurements used previously in a similar experiment.

It is perhaps of value to compare here the advantages and disadvantages of the solenoid with those of an electromagnet.

Advantages: *a*) The solenoid is easy to construct. *b*) A uniform field is automatically obtained over the cross section of the beam. *c*) If there is a spread of particle energies the two 90° precessions with a solenoid produce

a smaller spread of projected spins than a single 180° precession with an electromagnet. *d*) It could possibly be used in proton polarization experiments. Focussing effects of the solenoid magnetic field have then to be taken into account but as these do not affect the precession of the spin vectors and are the same for both directions of the solenoid field they should introduce no serious difficulty.

Disadvantages: *a*) The solenoid has rather larger power requirements. *b*) The solenoid cannot be used to rotate the spin vectors into or out of the beam direction as envisaged by WOLFENSTEIN [5] for triple scattering experiments.

* * *

We wish to extend our grateful thanks to the Special Plant Maintenance staff at A.E.R.E. for their help in the installation of the equipment and especially to Mr. G. PEAGRAM who contributed so much to the design and construction of the solenoid. Our thanks go to Prof. R. WILSON and Dr. R. VOSS for valuable discussions and loan of equipment; to the cyclotron crew for their cheerful co-operation and to Mr. F. URIDGE for helping with the experiment.

APPENDIX

Details and Design Features of the Solenoid.

It can easily be shown that

$$\int_{-\infty}^{\infty} \boldsymbol{H}\cdot d\boldsymbol{l} = l_0 H_0 ,$$

where l_0 is the length of the solenoid under consideration and $H_0 \quad 4\pi nI/10$ is the field at the centre of an infinite solenoid. n = number of turns per centimeter and I = current in amperes.

Hence for 100 MeV neutrons we require an integrated field

$$l_0 H_0 = \frac{vh}{4g\mu_n(1-\beta^2)^{\frac{1}{2}}} ,$$

or, if $N = l_0 n$,

we require $\quad NI = \dfrac{v}{1.46\cdot 10^4(1-\beta^2)^{\frac{1}{2}}}$ ampere turns $= 9.7\cdot 10^5$ ampere turns.

---

[5] L. WOLFENSTEIN: *Phys. Rev.*, **96**. 1654 (1954).

Space set a limit of 11 feet on the length of the coil and a readily available generator capable of providing 1 250 A at 60 V fixed the resistance. The coil was made from copper discs soldered together to form a single layer stepped spiral. 950 discs were stamped out of 0.125 inch electrical copper sheet. The disc had an outside diameter of 5 inches, a concentric hole 1.875 inches in diameter and a radial saw cut. Each disc was rotated 18° with respect to the previous one and the overlapping region between the sawcuts was soldered together to provide a coil of 903 turns. Spacers made of 0.003 inch polytetrafluoroethylene provided electrical insulation and prevented the solder from running into unwanted places. The coil was held rigid by Tufnol spacers and enclosed in a brass water jacket of 7 inches outside diameter. A heavy beryllium-copper spring and flexible electrical leads allowed for thermal expansion of the coil. Its weight was approximately 1 000 lbs. For cooling, demineralized water was circulated at the rate of 12 gallons per minute in direct contact with the solenoid winding. Under these conditions the temperature rise of the water was less than 15 °C and there was a maximum leakage current of 1.5 A to the case, the direction of this current being arranged to avoid depositing metal in the small gaps between the turns of the solenoid. This was in any case expected to be small. Power consumption at 1 200 A was 47 kW.

The field inside the solenoid was measured with a search coil and fluxmeter and found to be within 1 % of the calculated field and it increased linearly with current within the limits of the accuracy of measurement.

RIASSUNTO (*)

È stato costruito un solenoide di 11 piedi di lunghezza e con un numero massimo di $1.14 \cdot 10^6$ amperespire che permette di ruotare di 90° sulle due direzioni il piano di polarizzazione di un fascio di neutroni. Ciò permette di eseguire negli esperimenti di polarizzazione dei neutroni delle misure di asimmetria senza muovere l'apparecchiatura di rivelazione. Questo offre grandi vantaggi negli esperimenti in cui gli effetti di polarizzazione sono piccoli e le false asimmetrie, che possono nascere movendo il rivelatore, sono corrispondentemente difficili da eliminare con sufficiente esattezza. Il metodo è stato sperimentato usando il fascio di neutroni parzialmente polarizzato prodotto nel ciclotrone di Harwell con un bersaglio di berillio. Le misure di asimmetria sono state eseguite contando i neutroni diffusi ad un angolo di $\frac{1}{3}$° per mezzo di un diffusore di uranio. Furono impiegati quattro valori della corrente nel solenoide e i risultati ottenuti sono in buon accordo con quelli prevedibili teoricamente.

(*) *Traduzione a cura della Redazione.*

IL NUOVO CIMENTO Vol. IV, N. 1 1° Luglio 1956

An Attempt in the Theory of Elementary Particles.

T. Tati

Physics Department, Kanazawa University - Kanazawa, Japan

(ricevuto il 18 Aprile 1956)

Summary. — A quantum mechanical formulation of the fundamental law of Nature without using the space-time co-ordinates is presented. Matter is composed of various kinds of particles, each kind of which has the co-ordinate spaces characterized by the intrinsic quantities (m, σ) of the particle. (The co-ordinate space characterized by the mass m is the four dimensional momentum space of the particles of mass m). Probability amplitudes are functionals of the numbers of particles specified by their kind (m, σ) and co-ordinates. Phenomena are the transitions between the particles. The causality principle in our theory is the principle of the existence of the $\mathcal{W}$-matrix. The element $\mathcal{W}_{ji}$ means the probability of finding the state i in the observation O_1 of the observable Ω_1, and then the state j in the observation O_2 of the observable Ω_2, when we observe the system characterized by an operator $\mathcal{H}$; and $\mathcal{W}$ has the form $\mathcal{W} = C(O_1; O_2)W[\mathcal{H}, \Omega_1, \Omega_2]$, where W is the matrix determined by $\mathcal{H}$, Ω_1 and Ω_2, and C is the undetermined quantity independent from $\mathcal{H}$, Ω_1 and Ω_2. From this causality principle, we introduce $T(\boldsymbol{p})$ using an ideal $\boldsymbol{p}$-meson clock. Then the undetermined $C(O_1, O_2)$ is expressed as $C(O_1, O_2) = (2\pi/\hbar)T(\boldsymbol{p})$ with a universal constant $\hbar$ which has a dimension of [energy]·[T]. The formulation is described keeping the relation to the current theory as close as possible.

1. – Introduction.

Space and time were introduced in the theory of physics as geometrical co-ordinates to describe the motion of bodies quantitatively. The theory of relativity has enriched the contents of space-time and has bestowed on space-time the electromagnetic field quantities which are defined at each point of

its four-dimensional continuum and governed by field equations. The relativistic quantum field theory resulted from the combination of the quantum theory and the theory of relativity, gives a view of the world i.e. matter is composed of various kinds of elementary particles, they are created from and annihilated into vacuum. And phenomena in Nature are composed of these creations and annihilations. Elementary particles are described by quantized field quantities which are bestowed on space-time and governed by interacting field equations. In the field theory, matter is dissolved into an attribute of space-time and we may say figuratively that natural phenomena are complicated oscillations of space-time or in other words, the vacuum contains all the natural laws.

The relativistic quantum field theory is very successful in describing the nature and it is needless to say here of its great merits. However, as is well known, serious difficulties have appeared. The field theory which based on the four-dimensional continuum of space-time compels us to introduce the spatial extensions of elementary particles, while we can not do it consistently. Since the field theory has attributed the structure of the world to the structure of the space-time, it is evident that its difficulties are intimately related to the structure of space-time. The field theory is now in a stage where we have to reconsider about the concept of space-time which has remained unchanged when the classical theory has been reformed by the quantum mechanics. Phenomena—objects of our observations—are the changes of matter or in atomistical words, the transitions of elementary particles. The concept of space-time generates only in the case where the numerous transitions of elementary particles are observed, and has a similar character with the temperature of gases. The field theory seems to confer too substantial contents on space-time.

It is the purpose of this paper to discuss the possibility to formulate the fundamental law of interactions between elementary particles without using the concept of space-time. If this formulation could be done, space-time would become a statistical concept which could be expressed as a mean value of some sort, of more fundamental quantities in the numerous transitions of elementary processes which are governed by laws of quantum mechanical probabilities, in an analogous way that the thermodynamical quantities are expressed in the statistical mechanics as mean value of more fundamental quantities. And field equations would be derived having like character as thermodynamical equations.

In order to try to formulate the fundamental law independent from space-time, we have to tear ourselves away from the field theory hoping to get back there with a new point of view. An attempt and a program for a theory following these ideas are presented in this paper.

2. – Outline of the Field Theory.

We will outline here the construction of the quantum field theory [1] for comparison with our theory. The variables in the field theory are the field quantities of various kinds $k = 1, 2, \ldots$ of elementary particles

$$Q_{k\alpha}(x_\mu) , \tag{1}$$

Q's are covariant quantities which have several components in the Minkowski space and isotopic spin space, and are functions of space-time point $x_\mu(x, y, z, ict)$, and the transformation characters of Q's are related to the observable quantities of the elementary particles i.e. spin and isotopic spins. The existence of the relativistic invariant Lagrangian density,

$$L\left[Q_{k\alpha}(x_\mu),\ \frac{\partial}{\partial x_\mu} Q_{k\alpha}(x_\mu)\right] , \tag{2}$$

is assumed. The field equations are derived from $\delta \int L \, \mathrm{d}^4x = 0$, as Euler's equations,

$$\frac{\partial L}{\partial Q_{k\alpha}} - \sum_\mu \frac{\partial}{\partial x_\mu} \frac{\partial L}{\partial (\partial Q_{k\alpha}/\partial t)} = 0 . \tag{3}$$

The variables, canonical conjugates to $Q_{k\alpha}$, are derived by

$$P_{k\alpha} = \frac{\partial L}{\partial (\partial Q_{k\alpha}/\partial t)} , \tag{4}$$

and Hamiltonian density,

$$H = \sum P_{k\alpha} \frac{\partial Q_{k\alpha}}{\partial t} - L , \tag{5}$$

is constructed. Quantization is carried out by analogy with the quantum mechanics of particle systems. But this analogy is not complete, because we must assume anticommutation relations for Fermi fields. This incompleteness seems to suggest us the limits of the validity of the concept of fields. The commutation relations are determined in the forms

$$\begin{cases} [P_{k\alpha}(\boldsymbol{x}, t), Q_{l\beta}(\boldsymbol{x}'t)]_\pm = \text{const}\ \delta_{kl}\delta_{\alpha\beta}\delta(\boldsymbol{x} - \boldsymbol{x}') , \\ [Q_{k\alpha}(\boldsymbol{x}, t), Q_{l\beta}(\boldsymbol{x}'t)]_\pm = [P_{k\alpha}(\boldsymbol{x}t), P_{l\beta}(\boldsymbol{x}'t)]_\pm = 0 . \end{cases} \tag{6}$$

---

[1] W. Heisenberg and W. Pauli: *Zeits. f. Phys.*, **56**, 1 (1929); **59**, 168 (1930).

The probability amplitude,

$$\Psi[Q'_{k\alpha}(\boldsymbol{x}), t] , \tag{7}$$

is determined by the Schrödinger equation

$$i\hbar \frac{\partial}{\partial t} \Psi = \int H \, \mathrm{d}^3x \Psi . \tag{8}$$

The relativistic invariance of the theory is proved. The formulation of the modern covariant field theory (2) which has changed completely the style of the field theoretical calculations is derived from the above mentioned old theory. For convenience of comparison with our theory, we adopted the Schrödinger representation.

The field theory is now regarded as the fundamental theory of nature and gives successfully:

1) the description of the double nature of wave and particle of elementary particles,

2) the explanation of the existence of the relation between statistics and spin of elementary particles,

3) the heuristic description of properties of forces carried by elementary particles (e.g. the Coulomb potential and the Yukawa potential).

4) the method of calculation of transition probabilities in the interactions between elementary particles,

5) the concept of field reactions (e.g. explanations of the Lamb-shift and the anomalous magnetic moment of the electron in the Tomonaga-Schwinger theory), and some hope for the problem of bound states.

It is clear that we use, as a heuristic method, the concept of the field also in future physics. But we want in this paper to eliminate the concept of space-time from the fundamental law of nature and we hope to give a sort of statistical character to the field.

3. – A Tentative Description of the Fundamental Law of Elementary Particles.

3·1. *Fundamental co-ordinates and variables.* – Since we can not pass through the process of the quantization of the classical fields, we will try to describe

(2) S. Tomonaga: *Progr. Theor. Phys.*, **1**, 27 (1946); *Phys. Rev.*, **74**, 224 (1948); J. Schwinger: *Phys. Rev.*, **73**, 416 (1948); **74**, 1439 (1948); R. P. Feynman: *Rev. Mod. Phys.*, **20**, 367 (1948); *Phys. Rev.*, **76**, 749, 769 (1949); F. J. Dyson: *Phys. Rev.*, **76**, 749 (1949).

the interactions of elementary particles as directly as possible. We assume at the beginning the existence of elementary particles of which Nature is composed and which we are able to count. The same kind of the particles are assumed to be identical and not distinguishable. We start from the particle and hence from the quantum theory.

In this paper, variables mean the quantities which specify the state of the system, and co-ordinates mean the quantities which specify the variables since we have many variables. The variables and the co-ordinates may change and increase in the course of the progress of physics ([3]). In a first step towards desired theory, we want to preserve the relation to the current theory as close as possible and use the quantities which are already familiar with us, although we are free to choose variables and co-ordinates in so far as they specify the state and are independent from space-time.

We adopt in this paper as fundamental co-ordinates, the quantities $s(\sigma)$ which stand for co-ordinates of spin, isotopic spin, etc., and the momentum $p(m)$ of the elementary particles, and as variables the number $n_k(s, p)$ of elementary particles $k(\sigma, m)$ specified by the intrinsic quantities σ and m. Then the probability amplitudes are given by the functional

$$\Psi[n'_k(s, p)] \,. \tag{A}$$

p forms a four vector $(\boldsymbol{p}, p_0) = (p_1, p_2, p_3, p_4 = ip_0)$ with $p_0 = \sqrt{\boldsymbol{p}^2 + m^2c^4}$ in a four dimensional space which we will discuss in the next section. m is the mass of the elementary particle.

Here already we meet with a difficult problem. We do not know whether in the future theory, the mechanical mass can be calculated from the observed mass or if it disappears completely. The former expects that we can calculate the neutron proton mass difference in the future theory and the latter anticipates that the future theory is the description of the relations between only the observed quantities. We take the former standpoint in this paper to keep the intimate correspondence to the existing perturbation theory of the field reactions. Hence, n is the number of bare particles and m is the mechanical mass.

The concept of the energy and momentum is derived in mechanics using the concept of space and time. But the energy-momentum of the elementary particle is considered to be more fundamental and substantial than the space-time localization of the elementary particle. There exist conservation laws concernig energy-momentum. In our theory p in (A) must be considered

([3]) A. Pais: *Physica*, **19**, 869 (1953); M. Gell-Mann: *Phys. Rev.*, **92**, 833 (1953); T. Nakano and K. Nishijima: *Progr. Theor. Phys.*, **10**, 581 (1953); K. Nishijima: *Progr. Theor. Phys.*, **12**, 107 (1954).

to be more intrinsic to the elementary particles than is considered in the field theory. Figuratively speeking, p is the colour of the elementary particles although in general two observers may observe it as different colours. In the future theory p may be derived from a more fundamental quantity which we do not know at present. The meaning of our co-ordinates becomes more clear in the next Sect. 3·2.

It is needless to say that our theory is different from the theory of the second quantization starting from the particle aspect. In the foundation of our theory, we have not the Schrödinger equation containing time as we will mention in Sect. 3·4.

3·2. *Co-ordinate spaces.* – In the theory of elementary particles, we have the isotopic spin space which is independent from our Minkowski space. The isotopic spin space has been constructed to describe the isotopic spins which are intrinsic to the elementary particles. The importance of the isotopic spin space has very much increased recently in the description of the interactions between various new particles [3]. We can not move in the isotopic spin space but even in the field theory this space is postulated. In like manner, we introduce and postulate independently from space-time the co-ordinate spaces.

Our co-ordinate spaces mean the spaces which are introduced to describe the co-ordinates which specify the variables n. The kind k of elementary particles is specified by the intrinsic quantities m and σ where m is the mass and σ stands for $\sigma^{(1)}$, $\sigma^{(2)}$ ... $\sigma^{(f-1)}$, where $\sigma^{(1)}$ is the magnitude of isotopic spin, $\sigma^{(2)}$ is the magnitude of ordinary spin, etc. Each kind of elementary particles has f intrinsic spaces,

$$(\mathrm{A}_1) \qquad \Sigma^{(m)}(m)\,, \qquad \Sigma^{(1)}(\sigma^{(1)})\,, \qquad \Sigma^{(2)}(\sigma^{(2)})\,, \quad \ldots\,, \quad \Sigma^{(f-1)}(\sigma^{(f-1)})\,.$$

$\Sigma^{(1)}$ is constructed from isotopic spin matrices. We have three isotopic spin matrices T_1, T_2 and T_3, and the commutation relations between them. The isotopic spin state is determined by $\sigma^{(1)}$ and $s^{(1)}$ where $\sigma^{(1)}(\sigma^{(1)}+1)$ and $s^{(1)}$ are eigenvalues of $T_1^2 + T_2^2 + T_3^2$ and T_3. $\sigma^{(1)}$ is an intrinsic quantity of the particle and the space $\Sigma^{(1)}(\sigma^{(1)})$ is characterized by $\sigma^{(1)}$ i.e.

$$(\mathrm{A}_2) \qquad \Sigma^{(1)}(\sigma^{(1)}) = \left\{ s^{(1)};\ |s^{(1)}| \leqslant \sigma^{(1)} \right\} = (\sigma^{(1)},\ \sigma^{(1)}-1,\ \sigma^{(1)}-2,\ \ldots -\sigma^{(1)});$$

$\Sigma^{(2)}(\sigma^{(2)}) = \left\{ s^{(2)};\ s^{(2)} | \leqslant \sigma^{(2)} \right\}$ is constructed in similar way to $\Sigma^{(1)}(\sigma^{(1)})$. $\Sigma^{(1)} = \left\{ s^{(1)} \right\}$ and $\Sigma^{(2)} = \left\{ s^{(2)} \right\}$ are the assemblies of the discrete points.

$\Sigma^{(m)}(m)$ is the assembly of the points p_μ, which lies on the surface $p_1^2 + p_2^2 + p_3^2 + p_4^2 = -m^2c^4$, which is characterized by m in a four dimensional

p_μ space, i.e.

$$(A_3) \qquad \Sigma^{(m)}(m) = \{p_\mu;\ p_1^2 + p_2^2 + p_3^2 + p_4^2 = -m^2c^4\}.$$

$\sigma^{(1)}$, $\sigma^{(2)}$, $\Sigma^{(1)}$ and $\Sigma^{(2)}$ are derived from more fundamental spin and isotopic spin matrices. In like manner, m and $\Sigma^{(m)}$ will be derived in future theory from more fundamental quantities and m's will be the discrete eigenvalues of some quantity. It will be a central problem in the future theory to derive $\Sigma^{(m)}$ from more fundamental quantities and to obtain the relations between $\Sigma^{(i)}$'s.

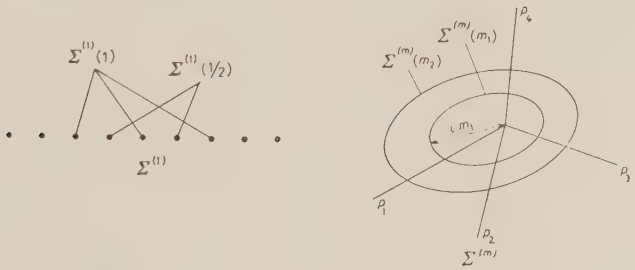

The illustration of the co-ordinate spaces.

We postulate the invariance of the theory with respect to the rotation of the p_μ-space. We expect that the relation between the Minkowski space and our p_μ-space will become clear after we construct the space-time from our fundamental law mentioned in Sect. 3·4.

3·3. *Hamiltonian.* – The densities in space-time of any quantities are not given to our theory at the beginning, but the Hamiltonian operator which represents the total energy of the system is given to us. We assume the existence of the Hamiltonian. Our Hamiltonian has not the meaning of the displacement operator in its basic character. The Hamiltonian may be replaced by a more fundamental quantity but we here again use the most familiar quantity.

We must be able to construct the Hamiltonian without the knowledge of the Lagrangian density. We introduce creation and annihilation operators $a_k^*(s, \boldsymbol{p})$ and $a_k(s, \boldsymbol{p})$ which satisfy

$$(B) \qquad \begin{cases} [a_k^*(s\boldsymbol{p}),\ a_l\,(r\boldsymbol{p}')]_\pm = \delta_{kl}\,\delta_{sr}\,\delta(p - p')\,, \\ [a_k^*(s\boldsymbol{p}),\ a_l^*(r\boldsymbol{p}')]_\pm = [a_k(s\boldsymbol{p}),\ a_l(r\boldsymbol{p}')]_\pm = 0\,, \\ n_k(s\boldsymbol{p}) = a_k^*(s\boldsymbol{p})a_k(s\boldsymbol{p})\,, \end{cases}$$

where $+$ for Fermi particles,

$-$ for Bose particles.

The Hamiltonian is assumed to have the form ,

$$\mathcal{H} = \sum n_k(s\boldsymbol{p})p_0 + \mathcal{H}_I \,. \tag{C}$$

We have to construct $\mathcal{H}_I$ after consultation with the observations of interactions. Even in the field theory, we can not construct interaction Hamiltonian density (or Lagrangian density) uniquely from the basic quantities of the elementary particles which participate in the interaction. Instead of the relativistic invariance which is a guiding principle to construct the interaction Hamiltonian density in the field theory, we have in our theory the invariance with respect to the rotation of the p_μ-space.

$\mathcal{H}_I$ has the form

$$\mathcal{H}_I = \sum \mathcal{A} \cdot G \,, \tag{D}$$

where $\mathcal{A}$ is a product of several creation and annihilation operators, and G is a function of co-ordinates which appear in $\mathcal{A}$. If we put $G = \delta(\sum \boldsymbol{p}) \cdot F$, choosing an appropriate function F, our G is reduced to the interaction Hamiltonian of the local field theory in the Schrödinger representation. We do not know at present the form of the function G. In our theory, the function G is considered to be determined only by the future observations (probably extremely high energy experiments), and at present we are free to presume the form of the G-function from the consistency of the theory. The difference between the theory of non-local interactions and ours is in that we have not space-time in the foundation of the theory and are not curbed by the space-time.

3·4. *Fundamental Law.* – Our theory is based on the quantum mechanical descriptions of observations (4). But since our observers have neither a rule nor a clock, equations of motion of the quantum mechanics are of no use for them. They can only distinguish the particles specified by the co-ordinates s and $\boldsymbol{p}$ and count them, and distinguish the order—of before and after—between two observations. Then, we want to give them laws in the sequence of two observations O_1 and O_2 using only the quantities appeared in (A), (B), (C) and (D). The postulates of the laws are given in following two cases separately. The observables in O_1 and O_2 are denoted by Ω_1 and Ω_2.

1) When Ω_1 is commutable with $\mathcal{H}$:

In this case, Ψ remains unchanged between O_1 and O_2. If the result in O_1 is ω, the expectation value of Ω_2 is given by

$$\langle \Psi_\omega | \Omega_2 | \Psi_\omega \rangle \,, \tag{E}$$

where $\Omega_1 \Psi_\omega = \omega \Psi_\omega$.

(4) P. A. M. Dirac: *The Principles of Quantum Mechanics* (Oxford, 1935).

2) When Ω_1 is not commutable with $\mathcal{H}$:

In this case our principal interest is in the transition of Ψ.

We postulate that the ratios $\mathcal{W}_{ji}/\mathcal{W}_{lk}$ $(i, j, k, l=1, 2, \ldots)$, where $\mathcal{W}_{ji}$ are the probabilities of finding the state i in O_1 and then the state j in O_2, are determined a priori, or in other words the matrix $\mathcal{W}$ has the form

$$\mathcal{W}[O_1, O_2; \mathcal{H}, \Omega_1, \Omega_2] = (C(O_1, O_2)W_{ji}[\mathcal{H}, \Omega_1, \Omega_2]) \,, \tag{F}$$

where W_{ji} is the quantity determined by $\mathcal{H}$, Ω_1 and Ω_2, and independent from O_1 and O_2; and C depends on O_1 and O_2, and is independent from $\mathcal{H}$, Ω_1 and Ω_2. This postulate (F) is the causality principle in our theory for the observer who has no clock. (O_1 and O_2 must satisfy certain conditions.)

Our law must give the method of the calculation of W. We restrict ourselves to the most important case,

$$\Omega_1 = \Omega_2 = \mathcal{K} \,, \tag{G$_1$}$$

where $\mathcal{K}$ represents the total Hamiltonian of the free observed (renormalized) particles. The extension to more general cases will not be difficult. We assume that we can separate $\mathcal{H}$ into two parts

$$\mathcal{H} = \mathcal{K} + (\mathcal{H} - \mathcal{K}) \,, \tag{G$_2$}$$

and

$$\mathcal{K}\Phi_i = E_i\Phi_i \,.$$

In practice, it is difficult to give $\mathcal{K}$ explicitely, but this difficulty is not characteristic of our theory. In principle, we can assume the existence of $\mathcal{K}$. Then, we postulate that W is given by the equations

$$W_{ji} = |\langle \Phi_j | \mathcal{H} - \mathcal{K} | \Psi_i^+ \rangle|^2 \delta(E_i - E_j) \,, \qquad (i \neq j) \tag{G$_3$}$$

where Ψ_i^+ is determined from

$$\Psi_i^+ = \Phi_i + \frac{1}{E_i - \mathcal{K} + i\varepsilon}(\mathcal{H} - \mathcal{K})\Psi_i^+ \,.$$

The description of our laws may be full of obscurities—e.g. conditions on O_1 and O_2—which are considered to be cleared in the developement of the theory. formulae in (G) are suggested from the scattering theory [5] and in future

[5] B. A. Lippman and J. Schwinger: *Phys. Rev.*, **79**, 469 (1950); C. Møller: *Kgl. Danske Videnskab. Selskab. Mat.-fyz. Medd.*, **23**, No. 1 (1945); M. Gell-Mann and M. L. Goldberger: *Phys. Rev.*, **91**, 398 (1953).

the postulate (F) may be expressed by another formula; but we want to say that we can calculate $\mathcal{W}$ except $C(O_1, O_2)$, from the quantities appeared in (A), (B), (C) and (D).

The matrix $\mathcal{W}$ has a similar character with Heisenberg's S-matrix [6]. But $\mathcal{W}$ contains the undetermined quantity $C(O_1, O_2)$ and has not the meaning of a transformation function.

4. – Introduction of Time and Determination of $C(O_1, O_2)$.

The introduction of the concept of time becomes necessary in order to make our fundamental law (F) useful. Time is introduced when we give a clock to our observer.

A figurative example of our clock may be a number of mesons which have the same co-ordinate $\boldsymbol{p}$. In the sequence of the observations O_0, O_1, O_2, ..., our observer is assumed to be able to count the numbers of mesons N_0, N_1, N_2, ..., in the clock simultaneously with each observation of O_0, O_1, O_2, ... Then, he can give the numbers $\tau(\boldsymbol{p}) \log N_0/N_0$, $\tau(\boldsymbol{p}) \log N_0/N_1$, $\tau(\boldsymbol{p}) \log N_0/N_2$, ... to O_0, O_1, O_2, ... respectively. The number $\tau(\boldsymbol{p}) \log (N_0/N_2) - \tau(\boldsymbol{p}) \log N_0/N_1$ corresponds to the time between two observations O_1 and O_2. The greater the number of mesons, the more exact the clock. $\tau(\boldsymbol{p})/C(O_1, O_2)$ is calculated from (F) and (G), and depends on the kind of mesons in the clock. Hence the number, which the clock gives to the observations, has a dimension. The dependence of $\tau(\boldsymbol{p})$ on $\boldsymbol{p}$ leads us to the delay of a clock in the theory of relativity. This is a problem of the next paper which is hoped to appear in near future.

There will be a more appropriate and more correct clock than the above mentioned one. However, it will be evident that any clock must involve the observations of numerous transitions governed by a probability matrix $\mathcal{W}$. For this reason, wewant to say that time is a statistical quantity.

Practically we can never construct any absolutely exact clock. The time co-ordinate fluctuates. An ideal clock must involve an infinite number of transitions which our observer can observe at the same time. Moreover the operators $\mathcal{H}$, Ω_1 and Ω_2 are very complicated ones in practical observations. They must contain the operators representing the effects of the apparatus for observations. Similar circumstances are found in the cases of determination of the temperature of gases. Temperature depends on the thermometer which are used to measure it. The thermodynamics introduced the temperature measured by the thermometer of an ideal gas.

In an analogy to the device of the thermodynamics we introduce an ideal

---

[6] W. Heisenberg: *Zeits. f. Phys.*, **120**, 513, 673 (1943).

$\boldsymbol{p}$-meson clock which is composed of infinite ideal mesons which have the same co-ordinates $\boldsymbol{p}$. The ideal clock gives numbers,

$$\text{(H)} \qquad T_0(\boldsymbol{p}), \quad T_1(\boldsymbol{p}), \quad T_2(\boldsymbol{p}), \quad \ldots$$

respectively to each of the observations O_0, O_1, O_2, ..., in a similar way as the before mentioned meson clock gives them the numbers $\tau(\boldsymbol{p}) \log N_0/N_0$, $\tau(\boldsymbol{p}) \log N_0/N_1$, ..., respectively. Then O_n is characterized by $T_n(\boldsymbol{p})$. It will be clear from the considerations of our meson clock that:

h_1) only the ratios $T_n(\boldsymbol{p})/T_m(\boldsymbol{p})$ $(n, m = 1, 2, \ldots)$ are determined, hence T has a dimension,

h_2) only the differences $T_n(\boldsymbol{p}) - T_m(\boldsymbol{p})$ $(n, m = 1, 2, \ldots)$ have a physical meaning,

h_3) the element of $\mathcal{W}$ is proportional to $T(\boldsymbol{p}) = T_2(\boldsymbol{p}) - T_1(\boldsymbol{p})$.

Now, we can determine $C(O_1, O_2)$ to give an unique value to $\mathcal{W}$, using $T(\boldsymbol{p})$. $C(O_1, O_2)$ is the function of $T(\boldsymbol{p})$ from h_2), and is proportional to $T(\boldsymbol{p})$ from h_3), i.e.

$$\text{(I)} \qquad C(O_1, O_2) = \gamma T(\boldsymbol{p}) \,.$$

The causality principle (F) demands γ to be an universal constant. From h_1), $T(\boldsymbol{p})$ has a dimension [T]. $\mathcal{W}$ is dimensionless by definition. From (G), the W matrix in (F) has the dimension of energy. Hence γ must have a dimension of inverse of [energy]·[T], and we can put

$$\text{(I}_1\text{)} \qquad \gamma = 2\pi/\hbar \,,$$

where $\hbar$ is an universal constant of dimension of [energy]·[T]. Now, we have a matrix the elements of which have unique values

$$\text{(I}_2\text{)} \qquad \mathcal{W}[T(\boldsymbol{p}); \mathcal{H}, \Omega_1, \Omega_2] = (2\pi/\hbar) T(\boldsymbol{p}) W[\mathcal{H}, \Omega_1, \Omega_2] \,,$$

$\mathcal{W}(1)$ is a matrix of transition probabilities per unit $T(\boldsymbol{p})$.

$\hbar$ appears in our theory when we construct T from the postulates (F) and (G).

5. – A Program for Further Investigations.

If we identify our co-ordinate $\boldsymbol{p}$ to the momentum of the particle, $\tau(\boldsymbol{p})$ to the life time of $\boldsymbol{p}$-mesons, $2\pi\hbar$ to the Planck constant and the function G in (D) to appropriate function, for the descriptions of the elementary process

there is no difference in practice between the current theory and ours. It will be a characteristc of our theory that we can chose the function G so as to avoid the unwanted infinities. The theory of relativity will not prevent our choice of G seriously, because in our theory, space-time is a derivable concept. The restriction in our theory is the invariance with respect to the rotation of p_μ-space.

In our theory, the wave nature of the particle is considered to be a statistical nature and to be studied with the introduction of the space co-ordinates into our theory.

We want to present a program for further investigations before we finish this article.

1) Introduction of the co-ordinates ($XYZT$). T has been already introduced in our theory. The universal constants h and c will play an important rôle when we introduce X, Y and Z. The invariance property of the theory in p_μ-space will imply the invariance property in ($XYZT$) or X_μ-space. (Lorentz-transformation).

2) Construction of the Schrödinger equation containing T and the field equations, in X_μ-space.

3) Construction of our covariant theory in p_μ-space. The field theory has achieved a substantial progress by the covariant formulations. It is hoped that our theory will be constructed so as to reveal the covariance property in the p_μ-space as much as possible.

4) Investigation for the existence of the functions G which gives a finite theory and consistent with observations, in a covariant way in p_μ-s space.

5) Examination of the obscurities with which our theory might be filled.

6) Complete description of our fundamental law.

RIASSUNTO (*)

Si presenta una formulazione della legge fondamentale della natura per mezzo della meccanica quantistica senza far uso di coordinate spazio-temporali. La materia si compone di varie specie di particelle, ogni specie delle quali ha gli spazi coordinati caratterizzati dalle grandezze intrinseche (m, σ) della particella. (Lo spazio coordinato caratterizzato dalla massa m è lo spazio quadridimensionale degli impulsi delle parti-

(*) *Traduzione a cura della Redazione.*

celle di massa m). Le ampiezze di probabilità sono funzionali dei numeri di particelle specificate dalle loro specie (m, σ) e coordinate. I fenomeni sono le transizioni fra le particelle. Il principio di causalità è nella nostra teoria il principio dell'esistenza della matrice $\mathcal{W}$. L'elemento $\mathcal{W}_{ji}$ significa la probabilità di trovare lo stato i osservando O_1 dell'osservabile Ω_1, e poi lo stato j osservando O_2 dell'osservabile Ω_2, se osserviamo il sistema caratterizzato da un operatore $\mathcal{H}$, e $\mathcal{W}$ ha la forma $\mathcal{W} = C(O_1 ; O_2) W[\mathcal{H}, \Omega_1, \Omega_2]$, dove W è la matrice determinata da $\mathcal{H}$, Ω_1 e Ω_2. Partendo da questo principio di causalità, introduciamo $T(\boldsymbol{p})$ servendoci di un orologio a mesoni $\boldsymbol{p}$ ideale. Allora il $C(O_1, O_2)$ indeterminato risulta espresso da $C(O_1, O_2) - (2\pi/\hbar) T(\boldsymbol{p})$ con una costante universale $\hbar$ che ha la dimensione di [energia]·[T]. La descrizione della formulazione si ottiene per quanto possibile alla teoria corrente.

On the Electron Capture Decay Energy of $^{153}_{64}$Gd.

R. K. Gupta and S. Jha

Tata Institute of Fundamental Research - Bombay

(ricevuto il 25 Aprile 1956)

Summary. — The summing technique in a scintillation spectrometer has been used to determine the electron capture decay energy of ^{153}Gd. The decay energy is 225^{+18}_{-13} keV. The internal conversion coefficients of the 102 keV γ-ray have been measured in the scintillation spectrometer. The K conversion coefficient of this γ-ray is 0.61 ± 0.03 and $K/(L+M) \sim 5$. It has been estimated that about 25% of the transitions go to the ground state of ^{153}Eu.

1. – Introduction.

It has been shown by Brysk and Rose [1] and Robinson and Fink [2] that a reliable value for the electron capture decay energy, when it is small, can be obtained from the ratio of the L and K electron captures. When the electron capture leads to the ground state only, one can obtain the decay energy only if the L fluorescence yield in the daughter atom is known. When, however, the electron capture decay leads to the excited states, and the decay scheme is accurately known, this method gives the decay energy even if the L fluorescence yield in the daughter atom is not known. In this case, one can find the total number of electron captures from the intensity of the γ-rays and their internal conversion coefficients, and the numbers of K captures from the intensity of K X-ray, the K conversion coefficient of γ-rays and the K fluorescence yield in the daughter atom. The electron capture decay energy of ^{153}Gd has been found by this method.

---

(1) H. Brysk and M. E. Rose: *ORNL* 1830 (1955).
(2) B. L. Robinson and R. W. Fink: *Rev. Mod. Phys.*, **27**, 424 (1955).

2. – Our Present Knowledge of the Decay Scheme of ^{153}Gd.

^{153}Gd was studied by CORK *et al.* [3], who found that the electron capture in ^{153}Gd leads to the excited state of ^{153}Eu at 102 keV, resulting in the emission of a 102 keV γ-ray, of which the K/L conversion ratio was measured to be 5.2 ± 1.0. MCGOWAN [4] found that the electron capture in ^{153}Gd leads to the 102 keV state, which de-excites itself in about $3 \cdot 10^{-9}$ s. He reports that the electron capture leads, in addition, to another state within a few keV of the 102 keV state. The γ-ray from the decay of this state, according to him, is in prompt coincidence ($T_{\frac{1}{2}} < 10^{-9}$ s) with the K X-ray from the electron capture and is 1.4 times as intense as the 102 keV γ-ray.

The properties of the excited states of ^{153}Eu have been studied also from the β^--decay of 47 h ^{153}Sm. In this process, the excited states are shown to occur at 102 keV, 170 keV and 540 keV [4-6], and in very weak intensities at about 84 keV and 195 keV [6]. The Coulomb excitation of ^{153}Eu [7-9] shows the levels at 84 keV and 195 keV. The value of the K conversion coefficient of the 102 keV γ-ray is rather uncertain; it has been measured to be 0.62 ± 0.15 [5] and 1.14 ± 0.2 [4,6]. The value of the K/L conversion ratio of this γ-ray was found from the study of β^--decay of ^{153}Sm to be 6.2 ± 0.15 [5,6].

3. – Object of the Present Work.

Since the K conversion coefficient of the 102 keV γ-ray from the decay of ^{153}Gd is uncertain, the object was to determine the decay energy by a method, which does not involve the knowledge of the internal conversion coefficient. The coincidence study of the K X-ray and the γ-ray gives the decay energy without involving the conversion coefficients. The coincidence study has been made here with a single crystal in the scintillation spectrometer by the summing technique. In order to find the percentage of transitions to the ground state and the log ft values, the electron spectrum has been measured in the scintillation spectrometer with a stilbene crystal, and the conversion coefficients of the γ-ray have thus been measured.

---

[3] J. M. CORK, J. M. LE BLANC, W. H. NESTER and F. B. STEMPF: *Phys. Rev.*, **88**, 685 (1952).
[4] F. K. MCGOWAN: *Phys. Rev.*, **93**, 163 (1954).
[5] M. R. LEE and R. KATZ: *Phys. Rev.*, **93**, 155 (1954).
[6] N. MARTY: *Journ. Phys. et Rad.*, **16**, 163 (1955).
[7] N. P. HEYDENBURG and N. TEMMER: *Phys. Rev.*, **100**, 150 (1955).
[8] H. MARK and G. T. PAULISSEN: *Phys. Rev.*, **100**, 813 (1955).
[9] E. M. BERNSTEIN and W. W. LEWIS: *Bull. Am. Phys. Soc.*, Jan. 30 (1956).

4. – The Determination of the Electron capture Decay Energy.

4·1. *The Description of the Procedure.* – If P_L and P_K are the probabilities of the capture of L electrons and K electrons respectively, the decay energy of an electron capturing isotope is given by the relation [10,1]

$$\frac{P_L}{P_K} \simeq \frac{P_{L_1}}{P_K} = \left(\frac{\psi_{L_1}}{\psi_K}\right)^2 \left(\frac{W_0 + W_L}{W_0 + W_K}\right)^2 ,$$

where P_{L_1} is the probability of the capture of L_1 electrons, and ψ_{L_1}, ψ_K the wave functions of the L_1 and K electrons respectively at the nucleus, W_L and W_K are the L and K electron binding energies, and $(W_0 + 1)$ is the decay energy. This relation holds for the allowed transitions, but HOFF and RASMUSSEN [11] have shown that this relation also holds, in normal cases, for the transitions of the type $\Delta J = \pm 1$, yes, and perhaps also for those of the type $\Delta J = \pm 0$, yes.

For the determination of the ratio P_L/P_K, the radiations from ^{153}Gd were studied in a scintillation spectrometer [12] using a NaI(Tl) crystal, $1\frac{1}{2}''$ in diameter and $\frac{1}{2}''$ thick, having an aluminium oxide and aluminium cover of thickness, t, which was about 200 mg/cm^2. One can see from the decay scheme given in Fig. 3 that the crystal would receive from the radioactive source the K X-rays of ^{153}Eu due to the K electron capture, and also due to the K conversion of the 102 keV γ-ray. It would also receive the 102 keV γ-ray, some quanta of which would be in coincidence with the K X-ray arising from the K capture.

If N is the total number of disintegrations of ^{153}Gd leading to the 102 keV state, of which N_K decays by the capture of the K electrons and N_L by the capture of L electrons, so that $N = N_K + N_L$, then the number of the 102 keV γ-ray detected by the crystal, is

$$I_\gamma = N(1 - x)\varepsilon_\gamma S \exp\left[-\mu_\gamma t\right] ,$$

where S is the solid angle subtended by the source at the crystal, ε_γ is the intrinsic efficiency of detection of the γ-ray and $\exp\left[-\mu_\gamma t\right]$ the transmission of the γ-ray through the cover of the crystal and

$$x = \frac{\text{Total no. of conversion electrons}}{\text{Total no. of conversion electrons} + \text{no. of the 102 kev } \gamma\text{-ray}} .$$

(10) R. E. MARSHAK: *Phys. Rev.*, **61**, 431 (1942).
(11) R. W. HOFF and J. O. RASMUSSEN: *Phys. Rev.*, **101**, 280 (1956).
(12) R. K. GUPTA and S. JHA: *Nuclear Physics*, **1**, 2 (1956).

The number of the 102 keV γ-ray which falls on the crystal simultaneously with the 42 keV K X-ray arising from the K capture, causing a sum peak to appear at 144 keV is given by

$$I_{\gamma X} = N_K \omega_K (1 - x) S^2 \varepsilon_\gamma \varepsilon_X \exp[-\mu_\gamma t] \exp[-\mu_X t] ,$$

where ε_X is the efficiency of detection of the K X-ray and $\exp[-\mu_K t]$ is the transmission of the K X-ray through the cover of the crystal. Then

$$(N_K/N) = (I_{\gamma X}/I_\gamma)(1/\omega_K \varepsilon_X S \exp[-\mu_X t]) .$$

We have

$$(P_L/P_K) = \{1 - (N_K/N)\}/(N_K/N) .$$

Thus from the ratio of the areas of the sum peak and the γ-ray peak, P_L/P_K can be calculated. The value of ε_X is taken to be 1. The value of $S \exp[-\mu_X t]$ was found from the numerical integration of

$$\int \exp[-\mu_X t] = \tfrac{1}{2} \int \exp[-\mu_X t(\alpha)] \sin\alpha \, d\alpha ,$$

for each geometry.

The spectrum of the electromagnetic radiations from ^{153}Gd is reproduced in Fig. 1.

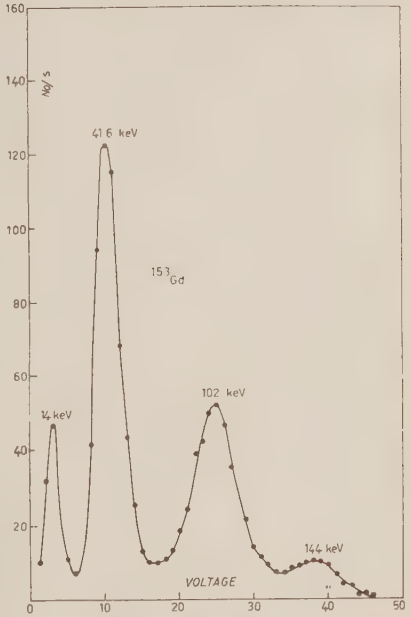

Fig. 1. - The pulse height spectrum of the electromagnetic radiations from ^{153}Gd with the scintillation spectrometer.

^{153}Gd was produced by the irradiation for four weeks at Harwell of 22 mg of spectroscopically pure Gd_2O_3. The radiations were studied after four months when short life activities had all died away. The spectrum shows four peaks at 14 keV, 42 keV, 102 keV and 144 keV. The peak at 14 keV is the escape peak due to the absorption of the 42 keV X-ray and the escape of the 28 keV iodine K X-rays from the crystal. The peak at 42 keV is due to the $_{63}$Eu K X-ray, and that at 102 keV is due to the γ-ray following the electron capture in ^{153}Gd. The peak at 144 keV arises from the simultaneous (within the pulse duration time of the spectrometer which is a microsecond) detection of the γ-ray and the K X-ray The spectra were taken with the source subtending three different solid angles at the crystal, and were repeated many times to give good statistics.

4·2. *Corrections.* – It was found experimentally that the area of the 14 keV escape peak was 24% of the area of the 42 keV K X-ray peak. One can see that some γ-ray pulses would sum up with the K X-ray pulses falling in the escape peak giving a sum peak at 116 keV, and that this sum peak area would be 24% of the area of the sum peak at 144 keV. The 144 keV sum peak area was therefore increased by 24% to give $I^*_{\gamma X}$. The measured area under the 102 keV peak gave I^*_γ. The γ-ray peak was shaped on the higher energy side to account for the escape sum peak, and on the lower energy side, the slope was made symmetrical. Thus the γ-ray peak was resolved from the sum peak of the two K X-rays, one arising in the K capture and the other in the K conversion of the γ-ray, this sum peak occuring at 84 keV. The ratio $I^*_{\gamma X}/I^*_\gamma$ was further corrected for the constant window width of the single channel analyser. The ratio $I^*_{\gamma X}/I^*_\gamma$ gives the finally corrected ratio $I_{\gamma X}/I_\gamma$ by the relation

$$I_{\gamma X}/I_\gamma = \frac{\left[E_\gamma/(E_\gamma + E_X)\right]^2 (I^*_{\gamma X}/I^*_\gamma)}{1 + \left[E_\gamma/(E_\gamma + E_X)\right]^2 (I^*_{\gamma X}/I^*_\gamma)},$$

where E_γ and E_X are the energies of the γ-ray and the K X-ray respectively.

4·3. *The Results.* – The results for the three solid angles are summarized below.

Solid angle	Observed sum peak area	$I^*_{\gamma X}$	I^*_γ	$Se^{-\mu_X t}$	$I_\gamma x/I_\gamma$	P_L/P_K
0.2890	421	522	2340	0.2310	0.1581 ± 0.005	$0{,}33 \pm 0.04$
0.3665	643	798	2894	0.2798	0.1884 ± 0.005	0.35 ± 0.04
0.4175	941	1166	3774	0.3062	0.2064 ± 0.006	0.35 ± 0.04

From these values of P_L/P_K, and taking the value of $(\psi_{L_1}/\psi_K)^2$ for $_{64}$Gd as 0.128 [1], and W_K for $_{63}$Eu as 0.91 [13], the value of the decay energy of ^{153}Gd to the 102 keV state of ^{153}Eu has been calculated. The transition energy, for the three solid angles, is

$$126^{+15}_{-10}\ \text{keV}, \quad 121^{+12}_{-8}\ \text{keV}, \quad \text{and} \quad 121^{+12}_{-8}\ \text{keV} \quad \text{respectively.}$$

the mean energy being 123^{+18}_{13} keV. This gives the decay energy to the ground state of ^{153}Eu

$$= 225^{+18}_{-13}\ \text{keV}\,.$$

By plotting the decay energy of the isotopes in which the transformation is

[13] E. H. S. BURHOP: *Auger Effect and other Radiationless Transitions* (1952).

of the type $\Delta I = A(N - Z) = 25 \rightleftarrows 27$ against the mass number ([11]), the decay energy of ^{153}Gd is expected to be about 250 keV which is in good agreement with what has been found in this work.

5. – The Measurements of the Internal Conversion Coefficient,

For the measurement of the electron spectrum of ^{153}Gd, a very thin deposit of the source was made on a stilbene crystal, about 3 mm × 3 mm in area and about one mm thick, which was placed on the photomultiplier. The electron spectrum is shown in Fig. 2.

A correction was made for back-scattering. According to PAUL and STEINWEDEL, ([15]) the back scattering is about 12% for the normal incidence, and about 18% for the diffuse angular distribution. A correction of 15% has been applied. The same source was used to measure the γ-ray with the NaI(Tl) crystal. The conversion coefficient α was found to be 0.73 ± 0.04 and $\alpha_K = 0.61 \pm 0.03$ and $K/(L + M) \sim 5$.

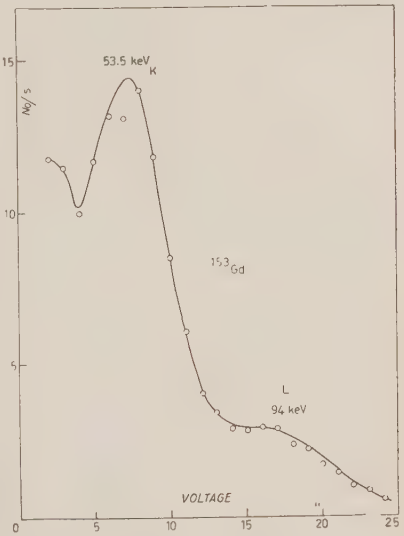

Fig. 2. – The spectrum of the conversion electrons from ^{153}Gd taken in the scintillation spectrometer with a stilbene crystal. The peak at 53.5 keV is the K conversion line of the 102 keV γ-ray and that at 94 keV is the L conversion line.

6. – The Ground State Transition,

If one uses the experimentally found value of the K conversion coefficient of the 102 keV γ-ray, P_L/P_K ratio for the transition to the 102 keV state, and the calculated value of P_L/P_K for the ground state, one can estimate the percentage of transitions to the ground state.

Let the total rate of disintegration of ^{153}Gd be n, of which a fraction (nf)

([14]) H. E. SUESS and J. H. D. JENSEN: *Ark. Fys.*, **3**, 577 (1951).

([15]) W. PAUL and H. STEINWEDEL: *Beta and Gamma Spectrometry*, Edited by KAI SIEGBAHN (1955).

goes to the 102 keV state, and the rest $n(1-f)$ goes to the ground state and let $(nf)_K$ and $[n(1-f)]_K$ be the disintegrations by the K electron capture. Then the K X-ray intensity

$$I_X = [(nf)_K\omega_K + (nf)x_K\omega_K + \{n(1-f)\}_K\omega_K]\varepsilon_X S \exp[-\mu_X t] .$$

and the intensity of the γ-ray as before is

$$I_\gamma = (nf)(1-f)\varepsilon_\gamma S \exp[-\mu_\gamma t] .$$

From the measured ratio of I_X/I_γ, the value of f can be calculated. The experimentally determined value of the decay energy to the ground state has been used to calculate the value of $[n(1-f)]_K/[n(1-f)]$ with the formula for allowed transitions. It has been found to be 0.830. The efficiency of detection of the γ-ray in the given geometry, was found by numerical integration to be 95%, and the transmission of this γ-ray through the cover of the crystal was 95%. The mean value of $(I_X \exp[-\mu_\gamma t]/I_\gamma \exp[-\mu_X t])$ is 2.3 ± 0.07, from which f comes out to be 0.75 ± 0.03, so that the transition to the ground state is about 25%.

7. – Discussion.

Lines of very low intensity in the decay of ^{153}Gd at 70 keV ([16,17]), 82 keV 90 keV, 115 keV and 170 keV ([17]) have been found in this laboratory using other methods. In order to look for lines of weak intensity, ^{153}Gd was placed in the well of a large well-type crystal, and to reduce the intensity of the strong K X-ray, the source was wrapped inside a tin foil (30 mg/cm^2). There was no peak between 144 keV and 250 keV with an intensity more than 3% of the intensity of the 102 keV γ-ray. If there are transitions to the levels of ^{153}Eu higher than the 102 keV level, they cannot be more than 5% in intensity, and their contribution to the intensity of the sum peak at 144 keV cannot be more than 3%, which is within the limits of error of our measurements. The coincidence technique with a single crystal used here for the determination of the electron capture decay energy is independent of the value of the K conversion coefficient of the 102 keV γ-ray.

From the knowledge of the relative percentage of transitions going to the 102 keV state and to the ground state, the log ft value for the former has been calculated ([18]) to be 6.1 and that for the latter 7.3. The values of ψ_K and ψ_{L_1}

([16]) S. K. Bhattacherjee: Private communication (1956).
([17]) M. C. Joshi: Private communication.
([18]) J. K. Major and L. C. Biedenharn: *Rev. Mod. Phys.*, **26**, 321 (1954).

are taken from BRYSK and ROSE (1). One can then represent the decay scheme as given in the Fig. 3.

The understanding of the log *ft* values is rendered difficult on account of the uncertainty in the parity assignment to the ground state of ^{153}Eu. The shell model predicts $d_{\frac{5}{2}}$ for the ground state but the magnetic moment of ^{153}Eu falls in the Schmidt diagram in the region $(l - \frac{1}{2})$. It is assumed here that its parity is even. The spin is known to be $\frac{5}{2}$. On the shell model, the 89th neutron in $^{153}_{64}Gd_{89}$, on the analogy of $^{143,145}_{64}$Nd and $^{141,149}_{62}$Sm is perhaps in the level $f_{\frac{7}{2}}$ and has the spin and parity $\frac{7}{2}^-$. The 102 keV state has been assigned $\frac{3}{2}^+$ (5,6,19). On this assignment, the electron capture decay of ^{153}Gd to the 102 keV state has to be of the type $\Delta J = 2$, yes, and that to the ground state of the type $\Delta J = 1$, yes, the known log *ft* values for such transitions being 9 and 7.5 respectively. Our results are consistent with the assignment by KING (20) of spin $\frac{7}{2}^+$ to the 102 keV state. With this assignment, both the transitions are of the first forbidden type, and the transition probabilities to the two states should be comparable as found in our experiment.

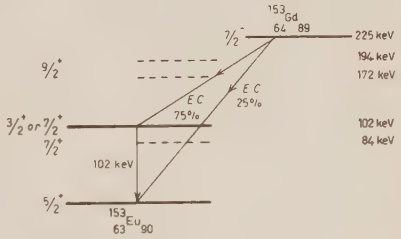

Fig. 3. – The decay scheme of ^{153}Gd.

* * *

Our thanks are due to Mr. M. C. JOSHI and Dr. S. K. BHATTHACHARJI of this laboratory for communicating their results to us. We are grateful to Dr. B. V. THOSAR for his help in the preparation of this paper.

(19) B. R. MOTTELSON and S. G. NILSSON: *Phys. Rev.*, **99**, 1615 (1955).
(20) R. W. KING: *Rev. Mod. Phys.*, **26**, 327 (1954).

RIASSUNTO (*)

La tecnica della sommazione è stata applicata ad uno spettrometro a scintillazione per determinare l'energia di decadimento per cattura elettronica del ^{153}Gd. L'energia decadimento è 225^{+13}_{-18} keV. I coefficienti di conversione interna del raggio γ di 102 keV sono stati misurati allo spettrometro a scintillazione. Il coefficiente di conversione K di questo raggio γ è 0.61 ± 0.03 e $K/(L + M) \sim 5$. Si stima che circa il 25% delle transizioni vadano allo stato fondamentale del ^{153}Eu.

(*) *Traduzione a cura della Redazione.*

β-γ Angular Correlation of $^{208}_{81}$Tl (ThC″).

F. Demichelis and R. A. Ricci

Istituto di Fisica Sperimentale del Politecnico - Torino

(ricevuto il 27 Aprile 1956)

Summary. — The angular correlation between the 2.37 MeV β radiation and the 2.62 MeV γ-ray in $^{208}_{81}\text{Tl} \rightarrow {}^{208}_{82}\text{Pb}$ decay has been measured and found anisotropic. The value of the anisotropic coefficient is $-(0.585 \pm 0.06)$. Assuming the spin and parity assignment for the excited levels of $^{208}_{82}$Pb suggested by Elliot *et al.*, we deduce $J = 4+$ for the $^{208}_{81}$Tl ground state. On the basis of the various experimental results, the most reliable assignment of the spin and parity for the $^{212}_{83}$Bi ground state should be $J = 1-$ or $2-$ according to the assignment suggested by Martin and Parry and to the order of forbiddeness of the $^{212}_{83}$Bi β transitions.

1. – Introduction.

In this paper, following our program of researches on the structure of some heavy radioactive nuclei, we report the results on the spins and parities of some nuclear levels of $^{212}_{83}$Bi, $^{208}_{81}$Tl.

$^{208}_{81}$Tl(ThC″), which arises from $^{212}_{83}$Bi(ThC') by α disintegration, decays, by emitting β particles, in $^{208}_{82}$Pb(TdD) according to the scheme of Fig. 1.

The most reliable assignment of spins and parities of the $^{208}_{82}$Pb levels has been suggested by Elliot, Graham, Walker, and Wolfson, on the basis of their internal conversion coefficient measurements and of the γ-γ angular correlation determination [1]; these assignments are indicated in Fig. 1.

The β transitions from the ground state of $^{208}_{81}$Tl to the first one and to the second excited state of $^{208}_{82}$Pb should be first forbidden [2]; their log *ft* values

[1] L. G. Elliot, R. L. Graham J. Walker and J. L. Wolfson: *Phys. Rev.*, **93**, 356 (1954).

[2] F. Demichelis, R. A. Ricci and G. Trivero: *Nuovo Cimento*, **3**, 377 (1956).

are in agreement with $\Delta J = 0, 1, 2$, parity change for the 2.37 MeV β transition and $\Delta J = 0, 1$, parity change for the 1.79 MeV β transition.

It follows that the ground state of $^{208}_{81}$Tl may be a 4+ or 5+ state.

KING ([3]) deduced an assignment $J = 5+$, according to the log *ft* value of the 1.79 MeV β transition.

WEALE ([4]), dealing with his experimental results on the α-γ angular correlation of $^{212}_{83}$Bi, assumed the same assignment.

A new source of information may be the study of the β-γ angular correlation of $^{208}_{81}$Tl.

Since the 2.37 MeV β transition is first forbidden ([2]) one would expect an anisotropical angular correlation between this radiation and the 2.62 MeV γ-ray.

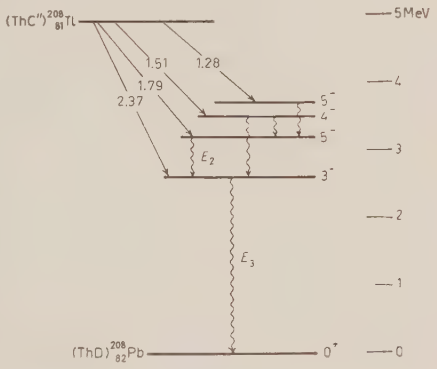

Fig. 1.

The aim of the present research is just the investigation of this angular correlation.

We will show that the ground state of $^{208}_{81}$Tl should have $J = 4-$ and that this result is satisfactory from the point of view of the shell model theory.

Finally, on the basis of the various experimental results on $^{212}_{83}$Bi and $^{208}_{81}$Tl, we will assign the spin and parity to the ground state of $^{212}_{83}$Bi. The most plausible assignment is $J = 1-$ or $2-$.

2. – Experimental Apparatus.

The experimental apparatus is the usual set up for coincidence measurements ([2,5]).

The source consists of a very thin layer of $^{228}_{90}$RdTh in equilibrium with its decay products (intensity ≈ 45 microcurie).

As β detector we use a stilbene crystal (3 mm thick, 13 mm diameter), and as γ detector a NaI(Tl) crystal (13 mm thick, 20 mm diameter); both the crystals are followed by 6291 Du Mont photomultipliers.

The resolving time of the coincidence circuit is $\tau = 1.36 \cdot 10^{-7}$ sec.

An aluminium sheet (3 mm thick) is placed in front of the β detector, in order to stop all the β radiations with energy lower than 1.80 MeV; only the

([3]) R. W. KING: *Rev. Mod. Phys.*, **26**, 327 (1954).
([4]) J. W. WEALE: *Proc. Phys. Soc.*, A **68**, 35 (1955).
([5]) F. DEMICHELIS and L. A. RADICATI: *Nuovo Cimento*, **3**, 152 (1956).

2.25 MeV β transition $^{2}_{83}Bi \rightarrow {}^{212}_{84}Po$ (ground to ground state) and the 2.37 MeV β transition from the ground state of $^{208}_{81}Tl$ to the first excited state of $^{208}_{82}Pb$, are detected.

The background (particularly γ-rays) of the β detector and the background coincidences (γ-γ coincidences) in the β-γ measurements, can be determined by covering the source with a beryllium absorber ($\approx 1.27\ g_m/(cm)^2$).

A lead sheet (1 mm thick) placed in front of the γ detector makes it insensitive to the β radiations and reduces the backscattered Compton photons.

Lead shieldings are also placed all round the detectors to avoid accidental coincidences due to the Compton photons scattered by the two crystals [6].

The β-γ coincidence rate was determined for the following values of θ: 90°, 120°, 150°, 180°; θ is the angle subtended by the two detectors at the source.

For every value of θ the total effective coincidences, with and without beryllium were $\approx 25\,000$.

The measurements have been made with the β detector fixed and the γ detector movable; the γ-ray rate was found to be constant with θ within 1%.

The usual corrections [7] have been made in order to take into account the asimmetry of the γ-ray source, the fluctuations with time of the efficiencies of the detectors, and the Compton scattered photons.

The β-γ angular correlation function depends on the angle θ and also on the β radiation energy; therefore we have made two sets of measurements: the first with 3.0 mm aluminium absorber (cut-off energy $E_c = 1.80$ MeV); the second with 3.5 mm aluminium absorber ($E_c = 2.00$ MeV).

For the β-γ coincidence rate we have:

$$n_{\beta\gamma} = (n_t - n_s) - (n'_t - n'_s)\,,$$

where: $n_{\beta\gamma}$ is the coincidence rate between the 2.37 MeV β transition and the 2.62 MeV γ-ray;

n_t and n_s are the total coincidence rate and the accidental coincidence rate respectively, without beryllium;

n'_t and n'_s are the total coincidence rate and the accidental coincidence rate respectively, with beryllium [5].

3. – Experimental Results.

In Fig. 2 are indicated the experimental points with their probable errors, obtained in the first measurement set.

([6]) H. FRAUENFELDER: *Ann. Rev. of Nuclear Science*, **2**, 129 (1953).
([7]) D. T. STEVENSON and M. DEUTSCH: *Phys. Rev.*, **83**, 1202 (1951).

We have plotted $\varepsilon(\theta) = (n_{e,\theta}/n_{e,90}) - 1 = W(\theta) - 1$ against θ. $n_{e,\theta}$ and $n_{e,90}$ are the effective β-γ coincidence rates for the values θ and 90° respectively.

The full line represents the differential angular correlation curve $[W(\theta) - 1]$, obtained by means of the least square method.

The good fit of the theoretical curve:

$$W(\theta) - 1 = a_2 \cos^2 \theta$$

confirms that the 2.37 MeV β transition is first forbidden ([2,8]).

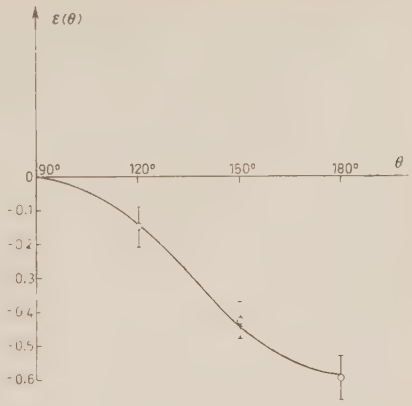

Fig. 2.

The anisotropy coefficient, corrected for the finite solid angle of the detectors ([9]) is: $a_2 = -0.585$.

The experimental value of $(n_{e,180}/n_{e,90}) - 1$ was found to be: (-0.59 ± 0.06) (see Fig. 2).

In the second measurement set the same expression was found to be: $-(0.61 \pm 0.06)$.

4. – Discussion.

The existence of an anisotropic angular correlation of the type:

$$W(\theta) = 1 + a_2 \cos^2 \theta \,,$$

with $a_2 \neq 0$, confirms that the β transition from the $^{208}_{81}$Tl ground state to the first excited state of $^{208}_{82}$Pb is first forbidden according to its log ft value (7.72) ([2]).

With this restriction we can assume that the β interaction contains only scalar, tensor, pseudoscalar terms ([10]).

We must now work out the anisotropy coefficient a_2 for the different choices of β-hamiltonian and for the different values of the spin and parity of the initial state involved in the 2.37 MeV β transition.

([8]) L. C. Biedenharn and M. E. Rose: *Rev. Mod. Phys.*, **25**, 729 (1953).
([9]) M. Walter, O. Huber and W. Zünti: *Helv. Phys. Acta*, **23**, 697 (1950).
([10]) D. C. Peaslee: *Phys. Rev.*, **91**, 1447 (1953).

The parameters b_ν for the β radiation, which appear in the $W(\theta)$ expression

$$W(\theta) = \sum_\nu b_\nu A_\nu P_\nu(\cos\theta),$$

are listed in Table X of the BIEDENHARN and ROSE's paper ([5]).

Since the b_ν parameters are function of the β energy, they must be averaged over the whole range of energies from the cut-off energy ($E_c - 4.43\ mc^2$ in the first measurement set, $E_c = 4.93\ mc^2$ in the second) to the maximum energy ($E_0 = 5.65\ mc^2$).

In order to determine the A_ν parameters, we have used the relationship (69*a*) of BIEDENHARN and ROSE, which relates A_ν with the F_ν coefficients.

The latter are listed in Table I of the BIEDENHARN and ROSE's paper, and for values of $J \geqslant 5$ they have been calculated by FERENTZ and ROSENZWEIG ([11]).

The results of the calculations for $L_1 = 1$ and $L_1 = 2$ respectively are summarized in Tables I and II.

TABLE I (*). – *Values of the anisotropy coefficient* a_2 *for* $L_1 = 1$.

Interaction \ J	2	3	4	5	Parity of the initial state
S $\lvert\int\beta\boldsymbol{r}\rvert^2$	0.221	— 0.236	0.0885	0	odd
T $\Sigma\lvert B^\beta_{ij}\rvert^2$	— 0.51	1.023	— 0.2345	0	odd
$\lvert\int\beta\boldsymbol{\sigma}\wedge\boldsymbol{r}\rvert^2$	— 0.0881	0.121	— 0.0384	0	odd
$\lvert\int\beta\boldsymbol{\alpha}\rvert^2 +$ $\lvert\int\beta\boldsymbol{\sigma}\wedge\boldsymbol{r}\rvert^2 +$ $\lvert\int\beta\boldsymbol{\alpha}\rvert\,\lvert\int\beta\boldsymbol{\sigma}\wedge\boldsymbol{r}\rvert$	— 0.0877	— 0.0361	0.1135	0	odd
P	0.221	— 0.236	0.0885	0	even

(*) The notations for the interaction terms are the same as those used by BIEDENHARN and ROSE.

L_1 represents the orbital angular momentum of the β transition (order of the β transition), according to the ordinary and relativistic selection rules ([12]), and for the following values of the spin of the initial state: $J = 2, 3, 4, 5$. The values $J = 0, 1$ are inconsistent with the type of $^{208}_{81}\mathrm{Tl} \rightarrow {}^{208}_{82}\mathrm{Pb}$ β transitions.

([11]) M. FERENTZ and N. ROSENZWEIG: *Table of F Coefficients*, Argonne National Laboratory 5324.

TABLE II (*). – *Values of the anisotropy coefficient a_2 for $L_1 = 2$.*

Interaction \ J	2	3	4	5	Parity of the initial state
S $\quad \lvert\int \beta \boldsymbol{r}\rvert^2$	— 0.0716	0.14	0.195	— 0.1178	even
T $\quad \Sigma \lvert B^{\beta}_{ij}\rvert^2$	0.254	— 0.353	— 0.462	0.414	even
$\lvert\int \beta \boldsymbol{\sigma} \wedge \boldsymbol{r}\rvert^2$	0.0337	— 0.06	— 0.0385	0.057	even
$\lvert\int \beta \boldsymbol{\alpha}\rvert^2 +$ $\lvert\int \beta \boldsymbol{\sigma} \wedge \boldsymbol{r}\rvert^2 +$ $\lvert\int \beta \boldsymbol{\alpha}\rvert \lvert\int \beta \boldsymbol{\sigma} \wedge \boldsymbol{r}\rvert$	0.0316	— 0.0562	— 0.076	0.053	even
P	— 0.0716	0.14	0.195	— 0.1178	odd

(*) The notations for the interaction terms are the same as those used by BIEDENHARN and ROSE.

The spins and the parities of the intermediate state and of the final state are assumed 3— and 0+ respectively (see Fig. 1).

According to Table I we can deduce that: the scalar and tensorial interactions are consistent with odd parity of the initial state; these interactions should then be excluded since, as said before, we must assume even parity for the $^{208}_{81}$Tl ground state; also the pseudoscalar interaction, which however is consistent with even parity of this state, should be excluded: the only one negative value of a_2 ($= \quad 0.236$), for $J = 3$, is lower than the experimental value ($a_2 = 0.595 \pm 0.06$).

The a_2 coefficient is the sum of the contributions from the different operators plus those arising from interference terms.

From Table I we can observe that the value corresponding to the sum of the operator terms only, is in disagreement with the experimental results.

Three modes of interference are possible in a β-γ angular correlation [13] and the difficulties in the calculation of the interference terms are remarkable. However the calculations will be performed within a short time.

It seems probable that in these calculations the terms of relativistic interaction ought to be taken into account.

With this assumption, we cannot exclude that the order of the β transition

---

[12] J. M. BLATT and V. F. WEISSKOPF: *Theoretical Nuclear Physics* (New York, 1952).

[13] H. FRAUENFELDER: *Beta and Gamma Ray Spectroscopy*, Ed. K. SIEGBAHN (Amsterdam), p. 569.

is $L_1 = 2$. In this case from the Table II we can deduce that: the only scalar and tensorial interactions are consistent with an even parity of the initial state; the a_2 value, sum of terms arising from the operators

$$\sum |B_{ij}^{\beta}|^2 \quad \text{and} \quad \left|\int \beta\boldsymbol{\alpha}\right|^2 + \left|\int \beta\boldsymbol{\sigma}\wedge\boldsymbol{r}\right|^2 + \left|\int \beta\boldsymbol{\alpha}\right| \left|\int \beta\boldsymbol{\sigma}\wedge\boldsymbol{r}\right|$$

($a_2 = -0.538$), is in agreement with the experimental results and with the type of the $^{208}_{81}\mathrm{Tl} \rightarrow {}^{208}_{82}\mathrm{Pb}$ β transitions.

In this case we have $J = 4+$ for the initial state.

The anisotropy coefficient calculated for the range energy $E = 4.93\ mc^2 \div \div E_0 = 5.65\ mc^2$ (corresponding to the second measurement set) is, for $J = 4+$, the sum of terms arising from the same operators as above and it results $a_2 = -0.59$ according to the experimental value $a_2 = -0.61 \pm 0.06$).

The assignment $J = 4+$ for the ground state of $^{208}_{81}\mathrm{Tl}$ is also consistent with the assignment $J = 4-$ and $J = 5-$ to the 3.48 MeV and 3.71 MeV levels respectively of $^{208}_{82}\mathrm{Pb}$ according to ELLIOT *et al.* [1], and with the assumption that all the β transitions of the $^{208}_{81}\mathrm{Tl} \rightarrow {}^{208}_{82}\mathrm{Pb}$ decay, are first forbidden.

We will discuss now the assignment $J = 4+$ from the point of view of the shell model theory [14].

$^{208}_{81}\mathrm{Tl}$ has 81 protons and 127 neutrons; the contribution of protons to the total spin should be $j_p = \frac{1}{2}$ (the greater pairing energy in the $1h_{11/2}$ orbital should explain one hole in the $3s_{\frac{1}{2}}$ orbital) [15].

According to the Jensen-Mayer model the neutron outside the closed shell occupies the $2g_{9/2}$ orbital and its spin would couple to $j_n = 9/2$.

The shell model predicts correctly the even parity of $^{208}_{81}\mathrm{Tl}$. According to the NORDHEIM's « weak rule » j_n and j_p would couple to a maximum total spin $J = |j_n + j_p| = 5$. The assignment $J = 4+$ is then consistent with the shell model theory.

Fig. 3 shows the decay schemes of the nuclides $^{212}_{83}\mathrm{Bi(ThC)}$, $^{212}_{84}\mathrm{Po(ThC')}$, $^{208}_{81}\mathrm{Tl(ThC'')}$ and the spins and parities for some levels [1,2,4,17,18].

The γ-ray (40 keV) from the first excited state to the ground state of $^{208}_{81}\mathrm{Tl}$ is certainly a M_1 transition [4,16]. Assuming $J = 4+$ for the ground state, the first excited state should have $J = 5+, 4+, 3+$.

[14] L. W. NORDHEIM: *Rev. Mod. Phys.*, **23**, 322 (1951); M. GOEPPERT MAYER J. H. D. JENSEN: *Elementary Theory of Nuclear Shell Structure* (New York, 1955).

[15] J. H. D. JENSEN: *Beta and Gamma Ray Spectroscopy*, Ed. K. SIEGBAHN (Amsterdam), p. 427.

[16] R. L. GRAHAM and R. E. BELL: *Canad. Journ. Phys.*, **31**, 377 (1953).

[17] D. G. E. MARTIN and G. PARRY: *Proc. Phys. Soc.*, A **68**, 1177 (1955).

[18] F. DEMICHELIS: *Nuovo Cimento*, **12**, 407 (1954).

Taking into account the experimental results on the α-γ angular correlation of $^{212}_{83}$Bi by WEALE (4), the spin and parity assignments of $^{212}_{83}$Bi ground state, consistent with $J = 4+$ for the $^{208}_{81}$Tl ground state, are summarized in Table III; L_α represents the minimum value of the orbital angular momentum of the α transition.

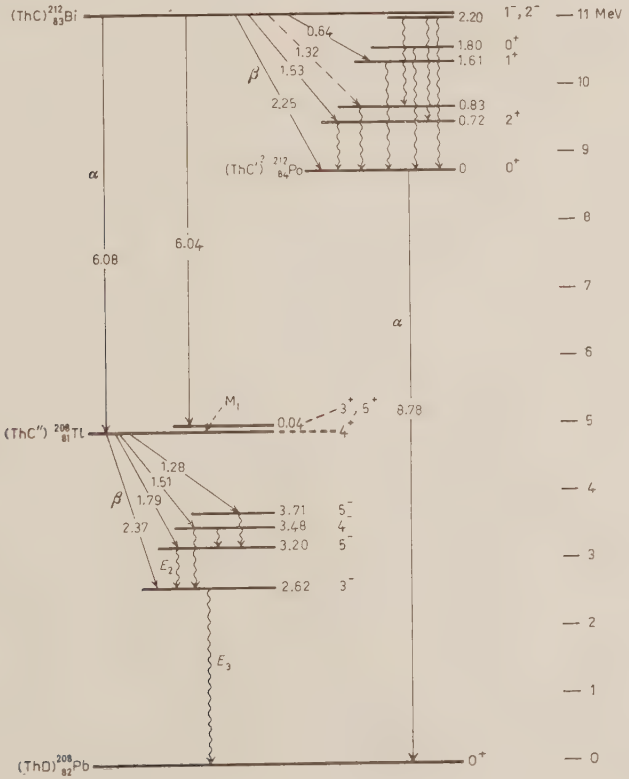

Fig. 3.

For the other assignments we have found a value of $W(\theta)$ too different from the experimental value obtained by WEALE:

$$[W(\theta) = 1 - (0.22 \pm 0.05)\cos^2\theta].$$

According to Table III we could deduce the following conclusions:

a) $J = 1+$ assignment to $^{212}_{83}$Bi ground state should be excluded. In fact the $^{212}_{83}$Bi β transitions are probably all first forbidden (2,17); particularly

the 2.25 MeV β transition from the ground state of $^{212}_{83}$Bi to the ground state of $^{212}_{84}$Po if first forbidden. By assuming the assignment $J = 0+$ to the latter (even-even nucleus) the former should have $J = 1-$ or $2-$.

Table III.

$W(\theta)$	$^{212}_{83}$Bi ground state	$^{208}_{81}$Tl first excited state	$^{208}_{81}$Tl ground state	L_α (6.04 MeV)	L_α (6.08 MeV)
$1 - 0.201 \cos^2\theta$	1+	3+	4+	2 parity favoured	4 parity unfavoured
$1 - 0.201 \cos^2\theta$	1−	3+	4+	3 parity unfavoured	3 parity favoured
$1 - 0.378 \cos^2\theta$	2−	5+	4+	3 parity favoured	3 parity unfavoured

b) $J = 1-$ assignment, suggested, by King ([3]) and by Martin and Parry ([17]) is consistent with the results of Weale and with the degree of forbiddeness of the $^{212}_{83}\text{Bi} \rightarrow {}^{212}_{84}\text{Po}$ ground to ground β transition.

However in this case the 6.04 MeV α transition to the first excited state of $^{208}_{81}$Tl, which should be less « hindered » than the 6.08 MeV α transition to the ground state, is « parity unfavoured » while the 6.08 MeV β transition is « parity favoured »; this is in disagreement with the usual selection rules for α particles ([12,19]).

c) $J = 2-$ assignment is consistent with the degree of forbiddeness of 2.25 MeV β transition and with the α particles selection rules, but the value of the anisotropy coefficient of the α-γ angular correlation is higher than the experimental value found by Weale.

The latter assignment agrees well with the shell model theory. The contribution of protons to the total spin of $^{212}_{83}$Bi (83 protons, 129 neutrons) should be $j_p = \frac{9}{2}$; the odd proton is in the orbital $1h_{\frac{9}{2}}$. We may assume that the three neutrons outside the closed shell occupy the orbital $2g_{\frac{9}{2}}$ ($j_n = \frac{9}{2}$), or that one of the neutrons has been raised to the $3d_{\frac{5}{2}}$ orbital ($j_n = \frac{5}{2}$).

The shell model predicts also the odd parity of $^{212}_{83}$Bi ground state.

([19]) I. Perlman and F. Asaro: *Ann. Rev. of Nuclear Science*, **4**, 157 (1954).

According to the Nordheim's « strong rule », one would expect that j_n and j_p couple to a total spin $J = |j_n - j_p|$. In our case we have $J = 0$ or 2.

If we exclude $J = 0$ — assignment, $J = 2$ — is then consistent with the shell model theory.

However also $J = 1$ — assignment must be considered, since it is in agreement with the experimental results on the α-γ angular correlation and with the type of $^{212}_{83}$Bi β transitions.

* * *

The authors are indebted to Prof. E. Perucca for his interest, to Prof. L. A. Radicati for some valuable discussion on this topic and to Ing. G. Trivero for his collaboration in the experimental measurements.

RIASSUNTO

È stata determinata la correlazione angolare tra la radiazione β di energia 2.37 MeV e il raggio γ di energia 2.62 MeV nel decadimento $^{208}_{81}$Tl → $^{208}_{82}$Pb. Il coefficiente di anisotropia risulta (0585 ± 0.06). Sulla base delle assegnazioni di spin e parità ai livelli eccitati del $^{208}_{82}$Pb, dedotte da Elliot e collaboratori, e d'accordo con i nostri risultati sperimentali, si è attribuito un valore J 4+ allo stato fondamentale del $^{208}_{81}$Tl. Con questa ipotesi, e tenendo conto dei risultati di Weale relativi alla correlazione angolare α-γ del $^{212}_{83}$Bi, l'assegnazione più plausibile per lo stato fondamentale del $^{212}_{83}$Bi, risulta $J = 1$ —, 2 —, in buon accordo con le assegnazioni suggerite da Martin e Parry e col grado di proibizione delle transizioni β del decadimento $^{212}_{83}$Bi → $^{212}_{84}$Po.

A Soluble Model of Meson-Nucleon S-State Scattering.

E. L. Lomon

Department of Physics The Weizmann Institute of Science - Rehovoth, Israel

(ricevuto il 2 Maggio 1956)

Summary. — We consider the interaction Hamiltonian

$$(1)\ (*) \qquad H_I = g\int \mathrm{d}_3x\,\bar{\psi}(x)\varphi(x)\cdot\varphi(x)\,\psi(x) + \lambda\int \mathrm{d}_3x\,\bar{\psi}(x)(\pi(x)\times\varphi(x))\cdot\tau\,\psi(x)\,.$$

There is evidence ([1,2]) that for meson-nucleon scattering (1) represents a large part of the $ps(ps)$ s-state interaction for intermediate as well as as weak coupling, providing that λ/g is suitably altered. The first term of (1) has long been known to be diagonalizable in the static nucleon limit ([3]). The isotopic spin coupling of the second term requires that the isotopic spin variable of the nucleon be left free (non-static) thus complicating the diagonalization. By combining the nucleon spin operator with the meson field operators we have succeeded in diagonalizing (1). The parameters determined by experiment are reasonable. One can examine many formal aspects. The point source limit exists.

Introduction.

It has been shown by G. F. Chew ([4]), by means of certain approximation methods, that the $ps(pv)$ interaction in the static nucleon limit can reproduce the p state scattering and photomeson production data. This interaction can

(*) g and λ coupling constants; ψ, $\bar{\psi}$ and φ, π are the field operators and their canonical conjugates for the nucleon and meson fields respectively.

([1]) T. Akiba and K. Sawada, *Prog. Theor. Phys.*, **12**, 94 (1954).

([2]) L. L. Foldy: *Phys. Rev.*, **84**, 168 (1951); F. J. Dyson: *Phys. Rev.*, **73**, 929 (1948); S. Tani: *Prog. Theor. Phys.*, **6**, 267 (1950); S. D. Drell and E. M. Henley: *Phys. Rev.*, **88**, 1053 (1952).

([3]) G. Wentzel: *Helv. Phys. Acta*, **15**, 111 (1942); G. Morpurgo and B. F. Touschek: *Nuovo Cimento*, **10**, 1681 (1953); A. Klein and B. N. McCormick: *Phys. Rev*, **98**, 1428 (1955).

([4]) G. F. Chew: *Phys. Rev.*, **94**, 1748, 1755 (1954); **95**, 1669 (1954).

be considered as the leading term (in powers of the coupling constant) of the Foldy type transformation (2) of the $ps(ps)$ interaction, providing the effect of the remaining terms on p-state meson interactions is small. If the nucleon is well localized, this stipulation is probably satisfied, due to the necessity of gradient coupling to cause a strong p-state interaction when close to the origin. As the $ps(pv)$ term has no effect on s-state scattering in the static nucleon limit, we must for our purposes consider the effect of the other terms of the transformed $ps(ps)$ Hamiltonian. In the weak coupling limit the leading order terms (to order f_s^2) are

$$H_I = g\int \mathrm{d}_3 x \bar{\psi}(x) q(x)\cdot q(x)\psi(x) + \lambda\int \mathrm{d}_3 x \bar{\psi}(x)\left(\tau(x)\times q(x)\right)\cdot\tau\psi(x)\ , \tag{1}$$

where $gM = 2f_s^2$ (M = nucleon mass; f_s is pseudoscalar coupling constant as defined by DRELL and HENLEY (2)), and $\lambda = -g/8M$.

Further, the work of AKIBA and SAWADA (1) in which they reorder the Foldy transformed $ps(ps)$ Hamiltonian with a cut-off at the nucleon mass, indicates that the scattering process is determined by (1), providing that $\lambda = -ag/8M$. The parameter a increases from 1 to 2 as the coupling goes from the weak to the strong limit, for their cut-off.

H_I has a form which makes it possible to exactly diagonalize the total Hamiltonian on the assumption that the nuclear field has a static spatial distribution. The isotopic spin of the nucleon field is left free and is taken into account properly. This is a necessary procedure due to the isotopic spin coupling of the second term of H_I, and the lack of any a priori reason for eliminating multiple isotopic spin-flip processes from consideration. In the case of the spatial dependence of ψ one may rely on the usual arguments depending on the large mass of the nucleon relative to the meson to eliminate the direct effects of recoil. Recoil is of course reflected in the nucleon form factor, and cut-off momentum A.

H_I is quadratic in both the meson and nucleon field operators. For this reason we may combine the two types of operators into « double operators ». As we shall show, the free meson Hamiltonian may also be written in this form when considering scattering. Thus the problem is reduced to diagonalizing a quadratic Hamiltonian in these « double operators ».

We write the Hamiltonian in terms of the Fourier transforms of the operators. The resulting Hamiltonian is first diagonalized in isotopic spin space and afterwards in momentum space. This separation, which makes the calculation possible, arises from the circumstance that, in isotopic spin space all the off-diagonal terms have the same momentum dependence and the diagonal terms are all equal.

We can then directly obtain an expression for the triplet and singlet phase shifts. In the limit of infinite cut-off one of the two phaseshifts may be non-zero. The zero energy experimental data ([5]) yield two conditions on the three parameters a, A and f_s. Energy dependence is a further restriction ([5]).

In this model the effect of infinite cut-off is not as drastic as in the case of the Lee model ([6]) or Wentzel pair theory ([3]) ($\lambda = 0$). Coupling is possible without « ghost states » ([7]).

1. – Diagonalization.

We consider

$$H = \bar{\psi}\mathcal{H}\psi\,, \qquad \text{where} \tag{2}$$

$$\psi = \begin{Vmatrix} p_1 & \chi_a \\ q_1 & \chi_a \\ p_2 & \chi_a \\ q_2 & \chi_a \\ p_3 & \chi_a \\ q_3 & \chi_a \\ p_1 & \chi_b \\ q_1 & \chi_b \\ p_2 & \chi_b \\ q_2 & \chi_b \\ p_3 & \chi_b \\ q_3 & \chi_b \end{Vmatrix} \qquad \bar{\psi} = (\bar{\chi}_a\bar{p}_1, \bar{\chi}_a\bar{q}_1, \ldots) \tag{3a}$$

$p_1 = |p_1(k')|$ a column matrix in k space, $\bar{p}_1 = (\ldots p_1(k) \ldots)$; $p_i(k)$ and $q_i(k)$ are the s-state components of the spherical Fourier transforms of $\pi_i(x)$ and $q_i(x)$ respectively. $p_i(k) = (1/\sqrt{2\pi R})\int \pi_i(x)((\sin Kr)/r)\mathrm{d}^3x$; $q_i(a) = (1/\sqrt{2\pi R})\cdot \int \varphi_i(r)((\sin Kr)/r)\,\mathrm{d}^3x$. R is the radius of the sphere of normalization. $i = 1, 2, 3$ indicate the isotopic spin component. χ_a is a neutron destruction operator, χ_b is a proton destruction operator, and $\bar{\chi}_a$, $\bar{\chi}_b$ are the creation operators.

([5]) *a*) J. Orear: *Phys. Rev.*, **96**, 176 (1954); *b*) H. A. Bethe and de Hoffmann: *Mesons and Fields*, II (Evanston, 1955).

([6]) T. D. Lee: *Phys. Rev.*, **95**, 1329 (1954).

([7]) G. Källén and W. Pauli: *Kong. Dan. Vid.*, **30**, No. 7 (1955).

$$
\mathcal{H} = \begin{pmatrix}
\delta_{k'k} & \lambda V_k V_{k'} & & & & & & & & & & i\lambda V_k V_{k'} \\
 & D_{k'k} & -\lambda V_k V_{k'} & & & & & & & & -i\lambda V_k V_{k'} & \\
 & -\lambda V_k V_{k'} & \delta_{k'k} & & & & & & & & & \lambda V_k V_{k'} \\
\lambda V_k V_{k'} & & & D_{k'k} & & & & & & & -\lambda V_k V_{k'} & \\
 & & & & \delta_{k'k} & & & -i\lambda V_k V_{k'} & & -\lambda V_k V_{k'} & & \\
 & & & & & D_{k'k} & i\lambda V_k V_{k'} & & \lambda V_k V_{k'} & & & \\
 & & & & & -i\lambda V_k V_{k'} & \delta_{k'k} & & & -\lambda V_k V_{k'} & & \\
 & & & & i\lambda V_k V_{k'} & & & D_{k'k} & \lambda V_k V_{k'} & & & \\
 & & & & & \lambda V_k V_{k'} & & \lambda V_k V_{k'} & \delta_{k'k} & & & \\
 & & & & -\lambda V_k V_{k'} & & -\lambda V_k V_{k'} & & & D_{k'k} & & \\
 & i\lambda V_k V_{k'} & & -\lambda V_k V_k & & & & & & & \delta_{k'k} & \\
i\lambda V_k V_{k'} & & \lambda V_k V_{k'} & & & & & & & & & D_{k'k}
\end{pmatrix}
$$

where $V_k = (1/\sqrt{2\pi}R)\int \mathrm{d}^3x\, U(x)((\sin Kr)/r)$, $U(x)$ being the nucleon form factor, and $D_{k'k} \equiv \omega_k^2\delta_{k'k} + gV_{k'}V_k$.

Thus (considering s-state components only):

$$H = \tfrac{1}{2}\sum_{kk'} \bar{\chi}\chi(\boldsymbol{p}^2(k) + \omega_{k'}\boldsymbol{q}^2(k))\,\delta_{kk'} + gV_kV_{k'}\bar{\chi}\chi\boldsymbol{q}(k)\boldsymbol{q}(k') + \\ + \lambda V_kV_{k'}\bar{\chi}(\boldsymbol{p}(k')\times\boldsymbol{q}(k) - \boldsymbol{q}(k')\times\boldsymbol{p}(k))\cdot\tau\chi\,, \tag{4}$$

where $\chi = \begin{pmatrix}\chi_a\\ \chi_b\end{pmatrix}$ and bold type signifies a vector in isotopic spin space.

The form $(\boldsymbol{p}\times\boldsymbol{q} - \boldsymbol{q}\times\boldsymbol{p})$ is used instead of simply $2\boldsymbol{p}\times\boldsymbol{q}$ to make the Hamiltonian Hermitian. It is the same as replacing $2p_1q_2$ by $p_1q_2 + q_2p_1$, etc. This then is exactly the Hamiltonian we desire except for the $\bar{\chi}\chi$ multiplying the free meson Hamiltonian $\boldsymbol{p}^2 + \omega^2\boldsymbol{q}^2$. However, due to the absence of operators changing the number of nucleons, we will be considering the operation of H only on state vectors containing one nucleon. For these state vectors the diagonal form $\bar{\chi}\chi = \bar{\chi}_a\chi_a + \bar{\chi}_b\chi_b$ has no effect. Thus H is exactly equivalent to the Hamiltonian we wish to consider for the scattering problem. In the point source limit it is the Fourier transform of $H_M + H_I$, where H_M is the free meson Hamiltonian. The cut-off is obtained by replacing the local interaction of equation (1) by the separable non-local interaction

$$H_I' = g\int\int \bar{\psi}(x')q(x')q(x)\psi(x)\,\mathrm{d}^3x'\,\mathrm{d}^3x + \lambda\int\int \bar{\psi}(x')(\pi(x')\times q(x))\cdot\tau\psi(x)\,\mathrm{d}^3x'\,\mathrm{d}^3x \tag{4a}$$

H is the Fourier transform of $H_M + H_I'$.

Our problem is now to find a unitary matrix S, such that $\mathcal{H}' = S^{-1}\mathcal{H}S$ is diagonal. The corresponding ψ' is given by $\psi' = S^{-1}\psi$. As $\mathcal{H}$ is a 12×12 matrix in isotopic spin space, it is fortunate that the problem can be done in steps. First we note that if we define the hermitian matrices

$$\Sigma = \left(\begin{array}{c|c} \delta_{k'k} & 0 \\ \hline 0 & \omega_k^2\delta_{k'k} + gV_kV_{k'} \end{array}\right) \quad \text{and} \quad \Pi = \left(\begin{array}{c|c} 0 & i\lambda V_kV_{k'} \\ \hline -i\lambda V_kV_{k'} & 0 \end{array}\right)$$

we may write:

$$2\mathcal{H} = \left(\begin{array}{cc|cc|cc} \Sigma & -i\Pi & & & & \Pi \\ i\Pi & \Sigma & & & & -i\Pi \\ \hline & & \Sigma & -\Pi & i\Pi & \\ & & -\Pi & \Sigma & i\Pi & \\ & & -i\Pi & -i\Pi & \Sigma & \\ \hline \Pi & i\Pi & & & & \Sigma \end{array}\right). \tag{5}$$

Now a unitary transformation of the form

$$S = \begin{bmatrix} S_{11} S_{12} S_{13} S_{14} S_{15} S_{16} \\ \cdot \\ \cdot \\ \cdot \\ \cdot \\ S_{61} \ldots\ldots\ldots\ldots \end{bmatrix}$$

where $S_{ij} = \begin{pmatrix} s_{ij} & 0 \\ 0 & s_{ij} \end{pmatrix}$ $i, j = 1, \ldots, 6$.

s_{ij} a matrix in k-space, will not change the matrices Π or Σ. Furthermore, the fact that all the diagonal elements of $\mathcal{H}$ are the same $= \Sigma$, together with the unitary conditions, guarantees that the off diagonal terms of $S^{-1}\mathcal{H}S$ are proportional only to Π. That is, the conditions for diagonalization are of the form $\Pi f(s_{ij}) = 0$ or $f(s_{ij}) = 0$. The form of Π and Σ do not appear (they of course enter into the diagonal elements). By diagonalizing the form (5) we will then be left with a problem non-diagonal only in p q space and in k space.

It may be shown that for this case, due to the « double operator » representation, the meson isospin and the nucleon isospin may be considered as the orbital and intrinsic angular momenta respectively of a single particle. The analogy may then be used to show that our diagonalization in isospin space is equivalent to finding the eigenvalue of the operator $L \cdot S$. One must revert however to the original problem to obtain the characteristics of the diagonalized Hamiltonian in Fock space. Because of this last problem, and because of the simplicity of direct diagonalization of (5), we neglect this method of solving the problem.

Blatt [8] has given the method for handling the diagonalization in p, q and k space and we will use a closely related method.

We may further simplify the problem by noting that the exchange of rows 3 and 6, and also columns 3 and 6 (exchanging both rows and columns is a unitary operation) transforms $\mathcal{H}$ into two 3×3 matrices. Thus we write $S = S_1 S_2$, where S_1 effects the required interchange of rows and columns.

If we have:

$$S_1 = \left[\begin{array}{c|c|c|c|c|c} 1 & & & & & \\ \hline & 1 & & & & \\ \hline & & & & & -1 \\ \hline & & & 1 & & \\ \hline & & & & 1 & \\ \hline & & 1 & & & \end{array}\right] \qquad \text{then} \qquad \mathcal{H}' = S_1^{-1}\mathcal{H}S = \left[\begin{array}{c|c|c|c|c|c} \Sigma & -i\Pi & \Pi & & & \\ \hline i\Pi & \Sigma & -i\Pi & & & \\ \hline \Pi & i\Pi & \Sigma & & & \\ \hline & & & \Sigma & i\Pi & \Pi \\ \hline & & & -i\Pi & \Sigma & i\Pi \\ \hline & & & \Pi & -i\Pi & \Sigma \end{array}\right]$$

[8] J. M. Blatt: *Phys. Rev.*, **72**, 466 (1947).

The phases of the elements in S_1 were chosen to give a simple relation between the two 3×3 matrices. We see that one is the complex conjugate of the other; and thus when we diagonalize one of the 3×3 matrices we can find the diagonalizing matrix for the other by taking the complex conjugate. The diagonal elements for both will be equal.

So we write:

$$S_2 = \begin{pmatrix} \bar{S}_2 & 0 \\ 0 & \bar{S}_2^* \end{pmatrix}$$

and find $\bar{S}_2$ to diagonalize the upper left hand quadrant of $\mathcal{H}'$. This is a simple task. The secular equation yields the eigenvalues

$$\Sigma - \Pi, \quad \Sigma - \Pi, \quad \text{and} \quad \Sigma + 2\Pi$$

and

$$\bar{S}_2 = \begin{bmatrix} \frac{1}{\sqrt{2}} & \frac{1}{\sqrt{6}} & \frac{1}{\sqrt{3}} \\ \frac{i}{\sqrt{2}} & \frac{-i}{\sqrt{6}} & \frac{-i}{\sqrt{3}} \\ 0 & \frac{2}{\sqrt{6}} & \frac{-1}{\sqrt{3}} \end{bmatrix}.$$

Thus

$$S = \left[\begin{array}{ccc|ccc} \frac{1}{\sqrt{2}} & \frac{1}{\sqrt{6}} & \frac{1}{\sqrt{3}} & 0 & 0 & 0 \\ \frac{i}{\sqrt{2}} & \frac{-i}{\sqrt{6}} & \frac{-i}{\sqrt{3}} & 0 & 0 & 0 \\ 0 & 0 & 0 & 0 & \frac{-2}{\sqrt{6}} & \frac{1}{\sqrt{3}} \\ \hline 0 & 0 & 0 & \frac{1}{\sqrt{2}} & \frac{1}{\sqrt{6}} & \frac{1}{\sqrt{3}} \\ 0 & 0 & 0 & \frac{-i}{\sqrt{2}} & \frac{i}{\sqrt{6}} & \frac{i}{\sqrt{3}} \\ 0 & \frac{2}{\sqrt{6}} & \frac{-1}{\sqrt{3}} & 0 & 0 & 0 \end{array}\right]$$

and

$$\mathcal{H}'' = S^{-1}\mathcal{H}S = \begin{pmatrix} \Sigma - \Pi & & & & & 0 \\ & \Sigma - \Pi & & & & \\ & & \Sigma + 2\Pi & & & \\ & & & \Sigma - \Pi & & \\ & & & & \Sigma - \Pi & \\ 0 & & & & & \Sigma + 2\Pi \end{pmatrix}.$$

It is clear from the multiplicity of the eigenvalues that $\Sigma - \Pi$ belongs to the isospin $\frac{3}{2}$ state, and $\Sigma + 2\Pi$ to the $\frac{1}{2}$ state. This is easily checked by examining the field operators $S^{-1}\psi$ belonging to the eigenvalues.

For instance $\psi_1' + \psi_4'$ (rows 1 and 4 of ψ' belong to the same eigenvalue of multiplicity $2\times\frac{3}{2}+1$) corresponds to, according to S,

$$\frac{1}{\sqrt{2}} \left[\begin{pmatrix} p_1 \\ q_1 \end{pmatrix} \chi_a - i \begin{pmatrix} p_2 \\ q_2 \end{pmatrix} \chi_a + \begin{pmatrix} p_1 \\ q_1 \end{pmatrix} \chi_b + i \begin{pmatrix} p_2 \\ q_2 \end{pmatrix} \chi_b \right].$$

This is the mixture appropriate to the state of isotopic spin $\frac{3}{2}$ with z component $\frac{3}{2}$.

We are now left with the task of diagonalizing $\Sigma - \Pi$ and $\Sigma + 2\Pi$ to obtain the $\frac{3}{2}$ and $\frac{1}{2}$ phase shifts respectively.

Thus, if we write $\psi_i = \begin{pmatrix} \tilde{p}_i \\ \tilde{q}_i \end{pmatrix}$ $\psi_i = (\bar{\tilde{p}}_i, \bar{\tilde{q}}_i)$ ($\tilde{p}_i$ and $\tilde{q}_i$ are thus « double operators ») we must diagonalize:

$$H_i = \tfrac{1}{2} \sum_{kk'} (\bar{\tilde{p}}_i(k')\tilde{p}_i(k) + \omega_k^2 \bar{\tilde{q}}_i(k')\tilde{q}_i(k))\delta_{kk'} + gV_kV_{k'}\bar{\tilde{q}}_i(k')\tilde{q}_i(k) + \\ + i\lambda_i V_k V_{k'}(\bar{\tilde{p}}_i(k')\tilde{q}_i(k) - \bar{\tilde{q}}_i(k')\tilde{p}_i(k)),$$

where $\lambda_i = \begin{cases} \lambda - \lambda^3 & i = 1, 2, 4, 5 \\ 2\lambda - \lambda^1 & i = 3, 6 . \end{cases}$

The commutation relations satisfied by our operators are (we neglect the subscript i, which need only be considered when we give λ_i a value):

$$[\tilde{p}(k), \tilde{p}(k')]_+ = [\tilde{q}(k), \tilde{q}(k')]_+ = [\tilde{p}(k), \tilde{q}(k')]_+ = 0$$

$$[\bar{\tilde{p}}(k), \tilde{p}(k')]_+ = [\bar{\tilde{q}}(k), \tilde{q}(k')]_+ = 0 + \text{« single operators »}$$

$$[\bar{\tilde{p}}(k), \tilde{q}(k')]_+ = -[\tilde{p}(k), \bar{\tilde{q}}(k')]_+ = -i\,\delta(k - k') + \text{« single operators »}.$$

as can easily be checked by the properties of S and of the components of $\boldsymbol{q}$.

We define new « double operators » $Q(k)$, $\bar{Q}(k)$, $P(k)$, $\bar{P}(k)$ by

$$(6)\qquad \begin{cases} \tilde{q}(k) = \sum\limits_{k'} \xi_{kk'} Q(k') + \eta_{kk'} P(k') \\ \bar{\tilde{q}}(k) = \sum\limits_{k'} \xi^*_{kk'} \bar{Q}(k') + \eta^*_{kk'} \bar{P}(k') \\ \tilde{p}(k) = \sum\limits_{k'} \varepsilon_{kk'} Q(k') + \lambda_{kk'} P(k') \\ \bar{\tilde{p}}(k) = \sum\limits_{k'} \varepsilon^*_{kk'} \bar{Q}(k') + \lambda^*_{kk'} \bar{P}(k') \,. \end{cases}$$

It is unnecessary to mix the barred with the unbarred operators, as the Hamiltonian is already diagonal with regard to the creation and destruction of nucleons.

In order that the new « double operators » satisfy the same commutation relations as the old operators, the requirements on ξ, η, ε and λ are

$$(7)\qquad \begin{cases} \sum\limits_{k} \xi_{k_1 k} \lambda^*_{k_2 k} - \eta_{k_1 k} \varepsilon^*_{k_2 k} = \delta_{k_1 k_2} \\ \sum\limits_{k} \xi_{k_1 k} \eta^*_{k_2 k} - \eta_{k_1 k} \xi^*_{k_2 k} = 0 \\ \sum\limits_{k} \varepsilon_{k_1 k} \lambda^*_{k_2 k} - \lambda_{k_1 k} \varepsilon^*_{k_2 k} = 0 \,. \end{cases}$$

The equations resulting from the requirement that H_i be diagonal in the new operators are

$$(8)\qquad \sum_{kk'} \lambda^*_{kk''} \lambda_{k'k'''} \delta_{kk'} + \omega_k^2 \eta^*_{kk''} \eta_{k'k'''} \delta_{kk'} + g V_k V_{k'} \eta^*_{kk''} \eta_{k'k'''} + \\ + i\bar{\lambda} V_k V_{k'} (\lambda^*_{kk''} \eta_{k'k'''} - \eta^*_{kk''} \lambda_{k'k'''}) = \delta_{k''k'''} \,,$$

$$(9)\qquad \sum_{kk'} \varepsilon^*_{kk''} \varepsilon_{k'k'''} \delta_{kk'} + \omega_k^2 \xi^*_{kk''} \xi_{k'k'''} \delta_{kk'} + g V_k V_{k'} \xi^*_{kk''} \xi_{k'k'''} + \\ + i\bar{\lambda} V_k V_{k'} (\varepsilon^*_{kk''} \xi_{k'k'''} - \xi^*_{kk''} \varepsilon_{k'k'''}) = \omega_{k''}^2 \delta_{k''k'''} \,,$$

$$(10)\qquad \sum_{kk'} \lambda^*_{kk''} \varepsilon_{k'k'''} \delta_{kk'} + \omega_k^2 \eta^*_{kk''} \xi_{k'k'''} \delta_{kk'} + g V_k V_{k'} \eta^*_{kk''} \xi_{k'k'''} + \\ + i\bar{\lambda} V_k V_{k'} (\lambda^*_{kk''} \xi_{k'k'''} - \eta^*_{kk''} \varepsilon_{k'k'''}) = 0 \,.$$

We have here utilized the fact that the energy eigenvalue of the coupled system, W_k^2, is equal to the free oscillator energy, ω_k^2, in the continuous limit [3]. We now can utilize (7) to linearize (8), (9) and (10).

For instance $\sum\limits_{k'''} - \varepsilon^*_{k_1 k'''} \times (8) + \lambda^*_{k_1 k'''} \times (10)$ leads to

$$(11)\qquad \omega^2_{k_1} \eta^*_{k_1 k''} + g V_{k_1} \sum_k V_k \eta^*_{kk''} + i\bar{\lambda} V_{k_1} \sum_k V_k \lambda^*_{kk''} = - \varepsilon^*_{k_1 k''}$$

and similarly we get

$$\lambda_{k_1k''} + i\bar{\lambda}V_{k_1}\sum_k V_k\eta_{kk''} = \xi_{k_1k''}\,, \tag{12}$$

$$\omega_{k_1}^2\xi_{k_1k''} + gV_{k_1}\sum_k V_k\xi_{kk''} - i\bar{\lambda}V_{k_1}\sum_k V_k\varepsilon_{kk''} = \omega_{k''}^2\lambda_{k_1k''}\,, \tag{13}$$

$$\varepsilon_{k_1k''} + i\bar{\lambda}V_{k_1}\sum_k V_k\xi_{kk''} = -\omega_{k''}^2\eta_{k_1k''}\,. \tag{14}$$

Putting (11) in (14) we have (if $V=\sum_k V_k^2$)

$$(\omega_j^2-\omega_i^2)\eta_{ij} = \bar{g}V_i\sum_k V_k\eta_{kj} - 2i\bar{\lambda}V_i\sum V_k\lambda_{kj}\,, \tag{15}$$

where $\bar{g}=g+\bar{\lambda}^2V$. (15) does not completely determine the dependence of η_{ij} on j. We thus write

$$\eta_{ij} = A_j\left(\delta_{ij}+\frac{V_iB_j}{\omega_j^2-\omega_i^2}\right) \tag{16}$$

which is the form determined by the singularities of (15).

Putting (16) in (15) we get

$$B(j) = \frac{\bar{g}V_j - 2i\bar{\lambda}\sum_k V_k\lambda_{kj}/A_j}{1-\bar{g}S_j}\,. \tag{17}$$

We now put (11) and (12) into (13)

$$(\omega_j^2-\omega_i^2)\lambda_{ij} = V_i\bar{g}\sum_k V_k\lambda_{kj} + i\bar{\lambda}V_i[2gV\sum_k V_k\eta_{kj} + \sum_k(\omega_i^2+\omega_k^2)V_k\eta_{kj}]\,.$$

Using (16) and (17) we have

$$(\omega_j^2-\omega_i^2)\lambda_{ij} = [\bar{g}(1-\bar{g}S_j)+2\bar{\lambda}^2(\omega_i^2+\omega_j^2)S_j]\frac{V_i}{(1-\bar{g}S_j)}\sum_k V_k\lambda_{kj} + \\ + \frac{i\bar{\lambda}V_iV_jA_j}{1-\bar{g}S_j}[\bar{g}V+\omega_i^2+\omega_j^2], \tag{18}$$

where $\bar{\bar{g}}=g-\bar{\lambda}^2V$. We now try

$$\lambda_{ij} = C_j\left(\delta_{ij}+\frac{V_iF_j}{\omega_j^2-\omega_i^2}+V_iG_j\right), \tag{18a}$$

where the last term is added due to the appearance of ω_i^2 in (18) removing

the $(\omega_j^2 - \omega_i^2)$ singularity for certain terms. Thus

$$F_j + (\omega_j^2 - \omega_i^2)G_j = [\bar{\bar{g}}(1 - \bar{\bar{g}}S_j) + 2\bar{\lambda}^2(\omega_i^2 + \omega_j^2)S_j](1 - \bar{g}S_j)^{-1} \cdot \cdot (V_j + S_jF_j + VG_j) + i\bar{\lambda}V_jA_jC_j^{-1}(1 - \bar{g}S_j)^{-1}(\bar{g}V + \omega_i^2 + \omega_j^2), \tag{19}$$

from which (equating coefficients of $(\omega_j^2 - \omega_i^2)$ and those independent of $(\omega_j^2 - \omega_i^2)$)

$$F_j = \frac{V_j}{1 - \bar{g}S_j}\left[(\bar{g}(1 - \bar{g}S_j) + 4\bar{\lambda}^2\omega_j^2S_j)\left(1 + \frac{S_jF_j + VG_j}{V_j}\right) + + i\bar{\lambda}A_jC_j^{-1}(\bar{g}V + 2\omega_j^2)\right], \tag{20}$$

$$G_j = \frac{V_j}{1 - \bar{g}S_j}\left[(-2\bar{\lambda}^2S_j)\left(1 + \frac{S_jF_j + VG_j}{V_j}\right) - i\bar{\lambda}A_jC_j^{-1}\right]. \tag{21}$$

(20) and (21) are two linear simultaneous equations for F_j and G_j. We can now obtain λ_{ij} from (18*a*), η_{ij} from (16) and (17), ε_{ij} from (11) and ξ_{ij} from (12); all in terms of A_j/C_j. A_j/C_j must be determined from (7). However, it does not enter in the phase shift experiment.

2. – Phase Shift Determination.

Let $\rangle$ represent the physical vacuum,

$$\bar{\alpha}_\beta(k) = -\frac{i}{\sqrt{2\omega_k}}\bar{\bar{p}}_\beta(k) + \sqrt{\frac{\omega_k}{2}}\bar{\bar{q}}_\beta(k)$$

is the creation operator for a state of a nucleon and s-state meson of momentum k, in the state of isotopic spin $\beta/2$. Similarly,

$$\bar{a}_\beta(k')\rangle \quad \left[\bar{a}_\beta(k') = \cdot \cdot \frac{i}{\sqrt{2\omega_{k'}}}\bar{p}_\beta(k) + \sqrt{\frac{\omega_k}{2}}\bar{Q}_\beta(k)\right]$$

represents the state vector for the real nucleon together with a stationary s-state meson of incoming momentum k', as $\bar{a}_\beta(k')$ is the operator in the diagonal form.

Consequently $\langle\alpha_\beta(k)\bar{a}_\beta(k')\rangle$ represents the component of our stationary state designated by k' that can be represented by a physical nucleon plus a meson of momentum k, i.e., it is the Fourier transform of the single meson wave function (in the state of isotopic spin $\beta/2$).

From equation (6)

$$\alpha_\beta(k) = \sum_{k''} [(M^\beta_{kk''} + N^\beta_{kk''})a_\beta(k'') + (M^\beta_{kk''} - N^\beta_{kk''})\bar{a}_\beta(k'')] , \tag{22}$$

where

$$M^\beta_{kk''} = \frac{1}{2}\left[\sqrt{\frac{\omega_k}{\omega_{k''}}}\,\xi^\beta_{kk''} + \frac{i}{\sqrt{\omega_k\omega_{k''}}}\,\epsilon^\beta_{kk''}\right]$$

and

$$N^\beta_{kk''} = \frac{1}{2}\left[\sqrt{\frac{\omega_{k''}}{\omega_k}}\,\lambda^\beta_{kk''} - i\sqrt{\omega_k\omega_{k''}}\,\eta^\beta_{kk''}\right] .$$

Using equation (22) and the commutation rules (for simplicity we omit the « single operators » which appear. They do not invalidate the following statements) we have

$$\langle \alpha_\beta(k)\bar{a}_\beta(k')\rangle = \sum_{k''} (M^\beta_{kk''} + N^\beta_{kk''})[\delta_{k'k''}\langle\ \rangle - \langle \bar{a}_\beta(k')a_\beta(k'')\rangle] + \tag{23}$$
$$+ \sum_{k''} (M^\beta_{kk''} - N^\beta_{kk''})\langle \bar{a}_\beta(k'')\bar{a}_\beta(k')\rangle .$$

As $\bar{a}_\beta(k')a_\beta(k'')$ is a projection of normalized states it can have no singularity on the energy shell. Neither can $\bar{a}_\beta(k'')\bar{a}_\beta(k')$, as it would imply the existence of real meson pairs (we restrict our conclusions to energies below that required for pair creation.).

As $(M^\beta_{kk''} + N^\beta_{kk''})$ has only a first order pole on the energy shell and $(M^\beta_{kk''} - N^\beta_{kk''})$ has no singularity there, we see that the only contribution to $\langle \alpha_\beta(k)\bar{a}_\beta(k')\rangle$ which will yield a phase shift is

$$(M^\beta_{kk'} + N^\beta_{kk'})\langle\ \rangle = X^\beta_{k'}\left[\delta_{kk'} + \frac{Y^\beta_{kk'}}{\omega^2_{k'} - \omega^2_k} + Z^\beta_{kk'}\right], \tag{24}$$

where $Y^\beta_{kk'}$ and $Z^\beta_{kk'}$ are not singular on the energy shell.

The wave function is

$$\psi^\beta(kr) = \sum_{k'} \frac{\sin k'r}{r}\,\langle \alpha_\beta(k)a_\beta(k')\rangle . \tag{25}$$

Inserting equation (24) in equation (25) we will obtain the phase shift

$$\delta_\beta(k) = \mathrm{tg}^{-1} - \frac{RY^\beta_{kk}}{2k} . \tag{26}$$

Equations (11), (12), (16), (17) and (18a) yield (omitting the superscript β until equation (29))

$$Y_{kk} = V_k \frac{F_k - \mu_k B_k}{1 - \mu_k} - \frac{V_a}{1 - \mu_k}\left[F_k - \frac{\mu_k \bar{g} V_k}{(1 - \bar{g}S_k)} - \frac{2\bar{\lambda}\bar{\omega}_k}{(1 - \bar{g}S_k)}(V_k + S_k F_k + VG_k)\right],$$

where $\mu_k = i\omega_k A_k C^{-1}_k$.

Using equation (20) to substitute for $V_k + S_k F_k + VG_k$

$$(27) \qquad Y_{kk} = \frac{V_k}{(1+\mu_k)}\left[F_k\left(1 - \frac{2\bar{\lambda}\omega_k}{(\bar{g}(1-\bar{g}S_k) + 4\bar{\lambda}^2\omega_k^2 S_k)}\right) - \frac{\mu_k V_k}{(1-\bar{g}S_k)}\left(\bar{g} - \frac{2\bar{\lambda}^2(\bar{g}V + 2\omega_k^2)}{(\bar{g}(1-\bar{g}S_k) + 4\bar{\lambda}^2\omega_k^2 S_k)}\right)\right].$$

From equations (20) and (21)

$$(28) \qquad [(1-\bar{g}S_k)^2 - 4\bar{\lambda}^2\omega_k^2 S_k^2]F_k = V_k[g(1 - gS_k) + 4\bar{\lambda}^2\omega_k^2 S_k] + 2\mu_k\bar{\lambda}V_k\omega_k .$$

Inserting equation (28) in equation (27)

$$(29) \qquad Y^{\beta}_{kk} = V_k^2[\bar{g}^{\beta}(1 - \bar{g}^{\beta}S_k) + 4(\lambda^{\beta})^2\omega_k^2 S_k - 2\lambda^{\beta}\omega_k][(1 - \bar{g}^{\beta}S_k)^2 - 4(\lambda^{\beta})^2\omega_k^2 S_k^2]^{-1} = V_k^2(\bar{g}^{\beta} - 2\lambda^{\beta}\omega_k)(1 - S_k(\bar{g}^{\beta} - 2\lambda^{\beta}\omega_k))^{-1} .$$

The dependence on μ_k has vanished, reflecting the independence of the phase-shift on the normalization factors.

3. – Properties of the Phase Shift.

We choose the particular form factor

$$u(r) = \frac{A^2 \exp[-Ar]}{4\pi r} \qquad V(k) = \frac{A^2 k}{\sqrt{2\pi}R(k^2 + A^2)} .$$

The general properties to be discussed depend only on the cut-off A, and not on the chosen form. We now have

$$S_k = \frac{A^3}{8\pi}\frac{k^2 - A^2}{(k^2 + A^2)^2} \quad \text{and} \quad V = \frac{A^3}{8} \quad \text{Thus} \quad \bar{g}^{\beta} = g - (\lambda^{\beta})^2\frac{A^3}{8\pi} .$$

Assuming a non-zero, finite ratio λ/g, g becomes negative for a sufficiently large cut-off. Thus, in contrast to the Wentzel Pair Theory, the denominator

of Y_{kk} vanishes for values of g going to zero through *positive* values, as $A \to \infty$. This is of importance, as g is the square of the fundamental coupling constant. Therefore we may proceed to the point source limit without the vanishing of the phase-shift or the invocation of « ghost states » (7). It is possible even in the point source limit to define a renormalized coupling constant (*) of arbitrary value.

$g_R^\beta = (g^\beta/(1 + g^\beta(A/8\pi))$. As g^β can be negative g_R^β is arbitrary. In the point source limit

$$\bar{g}^\beta = \operatorname*{Lim}_{A\to\infty} \frac{g_R^\beta}{1 - g_R^\beta(A/8\pi)} \qquad \text{or} \qquad (\lambda^\beta)^2 = \operatorname*{Lim}_{A\to\infty} \frac{8}{A^3}\left[g - \frac{g_R^\beta}{1 - g_R^\beta(A/8\pi)}\right].$$

This limit exists and is equal to zero for arbitrary finite g and g_R^β.

On the other hand, the adjustment of only one of the two λ^β, to effect a finite limit for Y_{kk}, is possible. In the point source limit only one of the isotopic spin states has non-zero scattering phase shift.

If has often been assumed (Drell and Henley (2)) that the contribution from the second term of (1) if of order μ/M compared to that of the first term. While this is true for the terms proportional to ω_k in equation (29), it is not true for $\bar{g}^\beta$. In this case the dimensionless ratio involved is A/M instead of μ/M. This considerably enhances the contribution of the second term of equation (1) and permits us to match experiment. In a non-cut-off theory the same effect would be produced by the order of the divergence involved.

4. – Comparison with Experiment.

We attempt to fit the phase shift analysis of Bethe and de Hoffman (5b) of the scattering results. For the zero energy slopes we use the values indicated by the radiative capture data in combination with the data obtained from the level shifts in π-mesonic atoms (page 108 of ref. (5b)). In case *b*) below, in order to better approximate the higher energy data, a somewhat larger value of the zero energy slope of δ_1 is used. However, this value is still smaller than that of Orear's analysis (5a) and is consistent with a negative level shift.

For both fits δ_3 is almost linear. On the other hand, for δ_1, the k/μ dependent terms (μ is the meson mass) are of the same order of magnitude as the k/μ independent terms. The slope of δ_1 decreases steadily with k, and δ_1 changes sign near $k/\mu = 2$.

(*) We refer to the renormalized coupling constant defined by zero energy ($k = \mu = 0$) scattering (9).

(9) S. Deser, W. E. Thirring and M. L. Goldberger: *Phys. Rev.*, **94**, 711 (1954).

We present one fit for a value of « a » between the weak and strong coupling values of AKIBA and SAWADA [1]. The character of the fit does not change greatly in this range. A/M decreases from 2.4 to 1.8 as « a » increases from 1 to 2.

a) For $A = 2M$ we have $a = 1.75$, $f_s^2/4\pi = 0.9$.

In both cases $f_s^2/4\pi$ is much smaller than the value (~ 12) given by the renormalized coupling constant of Chew's model [4]; and therefore much smaller than the value yielded by the unrenormalized coupling constant of that model. This is reminiscent of the disparity between the p state and s state renormalized coupling constants found from the low energy approximation to the $ps(ps)$ theory [9]. It is also similar to the disparity in the unrenormalized coupling constants required in the Tamm-Dancoff approximation of the same theory [10].

In our case, however, we can remove the discrepancy by allowing greater freedom to the parameter « a » than that indicated by AKIBA and SAWADA [1]. As our result has a different value for the cut-off, it is not necessarily inconsistent with their work.

b) If we choose $A = 3.5M$ then $a = 0.15$, $f_s^2/4\pi = 16.985$.

The positive features of the fits are (see Fig. 1).

1p) The ability to fit the zero energy data for a reasonable value of « a » or $f_s^2/4\pi$. Despite the availability of two parameters to fit the two slopes, in case *a*) the slope of δ_1 is the maximum possible while still fitting the slope of δ_3.

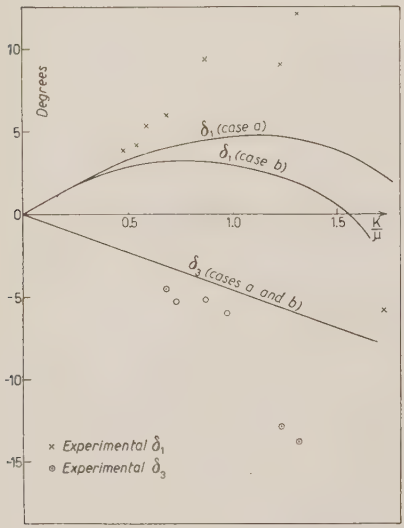

2p) The absence of resonances.

3p) The passing of δ_1 through a maximum and its change of sign near $k/\mu = 2$. This is particularly significant as all the parameters are determined by the zero energy slopes and the physical assumption for « a » or $f_s^2/4\pi$.

Fig. 1. – S-state meson-nucleon scattering phase shifts. The experimental phase shifts are taken from reference [5b]. The theoretical curves represent the parameters: Case *a*) $A = 2\ M$, $a = 1.75$, $f_s^2/4\pi = 0.9$; Case *b*) $A = 3.5M$, $a = 0.15$, $f_s^2/4\pi = 16.945$.

---

[10] M. H. KALOS and R. H. DALITZ: *Phys. Rev.*, **100**, 1515 (1955).

The negative aspects of the fits are:

1n) The maximum of δ_1 is not large enough.

2n) The magnitude of δ_3 does not increase with k as indicated by experiment.

Our cut-off is larger than that of CHEW ($\sim 0.85M$). As the recoil effects are different for s and p scattering, there is no reason to assume that the cut-offs, which are to a large extent the result of recoil, are the same. Due to the pair emission of mesons for the s state scattering, the recoil of the nucleon should be smaller, the mesons partially cancelling their own momenta.

5. – Discussion.

It seems to us that the above analysis indicates strongly that the $ps(ps)$ theory is adequate for S state scattering as well as p state phenomena. We have not considered the S state scattering due to recoil effects from the pseudovector term. As these would contribute an additional phase shift increasing as the square of the energy for low energies, it may rectify the deficiencies $1a$) and $2a$). On the other hand $1p$), $2p$), and $3p$) hold for values of « a » of the order of magnitude of unity and values of $f_s^2/4\pi$ in the range seemingly required by p state scattering. The appropriate value of $f_s^2/4\pi$ is not certain as the p state analysis is not exact, and it is only a hope that many particle effects are not appreciable. Also « a » is not well defined due to the uncertain contribution of the neglected terms of the Foldy transformed Hamiltonian. More extensive work like that of AKIBA and SAWADA [1] may clarify this.

The discrepancy of the low energy renormalized coupling constants [9] would be due to high order effects, according to our result which shows the two values to be consistent for certain values of « a ». Similarly, the failure of the Tamm-Dancoff approach [10] to reproduce s and p scattering with the same unrenormalized coupling constant, would be due to the omission of high order effects from this approximation. The importance of the high order effects is directly related to the fact that $(1 - g^2 S_1)$ is not very close to unity for our parameters.

The most general result is that the point source limit is possible without annihilating the scattering or destroying the physical integrity of the theory. The appearance in H_I of cross terms in $q(x)$ and its canonical conjugate $\pi(x)$ would appear to be responsible for this.

* * *

I am deeply indebted to Prof. M. CINI for suggesting the importance of H_I for s state scattering and for much help and criticism during the work.

Discussions with Dr. G. KÄLLÉN concerning the present treatment illuminated and simplified many aspects for me.

The work was supported in its initial stages by an overseas Postdoctoral Fellowship of the Canadian National Research Council and by a Rutherford Memorial Fellowship of the Royal Society of Canada. In the final stages it was supported by a Weizman Fellowship.

RIASSUNTO (*)

Consideriamo l'hamiltoniana

$$H_I = g\int \mathrm{d}_3 x\,\bar{\psi}(x)\varphi(x)\cdot\varphi(x)\psi(x) + \lambda\int \mathrm{d}_3 x\,\bar{\psi}(x)\big(\pi(x)\times\varphi(x)\big)\cdot\tau\psi(x)\,. \tag{1}$$

Esistono prove ([1,2]) che per lo scattering mesone-nucleone la (1) rappresenta larga parte dell'interazione di stato s $ps(ps)$ per accoppiamento sia intermedio che debole, purchè λ/g sia convenientemente modificato. Da tempo si sa che il primo termine della (1) è diagonalizzabile nei limiti del nucleone stabile ([3]). L'accoppiamento di spin isotopico del nucleone si lascia libera (non statica) complicando in tal modo la diagonalizzazione. Combinando l'operatore di spin del nucleone con gli operatori del campo mesonico siamo riusciti a diagonalizzare la (1). I parametri determinati sperimentalmente sono ragionevoli. Si possono esaminare molti aspetti formali. Esiste un limite di sorgente puntiforme.

(*) *Traduzione a cura della Redazione.*

On Intermetallic Diffusion in Gold-Lead System.

A. Ascoli, E. Germagnoli and L. Mongini

Laboratori CISE - Milano

(ricevuto il 26 Maggio 1956)

Summary. — Diffusion of gold in lead has been investigated by means of radioactive tracers method in the range of temperatures between 190 and 300 °C. In this temperature interval experimental values of the diffusion coefficient D fit the equation

$$D = 2.8 \cdot 10^{-3} \exp\left[-\frac{8.91 \cdot 10^3}{RT}\right] \text{cm}^2\,\text{s}^{-1},$$

whence an activation energy $Q = (8.91 \pm 0.18) \cdot 10^3$ cal mole^{-1} is obtained.

1. – Introduction.

Intermetallic diffusion has been studied in a number of binary and ternary systems. The interpretation of such phenomena, though still incomplete, can be of valuable help for a closer insight into some topics of solid state physics [1].

Experimental data concerning diffusion were already available many years ago but it was found somewhat difficult to interpret them clearly owing to the different experimental methods which in many cases had been used. Many parameters can in fact be expected to be important in this kind of phenomena and it is possible that the influence of some of them is greatly enhanced by a special experimental method; moreover not all these parameters have perhaps been adequately considered in early investigations. From an experimental point of view, chemical purities and structural features of materials are likely to be of outstanding importance.

The method of radioactive tracers and the present availability of radioactive

[1] A. D. Le Claire: *Progress in Metal Physics* (B. Chalmers Editor, London, 1949), 1.

sources of high specific intensity made investigations of diffusion and self-diffusion phenomena remarkably easier. Many diffusion coefficients have been measured with the help of this method and sometimes results have been obtained which were quite different from the previous ones: an analysis of many of the old data was done by NOWICK [2], who succeeded in showing that they did not seriously disagree with the more recent ones, if correctly interpreted.

Intermetallic diffusion experiments are most conveniently performed by plating a very thin layer of the metal to be diffused onto a flat surface of the solvent metal, letting them penetrate during a suitable annealing time and studying later the spatial distribution of the diffused metal within the solvent with the help of some radioactive counting method. Diffusion coefficients are so obtained as functions of annealing temperature and time.

With the above mentioned method the sensitivity can often be enormously increased, self diffusion investigations are possible, and, generally speaking, difficulties involved in chemical tracing out of very small amounts of elements are avoided. Moreover it is possible in this way to work with so small percentages of diffusing metals that complications due to the dependence of diffusion coefficients upon concentration can reasonably be avoided. The method of analyzing penetration curves has been discussed by JOHNSON [3].

In the above outlined experimental case the specific activity $A(x)$ of diffused metal is expected to be described by the following relationship

$$A(x) = \frac{C}{\sqrt{t}} \exp\left[-\frac{x^2}{4Dt}\right], \tag{1}$$

where x is the penetration within the solvent metal
t is the annealing time
D is the diffusion coefficient, which depends upon the annealing temperature.

(1) has been deduced under the hypothesis that only volume diffusion is important; this is usually true with single crystals of solvent metals and also with policrystalline materials at high temperatures.

Grain boundary and surface diffusion, conversely, seem to be important at temperatures reasonably lower than the melting point of solvent materials; these phenomena have been analyzed in detail by FISHER [4] who found that the penetration of solute is in this case exponentially dependent upon x.

From (1) or from analogous equations which have been derived by FISHER, the diffusion coefficients can be deduced as a function of temperature T.

---

[2] A. S. NOWICK: *Journ. Appl. Phys.*, **22**, 1182 (1951).
[3] W. A. JOHNSON: *Trans. Am. Inst. Mining Met. Engrs.*, **143**, 107 (1941).
[4] J. C. FISHER: *Journ. Appl. Phys.*, **23**, 741 (1951).

D has been experimentally found to obey in both cases the equation

$$D = D_0 \exp\left[-\frac{Q}{RT}\right]. \tag{2}$$

where D_0 is a diffusion constant
Q is the activation energy for the actual diffusion process
R is the gas constant.

The activation energy Q for the process can consequently be deduced directly from experimental values of D.

Diffusion in gold-lead system has been investigated by a few authors [5-10] many years ago. They all agreed in finding that diffusion coefficients are in this case very large even at low temperatures. As far as we know no recent determinations of these diffusion coefficients are available; it seemed consequently worthwhile to repeat such measurements with the above outlined method of radioactive tracers.

2. – Experimental Procedure.

The method of radioactive tracers provides an extremely sensitive technique of identifying very small amounts of gold within lead samples and offers in advance the possibility of checking the chemical purity of the solvent metal. This method is of general application and only a few details of it need be modified from case to case according to the particular features of the radioactive decay of used materials.

In the actual case a possible difficulty can arise from the fact that the half-life of ^{198}Au, which is produced by means of neutron irradiation of gold, is rather short (2.7 d) [11], but the very small activation cross sections of lead isotopes and their short half-lives permitted the avoidance of such difficulty as it will be discussed later.

Pure lead furnished by two different suppliers was used for the present investigation: the chemical purities of the two kinds of lead were not found to differ remarkably. A few measurements were also performed with less pure

---

[5] W. C. Roberts-Austen: *Phil. Trans. Roy. Soc.* (London), A **187**, 404 (1896).
[6] C. E. van Ostrand and F. C. Dewey: *U. S. Geol. Survey Prof. Paper* 1915, 956.
[7] G. V. Hevesy: *Zeits. f. Elektrochem.*, **39**, 490 (1933).
[8] W. Seith and A. Keil: *Zeits. f. Phys. Chem.*, **22** B, 350 (1933).
[9] W. Seith and H. Etzold: *Zeits. f. Elektrochem.*, **40**, 829 (1934).
[10] W. Seith and H. Etzold: *Zeits. f. Elektrochem.*, **41**, 122 (1935).
[11] J. M. Hollander, I. Perlman and G. T. Seaborg: *Rev. Mod. Phys.*, **25**, 469 (1953).

lead (99.98%) in order to investigate the possible influence of purity. A chemical analysis of one of the two kinds of pure lead is given in Table I and the results of a rough activation analysis performed by us are consistent with it.

Lead was melt, let to solidify slowly, and shaped in cylinders, 14 mm long and 10 mm in diameter. Microscope examination of the samples showed that its microstructure in most cases consisted of rather big grains (ranging from 1 to 9 mm in linear sizes). In some cases the lead cylinders can roughly be considered as single crystals.

TABLE I.

Impurity	Percentage
Ag	0.0002 %
Bi	< 0.0001
Cu	0.0009
Sb	0.002

Though the rather low healing temperature of lead makes it unlikely that permanent defects from mechanical treatment be produced within the samples, a careful preliminary annealing of them was performed in vacuo at the temperature of about 310 °C. No appreciable oxidation was noticed after this treatment, anyway one of the flat ends of the cylinders was etched with diluted cold HNO_3 which was neutralized later with NH_3; high purity gold (99.999%) was then evaporated in vacuo onto the so-treated ends of the cylinders. The thicknesses of gold layers were approximately 0.2 μm.

Diffusion annealing was subsequently performed at eight different temperatures ranging between 190 and 300 °C in an oven, the temperature of which was stabilized within $\pm$ 0.1 °C. The annealing times ranged correspondingly between 150 and 35 hours approximately in order to allow a sufficiently deep penetration of gold within lead. Some treatments were duplicated and some others were performed with different annealing times in order to check the reliability of the obtained results.

After diffusion the samples were sent to A.E.R.E. (Harwell) for slow neutron irradiation in a position within the nuclear reactor where the temperature was low (37 °C).

Activation of gold is due to the well known reaction

$$^{197}\mathrm{Au} + \mathrm{n} \rightarrow {}^{198}\mathrm{Au} \xrightarrow[(2.7\mathrm{d})]{} \beta^- + {}^{198}\mathrm{Hg} .$$

A few days after irradiation no appreciable activity could be attributed to lead isotopes and the only possible spurious activities could arise from long lived chemical impurities within the samples.

To illustrate this point two spectra of γ-rays emitted by one of the used probes are given in Figs. 1 and 2.

In Fig. 1 the γ spectrum of gold, as obtained during the few days in which activation measurements were done is reported: the small peak at ~ 550 keV has been attributed to ^{122}Sb (2.8 d half-life) ([11]) which is the main impurity according to the previously given chemical analysis. It has to be noticed that Fig. 1 represents a particularly unfavourable situation for the purpose of evaluating the amounts of impurities because only the portion of the lead probe which was opposite to the surface where gold had been evaporated was used. Activity of gold, averaged within this part of the samples, is reduced by a factor of at least 30 in comparison with the opposite end of the cylinder and the impurity peak was consequently enhanced.

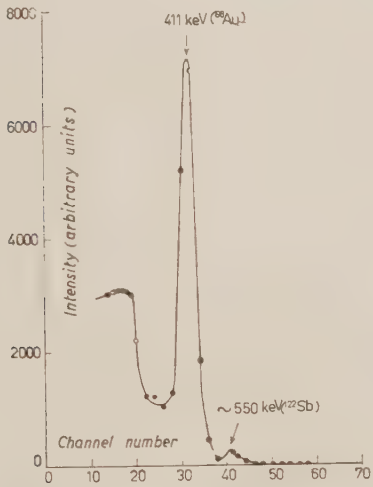

Fig. 1. – Energy spectrum of γ-rays emitted from an irradiated lead-gold sample. Spectrum obtained 2 days after the end of penetration measurements.

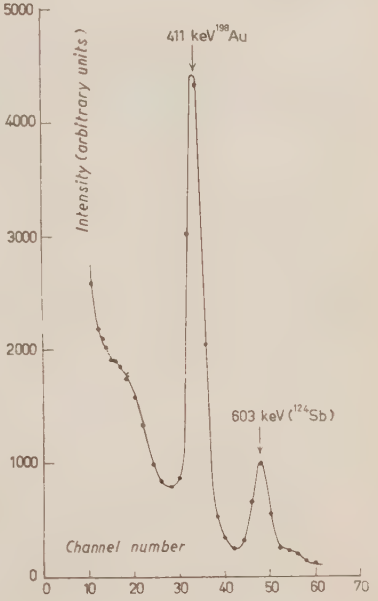

Fig. 2. – Energy spectrum of γ-rays emitted from an irradiated lead-gold sample. Spectrum obtained 23 days after the end of penetration measurements.

In these conditions, activity due to ^{122}Sb represents only a very small correction and was subtracted together with the cosmic background.

A similar spectrum, obtained about 20 days after the end of penetration measurements, is given in Fig. 2 and shows that the long lived (60 d half-life) ([11]) activity of ^{124}Sb has become more prominent, but it is estimated that its intensity was completely negligible at the time of measurements.

Activity of ^{198}Au was measured by means of a single crystal γ counter: a NaI(Tl) crystal, a RCA 5819 photomultiplier and a conventional amplifying chain were used for these measurements.

Samples were cut into slices 0.25 mm thick by means of a microtome and every penetration curve consisted of about 40 experimental points, corresponding to a total investigated depth of 10 mm or thereabout. Results are discussed in the next section.

3. – Results.

A typical penetration curve is given in Fig. 3; it shows the expected exponential dependence upon the squared distance, which is to be related to the volume diffusion phenomena. A noticeable deviation from such behaviour was found only with the probe which underwent diffusion annealing at the temperature of 189.5 °C and its meaning will be discussed in the next section.

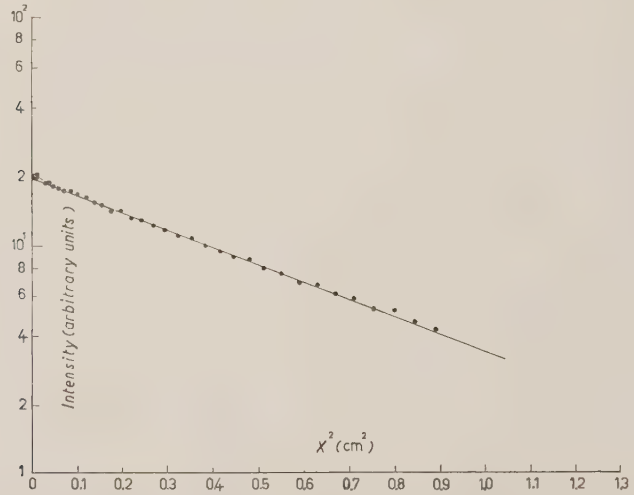

Fig. 3. – Typical penetration curve of gold in lead for cylindrical probes. Annealing temperature 280.4 °C; corrected annealing time 47.05 h.

In Table II the experimental data which have been obtained with the above described cylindrical probes are given. The quoted values for the diffusion coefficients D have been obtained assuming that the experimental curves showed fit equation (1).

The corrections to the annealing times, as they result from Table II, were introduced to take into account the rise in temperature in the oven before

TABLE II.

Temperature (°K)	Annealing time (s)	Corrected annealing time (s)	D ($cm^2\ s^{-1}$)
462.7	$5.032 \cdot 10^5$	$5.346 \cdot 10^5$	$1.67 \cdot 10^{-7}$
477.9	3.795	3.873	2.55
494.7	3.400	3.463	3.13
509.1	2.858	2.903	4.33
524.4	2.330	2.376	5.39
538.7	1.905	1.961	6.94
553.6	1.606	1.694	8.39
568.5	1.330	1.412	$1.09 \cdot 10^{-6}$

a steady temperature was reached and the decrease in temperature after the oven was switched down. Such corrections are straightforward and were calculated under the assumption that the oven reached the steady temperature and cooled down according to an exponential law; the « half-life » of the oven was measured and found to be independent from the steady temperature, at least for temperatures not too near room temperature, and equal to 2.74 hours.

The damped sinusoidal behaviour of the temperature immediately after the steady temperature had been reached was also taken into account but the corresponding correction is quite small.

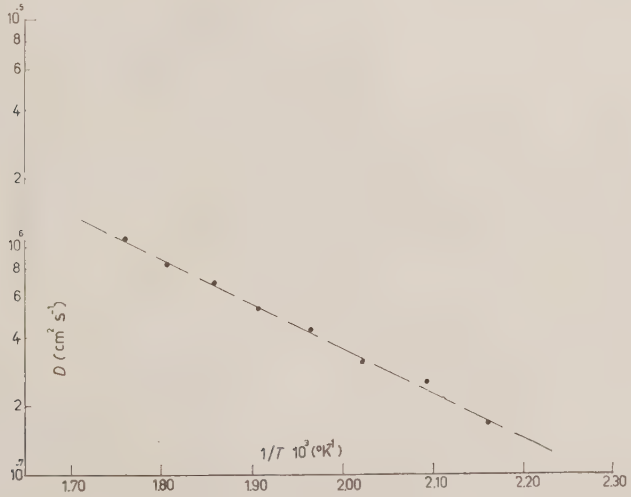

Fig. 4. – Dependence of diffusion coefficient upon T. Data obtained with cylindrical probes.

The corrected values for D, which are listed in Table II, were subsequently plotted logarithmically versus $1/T$; they are believed to be accurate within $\pm 3\%$ and their dependence upon the temperature is illustrated in Fig. 4 and results to be consistent with equation (2).

A least squares adjustment of the experimental data gave the following results:

$$D_0 = 2.8 \cdot 10^{-3} \text{ cm}^2 \text{ s}^{-1}$$

$$Q/R = (4.48 \pm 0.10) \cdot 10^3 \text{ °K}$$

whence an activation energy $Q = (8.91 \pm 0.18) \cdot 10^3$ cal mole^{-1} can be deduced.

4. – Discussion.

As it has been discussed in the introduction, three different kinds of intermetallic diffusion processes can be expected a priori: volume diffusion, grain boundary diffusion and surface diffusion. An attempt to investigate the possible influence of surface diffusion was done using lead samples having the same chemical purity as stated before but cut in the shape of rectangular slices one tenth of mm thick, 1 cm wide 4 cm long. Gold was evaporated at one of the ends of the samples in shape of rectangular spot 2 mm long and as wide as the samples themselves. Diffusion annealing was performed on these probes with the same modalities as with the cylindrical ones; in this case it is believed that surface diffusion, if important, should be greatly enhanced.

A typical penetration curve obtained in this set of measurements is given in Fig. 5 and the related diffusion data were analyzed as before. The least squares adjustment gave in this case:

$$D_0 = 2.5 \cdot 10^{-3} \text{ cm}^2 \text{ s}^{-1}$$

$$Q/R = (4.4 \pm 0.2) \cdot 10^3 \text{ °K} .$$

Though the self consistency of data here is somewhat poorer that in the case of cylindrical probes, we can safely assume that no experimental evidence could be found that surface diffusion was important in the investigated range of temperatures.

The exponential dependence of gold concentration in lead upon the squared penetration distance shows that volume diffusion was not affected by grain boundary diffusion in our experimental conditions and within the investigated range of temperatures ([3]). This result is in agreement with the fact that the structure of used probes was essentially oligocrystalline and consequently grain

boundary diffusion is not expected to be very important, at least at not too low temperatures.

To such purpose, it may be interesting to point out that a penetration curve which is remarkably different in shape from the typical one given in Fig. 3 was obtained from the cylindrical sample for which diffusion annealing had been done at 189.5 °C only. In this case the quoted value of D was obtained after extrapolation to $x^2=0$ of the experimental curve at higher values of x^2. When the extrapolated portion of the curve was subtracted from the experimental curve, a behaviour for the residual activity which is exponentially dependent upon x was put into evidence. This fact has been interpreted as an evidence that at low temperature grain boundary diffusion may be important also in our experimental conditions (4).

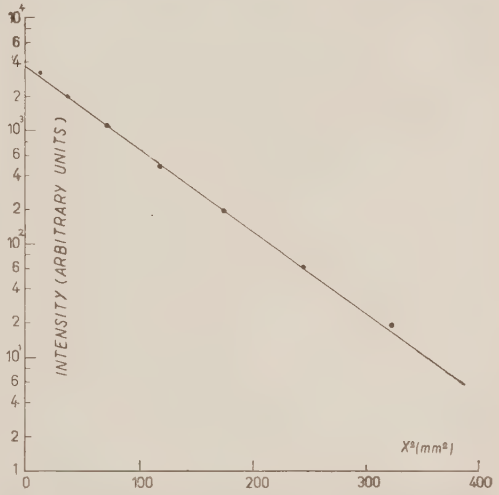

Fig. 5. Typical penetration curve of gold in lead for thin rectangular probes. Annealing temperature 235.9 °C; corrected annealing time 80.63 h.

Some slight indications of the influence of grain boundary diffusion could be observed also with a couple of other penetration curves; the affected distance interval was in every case 3 mm or less so that no reliable evaluation of the activation energy of grain boundary diffusion could be possible. It is not casual perhaps that the probes, which did not show any deviation from the behaviour described by the equation (1) showed a more definitely oligocrystalline structure.

5. – Conclusions.

Diffusion of gold in lead was investigated many years ago: in the most recent works by SEITH and KEIL (8), SEITH and ETZOLD (9), diffusion both of gold in lead and of gold-lead eutectic in lead were examined and the results given are rather different from those quoted in the present paper.

According to the average values reported by JOST (12) and BARRER (13)

(12) W. JOST: *Diffusion in Solids, Liquids, Gases* (New York, 1952), p. 236.
(13) R. M. BARRER: *Diffusion in and Through Solids* (Cambridge, 1951), p. 275.

the results

$$D_0 \sim 0.35 - 0.49 \text{ cm}^2 \text{ s}^{-1}$$

$$Q \sim 1.3 - 1.4 \cdot 10^4 \text{ cal mole}^{-1}$$

can be assumed as representative of previous works.

As far as the order of magnitude is concerned, our values for the diffusion coefficient D do not differ too much from the older ones: if we arbitrarily take $D_0 = 0.42$ cm^2 s^{-1} and $Q = 1.35 \cdot 10^4$ cal mole^{-1} as reference values for old data, a factor 2.5 represents the largest disagreement in the temperature interval investigated by us, but in our case the dependence upon the temperature is remarkably less steep; consequently the activation energy is smaller and D_0 results to have a quite lower value.

Owing to the differences in experimental methods used by the preceeding authors and by us, it is very difficult to understand the possible reasons for such disagreement. A few remarks are however possible: some measurements have also been performed by us with impure lead (99.98%) and with the previously described method. In this case the analysis of penetration curves was made more difficult by the rather high spurious activity of ^{122}Sb but it could be concluded that with less pure lead the activation energy becomes somewhat larger.

The purity of lead used by SEITH and ETZOLD, for instance, is not indicated in their paper. Moreover the larger concentrations of gold which have been used in the diffusion measurements of the above quoted authors can be effective in influencing the diffusion rates at different temperatures. At low temperatures at least, also the structure of lead may be of remarkable importance: the experimental conditions of SEITH and ETZOLD about this point are not clearly specified. Owing to these facts a comparison with the results of the previously mentioned authors is difficult.

However it is considered useful to repeat the above described measurements using both single crystals and policrystalline lead and to measure the diffusion coefficients in a wider range of temperatures.

* * *

We wish to thank the firm Montevecchio for having supplied a part of the pure lead, Ing. A. CACCIARI for the preparation of the lead samples, Dr. G. GIANNELLI for having built up the temperature stabilyzing device, and Prof. G. BOLLA for his kind interest in the present work.

Thanks are also due to Prof. F. FUMI for his helpful criticism and to Dr. M. ASDENTE for her help in the analysis of the experimental results.

RIASSUNTO

Il processo di diffusione intermetallica di oro in piombo è stato studiato coll'impiego del metodo dei traccianti radioattivi nell'intervallo di temperatura compreso tra 190 e 300 °C. I valori sperimentali del coefficiente di diffusione D possono essere rappresentati nel predetto intervallo di temperatura dalla relazione

$$D = 2.8 \cdot 10^{-3} \exp\left[-\frac{8.91 \cdot 10^3}{RT} \right] \text{cm}^2\,\text{s}^{-1} .$$

Di qui l'energia di attivazione del processo risulta essere $(8.91 \pm 0.18) \cdot 10^3$ cal mole^{-1}.

Tempo di decadimento del ZnS(Ag) e preparazione di ricevitori a ZnS(Ag).

B. Chinaglia, F. Demichelis e R. A. Ricci

Istituto di Fisica Sperimentale del Politecnico - Torino

(ricevuto il 3 Aprile 1956)

In ricerche di fisica nucleare si presenta spesso la necessità di usare ricevitori per particelle α particolarmente rapidi. Tale caratteristica diventa indispensabile in misure di coincidenze in cui si richiedano tempi di risoluzione $\leqslant \approx 10^{-8}$ s.

Un progresso in questo senso è stato realizzato con l'introduzione dei contatori a scintillazione in luogo dei contatori Geiger.

Con una opportuna scelta del cristallo scintillatore si possono ottenere sia ricevitori molto rapidi, sia ricevitori sensibili a un solo tipo di radiazioni.

Il ricevitore più adatto per particelle α è il ZnS(Ag) grazie alla sua alta efficienza per questo tipo di particelle; inoltre, essendo possibile ottenerlo in deposizioni sottili [$10 \div 20$ mg/cm^2], esso è inefficiente alle radiazioni β e γ.

Dalla bibliografia risulta che il tempo di decadimento τ del ZnS(Ag), definito come il tempo necessario perchè la intensità luminosa di scintillazione si riduca a $1/e$ del suo valore massimo, è maggiore di 1 μs per particelle α emesse dalle sostanze radioattive naturali [1].

Trattasi di una definizione convenzionale, ma sufficiente per il nostro caso, accettata anche quando la legge di decadimento non sia semplicemente esponenziale.

In lavori recentissimi si osserva un disaccordo tra i valori di τ precedentemente accettati e riconfermati da J. P. Anthony [2] e valori dell'ordine di 10^{-8} sec misurati da altri sperimentatori [3].

Ci siamo proposti di compiere una misurazione di τ relativa al ZnS(Ag) e a tale scopo abbiamo usato il seguente dispositivo.

La sorgente è $^{226}_{88}$Ra in equilibrio con i suoi prodotti di decadimento ed ha una intensità di $\approx$ 0.1 microcurie.

---

[1] H. W. Leverenz: *Luminescence of Solids* (New York, 1950); G. F. J. Garlick: *Progress in Nuclear Physics* (1952), p. 51; J. B. Birks: *Scintillation Counters* (Pergamon Press, London, 1953); S. C. Curran: *Luminescence and the Scintillation Counters* (Butterworths Scientific Publications, London, 1953); R. K. Swank: *Annual Review of Nuclear Science* (1954), p. 111; J. Sharpe: *Nuclear Radiation Detectors* (Methuen, London, 1955).

[2] J. P. Anthony: *Journ. de Phys. et Rad.*, **16**, 182 (1955).

[3] W. F. Hornyak: *Rev. Sci. Instr.*, **23**, 264 (1952); W. S. Emmerich: *Rev. Sci. Instr.*, **25**, 69 (1954); P. G. Kontz, G. R. Keepin and J. E. Ashley: *Rev. Sci. Instr.*, **26**, 352 (1955).

Il ricevitore ZnS(Ag) è costituito da un sottile disco di plexiglass sul quale è stata fatta una deposizione di cristallini di ZnS(Ag).

Si possono ottenere ricevitori di uniformità particolarmente notevole, secondo un procedimento suggerito e messo a punto da E. PERUCCA (v. oltre, in P.S.).

Gli impulsi uscenti da un fotomoltiplicatore DuMont 6292 sono inviati, attraverso un trasferitore catodico, direttamente ad un oscillografo Tektronix tipo 517A.

La costante di tempo $R \cdot C$ d'uscita del fotomoltiplicatore risulta minore di 10^{-8} s; in tal caso la durata degli impulsi non viene a dipendere dal valore di R ($R < 1\,000\ \Omega$). Il tempo di salita dell'amplificatore dell'oscillografo è $7 \cdot 10^{-9}$ s.

In fig. 1 è riportata la registrazione fotografica degli impulsi ottenuti col metodo descritto. Il fotogramma *a*) è stato ottenuto utilizzando come ricevitore ZnS(Ag). Il fotogramma *b*) è stato ottenuto con un cristallo di antracene; poichè il cristallo aveva spessore tale da rivelare anche particelle β e raggi γ emessi dalla sorgente di $^{226}_{88}$Ra, lo spettro ottenuto in questo caso è dovuto a tutti i tre tipi di radiazioni.

La scala dei tempi è data dalle ascisse del quadrigliato sovrapposto ai fotogrammi. Il lato ascissa di un quadratino corrisponde a $2 \cdot 10^{-8}$ s.

Per l'antracene risulta

$$\tau = (3 \div 4) \cdot 10^{-8} \text{ s}$$

in accordo con i valori generalmente accettati.

Per il ZnS(Ag) risulta

$$\tau = (7 \div 8) \cdot 10^{-8} \text{ s} .$$

L'esperienza ha dato lo stesso risultato per due ricevitori ZnS(Ag) di origine nettamente diversa, e formati da microcristalli di dimensioni differenti. Il valor medio delle dimensioni dei granuli era di 0.016 mm in un caso (polvere di ZnS(Ag) di origine USA, ottenuta da H. KALLMANN) e di 0.020 mm nell'altro (polvere di ZnS(Ag?) ugualmente di origine USA, ma ottenuta dalla ditta Italelettronica). Allo spessore medio del monostrato corrisponderebbe, per granuli cubici, una densità areale di 6.4 mg/cm² e 8.0 mg/cm² rispettivamente. Poichè i ricevitori usati avevano spessori di $5 \div 6$ mg/(cm)² e $7 \div 7.2$ mg/cm² rispettivamente, si può concludere che essi sono « mediamente » monostrati.

Viene dunque confermata la breve durata della luminescenza del ZnS(Ag)

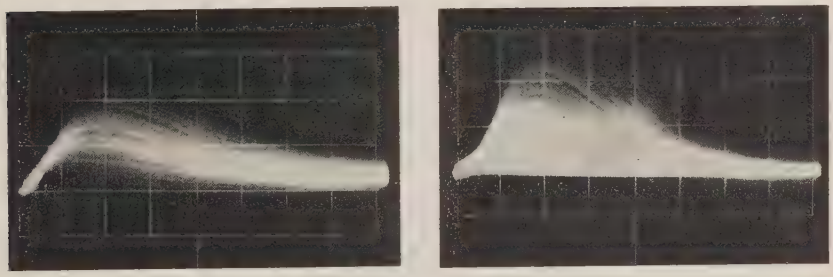

a *b*

Fig. 1 (*a*, *b*). – Diagrammi degli impulsi uscenti dal fotomoltiplicatore per l'arrivo di fiotti di luce generati rispettivamente nel ZnS(Ag) (*a*) e nell'antracene (*b*) da particelle α. L'ascissa è asse dei tempi; il confronto delle due registrazioni è sufficiente per stabilire il tempo di decadimento τ.

sotto azione delle particelle α e, in limiti ragionevoli, essa coincide con quella recentemente determinata da altri Autori [3].

L'impiego del classico ricevitore ZnS(Ag) per particelle α trae quindi nuova importanza e nuove possibilità di impiego.

P.S. – Perchè il ricevitore a ZnS(Ag) assuma carattere ragionevolmente « proporzionale » occorrerebbe anche per esso, come nei numerosi casi già in uso, disporre di un monocristallo. Sono caratteristici i casi del monocristallo NaI(Tl), classico ricevitore per raggi γ, e del monocristallo di antracene per raggi α e β.

Il più soddisfacente ricevitore a ZnS(Ag) deve oggi limitarsi ad uno strato sottile di cristallini, il più uniforme possibile.

Gli strati più soddisfacenti per l'efficienza alla rivelazione delle particelle α sono stati da noi ottenuti non secondo i procedimenti già noti e indicati nella bibliografia, ma secondo il metodo seguente (Perucca).

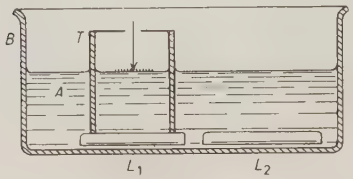

Fig. 2.

Nella bacinella B (Fig. 2) si ha uno strato alto ≈ 3 cm di acqua A. In questa sono immersi due dischi L_1 e L_2; ciò è comodo per le manipolazioni. Effettivamente L_2 è il disco utilizzato per il supporto dello scintillatore; esso è di plexiglass a facce ben piane.

T è un tubo di vetro a base ben smerigliata.

Poggiato T su L_1, sulla superficie dell'acqua entro T (diametro ≈ 3 cm) si lascia cadere delicatamente in grani ben sparsi la polvere di ZnS(Ag). Con un po' di cura si ottiene che la polvere galleggi e i grani si raccolgano a contatto. La parte di polvere eventualmente non tenuta dalla lamina superficiale di acqua cade su L_1.

Si ottiene molto facilmente uno strato di polvere uniforme, compatto, delle dimensioni volute, a contorno circolare; basta fare le cose con molta pulizia. E trattasi di una pellicola che si migliora scuotendo lievemente e ripetutamente il tubo T nell'acqua, poichè i granuli si addensano in un unico strato ben compatto.

Quindi si porta T su L_2; si solleva il « recipiente » TL_2 estraendolo così dall'acqua e lo si poggia su un altro supporto ad asciugare, ben al riparo dalla polvere. In effetti l'acqua può anche scolar via *lentissimamente* (varie ore) dal fondo, ove il tubo è semplicemente sovrapposto al disco di plexiglass.

A deposito asciutto, lo si fissa con una goccia di vernice diluitissima, incolore.

Le fotografie di Fig. 3 *a*), *b*), *c*) mostrano l'aspetto dei ricevitori così preparati.

Già uno strato di $7 \div 8$ mg/cm^2 di fosfòro raggiunge quel massimo di sensibilità col crescere dello spessore che, secondo Graves e Dyson [4], sarebbe raggiunto per spessori di ≈ 10 mg/cm^2.

Attribuiamo il lieve divario appunto alla più omogenea e uniforme deposizione da noi realizzata.

Il deposito delle polveri per precipitazione in acetato di amile [4] non ha dato risultati soddisfacenti. Risultati molto migliori si hanno precipitando la polvere in pseudosoluzione di gelatina (≈ 1.3 g in 100 g di acqua) atta a gelatinizzare a $\approx +2$ °C, e usando opportuni accorgimenti per la deposizione, l'asportazione della soluzione sovrabbon-

[4] J. D. Graves, J. P. Dyson: *Rev. Sci. Instr.*, **20**, 563, (1949).

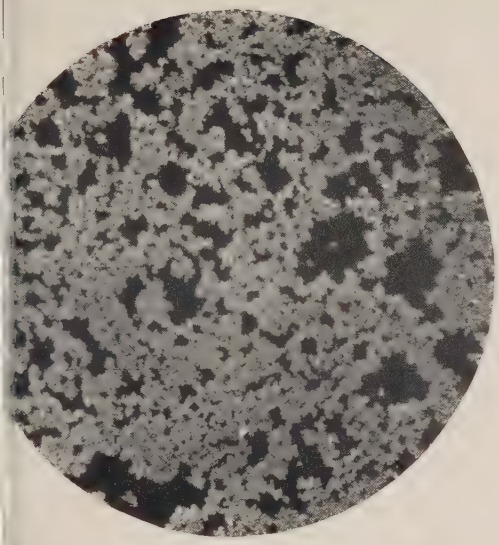

Fig. 3*a*). Aspetto di un monostrato di ZnS(Ag) ottenuto col procedimento di E. Perucca, ma non compatto.

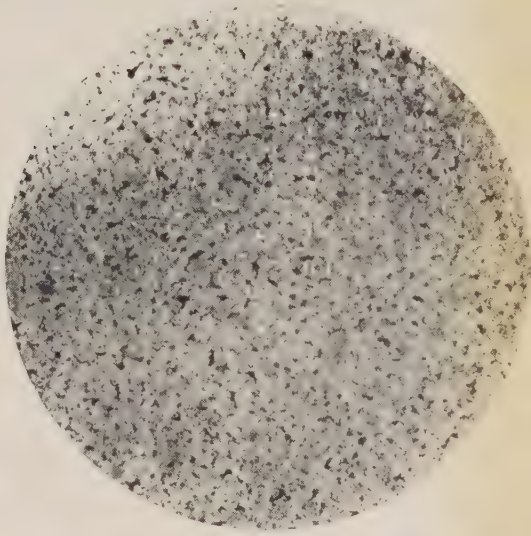

Fig. 3*b*). Aspetto di un ricevitore al ZnS(Ag) monostrato ottenuto con detto procedimento, ma reso compatto.

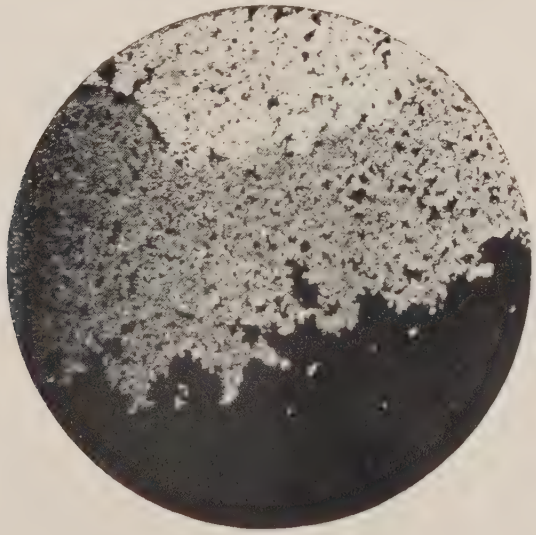

Fig. 3 *c*). – Aspetto della porzione ai bordi di un monostrato nella parte già ricoperta di vernice (più luminosa) e nella parte non verniciata.

Le tre fotografie sono state ottenute per luce riflessa; ingrandimento 25.

dante, ecc. Ma il procedimento è ben più impegnativo di quello sopra descritto, senza sensibili vantaggi, perciò non si insiste.

* * *

Ringraziamo vivamente il Prof. E. PERUCCA per il costante interessamento e per i suoi utili suggerimenti, su accennati, nel corso delle esperienze. Ringraziamo il Prof. H. KALLMANN (New York) e la Ditta Italelettronica (Roma) per averci fornito due campioni di ZnS(Ag). La misura dei tempi di decadimento è stata possibile grazie alla disponibilità dell'oscillografo Tektronix 517A del che ringraziamo il C.N.R.

On the Photodisintegration of the Deuteron and p-p Scattering.

Shih-Hui Hsieh

Physical Institute, Nagoya University

(ricevuto il 21 Aprile 1956)

In the previous letter [1] it was shown how we can make use of the photodisintegration of the deuteron to investigate the nature of nuclear force, combining it with the phase shift analysis on p-p scattering. However the treatment shown there was very crude, and here we wish to explain about our method in detail referring to more accurate phase shift analysis [2], and also on the nature of the nuclear force (indicated by our calculation).

In the photodisintegration of the deuteron, the angular distribution for the ejected proton with respect to the incident γ-ray in the center of mass system is given by

$$(a + b \sin^2 \vartheta)(1 + c \cos \vartheta) . \tag{1}$$

In which $a+b\sin^2\vartheta$ is due to m.d. (*), e.d., and m.q. The final states of these transitions are only singlet even and triplet odd states [3]. However these two states are just the states relating to p-p scattering. Therefore we may make use of phase shifts got from p-p scattering analysis, and see which set of the phase shifts is most favoured. In the formula (1), c is due to e.q., and its contribution to the total cross-section (σ_T) is very small at all energies.

Now in the calculation of m.d., e.d., and m.q., the required integral for the transition from $^3S_1$ state of the deuteron is given by [4]

$$\int u_0(1 + \Phi(r))u_d \left\{1 - \frac{1}{3!}(k_\gamma r)^2 + \frac{1}{5!}(k_\gamma r)^4\right\} dr - \int u_0(+ \Phi(r))u_d \frac{\sin (k_\gamma r)}{k_\gamma r} dr . \tag{2}$$

---

[1] S. Hsieh and M. Nakagawa: *Prog. Theor. Phys.*, **15**, 79 (1956).

[2] A. Garren: *Phys. Rev.*, **96**, 1710 (1954); **101**, 419 (1956).

(*) Magnet dipole is written as m.d., and so on.

[3] For formulas on the photodisintegration of the deuteron, see W. Rarita and J. Schwinger: *Phys. Rev.*, **59**, 556 (1941); N. Austern: *Phys. Rev.*, **85**, 283 (1951).

[4] Similarly the transition from the D-state of the deuteron can be given easily. Note that many previous calculations are uncorrect, because they expand the incident γ-ray into the power series. It corresponds to take only the 1st terms of (2) and (3).

$$(3)\qquad 3\int\left\{\frac{1}{1!\,3}-\frac{2}{3!\,5}(k_\gamma r)^2+\frac{3}{5!\,7}(k_\gamma r)^4\ldots\right\}u_t r u_d\,\mathrm{d}r+$$

$$+\frac{3\hbar}{2Mc}\cdot\frac{1}{k_\gamma}\int\left\{\frac{(3\cdot4-2)}{3!\,5}(k_\gamma r)^2-\frac{(5\cdot6-2)}{5!\,7}(k_\gamma r)^4\ldots\right\}u_t\left(\frac{\partial}{\partial r}-\frac{1}{r}\right)u_d\,\mathrm{d}r\,.$$

where u_d, u_0 and u_t represent the wave functions of the ${}^3S_1$ state of the deuteron, the radial part of ${}^1S_0$ and that of triplet odd states respectively. Also $\Phi(r)$ represents the contribution from the exchange current.

In the integral (2), u_0 may be taken in the form

$$(4)\qquad u_0=\sin(kr+\delta_0^0)(1-\exp[-\zeta(r-D_0)])\,,$$

where δ_0^0 is the phase shift of ${}^1S_0$, D_0 the hard core of singlet even, and ζ is to be varied according to energy. In (3), u_t may be taken in the form having the given phase shift (given by p-p scattering) at all points at energies not so high. (Because the inner region where potential is acting is not important in the integral.)

As the application, we show here the calculated result at $E_\gamma=108.7$ MeV, referring to the phase shifts on 213 MeV p-p scattering given by GARREN [2]. The possible sets of phase shifts in the analysis of p-p scattering are four. They are shown in Table I. Although it is certainly impossible to neglect waves with $L>2$ at such energy, we may still expect that it can be used as an approximation.

In the calculation we assumed that the hard core radius of triplet and singlet is the same and varied it from 0 to $0.3/\varkappa$ ($\varkappa=m_\pi c/\hbar$). u_d was taken as

$$(5)\qquad u_d=N(\exp[-\mu(r-D_0)]-\exp[-\nu(r-D_0)])\,,$$

where ν and N was varied according to D_0 (by the effective range theory). Also we put ζ of u_0 (see (4)) so that the correction factor $1-\exp[-\zeta(r-D_0)]$ changes u_0 only by 1 % or less at $r=1.0/\varkappa$. This is because the influence of potential is negligible at $r>1.0/\varkappa$ at such high energy.

The calculated σ_T and σ_{ip} ($=4\pi a$), using the phase shifts given in Table I, without including the exchange current moment, are shown in Fig. 1. Here σ_T is given by $\sigma_T=\sigma_{\mathrm{md}}+\sigma_{\mathrm{ed}}+\sigma_{\mathrm{mq}}$ (σ_{eq} is below 10^{-30} cm^2 at this energy.) The experimental value at this energy is approximately given by $\sigma_T\simeq 6.0\cdot10^{-29}$ cm^2, $\sigma_{ip}\simeq$ $\simeq 4.5\cdot10^{-29}$ cm^2 [5].

Among the four sets, the latter two where δ_0^0 is between $-30°$ and $-40°$ are better. For these two cases σ_T is about 80 % of the experimental value, and σ_{ip} about 50 %, when $D_0\simeq 0.2/\varkappa$. It is not impossible to account for the experimental result, if we adopt the exchange current operator of VILLARS or SUGIE and YOSHIDA [6], about which we shall explain in another place.

It is quite important to note that Yukawa potential of singlet even (+) (fitted to the effective range theory) which gives large value of δ_0^0, corresponds to small value of σ_{md} at all energies except the lowest. However if δ_0^0 is much smaller, the calculated σ_{md} is much larger, and is suitable to account for the large value of σ_T and

([5]) E. A. WHALIN: *Phys. Rev.*, **95**, 1362 (1954).

([6]) F. VILLARS: *Phys. Rev.*, **72**, 256 (1947); A. SUGIE and S. YOSHIDA: *Prog. Theor. Phys.*, **10**, 236 (1953).

(+) This potential gives $\delta_0^0\sim 30°$ at 213 MeV.

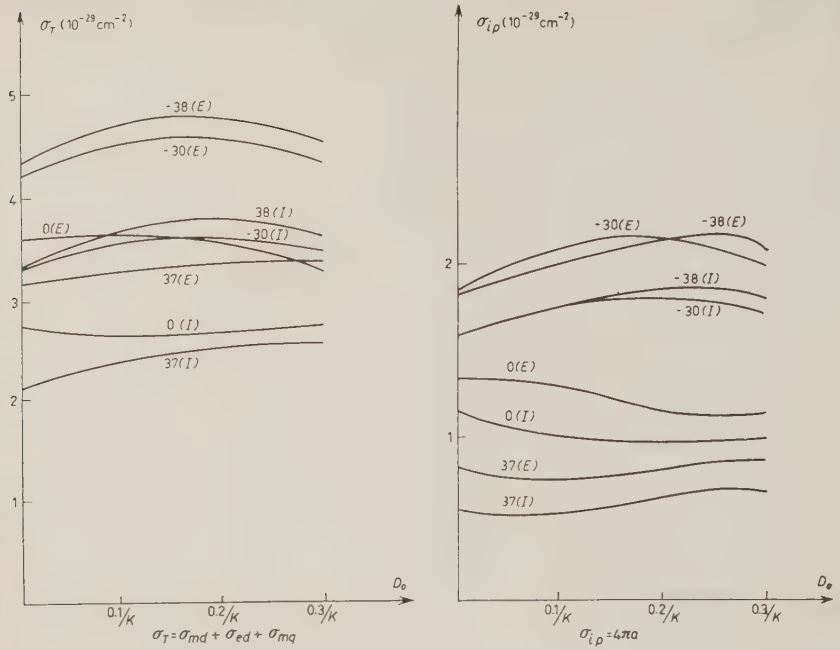

Fig. 1. – The total cross-section (σ_T) and the isotropic part (σ_{ip}) as the function of δ_0^0 and D_0 are shown. Figures written in the graphs are values of δ_0^0. (Compare with Table I). (1) indicates the case when only the 1st terms of $j_1(k_\gamma r)$ and $j_2(k_\gamma r)$ are taken in the calculation of σ_{md}, σ_{ed}, and σ_{mq}. (*E*) indicates the case when the exact formulas (2) and (3) are used.

σ_{ip} in the photodisintegration of the deuteron. Because this point is very important, we shall discuss it in another place together with other natures of nuclear force indicated by the photodisintegration of the deuteron and other experiments.

TABLE I.

The possible sets of phase shifts δ_L^J to account for 213 MeV p-p scattering given by GARREN [2]. The fitted data are: $\sigma(90°) = 3.56$ mb/ster, $\sigma(15°) = 1.02\,\sigma(90°)$, $P(45°) = 0.22$. The last column gives the polarization at 15°.

δ_0^0	δ_1^0	δ_1^1	δ_1^2	P (15°)
37	— 37	6	10	0.103
0	— 69	5	4	0.065
— 30	10	— 16	17	0.132
— 38	— 31	4	12	0.112

On the Field Theory in Functional Form.

K. YAMAZAKI

Research Institute for Fundamental Physics - Kyoto University

(ricevuto il 25 Aprile 1956)

In order to create a method which in no way is based upon the coupling constant as a parameter for iteration, EDWARDS and PEIERLS [1] formulated the field theory in the functional form starting from the functional differential equations given by SCHWINGER [2], and the final functional integral has been carried out by these authors for two special cases, and it is especially interesting in the matter of renormalization. But their derivation is rather complicated and it neglects the effects of the closed loops. The latter defect was removed by the work of MATTHEWS and SALAM [3]; their theory is the direct generalization of Feynman's «sum over histories» formulation (S.O.H.F.) of quantum particle mechanics to the field theory, but it leaves some points to be considered.

i) They introduced artificially the infinitesimal negative imaginary part $-i\varepsilon$ to the mass as the mathematical means in order to make the functional integral converge, whereas it should be required from the causal structure of the theory.

ii) Although their final answer is correct and it might be consistent in their framework, their functional integration over fermion variables seems to contain some dubious features, namely the integration over the so-called anticommuting c-numbers may not have the well defined mathematical meaning in spite of their explanation. At least their method does not agree with the Feynman type of sum over histories for the fermion field as recently shown in the detailed study of TOBOCMAN [4].

iii) As criticized by SUNAKAWA *et al.* [5], the boundary condition for the performance over the functional integral and where MATTHEWS and SALAM used it in their formalism are not clear, namely they made use of the condition saying that the field variables take the value zero ($\varphi = 0$, etc.) on the boundary surface, whereas

---

[1] S. F. EDWARDS and R. E. PEIERLS: *Proc. Roy. Soc.*, A **224**, 24 (1954).
[2] J. SCHWINGER: *Proc. N.A.S.*, **37**, 452, 455 (1951).
[3] P. T. MATTHEWS and A. SALAM: *Nuovo Cimento*, **2**, 120 (1955).
[4] W. TOBOCMAN: to be published.
[5] K. KANKI, K. MURATA and S. SUNAKAWA: *Soryusiron-kenkyu* (mimeographed circular in Japanese), **11**, No. 3 (1956).

the more usual formulation of GELL-MANN and LOW (6) gives that it should be the true vacuum state. Indeed they say they used the fact that boundary is the true vacuum, but then, by what condition is the true vacuum defined in their formalism? Their state must be defined by such a condition that $\varphi - \varphi'$ on σ, etc., and the concept such as the true vacuum must be borrowed from the canonical formalism (C.F.). Moreover their definition of the matrix element is not necessarily the same as it was originally given by FEYNMAN (7), if we do not allow for an artificial limiting procedure (5).

It is the purpose of this note to remove these defects and at the same time it would contribute to simplify the argument of EDWARDS and PEIERLS and supply the closed loop effects neglected by them. Our starting point is the C.F. and we deduce from it the results obtained by MATTHEWS and SALAM and thus this work completes the proof of the equivalence of the C.F. and the Lagrangian formalism or S.O.H.F. developed by FEYNMAN, in the case of field theory, and our method is based on the operator calculus formulation of field theory developed by FEYNMAN (8) and the present author (9). The connection between the dynamical principle of Schwinger and S.O.H.F. was pointed out by DYSON (10) and in I we have also discussed our method in relation to the Schwinger formalism.

Let us take the following propagator as an example,

$$(1) \qquad (\bar{\Psi}_0,\ T(\bar{\psi}(1)\psi(2)\bar{\psi}(3)\psi(4)A(5)A(6))\Psi_0)/(\Psi_0, \Psi_0)\ ,$$

where all symbols are nowadays customarily used in the literature in the Heisenberg representation, for example, Ψ_0 is the true vacuum state in the presence of the external field, and we assume for the interaction the form $-ig\bar{\psi}\Gamma\psi(A+A^e)$, where A^e is the external field. By using Gell-Mann and Low's relation between Ψ_0 and the free vacuum state Φ_0, the latter of which being the product of the free fermion vacuum Φ_f and the free boson vacuum Φ_b, we can transform (1) into the interaction representation. By means of the operator calculus as was explained in detail in I, we can take the expectation value $(\Phi_f \dots \Phi_f)$ and (1) can be written as (I. (3.9)) (A is the operator in the interaction representation.)

$$(2) \qquad (\Phi_b,\ T\{C_v^{A+A^e}A(5)A(6)(K_+^{A+A^e}(2,1)K_+^{A+A^e}(4,3) -$$

$$- K_+^{A+A^e}(2,3)K_+^{A+A^e}(4,1))\}\Phi_b) = (\Phi_b,\ T(C_v^{A+A^e})\Phi_b)\ ,$$

where T refers to the quantized A field, and $K_+^{A+A^e}$ satisfies the following integral equation (for the notations see I)

$$(3) \qquad K_+^{A+A^e} = K_+ - gK_+\Gamma(A + A^e)K_+^{A+A^e}\ .$$

$C_v^{A+A^e}$ represents the effects of the closed loops and is given by

$$(4) \qquad C_v^{A+A^e} = \exp[-L] = \exp[Sp \log\{1 + gK_+\Gamma(A + A^e)\}] =$$

$$= \det|1 + gK_+\Gamma(A + A^e)|\ .$$

---

(6) M. GELL-MANN and F. LOW: *Phys. Rev.*, **84**, 350 (1951).
(7) R. P. FEYNMAN: *Rev. Mod. Phys.*, **20**, 367 (1948).
(8) R. P. FEYNMAN: *Phys. Rev.*, **84**, 108 (1951).
(9) K. YAMAZAKI: *Prog. Theor. Phys.*, **7**, 449 (1952), to be referred to as I.
(10) F. J. DYSON: *Advanced Quantum Mechanics*, Cornell University Lectures (1951). Unpublished.

It should be noted that in (3) and (4) A must be operated in the time order. (If ψ obeys the bose statistics, $C_{\psi}^{a+A^e}$ becomes e^{+L}, as was shown in I).

In this way we can avoid the dubious functional integration over the fermion field. (In I we used the external spinors as convenient mathematical tools, but this has the clear physical meaning that they create or annihilate the external fermion line of the Feynman diagrams, and thus they should anticommute with each other, since they operate on the different fermions; yet if one will not use this sort of quantity, one can avoid it completely as we have already shown in the argument given in Sect. 3 of I.)

Now, as the natural extension of the Fourier transform from the finite number of variables ([11]) to the infinite number of variables (which is the standpoint of EDWARDS and PEIERLS and for the functional integral we use the notation of these authors), we can formally write for an arbitrary functional $f(A)$

$$T(f(A)) = \frac{1}{N}\int\int\delta a\,\delta\varphi\, f(a)\, T\left(\exp\left[i\int\varphi(x)(A(x)-a(x))\,\mathrm{d}^4x\right]\right). \tag{5}$$

N is the normalizing constant, which is so defined that the functional integral becomes 1, if $f(A)=1$. Note that in this equation $A(x)$ is the operator, and $\varphi(x)$ and $a(x)$ are the ordinary c-number functions.

Using obvious simplified notations and with the aid of the equality

$$\left(\Phi_b,\, T(\exp\,[i\varphi A])\Phi_b\right) = \exp\,[-\tfrac{1}{4}\varphi D_F\varphi]\,, \tag{6}$$

we have

$$\left(\Phi_b,\, T(f(A))\Phi_b\right) = \frac{1}{N}\int\int\delta a\,\delta\varphi\, f(a)\,\exp\,[-i\varphi a - \tfrac{1}{4}\varphi D_F\varphi]\,. \tag{7}$$

Thus we see that $i\varepsilon$ in D_F comes from the causal structure of the theory. To evaluate (7), write

$$\varphi = \varphi' - 2iD_F^{-1}a\,, \tag{8}$$

then

$$(\Phi_b,\, T(f(A))\,\Phi_b) = \frac{1}{N}\int\delta\varphi'\,\exp\,[-\tfrac{1}{4}\varphi' D_F\varphi']\int\delta a\, f(a)\,\exp\,[-aD_F^{-1}a] = \tag{9}$$

$$= \frac{C}{N}\int\delta a\, f(a)\,\exp\,[-aD_F^{-1}a]\,,$$

C is defined by the last equality. Introducing (9) into (2) we finally obtain

$$\int\delta a\,\exp\,[iI_b]\,C_{\psi}^{a+A^e}\,a(5)\,a(6)(K_+^{a+A^e}(2,1)\,K_+^{a+A^e}(4,3) - K_+^{a+A^e}(2,3)\,K_+^{a+A^e}(4,1)) \div \tag{10}$$

$$\div\int\delta a\,\exp\,[iI_b]\,C_{\psi}^{a+A^e}\,.$$

([11]) See the reference ([8]), Appendix A.

where I_b is the free action for the boson field

$$(11) \qquad I_b = \frac{1}{2}\int a(a)(\Box - \varkappa^2 + i\varepsilon)\, a(x)\, \mathrm{d}^4x = -\frac{1}{2}\int a(k)(k^2 + \varkappa^2 - i\varepsilon)\, a(k)\, \mathrm{d}^4k\,.$$

This is the well-known result given by MATTHEWS and SALAM. And thus we can prove that the orthodox C.F. is quite equivalent to the functional integral formulation (F.I.F.), namely if we know the classical solution $f(a)$, we can obtain the quantum solution by multiplying it by $\exp[iI_b]$ and integrating it over all possible classical fields $a(x)$. The above proof, especially eq. (7), manifests that the connection between C.F. and F.I.F. is like that between the coordinate space and momentum space treatment; namely in the C.F. it is the operator equation or functional differential equation such as $\delta/\delta J(x)$ in Schwinger's theory (i.e., it corresponds to $-i(\partial/\partial x)$), whereas in F.I.F. it is the c-number equation but the integration over $a(x)$ (i.e., p) must be performed.

The significant point of (5) is that it is completely covariant in the space time coordinate and the causal structure of the theory is guaranteed by T. Thus the starting point of our theory is C.F. but the final solution in functional form is covariant, and it has some similarity with Coester's theory [12] and the over all space time quantization method [13]. To see this similarity it is easier to write our solution in the momentum space like in the latter equality in (11), and δa means $\prod_k \mathrm{d}a(k)$. In Coester's theory are introduced first the completely four dimensional variables c_k and c_k^* satisfying $[c_k, c_{k'}^*] = \delta^4(k - k')$, which correspond in our theory to integrate over $\mathrm{d}a(k)$ for all possible values of k without any restriction on k_1, k_2, k_3 and k_4. Then in the former theory a special combination of c_k and c_k^* is significant, while in the latter the multiplication by $\exp[iI_b]$ and integration over $\mathrm{d}a(k)$ plays the role of selecting out this special combination; and why this is so will be clear in our derivation given in this note.

---

[12] F. COESTER: *Phys. Rev.*, **95**, 1381 (1954).
[13] Y. KATAYAMA, Z. TOKUOKA and K. YAMAZAKI: *Nuovo Cimento*, **2**, 728 (1955).

Some Considerations on the Charge-Exchange Scattering of Antinucleons on Nucleons (*).

D. Amati and B. Vitale (+)

Istituto di Fisica dell'Università - Roma
Istituto Nazionale di Fisica Nucleare - Sezione di Roma

(ricevuto l'8 Maggio 1956)

Experimental data will be available in a short time on the nuclear scattering of antiprotons, from track scanning in nuclear emulsions (interactions with complex nuclei) and from the interactions in Hydrogen bubble chambers (proton-antiproton scattering). In both cases, if the absorption processes are not predominant on the elastic scattering processes, it will be possible to measure the ratio between elastic and charge-exchange scattering of antiprotons on nucleons. The data have to be previously corrected for the effect of the « shadow scattering », due to the presence of absorption processes, that, of course, does not contribute to the charge-exchange scattering; and for the absorptions in flight of antiprotons, not followed by emission of charged secondaries. Also the antineutron-proton charge-exchange scattering can present some interest, as a possible method for the detection of antineutrons.

Assuming that the transitions are consequence of a « strong » interaction—to say, that isotopic spin and its third component are conserved—the cross-sections for nucleon-antinucleon scattering involve, as for the nucleon-nucleon case, only two independent transition amplitudes. They correspond to transitions between states with, respectively, $T=0$ and $T=1$.

It has been noticed by Kobsarev *et al.* [1] that there exist no relations between the cross-sections for the different scattering processes, depending on the isotopic spin invariance of the interaction. They can derive, however, the following inequalities:

$$(1)\qquad \begin{cases} |\sqrt{\sigma}(\bar{p}p/\bar{n}n) - \sqrt{\sigma}(\bar{p}n/\bar{p}n)| \leqslant \sqrt{\sigma}(\bar{p}p/\bar{p}p) \leqslant \sqrt{\sigma}(\bar{p}p/\bar{n}n) + \sqrt{\sigma}(\bar{p}n/\bar{p}n) \\ |\sqrt{\sigma}(\bar{p}p/\bar{n}n) - \sqrt{\sigma}(\bar{p}p/\bar{p}p)| \leqslant \sqrt{\sigma}(\bar{p}n/\bar{p}n) \leqslant \sqrt{\sigma}(\bar{p}p/\bar{n}n) + \sqrt{\sigma}(\bar{p}p/\bar{p}p) \\ |\sqrt{\sigma}(\bar{p}n/\bar{p}n) - \sqrt{\sigma}(\bar{p}p/\bar{p}p)| \leqslant \sqrt{\sigma}(\bar{p}p/\bar{n}n) \leqslant \sqrt{\sigma}(\bar{p}n/\bar{p}n) + \sqrt{\sigma}(\bar{p}p/\bar{p}p) \end{cases}$$

(*) After sending this letter we have read a letter of I. Ja. Pomerančuk [*Zu. Éksper. Teor. Fiz. SSSR*, **30**, 423 (1956)] where many of the relations contained in our letter are also obtained. At high energy, Pomerančuk foresees $a) = c)$, and $b)$ negligible with respect to $c)$ (see eq. (2)).

(+) Now at the *Department of Mathematical Physics-University of Birmingham* (England).

(1) I. Kobsarev and I. Schmuschkevic: *Dokl. Akad. Nauk SSSR*, **102**, 929 (1955).

These inequalities can be very easily understood considering the relations between the two complex a_0 and a_1; transition amplitudes corresponding, respectively, to $T=0$ and $T=1$ transitons. We have, indeed, for the differential (at a given fixed angle) or total cross-sections for the different possible physical processes:

$$(2)\qquad \begin{cases} a) & \sigma(\bar{p}p/\bar{p}p) = \sigma(\bar{n}n/\bar{n}n) = 1/4\,|a_0 + a_1|^2 \\ b) & \sigma(\bar{p}p/\bar{n}n) = \sigma(\bar{n}n/\bar{p}p) = 1/4\,|a_0 - a_1|^2 \\ c) & \sigma(\bar{p}n/\bar{p}n) = \sigma(\bar{n}p/\bar{n}p) = |a_1|^2 . \end{cases}$$

From the relations (2) and representing the transition amplitudes in the complex plane, the relations (1) follow immediately. It should be noted, moreover, that in the total cross-sections the interference terms do not disappear, because of the lack of a definite state of symmetry for the final states.

The two transition amplitudes a_0 and a_1 are by no means compelled to be of the same order of magnitude; as a typical example, take the pion-nucleon scattering at about 200 MeV, where the experimental results are in good agreement with all transitions being between $T=3/2$ states of the pion-nucleon system. If something alike happens in the nucleon-antinucleon scattering, there will be definite relationships between the cross-sections corresponding to the various possible physical processes. We write down the ratio between the processes *a*), *b*) and *c*) in the assumption of definite values of, or relations between, a_0 and a_1. We obtain:

$$(3)\qquad \begin{cases} \text{if} \quad a_0 = a_1 & a) : b) : c) :: 1 : 0 : 1 \\ \quad\;\; a_1 = 0 & a) : b) : c) :: 1 : 1 : 0 \\ \quad\;\; a_0 = 0 & a) : b) : c) :: 1 : 1 : 4 \end{cases}$$

We note now that the one pion annihilation graphs, that play an important role in nucleon-antinucleon scattering in the pseudoscalar theory with pseudoscalar coupling, are allowed only for initial states with $T=1$; and that the « meson-exchange » graphs, present also in the nucleon-nucleon scattering, involve the virtual meson in a $t=\frac{1}{2}$ or $t=\frac{3}{2}$ state ($T=1$) and only in a $t=\frac{1}{2}$ state for $T=0$ (t refers to the isotopic spin of the virtual pion+emitting nucleon sub-system; all of these rough considerations are made for only lowest order processes, disregarding also self-energy modifications, and can have some validity only if these processes are preponderant on the others). Therefore we should be willing to foresee that, for not too high energies, it is probable that the experimental data will fit, or will be close, to the third of the relations (3); namely, that the ratio between the various physical processes will be close to:

$$(4)\qquad \begin{cases} \sigma(\bar{p}p/\bar{p}p) : \sigma(\bar{p}p/\bar{n}n) : \sigma(\bar{p}n/\bar{p}n) :: 1 : 1 : 4 \\ \sigma(\bar{n}n/\bar{n}n) : \sigma(\bar{n}n/\bar{p}p) : \sigma(\bar{n}p/\bar{n}p) :: 1 : 1 : 4 . \end{cases}$$

* * *

One of us (B.V.) wishes to thank Dr. R. H. Dalitz for a useful discussion on this subject.

Sulla polarizzazione della Bremsstrahlung.

R. Ascoli e G. Bussetti

Istituto di Fisica dell'Università - Torino
Istituto Nazionale di Fisica Nucleare - Sezione di Torino

(ricevuto il 14 Maggio 1956)

In un precedente lavoro uno di noi [1] ha studiato l'emissione di fotoni da parte di un elettrone che passi da uno stato di impulso iniziale $\boldsymbol{p}_0$ determinato ad uno stato di impulso finale $\boldsymbol{p}$ pure determinato, diverso da quello iniziale. Si è trascurata la reazione della radiazione emessa sull'elettrone, e lo studio è stato effettuato nel sistema di riferimento di riposo dell'elettrone nello stato finale. Uno dei risultati che valgono in questo sistema di riferimento è che i fotoni emessi sono interamente polarizzati col vettore elettrico giacente nel piano di emissione (piano contenente l'impulso iniziale dell'elettrone e l'impulso del fotone).

Un risultato analogo vale nel sistema di riferimento di riposo dell'elettrone nello stato iniziale: precisamente in tale sistema i fotoni emessi sono polarizzati col vettore elettrico giacente nel piano dell'impulso finale dell'elettrone e dell'impulso del fotone. A tale conclusione si giunge direttamente o partendo dal risultato valido nel sistema di riposo finale con una immediata trasformazione di Lorentz.

D'altra parte lo studio della bremsstrahlung singola effettuato col metodo perturbativo [2], conduce, come è noto, al risultato che i fotoni emessi sono prevalentemente polarizzati col vettore elettrico perpendicolare al piano di emissione almeno quando l'angolo di emissione ϑ_0 [3] è compreso in un certo intervallo di valori. Se $\cos\vartheta_0 = \beta_0$ (essendo $\beta_0 = v_0$ la velocità iniziale dell'elettrone [4]) i fotoni sono anzi totalmente polarizzati col vettore elettrico perpendicolare al piano di emissione, quando si fa tendere a 0 la loro energia [5]. Questi risultati sono dedotti naturalmente nel sistema di laboratorio.

Ci proponiamo qui di mostrare come l'apparente diversità dei risultati citati, concernenti la polarizzazione dei fotoni emessi, sia unicamente dovuta alla diver-

---

[1] R. Ascoli: *Nuovo Cimento*, **2**, 1 (1955).

[2] G. C. Wick: *Phys. Rev.*, **81**, 467 (1951); M. May e G. C. Wick: *Phys. Rev.*, **81**, 628 (1951); M. May: *Phys. Rev.*, **84**, 265 (1951); R. L. Gluckstern, M. H. Hull jr. e G. Breit: *Phys. Rev.*, **90**, 1026 (1953); R. L. Gluckstern e M. H. Hull jr.: *Phys. Rev.*, **90**, 1030 (1953).

[3] Angolo tra l'impulso $\boldsymbol{k}$ del fotone e quello $\boldsymbol{p}_0$ iniziale dell'elettrone.

[4] Usiamo unità per cui $\hbar = c = 1$.

[5] R. L. Gluckstern e M. H. Hull jr.: *Phys. Rev.*, **90**, 1030 (1953).

sità del sistema di riferimento in cui il fenomeno è studiato. Precisamente partendo dai risultati validi nel sistema di riposo iniziale dell'elettrone [6] dedurremo, con semplici considerazioni geometriche, quelli validi nel sistema di laboratorio. Poichè il risultato molto semplice valido nel sistema di riposo iniziale (come pure quello valido nel sistema di riposo finale) si può ritenere evidente, la deduzione può essere considerata una prova intuitiva delle conclusioni, a prima vista inaspettate, valide nel sistema di laboratorio.

Indichiamo con un apice le grandezze relative al sistema di riposo iniziale (sistema in cui $\boldsymbol{p}_0' = 0$). Rispetto a questo sistema di riferimento, il sistema di laboratorio si muove con velocità $-\boldsymbol{v}_0$, essendo $\boldsymbol{v}_0$ la velocità iniziale dell'elettrone (nel sistema di laboratorio).

Prendiamo in considerazione l'emissione di fotoni di energia k molto minore di quella dell'elettrone (nel sistema di laboratorio). Si ha allora $p \cong p_0$ [7]. Osserviamo inoltre che il maggior contributo alla sezione d'urto si ha per valori molto piccoli dell'angolo α tra i vettori $\boldsymbol{p}$ e $\boldsymbol{p}_0$ [8]; i valori di α che maggiormente contribuiscono nel fenomeno tendono anzi a zero quando l'energia del fotone emesso tende a zero.

Ora indicando con α' l'angolo tra i vettori $\boldsymbol{p}'$ (impulso finale dell'elettrone nel sistema di riposo iniziale) e $\boldsymbol{v}_0$ si ha, dalle formule della trasformazione di Lorentz, che α' è legato ad α dalla:

$$\operatorname{tg} \alpha' = \left(\gamma_0 \operatorname{tg} \frac{\alpha}{2}\right)^{-1},$$

dove

$$\gamma_0 = (1 - \beta_0^2)^{-\frac{1}{2}}.$$

da cui si vede che se α è prossimo a zero, α' è prossimo a $\pi/2$. Risulta quindi che, almeno per l'emissione di fotoni di bassa energia, nei casi che maggiormente contribuiscono alla sezione d'urto, $\boldsymbol{p}'$ è approssimativamente perpendicolare a $\boldsymbol{v}_0$.

Esaminiamo ora in particolare i fotoni di bassa energia emessi nel sistema di laboratorio con l'angolo di emissione ϑ_0 dato da $\cos \vartheta_0 = \beta_0$. Si trova che nel sistema di riferimento in cui l'impulso iniziale dell'elettrone è nullo tali fotoni sono emessi con un impulso $\boldsymbol{k}'$ perpendicolare alla velocità $\boldsymbol{v}_0$.

Ora in questo sistema la radiazione è polarizzata col vettore elettrico $\boldsymbol{E}'$ parallelo al piano dei vettori $\boldsymbol{p}'$, $\boldsymbol{k}'$. Da ciò, e dal fatto che $\boldsymbol{p}' \perp \boldsymbol{v}_0$ e $\boldsymbol{k}' \perp \boldsymbol{v}_0$ risulta che anche $\boldsymbol{E}'$ è perpendicolare a $\boldsymbol{v}_0$ (vedi Fig. 1).

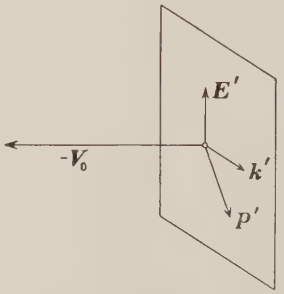

Fig. 1. – Posizione dei vettori nel sistema di riferimento di riposo dell'elettrone nello stato iniziale ($\boldsymbol{p}_0' = 0$), nel caso di angolo di emissione ϑ_0 dei fotoni nel sistema di laboratorio dato da $\cos \vartheta_0 = \beta_0$. Il piano di $\boldsymbol{k}'$, $\boldsymbol{p}'$, $\boldsymbol{E}'$ è perpendicolare a $\boldsymbol{V}_0$.

Passiamo ora al sistema di laboratorio. Il vettore elettrico $\boldsymbol{E}$ in quest'ultimo si ottiene dalla formula di trasformazione [9]:

$$\boldsymbol{E} = \gamma \boldsymbol{E}' + \boldsymbol{v} \frac{\boldsymbol{v} \cdot \boldsymbol{E}'}{v^2} (1 - \gamma) \quad \gamma \boldsymbol{v} \wedge \boldsymbol{H}',$$

dove $\boldsymbol{H}'$ è il campo magnetico, e nel

[6] Tale risultato è ottenuto trascurando la reazione dei fotoni sull'elettrone. Perciò esso dà luogo a conclusioni esatte quando l'energia dei fotoni tenda a 0; approssimative altrimenti.

[7] Poniamo $p = |\boldsymbol{p}|$, $p_0 = |\boldsymbol{p}_0|$.

[8] Ciò è dovuto al fatto che la sezione d'urto per lo scattering di un elettrone in un campo coulombiano contiene il fattore $1/\sin^4(\alpha/2)$.

[9] Vedi p. es.: C. MOLLER: *The theory of relativity* (Oxford, 1952), p. 110.

nostro caso $\boldsymbol{v} = -\boldsymbol{v}_0$. Ora

$$\boldsymbol{H}' = \frac{\boldsymbol{k}'}{|\boldsymbol{k}'|} \wedge \boldsymbol{E}' ,$$

e perciò, dato che $\boldsymbol{E}' \perp \boldsymbol{v}$ e $\boldsymbol{k}' \perp \boldsymbol{v}$, il secondo ed il terzo termine si annullano e si trova $\boldsymbol{E} = \gamma \boldsymbol{E}'$. Perciò anche nel sistema di laboratorio il vettore elettrico $\boldsymbol{E}$ risulta perpendicolare a $\boldsymbol{v}_0$. Quindi esso è perpendicolare a $\boldsymbol{p}_0$, e dovendo risultare perpendicolare a $\boldsymbol{k}$, è perpendicolare al piano di emissione.

Si conclude pertanto che nel sistema di laboratorio i fotoni di bassa energia emessi con angolo di emissione ϑ_0 dato da $\cos \vartheta_0 = \beta_0$ sono interamente polarizzati col vettore elettrico perpendicolare al piano di emissione. Se l'angolo di emissione non è esattamente quello dato da $\cos \vartheta_0 = \beta_0$, la polarizzazione è solo parziale. Altrettanto accade se l'energia dei fotoni non è sufficientemente bassa.

I risultati relativi ai due sistemi di riferimento sono stati dedotti l'uno dall'altro, e risulta pertanto chiarita l'apparente contraddizione suaccennata.

Estensione del metodo parametrico di Davison al caso di potenziali cinetici.

R. Cirelli

Istituto di Scienze Fisiche dell'Università - Milano
Istituto Nazionale di Fisica Nucleare - Sezione di Milano

M. Pusterla

Istituto di Fisica dell'Università - Pavia
Istituto Nazionale di Fisica Nucleare - Sezione di Milano

(ricevuto il 14 Maggio 1956)

È noto come il propagatore quantistico per un sistema dinamico si possa calcolare con la prescrizione di Feynman [1] che risulta equivalente alla meccanica quantistica nella formulazione solita.

Davison [2] ha mostrato che l'integrale di Feynman sui cammini coincide con quella soluzione del sistema funzionale

$$(1)\qquad \begin{cases} \alpha) = K(x, t\,|\,x_0, t_0;\, L) = \exp\left[\dfrac{i}{\hbar}\displaystyle\int_{t_0}^{t} L(x_c\,|\,\dot{x}_c)\,\mathrm{d}t'\right] K(\xi, t\,|\,\xi_0, t_0;\, \tilde{L}) \\ \beta) = K(x, t\,|\,x_0, t_0;\, L) = \displaystyle\int_{-\infty}^{\infty} K(x, t\,|\,x', t';\, L)\,\mathrm{d}x'\, K(x', t'\,|\,x_0, t_0;\, L) \end{cases}$$

che non coinvolge l'introduzione di nuove costanti universali arbitrarie. Il sistema suddetto, per potenziali scalari, ammette una unica soluzione ottenibile per altro attraverso il calcolo di un integrale infinitamente multiplo che parametrizza in una fissata base il funzionale di Feynman.

Qui si vuole mostrare come il sistema funzionale di Davison e l'integrale infinitamente multiplo possano essere usati anche nel caso di potenziali vettori molto

---

[1] R. P. Feynman: *Rev. Mod. Phys.*, **20**, 367 (1948); W. Pauli: *Ausgewahlte Kapitel aus der Feldquantisierung* (Zürich, 1951), p. 139.

[2] B. Davison: *Proc. Roy. Soc.*, **225** A, 252 (1954); W. K. Burton e A. De Borde: *Nuovo Cimento*, **2**, 197 (1955).

semplici. Si studia pertanto il caso di una particella carica in un campo magnetico uniforme e si ricava per l'una e l'altra via l'espressione già nota del propagatore, pensando che il lato interessante dello studio di tale caso particolare stia nell'implicita possibilità dell'estensione del metodo a potenziali vettori più generali.

$$L = \frac{1}{2} m (\dot{x}_1^2 + \dot{x}_2^2 + \dot{x}_3^2) - m\omega(\dot{x}_1 x_2 - \dot{x}_2 x_1) \qquad \left(\omega = \frac{eH}{2mc}\right).$$

Prendendo per $\boldsymbol{x}_c(t')$ la traiettoria classica

$$x_{1c}(t') = a + R \sin [2\omega(t' - t_0) + \alpha]$$

$$x_{2c}(t') = b + R \cos [2\omega(t' - t_0) + \alpha]$$

$$x_{3c}(t') = \frac{x_3 - x_{30}}{t - t_0} (t' - t_0) + x_{30} \quad \text{con}$$

$$a = \frac{1}{2}\left[x_1 + x_{10} + (x_2 - x_{20}) \operatorname{ctg} \omega(t - t_0)\right]; \quad b = \frac{1}{2}\left[x_2 + x_{20} - (x_1 - x_{10}) \operatorname{ctg} \omega(t - t_0)\right];$$

$$R = \frac{\sqrt{(x_1 - x_{10})^2 + (x_2 - x_{20})^2}}{2 \sin \omega(t - t_0)}; \quad b = x_{20} - R,$$

risulta

$$\int_{t_0}^{t} \tilde{L}(\xi \,|\, \dot{\xi})\, \mathrm{d}t' = \int_{t_0}^{t} L(\xi \,|\, \dot{\xi})\, \mathrm{d}t'$$

e quindi

$$K(x, t \,|\, x_0, t_0;\, L) = \exp\left[\frac{i}{\hbar} \int_{t_0}^{t} L(x_c \,|\, \dot{x}_c)\, \mathrm{d}t'\right] K(0, t \,|\, 0, t_0;\, L) = \exp\left[\frac{i}{\hbar} m \frac{(x_3 - x_{30})^2}{2(t - t_0)} - \right.$$

$$\left. + \frac{i}{\hbar} m\omega \left(\frac{(x_1 - x_{10})^2 + (x_2 - x_{20})^2}{2} \operatorname{cotg} \omega(t - t_0) + x_2 x_{10} - x_1 x_{20}\right)\right] K(0, t \,|\, 0, t_0;\, L).$$

Valendosi della (1 β) per valutare $K(0, t \,|\, 0, t_0)$ si ha:

$$K(0,t\,|\,0,t_0) = K(0,t\,|\,0,t')\, K(0,t'\,|\,0,t_0) \left[\frac{2\pi i\hbar (t - t')(t' - t_0)}{m(t - t_0)}\right]^{\frac{1}{2}} \frac{2\pi i\hbar \sin \omega(t - t') \sin \omega(t' - t_0)}{m\omega \sin \omega(t - t_0)},$$

di cui l'unica, più generale soluzione che non coinvolga l'introduzione di nuove costanti universali è

$$K(0, t \,|\, 0, t_0) = \left(\frac{m}{2\pi\hbar i(t - t_0)}\right)^{\frac{1}{2}} \frac{m\omega}{2\pi\hbar i \sin \omega(t - t_0)}.$$

Si ha quindi per il propagatore

$$K(x, t \,|\, x_0, t_0) = \left(\frac{m}{2\pi\hbar i(t - t_0)}\right)^{\frac{1}{2}} \frac{m\omega}{2\pi\hbar i \sin \omega(t - t_0)} \cdot$$

$$\cdot \exp\left[\frac{i}{\hbar} m \frac{(x_3 - x_{30})^2}{2(t - t_0)} + \frac{i}{\hbar} m\omega \left(\frac{(x_1 - x_{10})^2 + (x_2 - x_{20})^2}{2} \operatorname{cotg} \omega(t - t_0) + x_2 x_{10} - x_1 x_{20}\right)\right].$$

Vogliamo ora dedurre lo stesso risultato utilizzando l'integrazione parametrica che, attesa l'unicità della soluzione del sistema funzionale (1) deve necessariamente portare al medesimo risultato.

Per maggiore semplicità basterà fare il calcolo con due gradi di libertà:

$$L = \tfrac{1}{2} m(\dot{x}^2 + \dot{y}^2) - m\omega(\dot{x}y - \dot{y}x) .$$

Usando la base di Fourier per lo sviluppo di $\dot{x}(t')$ e $\dot{y}(t')$ nell'intervallo $(0, t)$:

$$\dot{x}(t') = \left(\frac{2\pi\hbar}{mt}\right)^{\frac{1}{2}} \left[a_0 + \sum_{n=1}^{\infty} \sqrt{2} \left(a_n \sin 2\pi n \frac{t'}{t} + b_n \cos 2\pi n \frac{t'}{t}\right)\right]$$

$$\dot{y}(t') = \left(\frac{2\pi\hbar}{mt}\right)^{\frac{1}{2}} \left[c_0 + \sum_{n=1}^{\infty} \sqrt{2} \left(c_n \sin 2\pi n \frac{t'}{t} + d_n \cos 2\pi n \frac{t'}{t}\right)\right]$$

da cui integrando:

$$x(t') = \left(\frac{2\pi\hbar}{mt}\right)^{\frac{1}{2}} \left\{a_0 t' + \sum_{n=1}^{\infty} \left[\frac{-\sqrt{2}\, t a_n}{2\pi n} \cos 2\pi n \frac{t'}{t} + \frac{\sqrt{2}\, t b_n}{2\pi n} \sin 2\pi n \frac{t'}{t} + \frac{\sqrt{2}\, t a_n}{2\pi n}\right] + \left(\frac{mt}{2\pi\hbar}\right)^{\frac{1}{2}} x_0\right\}$$

$$y(t') = \left(\frac{2\pi\hbar}{mt}\right)^{\frac{1}{2}} \left\{c_0 t' + \sum_{n=1}^{\infty} \left[\frac{-\sqrt{2}\, t c_n}{2\pi n} \cos 2\pi n \frac{t'}{t} + \frac{\sqrt{2} t d_n}{2\pi n} \sin 2\pi n \frac{t'}{t} + \frac{\sqrt{2}\, t c_n}{2\pi n}\right] + \left(\frac{mt}{2\pi\hbar}\right)^{\frac{1}{2}} y_0\right\}$$

si ha:

$$\frac{i}{\hbar} \int L \, \mathrm{d}t' = i\pi \left[a_0^2 + c_0^2 + \sum_{n=1}^{\infty} (a_n^2 + b_n^2 + c_n^2 + d_n^2)\right] -$$

$$- i2\pi\omega \left\{\left(\frac{mt}{2\pi\hbar}\right)^{\frac{1}{2}} (a_0 y_0 - c_0 x_0) + \sum_{n=1}^{\infty} \frac{t}{\pi n} [a_0\sqrt{2}\, c_n - c_0\sqrt{2}\, a_n + a_n d_n - b_n c_n]\right\} .$$

L'integrale infinitamente multiplo è quindi:

$$\frac{m}{2\pi\hbar i t} \exp\left[i\pi \left(a_0^2 + c_0^2 - \omega \left(\frac{2mt}{\pi\hbar}\right)^{\frac{1}{2}} (a_0 y_0 - c_0 x_0)\right)\right] \cdot \int_{-\infty}^{\infty} \frac{\mathrm{d}a_0}{\sqrt{-i}} \int_{-\infty}^{\infty} \frac{\mathrm{d}b_0}{\sqrt{-i}} \int_{-\infty}^{\infty} \frac{\mathrm{d}c_0}{\sqrt{-i}} \int_{-\infty}^{\infty} \frac{\mathrm{d}d_0}{\sqrt{-i}} \cdots \cdot$$

$$\cdot \exp\left[i\pi \sum_{n=1}^{\infty} (a_n^2 + b_n^2 + c_n^2 + d_n^2) - 2i\omega t \sum_{n=1}^{\infty} \frac{1}{n} (a_0\sqrt{2}\, c_n - c_0\sqrt{2}\, a_n + a_n d_n - b_n c_n)\right] .$$

Usando la formula:

$$\int_{-\infty}^{\infty} \mathrm{d}x \int_{-\infty}^{\infty} \mathrm{d}x \exp\left[i\left[\alpha(x^2 + y^2) + \beta xy + \gamma x\right)\right] = \left(\frac{i\pi}{\alpha}\right)^{\frac{1}{2}} \left(\alpha - \frac{i\alpha}{(\beta^2/4\alpha)}\right)^{\frac{1}{2}} \exp\left[\frac{i\gamma^2}{4\alpha - (\beta^2/\alpha)}\right]$$

e tenendo presenti gli sviluppi

$$\prod_{n=1}^{\infty}\left(1 - \frac{z^2}{n^2}\right) = \frac{\sin \pi z}{\pi z}$$

$$\frac{1}{z} + \sum_{n=1}^{\infty} \frac{2z}{z^2 - \pi^2 n^2} = \operatorname{cotg} z$$

e

$$a_0^2 = \frac{m}{2\pi\hbar t}(x - x_0)^2 , \qquad c_0^2 = \frac{m}{2\pi\hbar t}(y - y_0)^2$$

si ottiene il propagatore

$$K(x, y, t \mid x_0, y_0, 0) = \frac{m\omega}{2\pi\hbar i \sin \omega t} \exp\left[\frac{i}{\hbar} m\omega \left[\frac{(x - x_0)^2 + (y - y_0)^2}{2} \operatorname{cotg} \omega t - y x_0 \quad x y_0\right]\right].$$

Osserviamo infine che, come potrebbe dimostrarsi con argomenti analoghi a quelli di Davison, i metodi di calcolo qui usati possono univocamente definire la funzione di Green di una particella in un campo magnetostatico uniforme ed elettrostatico qualunque.

* * *

Desideriamo ringraziare il prof. P. Caldirola per l'interessamento dimostratoci, il prof. A. Loinger e il dott. G. M. Prosperi per le proficue discussioni sull'argomento.

On the Anelasticity of Cosmic Ray Jets.

A. Wataghin (*)

Istituto di Fisica dell'Università - Torino

(ricevuto il 16 Maggio 1956)

35 jets found in nuclear emulsions exposed in ballon flights at altitudes ~ 30 km have been analyzed. The energy of each jet was calculated from the angular distribution with the method proposed by Castagnoli *et al.* [1]. Since the maximum energy included in the statistics is 600 GeV and the altitude is ~ 30 km, most of the primaries of the jets should be nucleons.

The mean energy E of the mesons in the center of mass system (C-system) and the degree of anelasticity K of each jet may be evaluated with a method used by Dilworth *et al.* [2]. K is defined as the ratio of the total energy taken by the mesons in C-system to the kinetic energy available before the collision (also in C-system).

The number n_h of black and gray tracks present in the star from which the core of relativistic particles was ejected was $\leqslant 4$ (75% had $n_h \leqslant 2$). If a jet had an apparent K significantly > 1 it was not included in the statistics. No track was excluded from the jets considered.

The energies of the considered jets are in the interval from 6 GeV to 600 GeV. The mean number of charged relativistic particles $\bar{n}$ is 6.5 ± 0.3. The average energy of the mesons in the C-system is 0.52 ± 0.05 GeV. The average anelasticity $\bar{K}$ is 0.65 ± 0.05.

If in spite of the scarcity of the data we divide our jets in two energy regions we notice a tendency for K to decrease with increasing energy in the range investigated (from 0.85 to 0.5).

The errors given are standard errors obtained in a purely statistical manner from the square of the deviations of the experimental data from the mean. But there are uncertainties due to our present lack of knowledge, such as: *a*) we do not observe the neutral particles; *b*) in the range of energies investigated we assumed all the produced mesons to be π-mesons, while heavier mesons and pairs of antinucleons are present in a certain proportion; *c*) our analysis was made in the hypothesis that the chosen jets were produced in only one nucleon-nucleon collision.

It is nevertheless interesting to observe that our results are intermediate

(*) On leave of absence from S. Paulo University, Brazil, with a fellowship from C.N.P. of Brazil.

(1) C. Castagnoli, G. Cortini, C. Franzinetti, A. Manfredini and D. Moreno: *Nuovo Cimento*, **10**, 1539 (1953).

(2) C. C. Dilworth, S. J. Goldsack, T. F. Hoang and L. Scarsi: *Nuovo Cimento*, **10**, 1261 (1953).

between a few available data belonging to lower and higher energy ranges than the interval analyzed by us.

A case observed with a cloud-chamber exposed to neutrons from Berkeley's bevatron ([3]) gives $K \cong 0.75$, for a seven prong event produced by a 4.7 GeV neutron.

Considerations made on results on extensive showers ([4]) for energies $\gtrsim 10^{11}$ eV (higher than those of our jets), gave for K the value of 0.4.

Analyses made on the N-component of cosmic rays ([5,6]), give for K 0.3, 0.25 respectively.

The K quoted from results from cosmic ray showers refer to the fraction of energy given to the meson in a collision with a nucleus of the air, but it is interesting to notice that if each collision with a nucleus is considered as composed of more than one collision with nucleons inside it, the evaluated K would get still lower.

Heisenberg's turbulence theory ([7]) predicts in our energy region a number of charged particles from 5 to 7 which is in agreement with our data. The predicted anelasticity (0.2 for 600 GeV and 0.65 for 6 GeV) is a little lower than the one we found. Fermi's thermodynamical theory ([8]), on the other hand supposes $K = 1$.

An important part of the jets analyzed in this work were analyzed with different criteria by BERTOLINO ([9]). Partly because of the different criteria he finds anelasticities somewhat lower than ours.

* * *

I thank Dr. G. BERTOLINO for having put at our disposal his measurements of jets. I thank Prof. G. LOVERA, for stimulating discussions. I want also to express my gratitude for the hospitality I received in the Institute of Physics of the University of Turin, where I had the opportunity of studying some problems of the nuclear emulsion technique.

([3]) FOWLER *et al.* *Phys. Rev.*, **101**, 911 (1956).

([4]) DOBROTIN *et al.*: *III Congress on Cosmic Rays* in *Isz. Ac. Sc. USSR*, 666 (1955).

([5]) G. WATAGHIN: *Phys. Rev.*, **75**, 693 (1949).

([6]) M. CINI and G. WATAGHIN: *Nuovo Cimento*, **8**, 135 (1950).

([7]) W. HEISENBERG: *Kosmische Strahlung* (Berlin, 1953).

([8]) E. FERMI: *Elementary Particles* (Yale University Press, 1951).

([9]) G. BERTOLINO: *Nuovo Cimento*, **1**, 141 (1956).

High Resolution Millimicrosecond Time Interval Measurements Based Upon Frequency Conversion.

C. Cottini, E. Gatti and G. Giannelli
Laboratori CISE - Milano

(ricevuto il 17 Maggio 1956)

The measurement of the time interval between electrical pulses in the millimicrosecond region is of paramount importance for nuclear physics experiments. In fact several apparatuses have been developed and described very recently [1-6].

A new method is under development in our laboratories that has already reached the highest resolutions till now obtained and seems to be suitable to achieve even higher resolutions. Each of the two pulses, whose interval is to be measured, excites a different high Q oscillating circuit. The resonant frequencies of the two circuits are made slightly different (for instance 1%).

The two damped oscillations excited by the incoming pulses are mixed in a germanium diode ring demodulator; its output results to be a damped low frequency oscillation whose phase, measured in respect of the time of arrival of the input pulses, is equal to the initial phase difference between the two damped high frequency oscillations. Time measurements are obtained measuring the phase of the damped low frequency oscillation and are in this way shifted to time intervals many times larger (i.e. a factor of 100 for the quoted 1% frequency difrefence).

In our first set up the two input pulses cut-off two sharp cut-off pentodes having as plate load the two oscillating circuits. These are tuned to frequencies differing by 1% and centered around 30 MHz.

One volt is sufficient to cut-off the pentodes and as it was expected, a time difference of $5 \cdot 10^{-9}$ appeared as a shift

(1) W. Weber, C. W. [Johnstone and L. Cranberg: *Rev. Scient. Instr.*, **27**, 166 (1956).

(2) F. Lepri, L. Minetti and G. Stoppini: *Rev. Scient. Instr.*, **26**, 936 (1955).

(3) G. K. O. Neill: *Rev. Scient. Instr.*, **26**, 285 (1955).

(4) J. W. Keuffel, F. B. Harrison, T. N. K. Goodfrey and G. T. Reynolds: *Phys. Rev.*, **87**, 942 (1952).

(5) J. W. Keuffel: *Rev. Scient. Instr.*, **20**, 197 (1949).

(6) S. H. Neddermayer, E. J. Althaus, W. Allison and R. Schatz: *Rev. Scient. Instr.*, **18**, 488 (1947).

of $0.5 \cdot 10^{-6}$ in the position of the first zero of the low frequency modulation product.

Obviously a conventional coincidence is provided for rejecting coincident pulses whose time separation is larger than a cycle of the high frequency oscillations.

Possibility of exciting ballistically the two resonant circuits with the current pulses of the phototubes has been taken into account. This leads to the possibility of defining the instant of occurrence of the input pulses indipendently from their amplitude. In this way the instant of occurrence of a pulse is affected by an average error of about $\tau/\sqrt{N}$, where τ is the decay time of the phosphor and N the total number of photoelectrons of the considered pulse.

Two Examples of Mesonic Decay of Hyperfragments.

P. H. Fowler (*) and K. H. Hansen

Institute for Theoretical Physics, University of Copenhagen
Copenhagen, Denmark

(ricevuto il 17 Maggio 1956)

The first observation of the emission of an unstable fragment from a nuclear disintegration by Danysz and Pniewski (1) has been followed by many examples supporting their finding. It has been possible to show that most of these events are consistent with the assumption that a Λ^0 is bound into the nuclear structure of the unstable fragment.

Two recent examples, on which detailed measurements were performed, have been observed in this laboratory and are described in the present note. They have previously been briefly commented on by one of us (P.H.F.) at the Pisa Conference in 1955.

1. – An Example of the Decay of $^4_2$He* in Flight.

An unstable fragment (A in Fig. 1) is emitted from a 4+2n star .

After traversing 5.18 mm of the emulsion, the fragment decays, apparently in flight, into four charged particles; of these, the one producing track D is a negative π-meson which comes to rest after a pathlength of 10.05 mm of emulsion and produces a 4-pronged σ-star.

The appearance of track A suggests that the decay took place in flight. Measurements on the distribution of δ-rays along the track make it possible to estimate the charge and residual range of the particle producing the track. Relevant details of the δ-ray measurements and the method used for determining the residual range at decay are given in the appendix. From our measurements the charge of the particle was found to be 2.05 ± 0.15, and the residual range at decay (350 ± 100) μm, assuming the particle to be $^4_2$He*.

(*) On leave from the University of Bristol, summer 1955.
(1) M. Danysz and J. Pniewski: *Phil. Mag.*, **44**, 348 (1953).

From charge-conservation, the particles producing tracks B, C, and E must be singly charged. Assuming tracks B and C to be due to protons, a possible interpretation of the decay is

(*a*) $$ {}^4_2\mathrm{He}^* \rightarrow \mathrm{P} + \mathrm{P} + \mathrm{D} + \pi^- + Q_1 , $$

where no neutral particle is emitted and track E is ascribed to a deuteron.

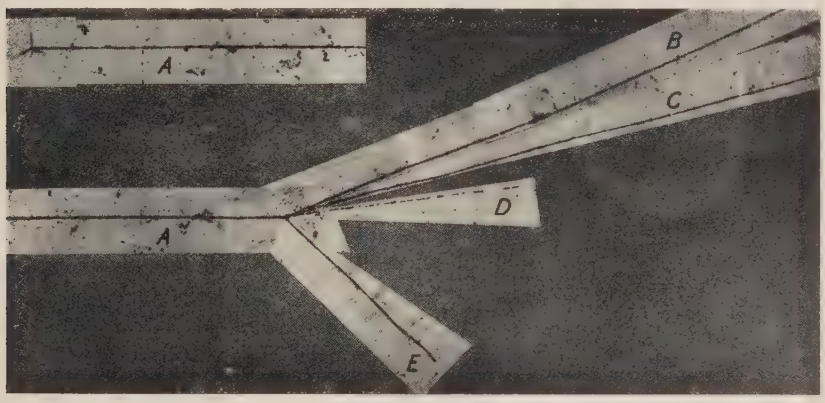

Fig. 1. – Microphotography of the ${}^4_2\mathrm{He}^*$ event.

The relevant data are shown in Table I.

Within the errors of measurement track A lies in the plane of the emulsion. ϑ is the angle between the direction of A and the projected directions of B, C, D, and E, respectively.

TABLE I.

Track	Identity	Range μm	Energy E MeV	Momentum p MeV/c	dip angle (°)	χ(°)
A	${}^4_2\mathrm{He}^*$	5180(*)	—	—	0.0	0.0
B	P	898	13.4 ± 0.1	158.7 ± 0.8	+ 8.1	22.7
C	P	565	10.2 ± 0.1	138.9 ± 0.7	— 25.5	16.1
D	π	10050	23.6 ± 0.5	84.5 ± 0.8	+ 43.8	12.9
E	D	136	5.70 ± 0.05	146.2 ± 0.7	— 8.1	43.8

(*) Observed track length from parent star to decay in flight.

The dip angle is counted positive towards surface, negative towards glass.

The range-energy curve used is that of BARONI *et al.* [2].

[2] G. BARONI, C. CASTAGNOLI, G. CORTINI, C. FRANZINETTI and A. MANFREDINI: *Bureau of Standards, Cern Bulletin*, no. 9 (1954).

The errors quoted do not contain systematic errors in the range-energy relation.

The transverse momentum in the plane of emulsion is found to be (9 ± 2) MeV/c and perpendicular to this plane (0.7 ± 2) MeV/c. The momentum along the direction of motion of track A of the four secondary particles is (429 ± 2) MeV/c. This corresponds to a residual range for a ${}^4_2\mathrm{He}^*$ of (240 ± 5) μm in agreement with the estimate from δ-ray measurements. The total momentum vector is within 1° colinear with A, so that, within the errors, momentum balance can be obtained without introducing any neutral decay products. The corresponding value of Q is (29.6 ± 0.6) MeV; when the value 36.9 MeV for the Q of $\Lambda^0 \to \mathrm{P} + \pi^- + Q$ ([3]) is used, one obtains a binding energy $\mathrm{BE} = (1.9 \pm 0.6)$ MeV of the Λ^0 in ${}^4_2\mathrm{He}^*$. This is in agreement with previous measurements on ${}^4_2\mathrm{He}^*$ ([4]).

Unfortunately, momentum considerations alone cannot rule out the possibility that one or more neutral particles are emitted in the decay. If one interprets the decay as

$$(b) \qquad {}^4_2\mathrm{He}^* \to \mathrm{P} + \mathrm{P} + \mathrm{P} + \pi^- + \mathrm{N} + Q_2 ,$$

the momentum of the neutron must be determined from the δ-ray estimate of the residual range of the ${}^4_2\mathrm{He}^*$. This procedure gives a rather inaccurate determination of the binding energy $\mathrm{BE} = (3 \pm 5)$ MeV. The value is reasonable, but such an interpretation requires that the neutron and proton E are emitted in such a way that the momentum balance can also be obtained by assuming the decay scheme (a) which does not involve any neutral particle. Such a coincidence is improbable, and thus the scheme is given no further consideration.

The possibility of a ${}^3_2\mathrm{He}^*$ is ruled out by lack of momentum balance. This also applies to the case of ${}^3_2\mathrm{He}^*$ without any neutral decay products. The assumption

$$ {}^5_2\mathrm{He}^* \to \mathrm{P} + \mathrm{P} + \mathrm{D} + \pi^- + \mathrm{N} + Q$$

leads to a negative value of BE of the Λ^0.

The same argument based on the visible momentum balance shows that it is unlikely that the event was actually a nuclear interaction of the hyperfragment.

The time of flight of the fragment was $7.7 \cdot 10^{-11}$ s.

2. – An Example of ${}^5_2\mathrm{He}^*$ Decaying at Rest.

This example together with another one reported by CRUSSARD at the Pisa conference in 1955 are believed to be the first cases which give evidence for ${}^5_2\mathrm{He}^*$. Our fragment comes from a 19 + 3p star and reaches the end of its range before decay. The path length of the fragment is 122 μm.

A is the track of the fragment. D is a negative π-meson which comes to rest after having traversed 9.28 mm of emulsion; it ends as a ρ-meson without any

([3]) M. W. FRIEDLANDER, D. KEEFE, M. G. K. MENON and M. MERLIN: *Phil. Mag.*, **45**, 533 (1954).

([4]) R. D. HILL, E. O. SALANT, M. WIDGOFF, L. S. OSBORNE, A. PEVSNER, D. M. RITSON, J. CRUSSARD, and W. D. WALKER: *Phys. Rev.*, **94**, 797 (1954); J. E. NAUGLE, E. P. NEWY, P. S. FREIER, and W. B. CHESTON: *Phys. Rev.*, **96**, 1383 (1954); W. F. FRY, J. SCHNEPS and M. S. SWAMI: *Phys. Rev.*, **99**, 1561 (1955).

decay products. C has a length of 275 μm and is supposed to be a proton. Track B is only 22 μm long and steeply dipping.

Within the error of measurement, the tracks B, C and D are coplanar (actually a non-coplanarity of 1.7 degrees is found). It is therefore reasonable to assume that no neutral particles are emitted.

When C is assumed to be a proton, the momentum along B is (192 ± 2) MeV/c. With this momentum the range is 35 μm for a ${}_2^3\mathrm{He}$, 21 μm for a ${}_2^4\mathrm{He}$, and 13 μm for a ${}_2^5\mathrm{He}$ nucleus. The hydrogen isotopes would have much longer ranges, and nuclei with $Z \geqslant 3$ much shorter ranges than the observed 22 μm.

Therefore

$${}_2^5\mathrm{He}^* \to {}_2^4\mathrm{He} + \mathrm{P} + \pi^- + Q$$

is a reasonable interpretation. The data are shown in Table II.

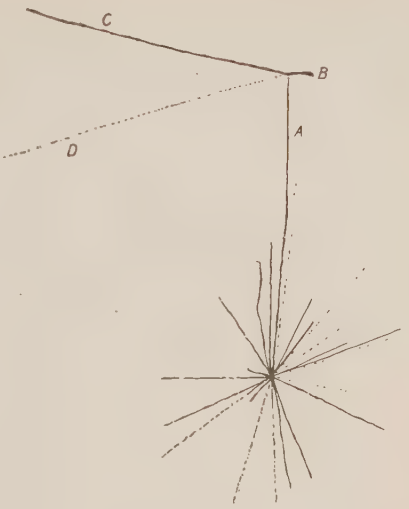

Fig. 2. – Projection drawing of the ${}_2^5\mathrm{He}^*$ event.

TABLE II.

Track	Identity	Range μm	Energy E MeV	Momentum p MeV/c	dip angle(°)	ϑ(°)
B	${}_2^4\mathrm{He}$	22.4	5.3 ± 0.2	198.9 ± 4	-67	—
C	P	275	6.7 ± 0.1	112.2 ± 0.6	$+63.5$	16.7
D	π	9 280	22.4 ± 0.4	82.2 ± 0.8	$+55.0$	10.2

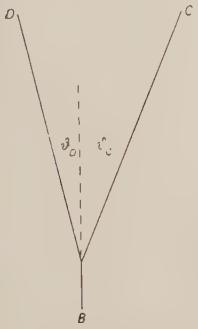

Fig. 3. – Projection in the plane of emulsion.

We obtain a momentum balance in the decay plane of

$$(8 \pm 3) \text{ MeV/c} \perp B,$$

$$(6 \pm 4) \text{ MeV/c} \parallel B.$$

The best value for the energy of the α-particle is obtained from the momentum balance, and is (4.92 ± 0.05) MeV. Thus, the Q-value becomes (34.0 ± 0.5) MeV and, hence, the BE of the Λ^0 is (2.9 ± 0.5) MeV. This value suggests that the binding energy of Λ^0 is larger in ${}_2^5\mathrm{He}^*$ than in ${}_1^3\mathrm{H}^*$ or ${}_2^4\mathrm{He}^*$.

If we consider the possibilities

$${}_1^4\mathrm{H}^* \to \mathrm{P} + \mathrm{D} + \pi^- + \mathrm{N} + Q$$

or

$$^{3}_{1}\mathrm{H}^{*} \rightarrow \mathrm{P} + \mathrm{P} + \pi^{-} + \mathrm{N} + Q$$

we find negative values for the BE's of the Λ^0. Therefore these schemes are neglected.

The possibility of

$$^{6}_{2}\mathrm{He}^{*} \rightarrow \mathrm{P} + {}^{4}_{2}\mathrm{He} + \pi^{-} + \mathrm{N} + Q$$

is considered improbable, since the neutron would have to be sent out with the very small energy of ~ 50 keV.

The values of BE (Λ^0) 1.9 MeV in $^{4}_{2}$He* and 2.9 MeV in $^{5}_{2}$He* are in accordance with the view that the Λ^0 is unrestricted by the Pauli principle. The corresponding binding energies for neutrons are 20.6 MeV in $^{4}_{2}$He, and negative in $^{5}_{2}$He.

Appendix

Estimate of the Residual Range of $^{4}_{2}$He* from the δ-Ray Distribution.

The observations of the δ-rays over the last sections of the track are summarized in Table III.

Table III.

Distance from Decay μm	Number of δ-rays observed	
	2 and 3 grains	⩾4 grains
0 ÷ 200	6	0
200 ÷ 400	14	4
400 ÷ 600	Not useful	7

For convenience we summarize, in Table IV, the average numbers of δ-rays to be expected in intervals of different residual ranges on the track of $^{4}_{2}$He* which comes to rest. The data are taken from the figures given by Dainton and Fowler [5], modified for use with double charged particles of mass number 4.

For each assumed value of the residual range at decay, Table IV gives the average number of δ-rays expected in the three sections. We can then readily calculate the probability P of obtaining the observed set of 5 numbers (Table III) if we assume for each section that the distribution of δ-rays is poissonian around the appropriate mean.

---

[5] A. D. Dainton and P. H. Fowler: *Proc. Roy. Soc.*, A **221**, 414 (1954).

TABLE IV.

Residual range μm	Number of δ-rays expected	
	2 and 3 grains	⩾4 grains
0 ÷ 200	2.0	0.12
100 ÷ 300	4.0	0.20
200 ÷ 400	7.6	0.36
300 ÷ 500	10.8	0.72
400 ÷ 600	12.0	1.36
500 ÷ 700	12.4	2.00
600 ÷ 800	12.4	2.84
700 ÷ 900	13.6	4.16
800 ÷ 1000	14.4	5.24
900 ÷ 1100	—	5.44

TABLE V

Residual range at decay μm	Relative probabilities		Total ln P
	2 and 3 grains δ-rays ln P	⩾4 grains δ-rays ln P	
0	0	0	0
100	3.91	5.38	9.29
200	4.41	7.78	12.16
300	3.31	9.64	12.95
400	2.74	10.10	12.84
500	—	9.73	—

P is found to vary with R as shown in Table V. It is clear that the δ-ray counts indicate most strongly that the particle was not at rest when it decayed. P is a maximum for values of R from 300 ÷ 400 μm. Hence the best value of R obtained from these δ-rays measurements is (350 ± 100) μm.

Effect of Centre-of-Mass Motion on Nuclear Moments.

J. P. Elliott and T. H. R. Skyrme

Atomic Energy Research Establishment - Harwell, Berks.

(ricevuto il 21 Maggio 1956)

In a recent paper on the description of collective motion, Lipkin, de Shalit and Talmi [1] assert a value for the magnetic moment of a nucleus whose shell-model description has a single neutron outside a core. Their value for the orbital contribution does not appear to us to be generally valid, being in contradiction with a result found by us [2] for a particular case.

In that paper [2] we have discussed in detail the separation of the centre of mass motion in the case of an oscillator potential, when the algebra is simple and explicit. A complete set of states of internal motion is obtained by selecting those and only those shell-model states (referred to a fixed well-centre) in which the centre of mass is in one assigned state of motion, chosen for convenience as a 1*s* state. Such shell-model states are referred to as good states, in contrast to the spurious ones which involve some displacement of the centre-of-mass.

It was then shown that the usual method of evaluating nuclear moments with the shell-model gave correct answers, provided the states were limited to the good ones described above. In particular one neutron in the lowest state outside a closed oscillator shell defines a good state, and its orbital magnetic moment is zero. The discrepancy with the result of Lipkin, de Shalit and Talmi [eq. (3.10)] appears to arise from their incomplete antisymmetrization of the wave-function.

The magnetic dipole operator of the internal motion is $\boldsymbol{M}' = \sum_i \frac{1}{2}(1 - \tau_3^i)\boldsymbol{L}_i'$, where as in Lipkin *et al.* [eq. (3.9)]

$$\boldsymbol{L}_i' = (\boldsymbol{x}_i - \sum \boldsymbol{x}_j/A) \times (\boldsymbol{p}_i - \sum \boldsymbol{p}_k/A) \,.$$

This expression for M' may be broken down into three parts

$$\boldsymbol{M}' = \boldsymbol{M} + \boldsymbol{M}_1 + \boldsymbol{M}_2 = \sum \tfrac{1}{2}(1 - \tau_3^i)(\boldsymbol{x}_i \boldsymbol{p}_i) + \\ + A^{-2} \sum [Z - A(1 - \tau_3^i)](\boldsymbol{x}_i \boldsymbol{p}_i) + A^{-2} \sum_{j \neq k} \sum [Z - A(1 - \tfrac{1}{2}\tau_3^j - \tfrac{1}{2}\tau_3^k)](\boldsymbol{x}_j \boldsymbol{p}_k) \,,$$

---

[1] H. J. Lipkin, A. de Shalit and I. Talmi: *Nuovo Cimento*, **2**, 773 (1955).

[2] J. P. Elliott and T. H. R. Skyrme: *Proc. Roy. Soc.*, **232**, 561 (1955).

of which the first M, the simple shell-model operator, will give zero for the state considered. The second term M_1 is a single particle operator that gives the result of Lipkin *et al.* The last term would vanish if the anti-symmetrization were not extended to the neutron outside the core, but in the circumstances that we have considered it will exactly cancel the contribution of M_1; we have verified this explicitly for the configuration s^4p.

A related apparent difficulty arises in connection with the well-known dipole sum-rules [3]. It has been pointed out to us [4] that the use of the simple electric dipole operator $\sum z_i$ would apparently lead to the result $(\frac{3}{4}\pi)Ze^2$ instead of the correct result $(\frac{3}{4}\tau)(NZ/A)e^2$ found when the dipole operator of relative motion is used. This apparent discrepancy is removed when it is remembered that only good states must be used with the uncorrected operators; then it is not possible to apply the completeness theorem in the same way summing over all intermediate states. But if the relative operator is used this can only have non-vanishing matrix elements with good states (assuming that the initial state is one) and the summation can be extended to all states without affecting the answer. Thus in this case it is convenient to use the relative operator and all states, whereas in the previous discussion it was preferable to use the uncorrected operator with a good state.

It should be emphasized that our result for the magnetic moment has been established only for an oscillator well, and there may be circumstances in which the « classical » result of Lipkin *et al.* may be better approximation. Unfortunately it is difficult to carry out the calculations in any other than this simple case.

---

[3] J. M. Blatt and V. F. Weisskopf: *Theoretica Nuclear Physics* (New York, 1952), p. 641.
[4] D. K. Wilkinson: private communication.

Su una nuova equazione relativistica dell'elettrone proposta da Zaitsev.

R. Pappalardo

Istituto di Fisica dell'Università - Pavia

(ricevuto il 26 Maggio 1956)

In un recente articolo [1] G. A. Zaitsev, basandosi su un formalismo spinoriale che fa uso di sole grandezze *reali*, ha dedotto un nuovo sistema di equazioni relativistiche per la particella a spin $\frac{1}{2}$.

Tale sistema è presentato dall'autore come una sostanziale novità rispetto alla consueta teoria di Dirac.

Tuttavia, il fatto che la formula di struttura fina dei livelli energetici dell'atomo di idrogeno ricavata da Zaitsev coincida con quella dedotta partendo dall'equazione di Dirac, induce a ritenere che esista una stretta parentela tra le due teorie.

In questa lettera ci proponiamo di dimostrare che in effetti esiste tra tali teorie una completa identità.

Il sistema di equazioni proposto da Zaitsev è, con le usuali notazioni, il seguente [cfr. eq. (58), (59) loc. cit.]:

$$(1) \qquad \left[\sum_1^3{}_k \sigma_k \left(\frac{\partial}{\partial x_k} + \frac{ie}{\hbar c} A_k\right) + \frac{1}{c}\left(\frac{\partial}{\partial t} - \frac{ie}{\hbar}\varphi\right)\right] \xi = \frac{m_0 c}{\hbar} \sigma_2 \bar{\eta} \,,$$

$$(2) \qquad \left[\sum_1^3{}_k \sigma_k \left(\frac{\partial}{\partial x_k} - \frac{ie}{\hbar c} A_k\right) + \frac{1}{c}\left(\frac{\partial}{\partial t} + \frac{ie}{\hbar}\varphi\right)\right] \eta = \frac{m_0 c}{\hbar} \sigma_2 \bar{\xi} \,,$$

ove $\sigma_1, \sigma_2, \sigma_3$ sono le matrici di Pauli nella consueta rappresentazione, ξ ed η sono due semivettori, $\bar{\xi}$ e $\bar{\eta}$ i loro complessi coniugati.

Osserviamo ora che la (1) e la complessa coniugata della (2) si possono conglobare nell'unica equazione:

$$(3) \qquad \left[\sum_1^3{}_k \begin{pmatrix} \sigma_k & 0 \\ 0 & \bar{\sigma}_k \end{pmatrix} \cdot \left(\frac{\partial}{\partial x_k} + \frac{ie}{\hbar c} A_k\right) + \frac{1}{c}\left(\frac{\partial}{\partial t} \quad \frac{ie}{\hbar}\varphi\right) \quad \frac{m_0 c}{\hbar}\begin{pmatrix} 0 & \sigma_2 \\ \bar{\sigma}_2 & 0 \end{pmatrix}\right]\begin{pmatrix} \xi \\ \bar{\eta} \end{pmatrix} = 0 \,,$$

dove le $\bar{\sigma}_k$ sono le complesse coniugate delle matrici di Pauli.

[1] G. A. Zaitsev: *Soviet Physics JETP*, **1**, 491 (1955).

Riscritta la (3) nella forma:

$$(4) \qquad \left[\sum_1^3{}_k \begin{pmatrix} \sigma_k & 0 \\ 0 & \bar{\sigma}_k \end{pmatrix} \cdot \left(\frac{\partial}{\partial x_k} + \frac{ie}{\hbar c} \Phi_k \right) + i \left(\frac{\partial}{\partial x_4} + \frac{ie}{\hbar c} \Phi_4 \right) - \frac{m_0 c}{\hbar} \begin{pmatrix} 0 & \sigma_2 \\ \bar{\sigma}_2 & 0 \end{pmatrix} \right] \begin{pmatrix} \xi \\ \eta \end{pmatrix} = 0 ,$$

con $x_4 = ict$; $\Phi_k = A_k$; $\Phi_4 = i\varphi$, moltiplichiamo a sinistra per la matrice $\begin{pmatrix} 0 & \sigma_2 \\ \bar{\sigma}_2 & 0 \end{pmatrix}$, tenendo presente che, nella consueta rappresentazione delle matrici di Pauli, $\sigma_l \cdot \sigma_l$ per $l = 1, 3$ e $\bar{\sigma}_2 = -\sigma_2$.

Si ottiene in tal modo:

$$(5) \qquad \left[\sum_1^4{}_\nu \lambda_\nu \left(\frac{\partial}{\partial x_\nu} + \frac{ie}{\hbar c} \Phi_\nu \right) + \frac{m_0 c}{\hbar} \right] \begin{pmatrix} \xi \\ \eta \end{pmatrix} = 0 ,$$

dove:

$$\lambda_1 = \begin{pmatrix} 0 & i\sigma_3 \\ i\sigma_3 & 0 \end{pmatrix} = \gamma_3 ; \qquad \lambda_2 = \begin{pmatrix} 0 & I \\ I & 0 \end{pmatrix} = \gamma_4 ;$$

$$\lambda_3 = \begin{pmatrix} 0 & i\sigma_1 \\ -i\sigma_1 & 0 \end{pmatrix} = \gamma_1 ; \qquad \lambda_4 = \begin{pmatrix} 0 & i\sigma_2 \\ -i\sigma_2 & 0 \end{pmatrix} = \gamma_2 ,$$

e i γ_μ sono gli operatori di Dirac nella rappresentazione di van der Waerden. Ma è ora evidente che, soddisfacendo i λ_μ le relazioni di anticommutazione:

$$\lambda_\mu \lambda_\nu + \lambda_\nu \lambda_\mu = 2\delta_{\mu\nu} ,$$

l'eq. (5) non è altro che l'equazione di Dirac, come si voleva mostrare.

* * *

Ringrazio cordialmente gli amici P. Bocchieri e A. Loinger per un'utile discussione.

ERRATA-CORRIGE

T. Tietz: **The Solution of the Schrödinger Equation for an Approximate Atomic Field,** *Nuovo Cimento*, **3**, 486 (1956).

In equation (3), pag. 487, read φ instead of μ; in equation (9), *ibidem*, read $-(n-1)$ instead of $(n-1)$.

G. Bertolini, M. Bettoni and E. Lazzerini: **Gamma-Gamma Angular Correlation in ^{160}Dy,** *Nuovo Cimento*, **3**, 1162 (1956).

In Fig. 4 of the above paper the ordinate axis should be labelled $W(\theta)/W(90^\circ)$ instead of $W(\theta)$.

Determination of the p-Wave Coupling Constant f^2 of Pion-Nucleon Scattering from Analysis of the α_{31} Phase-Shift.

A. Stanghellini

Istituto di Fisica dell'Università - Bologna

(ricevuto il 26 Maggio 1956)

1. – Introduction.

The main result of Low's equation consists in the determination of all the p-wave phase-shifts of pion-nucleon scattering with only one renormalized coupling constant f^2.

It is therefore important to test whether the coupling constants deduced from experimental data for the four p-wave phase-shifts are the same.

In a previous work, Cini, Fubini, Stanghellini [1], have determined f^2 introducing the experimental data for α_{33} in Low's equation, considered as an exact sum rule.

At the time of the 1955 Rochester Conference it was remarked that the uncertain experimental results then available for the other phase-shifts did not disagree with the f^2 determination of Chew and Low, determination which may be considered as a first approximation of that given by C.F.S.

In this work the new experimental data for the phase-shifts α_{31} are analized in order to determine the f^2 coupling constant.

2. – Following C. F. S. we write the 2-nd Low equation as

$$\text{(1)} \qquad \operatorname{Re} g_2(\omega_q) = -\frac{2}{3}\frac{q^3}{\omega_q} f^2 v^2(q) + \frac{q^3}{\pi} v^2(q) P \int_1^\infty \frac{\mathrm{d}\omega_p}{v^2(p) p^3} \cdot \left(\frac{\operatorname{Im} g_2(\omega_p)}{\omega_p - \omega_q} + \frac{1}{9} \frac{4 \operatorname{Im} g_3(\omega_p) - 2 \operatorname{Im} g_1(\omega_p) + 7 \operatorname{Im} g_2(\omega_p)}{\omega_p + \omega_q} \right).$$

Putting $v^2(q) = 1$ in the energy interval under the cut-off ξ and defining

[1] M. Cini, S. Fubini and A. Stanghellini: *Nuovo Cimento*, **3**, 1380 (1956). In the following we shall quote this work as C.F.S.

$Y'=$ all the contributions to the integral of energy interval from the cut-off to ∞

$$X' = \frac{1}{\pi} P \int_1^{\xi} \frac{d\omega_p}{p^3} \left(\frac{\text{Im } g_2(\omega_p)}{\omega_p - \omega_q} + \frac{4}{9} \frac{\text{Im } g_3(\omega_p)}{\omega_p + \omega_q} \right), \tag{2}$$

where the little phase-shifts are neglected, we can rewrite equation (1) as

$$\sin \alpha_{31} \cos \alpha_{31} = -\frac{2}{3} \frac{q^3}{\omega_q} f^2 + q^3 X' + q^3 Y' \,. \tag{3}$$

Let us suppose that $X' = Y' = 0$. The a posteriori explicit calculation given later in this paper proves the feasibility of this approximation.

Since α_{31} is experimentally small, i.e. of the order of few degrees, equation (3) becomes:

$$\alpha_{31} = -\frac{2}{3} \frac{q^3}{\omega_q} a_{31} \,, \tag{4}$$

where we have substituted f^2 with the parameter a_{31} in order to make explicit the fact that we have introduced an approximation.

This behaviour of α_{31} given by (4) can be deduced also from the approximate solution of Low's equation:

$$-\frac{2}{3} \frac{q^3}{\omega^*} \text{cotg } \alpha_{31} = \frac{1}{f^2} \left(1 + \frac{X\omega^*}{\omega_0} \right),$$

putting $X = 0$.

This is legitimate since this quantity is fairly small as suggested by Low.

Using the results of 14 experiments [2] (Fig. 1) we have obtained

$$a_{31} = 0.083 \pm 0.020 \,, \tag{5}$$

where the error is the standard error calculated from the 7 experiments in which the errors are given.

If one computes the mean square deviation, one gets:

$$0.007 \,,$$

which proves the reliability of the value obtained for a_{31}.

(2) J. TINLOT and A. ROBERTS: *Phys. Rev.*, **95**, 137 (1954); D. BODANSHY, A. SACHS and J. STEINBERGER: *Phys. Rev.*, **93**, 1367 (1954); H. L. ANDERSON, E. FERMI, R. MARTIN and D. E. NAGLE: *Phys. Rev.*, **91**, 155 (1953); G. PUPPI: 1956 *Rochester Conference* (scattering of π^+-mesons by protons at 80, 100, 114 and 124 MeV); J. ASHKIN, J. P. BLASER, F. FEINER and M. O. STERN: *Phys. Rev.*, **101**, 1149 (1956); H. L. ANDERSON, W. C. DAVIDON, M. GLIKSMAN and V. E. KRUSE: *Phys. Rev.*, **100**, 279 (1955); O. TAFT: *Phys. Rev.*, **101**, 1116 (1956); J. ASHKIN: private communication; R. S. MARGULEIS: *Bull. of Amer. Society*, **7** (1955).

This result can be interpreted in two ways:

a) as an approximated determination of f^2;

b) as a good fit of experimental data for α_{31}.

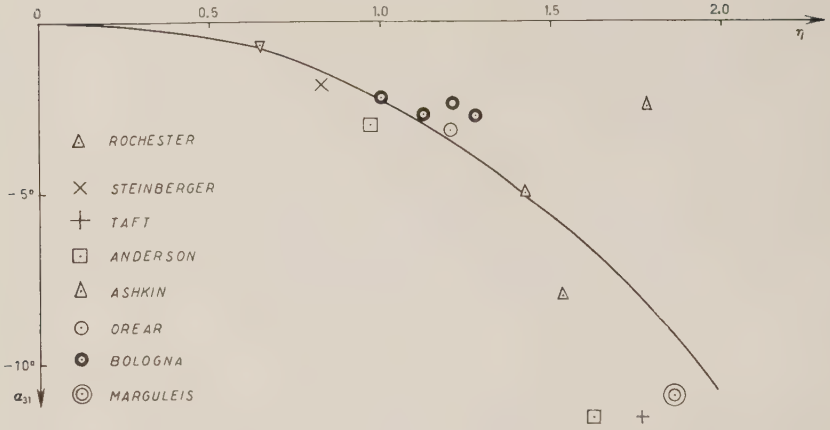

Fig. 1. – The experimental points of α_{31} phase-shift are plotted versus $\eta = p/\mu c$, the pion momentum in c.m.s., and fitted with the curve $\alpha_{31} = -\frac{2}{3}(0.083 \pm 0.020)(q^3/\omega_q)$.

Taking the point of view (*b*) we have calculated the integral X' and therefore the correction to the f^2 of the point of view (*a*).

We have:

$$\operatorname{Im} g_2 = \alpha_{31}^2 .$$

The first term of X' becomes:

$$\frac{1}{\pi}\frac{4}{3}\alpha_{31}^2 P \int_1^{\xi} \frac{\mathrm{d}\omega_p}{\omega_p^2} \frac{p^3}{\omega_p - \omega_q} .$$

which can be calculated numerically after subtraction of the singularity.

The calculations were carried out for two limiting cases: first that the integral is limited between 1 and $2.5\omega_p$; second that the behaviour (4) can be extrapolated to $6\omega_p$ ($\alpha_{31} \sim 100°$). One finds that in both cases the integrals are the same within the errors, for the energy range between 1 and $2\omega_q$:

The main contribution of the integral X' comes for the second term which contains α_{33} already calculated in C.F.S.

From the equation (3) we have:

$$(a_{31} + \tfrac{3}{2}X'\omega_q) = f^2 - \tfrac{3}{2}Y'\omega_q .$$

The term $\frac{3}{2}X'\omega_q$ is found to be constant within the errors in the energy interval $1.4 \lesssim \omega_q \lesssim 1.9$ therefore $Y' = 0$.

The average of $\frac{3}{2}X'\omega_q$ for the two limiting cases mentioned above is:

$$\frac{3}{2}X'\omega_q \begin{cases} \nearrow 0.023 \pm 0.004 \\ \searrow 0.032 \pm 0.007 . \end{cases}$$

For f^2 we have

$$f^2 = 0.106 \pm 0.024 .$$

$$f^2 = 0.117 \pm 0.027 .$$

If we take the mean value of these results we can conclude that the coupling constant derived from α_{31} is

$$f^2 = 0.11 \pm 0.025 .$$

which is in a good agreement with the determination of f^2 from α_{33}

$$f^2 = 0.107 \pm 0.006 .$$

We can therefore conclude:

1) That the behaviour (3) for α_{31} based on the assumption that X' and Y' are small is reliable.

2) That this determination of f^2 agrees with that in C.F.S.

3) That the contribution of energies above the cut-off is small.

We want to emphasize that introducing the experimental phase-shifts in Low equation is equivalent to assuming that the contribution of the nucleon recoil to the interaction does not involve the P-waves.

An explicit calculation of f^2 with dispersion formulae should provide a verification of the reliability of this assumption.

* * *

I wish to thank Profs. Cini, Fubini and Puppi for many advices and discussions.

ERRATA-CORRIGE

D. Amati and B. Vitale: **On the Pion Annihilation of Nucleon-Antiproton Pairs**, *Nuovo Cimento*, 3, 1411 (1956).

Owing to a misprint, a note that should have been added in proof to the letter « Some Considerations on the Charge-Exchange Scattering of Antinucleons on Nucleons » of the same Authors, appearing in this issue, pag. 145, was erroneously appended to aforesaid paper.

Simboli e Unità.

Il prof. J. De Boer, Segretario della Commissione dei Simboli, Unità e Nomenclatura (S.U.N.) dell'Unione Internazionale di Fisica pura e applicata, ci prega di pubblicare il seguente « Document U.I.P. 6, (1955) », relativo alle ultime decisioni della Commissione S.U.N.

Aderiamo ben volentieri alla richiesta del prof. De Boer, e prendiamo occasione da questa pubblicazione per raccomandare agli Autori di seguire, per quanto è possibile, le norme date in questo Documento.

La Direzione del *Nuovo Cimento*

Symbols and Units

INTERNATIONAL UNION OF PURE AND APPLIED PHYSICS

S.U.N. COMMISSION

Symboles et Unités

UNION INTERNATIONALE DE PHYSIQUE PURE ET APPLIQUÉE

COMMISSION S.U.N.

Document U.I.P. 6

(1955)

I.

II.

III.

MATHEMATICAL OPERATIONS AND SYMBOLS

OPÉRATIONS ET SYMBOLES MATHÉMATIQUES

IV.

SYMBOLS FOR UNITS

SYMBOLES DES UNITÉS

Remark.

This report, composed by the Commission of Symbols, Units and Nomenclature of the I.U.P.A.P. has been approved by the General Assemblies of the Union of Physics, held im 1948, 1951 and 1954.

The recommendations on the use of symbols for units, for physical quantities and for mathematical constants and operations contained in this report are in general in agreement with important international recommendations, *viz.*:

Remarque.

Ce rapport, composé par la Commission des Symboles, Unités et Nomenclature de l'U.I.P.P.A., a été approuvé par les Assemblées Générales de l'Union de Physique, tenues en 1948, 1951 et 1954.

Les recommandations concernant l'usage des symboles pour les unités, les grandeurs physiques et pour les constantes et opérations mathématiques, contenues dans ce rapport s'accordent en général avec des recommendations importantes internationales, *c. à. d.*:

(1) International Standardising Organisation (I.S.O.) — Project ISO. TC 12.
(2) Conférence Générale des Poids et Mesures (9ème C.G. 1948; 10ème C.G. 1954).
(3) Union Internationale de Chimie Pure et Appliquée (1947, 1949, 1951).
(4) International Electrotechnical Committee (Int. Letter Symbols Publ. 27, 1953).

I.

GENERAL PRINCIPLES AND RECOMMENDATIONS

1. Physical quantities.

(1) Symbols for physical quantities should be printed in italic (cursive) type.

The symbol for a physical quantity (« grandeur physique » in France, « physical magnitude » in America, « physikalische Größe » in Germany) is equivalent to the product of the numerical value or measure, being a pure number, and a unit:

physical quantity =
= numerical value × unit.

(2) Abbreviations, i.e. shortened forms of names or expressions, should not be used in physical equations. In the text the abbreviations should be written in ordinary roman type (e.g.: pf for partition function, EMF for electromotive force, etc.).

2. Units.

(1) Symbols for units of physical quantities should be printed in roman (upright) type.

(2) Symbols for units should *not* be followed by a full stop.

(3) Symbols for units derived from proper names should start with a capital roman letter. All other units should be printed in lower case romane type.

(4) Symbols for prefixes should be printed in lower case roman type, with the single exception of the prefixes: M = mega, G = giga and T = tera.

(5) Symbols for units should *not* be written in plural (e.g. do *not* write: 7 watts, but: 7 watt or 7 W).

PRINCIPES ET RECOMMANDATIONS GÉNÉRAUX

1. Grandeurs phisiques.

(1) Les symboles des grandeurs physiques seront imprimés en caractères italiques (cursives).
Le symbole d'une grandeur physique (« physical quantity » en Angleterre, « physical magnitude » en Amérique, « physikalische Größe » en Allemagne) est équivalent au produit de la valeur numérique (ou mesure), qui est un nombre pur, et d'une unité:

grandeur physique =
= valeur numérique × unité.

(2) Des abréviations, des noms ou des expressions abrégées, ne seront pas utilisées dans des équations physiques. Dans le texte, les abréviations seront écrites en caractères romains ordinaires (p. ex.: fp au lieu de fonction de partition; F.E.M. au lieu de force électromotrice, etc.).

2. Unités.

(1) Les symboles des unités des grandeurs physiques seront imprimés en caractères romains (droits).

(2) Les symboles des unités ne seront *pas* suivis d'un point.

(3) Les symboles des unités dérivées de noms propres seront imprimés en commençant avec un caractère majuscule romain. Toutes les autres unités seront imprimées en caractères minuscules romains.

(4) Les symboles pour préfixes seront imprimés en caractères minuscules romains, excepté les préfixes: M = mega, G = giga et T = téra.

(5) Les symboles des unités ne seront *pas* écrits au pluriel (p. ex. n'écrivez *pas*: 7 watts, mais: 7 watt ou 7 W).

3. Mathematical operations.

(1) Symbols for mathematical operations should be printed in roman (upright) type. (e.g. $\sin kx$, $\exp at$, $\log A$).

(2) Symbols for mathematical operations should *not* be followed by a full stop.

(3) Numbers should be printed in upright figures. A comma or point may be used only to separate the whole numbers from the decimals.

(4) To facilitate the reading of large numbers the figures may be grouped in groups of three but *no* comma or point should be used (e.g. 2 573.421 736).

4. Chemical elements.

(1) Symbols for chemical elements should be written in roman (upright) type and are not followed by a full stop (e.g. Ca, C, H, D, He).

(2) The attached numerals should have the following meaning:

mass number ^{14}
atomic number $_{7}$
N_{2} atoms/molecule

The right superscript place is left for indicating, if required, a state of ionisation or nuclear excited states (e.g. Ca^{2+}, PO_4^{3-}). It may be of advantage to omit the atomic number when there is no special reasons for indicating it.

(3) A species of atoms identical as regards atomic number and mass-number should be indicated by the word *nuclide*. The name *isotopes* should be reserved for atoms with the same atomic number, whereas *isobars* are atoms having the same mass number.

3. Opérations mathématiques.

(1) Les symboles des opérations mathématiques seront imprimés en caractère romains (droits) (p. ex. $\sin kx$, $\exp \alpha t$, $\log A$).

(2) Les symboles des opérations mathématiques ne seront *pas* suivis d'un point.

(3) Les nombres seront imprimés en chiffres droits. La virgule ou le point est utilisé seulement pour séparer les nombres entiers des nombres décimaux.

(4) Pour faciliter l'écriture, les grands nombres peuvent être partagés en tranches de trois chiffres mais ne doivent *pas* être séparés par des points ni par des virgules (p. ex. 2 573,421 736).

4. Éléments chimiques.

(1) Les symboles des éléments chimiques seront imprimés en caractères romains (droits) et ne sont pas suivis d'un point (p. ex. Ca, C, H, D, He).

(2) Les indices attachés aux symboles des éléments ont les sens suivants:

nombre de masse ^{14}
nombre atomique $_{7}$
N_{2} atomes/molecule

L'indice en haut à droite est réservé pour indiquer l'état d'ionisation ou des états nucléaires excités (p. ex. Ca^{2+}, PO_4^{3-}). S'il n'y a pas de raisons spéciales pour indiquer le nombre atomique, il peut être préférable de le supprimer.

(3) Une espèce d'atomes identiques dans leur nombre atomique et nombre de masse serà désignée par le mot *nuclide*. Le nom *isotopes* sera réservé pour des atomes ayant le même nombre atomique, tandis que des *isobares* sont des atomes ayant le même nombre de masse.

II.

SYMBOLS FOR PHYSICAL QUANTITIES

Remarks.

(1) Where several symbols are given for one quantity, and no special indication is made, they are on equal footing.

(2) In general no special attention is paid to the name of the quantity.

1. Space and time.

length	l
breadth	b
height	h
radius	r
diameter: $d = 2r$	d
path: $L = \int ds$	L, s
area	A, S
volume	V, v
plane angle	$\alpha, \beta, \gamma, \theta, \vartheta, \varphi$
solid angle	ω, Ω
wave length	λ
wave number: $\sigma = 1/\lambda$	σ, $\tilde{\nu}$ (*)
circular number: $k = 2\pi/\lambda$	k
time	t
period	T
frequency: $\nu = 1/T$	ν, f (**)
pulsatance: $\omega = 2\pi\nu$	ω
velocity: $v = \mathrm{d}s/\mathrm{d}t$	v
angular velocity: $\omega = \mathrm{d}\varphi/\mathrm{d}t$	ω
acceleration: $a = \mathrm{d}v/\mathrm{d}t$	a
angular acceleration: $\alpha = \mathrm{d}\omega/\mathrm{d}t$	α
gravitational acceleration	g
standard gravitational acceleration	g_n
v/c	β

(*) $\tilde{\nu}$ is exclusively used in molecular spectroscopy.

(**) In physics: ν.

SYMBOLES DES GRANDEURS PHYSIQUES

Remarques.

(1) Lorsque plusieurs symboles sont indiqués pour une même grandeur sans indication spéciale, ces symboles sont admissibles au même titre.

(2) En général on n'a pas accordé une attention spéciale au nom de la grandeur.

1. Espace et temps.

longueur	l
largeur	b
hauteur	h
rayon	r
diamètre: $d = 2r$	d
parcours: $L = \int ds$	L, s
surface	A, S
volume	V, v
angle plan	$\alpha, \beta, \gamma, \theta, \vartheta, \varphi$
angle solide	ω, Ω
longueur d'onde	λ
nombre donde: $\sigma = 1/\lambda$	σ, $\tilde{\nu}$ (*)
nombre circulaire: $k = 2\pi/\lambda$	k
temps	t
période	T
fréquence: $\nu = 1/T$	ν, f (**)
pulsation: $\omega = 2\pi\nu$	ω
vitesse: $v = \mathrm{d}s/\mathrm{d}t$	v
vitesse angulaire: $\omega = \mathrm{d}\varphi/\mathrm{d}t$	ω
accélération: $a = \mathrm{d}v/\mathrm{d}t$	a
accélération angulaire: $\alpha = \mathrm{d}\omega/\mathrm{d}t$	α
accélération de la pesanteur	g
accélération de la pesanteur normale	g_n
v/c	β

(*) $\tilde{\nu}$ est utilisé exclusivement en spectroscopie moléculaire.

(**) En physique: ν.

2. Mechanics.

mass	m
reduced mass	μ
density: $\varrho = m/V$	ϱ
momentum: $p = mv$	$\boldsymbol{p}$, p
moment of inertia: $I = \int r^2 \mathrm{d}m$	I, J
force	$\boldsymbol{F}$, F
weight	G, (W) (*)
force moment	$\boldsymbol{M}$, M
pressure	p
traction	σ
shear stress	τ
gravitational constant: $F(r) = G m_1 m_2 / r^2$	G
modulus of elasticity, Youngs modulus: $\sigma = E \Delta l / l$	E
shear modulus: $\tau = G \operatorname{tg} \gamma$	G
compressibility: $\varkappa = -(1/V)\,\mathrm{d}V/\mathrm{d}p$	$\varkappa$
bulk modulus: $K = 1/\varkappa$	K
viscosity	η
kinematic viscosity: $\nu = \eta/\varrho$	ν
friction coefficient	f
surface tension	γ, σ
energy	E, U
potential energy	V, E_p
kinetic energy	T, E_k
work	W, A
power	P
efficiency	η
Hamiltonian function	H
Lagrangian function	L
relative density	d

3. Kinetic theory of gases.

number of molecules	N
number of molecules per mole	N_0, N
number of molecules per volume, number density	n
molecular velocity vector with components	$\boldsymbol{c}$ (c_x, c_y, c_z) $\boldsymbol{u}$ (u_x, u_y, u_z)
molecular position vector with components	$\boldsymbol{r}$ (x, y, z)
molecular momentum vector with components	$\boldsymbol{p}$ (p_x, p_y, p_z)
average velocity	c_0, u_0, $\bar{c}$, $\bar{u}$

(*) Preferred symbol: G.

2. Mécanique.

masse	m
masse réduite	μ
masse volumique: $\varrho = m/V$	ϱ
moment: $p = mv$	$\boldsymbol{p}$, p
moment d'inertie: $I = \int r^2 \mathrm{d}m$	I, J
force	$\boldsymbol{F}$, F
poids	G, (W) (*)
moment d'une force	$\boldsymbol{M}$, M
pression	p
traction	σ
tension de cisaillement	τ
constante de la gravitation: $F(r) = G m_1 m_2 / r^2$	G
module d'élasticité: $\sigma = E \Delta l / l$	E
module de torsion $\tau = G \operatorname{tg} \gamma$	G
compressibilité: $\varkappa = -(1/V)\,\mathrm{d}V/\mathrm{d}p$	$\varkappa$
module de compression: $K = 1/\varkappa$	K
viscosité	η
viscosité cinématique $\nu = \eta/\varrho$	ν
coefficient de frottement	f
tension superficielle	γ, σ
énergie	E, U
énergie potentielle	V, E_p
énergie cinétique	T, E_k
travail	W, A
puissance	P
rendement	η
fonction de Hamilton	H
fonction de Lagrange	L
densité relative	d

3. Théorie cinétique des gaz.

nombre de molécules	N
nombre de molécules par mole	N_0, N
nombre de molécules par volume	n
vecteur de la vitesse moléculaire et ses composantes	$\boldsymbol{c}$, (c_x, c_y, c_z) $\boldsymbol{u}$, (u_x, u_y, u_z)
vecteur de position moléculaire et ses composantes	$\boldsymbol{r}$, (x, y, z)
vecteur du moment moléculaire et ses composantes	$\boldsymbol{p}$, (p_x, p_y, p_z)
vitesse moyenne	c_0, u_0, $\bar{c}$, $\bar{u}$

(*) Symbole préféré: G.

most probable speed	$\hat{c}$, $\hat{u}$
mean free path	l
velocity distribution function: $n = \int f \mathrm{d}u_x \mathrm{d}u_y \mathrm{d}u_z$	$f(c)$
Boltzmann's function	H
generalized co-ordinate	q
generalized momentum	p
volume in γ phase space	Ω
thermodynamic temperature	T, (Θ) ( )
Boltzmann's constant	k
$1/kT$ in exponential functions	β
gas constant per mole	R
characteristic temperature	Θ
Debye temperature: $\Theta_D = h\nu_D/k$	Θ_D
Einstein temperature: $\Theta_E = h\nu_E/k$	Θ_E
rotational temperature: $\Theta_r = h^2/8\pi^2 Ik$	Θ_r
vibrational temperature: $\Theta_v = h\nu/k$	Θ_v

vitesse la plus probable	$\hat{c}$, $\hat{u}$
libre parcours moyen	l
fonction de distribution des vitesses $n = \int f \mathrm{d}u_x \mathrm{d}u_y \mathrm{d}u_z$	$f(c)$
fonction de Boltzmann	H
coordonnée généralisée	q
moment généralisé	p
volume dans l'espace γ	Ω
température thermodynamique	T, (Θ) ( )
constante de Boltzmann	k
$1/kT$ dans les fonctions exponentielles	β
constante molaire des gaz	R
température caractéristique	Θ
température de Debye: $\Theta_D = h\nu_D/k$	Θ_D
température d'Einstein: $\Theta_E = h\nu_E/k$	Θ_E
température de rotation: $\Theta_r = h^2/8\pi^2 Ik$	Θ_r
température de vibration: $\Theta_v = h\nu/k$	Θ_v

4. Thermodynamics.

quantity of heat	Q
work	W, A
temperature	t, (ϑ) (*)
thermodynamic temperature	T, (Θ) (**)
entropy	S
internal energy	U
free energy, Helmholtz function: $F = U - TS$	F
enthalpy, heat function: $H = U + pV$	H
Gibbs function: $G = U + pV - TS$	G
linear expansion coefficient	α
cubic expansion coefficient	γ
thermal conductivity	λ
specific heat	c_p, c_v
molar heat capacity	C_p, C_v
Joule-Thomson coefficient	μ
ratio of specific heats	$\varkappa$, γ

(+) Preferred symbol: T.
(*) Preferred symbol: t.
(**) Preferred symbol: T.

4. Thermodynamique.

quantité de chaleur	Q
travail	W, A
température	t, (ϑ) (*)
température thermodynamique	T, (Θ) (**)
entropie	S
énergie interne	U
énergie libre, fonction de Helmholtz: $F = U - TS$	F
enthalpie: $H = U + pV$	H
enthalpie libre, fonction de Gibbs: $G = U + pV - TS$	G
coefficient de dilatation linéaire	α
coefficient de dilatation cubique	γ
conductivité calorifique	λ
chaleur spécifique	c_p, c_v
capacité thermique molaire	C_p, C_v
coefficient de Joule-Thomson	μ
rapports des chaleurs spécifiques	$\varkappa$, γ

(+) Symbole préféré: T.
(*) Symbole préféré: t.
(**) Symbole préféré: T.

5. Electricity.

quantity of electricity	Q
charge density	ϱ
surface charge density	σ
electric potential	V
electric field	$\boldsymbol{E}$, E
electric displacement	$\boldsymbol{D}$, D
capacity	C
permittivity: $\varepsilon = D/E$	ε
permittivity of vacuum	ε_0
relative permittivity	ε_r
dielectric polarization: $\boldsymbol{D} = \varepsilon_0\boldsymbol{E} + \boldsymbol{P}$ (†)	$\boldsymbol{P}$, P
electric susceptibility	χ_e
electric dipole moment	$\boldsymbol{p}$ p
electric current	I
electric current density	$\boldsymbol{J}$, J
magnetic field	$\boldsymbol{H}$, H
magnetic induction	$\boldsymbol{B}$, B
magnetic flux	Φ
permeability: $\mu = B/H$	μ
permeability of vacuum	μ_0
relative permeability $\mu_r = \mu/\mu_0$	μ_r
magnetization: $\boldsymbol{B} = \mu_0(\boldsymbol{H} + \boldsymbol{M})$ (†)	$\boldsymbol{M}$, M
magnetic susceptibility	χ_m
electromagnetic moment	$\boldsymbol{\mu}$, μ
magnetic polarization: $\mu_0\boldsymbol{M}$	(*)
magnetic dipole moment	$\boldsymbol{m}$, m
resistance	R
reactance	X
impedance: $Z = R + iX$	Z
conductance: $G = R/Z^2$	G
susceptance: $B = -X/Z^2$	B
admittance $Y = 1/Z = G + iB$	Y
resistivity	ϱ
conductivity: $1/\varrho$	γ, σ
self inductance	L
mutual inductance	M, L_{12}
phase number	m
loss angle	δ
number of turns	N
power	P
Poynting vector	$\boldsymbol{S}$, S
vector potential	$\boldsymbol{A}$

(†) Written in the rational form. See page 176.

(*) No symbol is recommended.

5. Électricité.

quantité d'électricité	Q
densité électrique	ϱ
densité électrique superficielle	σ
potentiel électrique	V
champ électrique	$\boldsymbol{E}$, E
déplacement électrique	$\boldsymbol{D}$, D
capacité	C
permittivité: $\varepsilon = D/E$	ε
permittivité du vide	ε_0
permittivité relative: $\varepsilon_r = \varepsilon/\varepsilon_0$	ε_r
polarisation diélectrique: $\boldsymbol{D} = \varepsilon_0\boldsymbol{E} + \boldsymbol{P}$ (†)	$\boldsymbol{P}$, P
susceptibilité électrique	χ_e
moment dipolaire électrique	$\boldsymbol{p}$, p
courant électrique	I
densité de courant électrique	$\boldsymbol{J}$, J
champ magnétique	$\boldsymbol{H}$, H
induction magnétique	$\boldsymbol{B}$, B
flux magnétique	Φ
perméabilité: $\mu = B/H$	μ
perméabilité du vide	μ_0
perméabilité relative: $\mu_r = \mu/\mu_0$	μ_r
aimantation: $\boldsymbol{B} = \mu_0(\boldsymbol{H} + \boldsymbol{M})$ (†)	$\boldsymbol{M}$, M
susceptibilité magnétique	χ_m
moment électromagnétique	$\boldsymbol{\mu}$, μ
polarisation magnétique: $\mu_0\boldsymbol{M}$	(*)
moment magnétique dipolaire	$\boldsymbol{m}$, m
résistance	R
réactance	X
impédance: $Z = R + iX$	Z
conductance: $G = R/Z^2$	G
susceptance: $B = -X/Z^2$	B
admittance: $Y = 1/Z = G + iB$	Y
résistivité	ϱ
conductivité: $1/\varrho$	γ, σ
inductance propre	L
inductance mutuelle	M, L_{12}
nombre de phases	m
angle de pertes	δ
nombre de tours	N
puissance	P
vecteur de Poynting	$\boldsymbol{S}$, S
potentiel vecteur	$\boldsymbol{A}$

(†) Écrite sous la forme rationalisée. Voir la page 176.

(*) Pas de symbole recommandé.

6. Light.

quantity of light	Q
flux of light	Φ
luminous intensity: $\mathrm{d}\Phi/\mathrm{d}\omega$	I
illumination: $\mathrm{d}\Phi/\mathrm{d}S$	E
luminance: $\mathrm{d}I/\mathrm{d}S \cos\vartheta$	$L,\ B$
luminous radiance: $\mathrm{d}\Phi/\mathrm{d}S$	H
absorption factor: Φ_a/Φ_0	α
reflection factor: Φ_r/Φ_0	ϱ
transmission factor: Φ_{tr}/Φ_0	τ
absorption coefficient	a
extinction coefficient	$\varkappa$
speed of light in empty space	c
refractive index: $n = c/c_n$	n

7. Atomic physics.

atomic number	Z
mass number	A
proton number: $P = Z$	P
neutron number: $N = A - Z$	N
charge of electron	$-e$
electron mass	m
proton mass	M_p
neutron mass	M_n
meson mass	$m_\pi,\ m_\mu$
nuclear mass	M
atomic mass	M_a
magnetic moment of particle	μ
magnetic moment of proton	μ_p
magnetic moment of neutron	μ_n
magnetic moment of electron	μ_e
Bohr magneton	$\mu_B,\ \beta$
principal quantum number	$n,\ n_i$
orbital angular momentum quantum number	$L,\ l_i$
spin quantum number	$S,\ s_i$
total angular momentum quantum number	$J,\ j_i$
magnetic quantum number	$M,\ m_i$
nuclear spin quantum number	I
hyperfine quantum number	F
rotational quantum number	$J,\ K$
vibrational quantum number	v
quadrupole moment	Q
Rydberg constant	R

6. Lumière.

quantité de lumière	Q
flux de lumière	Φ
intensité lumineuse: $\mathrm{d}\Phi/\mathrm{d}\omega$	I
éclairement: $\mathrm{d}\Phi/\mathrm{d}S$	E
luminance: $\mathrm{d}I/\mathrm{d}S \cos\vartheta$	$L,\ B$
émittance lumineuse: $\mathrm{d}\Phi/\mathrm{d}S$	H
facteur d'absorption: Φ_a/Φ_0	a
facteur de réflexion: Φ_r/Φ_0	ϱ
facteur de transmission: Φ_{tr}/Φ_0	τ
coefficient d'absorption	a
coefficient d'estinction	$\varkappa$
vitesse de la lumière dans le vide	c
indice de réfraction: $n = c/c_n$	n

7. Physique atomique.

nombre atomique	Z
nombre de masse	A
nombre de protons: $P = Z$	P
nombre de neutrons: $N = A - Z$	N
charge électrique de l'électron	$-e$
masse de l'électron	m
masse du proton	M_p
masse du neutron	M_n
masse du méson	$m_\pi,\ m_\mu$
masse nucléaire	M
masse atomique	M_a
moment magnétique d'une particule	μ
moment magnétique du proton	μ_p
moment magnétique du neutron	μ_n
moment magnétique électronique	μ_e
magnéton de Bohr	$\mu_B,\ \beta$
nombre quantique principal	$n,\ n_i$
nombre quantique du moment angulaire	$L,\ l_i$
nombre quantique du spin	$S,\ s_i$
nombre quantique du moment total	$J,\ j_i$
nombre quantique magnétique	$M,\ m_i$
nombre quantique du spin nucléaire	I
nombre quantique hyperfin	F
nombre quantique de rotation	$J,\ K$
nombre quantique de vibration	v
moment quadripolaire	Q
constante de Rydberg	R

III.

MATHEMATICAL OPERATIONS AND SYMBOLS

1. Analysis.

equal to	$=$
approximately equal to	$\backsim$, $\approx$
proportional to	$\propto$
tends to	$\rightarrow$
asymptotically equal to	$\sim$
corresponds to	$\widehat{=}$
plus or minus	$\pm$
sum of	Σ
product of	Π
infinity	∞
pi	π
base of natural logarithm	e
factorial n	$n!$
binomial coefficient: $n!/p!\,(n-p)!$	$\binom{n}{p}$
variation of x	∂x
increase of x	Δx (*)
exponential of x	$\exp x$, e^x
decadic logarithm of x	$\log x$ (**)
natural logarithm of x	$\ln x$
real part of z	$\mathrm{Re}\, z$
imaginary part of z	$\mathrm{Im}\, z$
modulus of z	$\lvert z \rvert$
complex conjugate of z	z^*
complex conjugate of matrix A: $(A^*)_{ik} = (A_{ik})^*$	A^*
Hermitian conjugate of matrix A: $(A^\dagger)_{jk} = A^*_{kj}$	$A^\dagger$
adjoint of matrix A: $\tilde{A}_{jk} = A_{kj}$	$\tilde{A}$

2. Vectors and tensors.

To avoid the usage of subscripts it is often recommended to indicate vectors and tensors of the second rank by letters of a special type.

The following choice is recommended:

(*) Greek capital delta, not triangle

(**) In case of ambiguity ${}^{10}\log x$ or $\log_{10} x$.

OPÉRATIONS ET SYMBOLES MATHÉMATIQUES

1. Analyse.

égal à	$=$
égal environ à	$\backsim$, $\approx$
proportionnel à	$\propto$
tend vers	$\rightarrow$
asymptotiquement égal à	$\sim$
correspond à	$\widehat{=}$
plus ou moins	$\pm$
somme de	Σ
produit de	Π
infini	∞
pi	π
base des logarithmes naturels	e
factoriel n	$n!$
coefficient du binome: $n!/p!\,(n-p)!$	$\binom{n}{p}$
variation de x	∂x
accroissement de x	Δx (*)
exponentielle de x	$\exp x$, e^x
logarithme décimal de x	$\log x$ (**)
logarithme naturel de x	$\ln x$
partie réelle de z	$\mathrm{Re}\, z$
partie imaginaire de z	$\mathrm{Im}\, z$
module de z	$\lvert z \rvert$
conjuguée complexe de z	z^*
conjuguée complexe de la matrice A: $(A^*)_{jk} = (A_{jk})^*$	A^*
conjuguée Hermitienne de la matrice A: $(A^\dagger)_{jk} = A^*_{kj}$	$A^\dagger$
adjoint de la matrice A: $\tilde{A}_{jk} = A_{kj}$	$\tilde{A}$

2. Vecteurs et tenseurs.

Pour éviter l'usage d'indices il est souvent recommandé d'indiquer les vecteurs et les tenseurs du second ordre par des caractères spéciaux.

Le choix suivant est recommandé:

(*) Delta capitale grecque et non triangle

(**) En cas d'ambiguité ${}^{10}\log x$ ou $\log_{10} x$.

(1) *Vectors should be printed in bold type by preference bold italic type.*

(2) *Tensors of the second rank should be printed in sans serif type.*

(3) In manuscripts vectors may be indicated by an arrow and tensors by a double arrow on top.

vector	$\boldsymbol{A}$, $\boldsymbol{a}$
absolue value	$\lvert\boldsymbol{A}\rvert$, $\lvert\boldsymbol{a}\rvert$
scalar product	$\boldsymbol{A}\cdot\boldsymbol{B}$
vector product	$\boldsymbol{A}\wedge\boldsymbol{B}$, $\boldsymbol{A}\times\boldsymbol{B}$
nabla operator	∇
gradient	grad φ, $\nabla\varphi$
divergence	div $\boldsymbol{A}$
curl	curl $\boldsymbol{A}$, rot $\boldsymbol{A}$
Laplacian	$\Delta\varphi$, $\nabla^2\varphi$
dyadic product	$\boldsymbol{AB}$
tensor	T
tensor product: $\Sigma_k S_{ik} T_{kl}$	$\mathsf{S}\cdot\mathsf{T}$
scalar product: $\Sigma_k\Sigma_i S_{ik} T_{ki}$	$\mathsf{S}:\mathsf{T}$
product of vector and tensor: $\Sigma_k A_k T_{ki}$, $\Sigma_i T_{ki} A_i$	$\boldsymbol{A}\cdot\mathsf{T}$, $\mathsf{T}\cdot\boldsymbol{A}$

(1) *Les vecteurs seront imprimés en caractères gras, de préférence en caractères italiques.*

(2) *Les tenseurs du second ordre seront imprimeés en caractères sans sérif.*

(3) Dans le manuscrits les vecteurs peuvent être indiqués par une flèche et les tenseurs par deux flèches surmontant la lettre.

vecteur	$\boldsymbol{A}$, $\boldsymbol{a}$
valeur absolue	$\lvert\boldsymbol{A}\rvert$, $\lvert\boldsymbol{a}\rvert$
produit scalaire	$\boldsymbol{A}\cdot\boldsymbol{B}$
produit vectoriel	$\boldsymbol{A}\wedge\boldsymbol{B}$, $\boldsymbol{A}\times\boldsymbol{B}$
opérateur nable	∇
gradient	grad φ, $\nabla\varphi$
divergence	div $\boldsymbol{A}$
rotationnel	curl $\boldsymbol{A}$, rot $\boldsymbol{A}$
Laplacien	$\Delta\varphi$, $\nabla^2\varphi$
produit dyadique	$\boldsymbol{AB}$
tenseur	T
produit tensoriel: $\Sigma_k S_{ik} T_{kl}$	$\mathsf{S}\cdot\mathsf{T}$
produit scalaire: $\Sigma_k\Sigma_i S_{ik} T_{ki}$	$\mathsf{S}:\mathsf{T}$
produit d'un vecteur et d'un tenseur: $\Sigma_k A_k T_{ki}$, $\Sigma_i T_{ki} A_i$	$\boldsymbol{A}\cdot\mathsf{T}$, $\mathsf{T}\cdot\boldsymbol{A}$

IV.

SYMBOLS FOR UNITS

1. Prefixes.

deci $(= 10^{-1})$	d
centi $(= 10^{-2})$	c
milli $(= 10^{-3})$	m
micro $(= 10^{-6})$	μ
nano $(= 10^{-9})$	n
pico $(= 10^{-12})$	p
kilo $(= 10^{3})$	k
mega $(= 10^{6})$	M
giga $(= 10^{9})$	G
tera $(= 10^{12})$	T

2. CGS units.

l, b, h	centimetre	cm
t	second	s
m	gram	g
f, ν	hertz $(= s^{-1})$	Hz
F	dyne	dyn

SYMBOLES DES UNITÉS

1. Préfixes.

déci $(= 10^{-1})$	d
centi $(= 10^{-2})$	c
milli $(= 10^{-3})$	m
micro $(= 10^{-6})$	μ
nano $(= 10^{-9})$	n
pico $(= 10^{-12})$	p
kilo $(= 10^{3})$	k
méga $(= 10^{6})$	M
giga $(= 10^{9})$	G
téra $(= 10^{12})$	T

2. Unités CGS.

l, b, h	centimètre	cm
t	seconde	s
m	gramme	g
f, ν	hertz $(= s^{-1})$	Hz
F	dyne	dyn

E	erg	erg
p	barye (= dyn/cm²)	barye
η	poise (= dyn s/cm²)	P
T	degree Kelvin	°K
t	degree Celsius	°C
H	oersted	Oe
B	gauss	G
Φ	maxwell	Mx
F_M	gilbert	Gi
I	candela	cd
Φ	lumen (= cd·sr)	lm
L, B	stilb (= cd/cm²)	sb
E	phot (= lm/cm²)	phot
α	radian	rad
ω	steradian	sr

3. MKSA units.

l, b, h	metre	m
t	second	s
m	kilogramme	kg
ν, f, ω	hertz	Hz
F	newton	N
E	joule	J
P	watt	W
I	ampere	A
Q	coulomb	C
V	volt	V
C	farad	F
R	ohm	Ω
L	henry	H
Φ	weber	Wb
I	candela	cd
Φ	lumen	lm
L, B	nit (= cd/m²)	nt
E	lux (= lm/m²)	lx

4. Non-coherent units.

l	ångström	Å
V	liter	l
t	minute	min
t	hour	h
p	atmosphere	atm
p	bar (= 10^5 barye)	bar
E,W	kilowatt-hour	kWh
Q	calorie	cal
Q	kilocalorie	kcal
m	tonne (= 1000 kg)	t

E	erg	erg
p	barye (= dyn/cm²)	barye
η	poise (= dyn s/cm²)	P
T	degré Kelvin	K
t	degré Celsius	°C
H	oersted	Oe
B	gauss	G
Φ	maxwell	Mx
F_M	gilbert	Gi
I	candéla	cd
Φ	lumen (= cd·sr)	lm
L, B	stilb (= cd/cm²)	sb
E	phot (= lm/cm²)	phot
α	radian	rad
ω	stéradian	sr

3. Unités MKSA.

l, b, h	mètre	m
t	seconde	s
m	kilogramme	kg
ν, f, ω	hertz	Hz
F	newton	N
E	joule	J
P	watt	W
I	ampère	A
Q	coulomb	C
V	volt	V
C	farad	F
R	ohm	Ω
L	henry	H
Φ	weber	Wb
I	candéla	cd
Φ	lumen	lm
L, B	nit (= cd/m²)	nt
E	lux (= lm/m²)	lx

4. Unités non-cohérentes.

l	ångström	Å
V	litre	l
t	minute	min
t	heure	h
p	atmosphère	atm
p	bar (= 10^5 barye)	bar
E,W	kilowatt-heure	kWh
Q	calorie	cal
Q	kilocalorie	kcal
m	tonne (= 1000 kg)	t

Remark on rationalisation.

(1) In 1951 the I.U.P.A.P. accepted the following *resolution*:

« The General Assembly of the Union of Physics considers that, in the case that the equations are rationalised, the rationalisation should be effected by the introduction of new quantities. »

(2) When confusion is possible between rational and non-rational quantities it is recommended to add to the name of the quantity the adjective « *rational* » or « *non-rational* » and to provide the symbol of the quantity with a left subscript n or r respectively. E.g.:

non-rational magnetic field = ${}_{n}H$,
rational magnetic field = ${}_{r}H$,

${}_{r}D = {}_{n}D/4\pi$ but ${}_{n}E = {}_{r}E = E$,
${}_{r}H = {}_{n}H/4\pi$ but ${}_{n}B = {}_{r}B = B$,

(3) In order to transform an equation between non-rational quantities into an equation between rational quantities, the following table gives the rational quantities and the equivalent espressions in terms of the non-rational quantities:

Remarque sur la rationalisation.

(1) En 1951 l'U.I.P.P.A. à adopté la *résolution* suivante:

« L'Assemblée Général de l'Union de Physique considère que, dans le cas où les équations sont rationalisées, la rationalisation doit être obtenue par l'introduction de grandeurs nouvelles. »

(2) Quand il y a une possibilité de confusion entre grandeurs rationnelles et non-rationnelles il est recommandé d'ajouter l'adjective « *rationnel* » ou « *non-rationnel* » et de munir le symbole de la grandeur d'un indice en bas à gauche n ou r respectivement. P. ex.:

champ magnétique non-rationnel = ${}_{n}H$
champ magnétique rationnel = ${}_{r}H$

${}_{r}D = {}_{n}D/4\pi$ mais ${}_{n}E = {}_{r}E = E$
${}_{r}H = {}_{n}H/4\pi$ mais ${}_{n}B = {}_{r}B = B$

(3) Afin de transformer une équation entre grandeurs rationnelles en une équation entre grandeurs non-rationnelles, le tableau suivant donnes les grandeurs rationnelles et les expressions équivalentes exprimées en grandeurs non-rationnelles:

rat.	non-rat.	rat.	non-rat.
Q	Q	I	I
ρ	ρ	J	J
E	E	B	B
D	$D/4\pi$	H	$H/4\pi$
P	P	M	M
ε	$\varepsilon/4\pi$	μ	$4\pi\mu$
ε_0	$\varepsilon_0/4\pi$	μ_0	$4\pi\mu_0$
ε_r	ε_r	μ_r	μ_r

(4) *Example*:

The horizontal component of the magnetic induction of the earth's magnetic field is in Europe approximately

$$B = 0.2 \text{ G} = 0.2 \times 10^{-4} \text{ Wb/m}^2 .$$

This value *is unaffected by rationalisation.*

The corresponding non-rational magnetic field is:

$${}_{n}H = 0.2 \text{ Oe} = 0.2 \times 10^{3} \text{ A/m}$$

and the corresponding rational magnetic field is:

$${}_{r}H = (0.2/4\pi) \text{ Oe} = (0.2 \times 10^{3}/4\pi) \text{ A/m} = 15.9 \text{ A/m} .$$

As the numerical value of the magnetic field *is affected by rationalisation*, it is advisable to use when possible the magnetic induction expressed in gauss or in Wb/m².

(4) *Exemple*:

La composante horizontale de l'induction magnétique du champ magnétique terrestre en Europe est approximativement

$$B = 0{,}2 \text{ G} = 0{,}2 \times 10^{-4} \text{ Wb/m}^2 .$$

Cette valeur *ne dépend pas de la rationalisation.*

L'intensité du champ magnétiques non-rationnel correspondant est

$${}_{n}H = 0{,}2 \text{ Oe} = 0{,}2 \times 10^{3} \text{ A/m}$$

et l'intensité du champ magnétique rationnel correspondant est:

$${}_{r}H = (0{,}2/4\pi) \text{ Oe} = (0{,}2 \times 10^{3}/4\pi) \text{ A/m} = 15{,}9 \text{ A/m} .$$

La valeur numérique de l'intensité du champ magnétique *dépendant de la rationalisation*, il est recommandable d'utiliser si possible l'induction magnétique exprimée en gauss ou en Wb/m².

LIBRI RICEVUTI E RECENSIONI

L. BIEBERBACH – *Analytische Fortsetzung.* Springer-Verlag, Berlin-Göttingen - Heidelberg, 1955, p. 168.

Questo volume tratta delle più recenti ricerche sui legami fra le proprietà dei coefficienti di un elemento analitico (serie di potenze) e le proprietà in grande della funzione analitica definita da tale elemento (secondo il prolungamento analitico di Weierstrass). Si tratta di questioni assai difficili che interessano quasi esclusivamente il matematico puro.

Dopo un capitolo ove sono raccolti nozioni e teoremi ausiliari si inizia (Cap. II e III) l'esposizione della teoria dando i più raffinati teoremi relativi all'ubicazione dei punti singolari della funzione analitica sulla circonferenza che limita il cerchio di convergenza dell'elemento analitico assegnato ed alla natura del campo di esistenza della funzione stessa.

Segue (Cap. IV) lo studio degli elementi analitici prolungabili o non prolungabili, allo scopo di mostrare che, in un certo senso, questi ultimi costituiscono la regola ed i primi l'eccezione. I tre capitoli successivi trattano del cosiddetto teorema di moltiplicazione di Hadamard e di varie altre questioni dipendenti dai caratteri aritmetici dei coefficienti dell'elemento analitico assegnato.

Vasta ed accurata è la bibliografia posta in fine al volume.

Si tratta di una pregevole monografia di grandissimo interesse teorico, dalla quale però non sembra possibile dedurre immediatamente delle applicazioni di carattere fisico-matematico.

ALDO GHIZZETTI

Niels Bohr and the development of Physics (Essay dedicated to Niels Bohr on the occasion of his seventieth birthday). Edited by W. PAULI with the assistance of L. ROSENFELD and V. WEISSKOPF, pp. 1-195; Pergamon Press, London, 1955. Prezzo 30 sh.

Come il titolo dice questo volume è una raccolta di saggi riguardanti le questioni fondamentali allo sviluppo delle quali NIELS BOHR contribuì, scritto per onorare il 70-esimo compleanno del grande fisico.

I titoli dei vari saggi ed i loro autori sono i seguenti: 1) La scoperta del numero atomico - C. G. DARWIN; 2) Lo sviluppo dell'interpretazione della teoria dei quanti - W. HEISENBERG; 3) Principio di esclusione, gruppo di Lorentz, riflessione spazio temporale e coniugio di carica - W. PAULI; 4) Teoria quantistica dei campi - L. D. LANDAU; 5) Elettrodinamica quantistica - L. ROSENFELD; 6) Teoria dei quanti e relatività - O. KLEIN; 7) Superconduttività - H. B. G.

CASIMIR; 8) Il nucleo composto - F. L. FRIEDMAN e V. F. WEISSKOPF; 9) Fissione nucleare e stabilità nucleare - J. A. WHEELER; 10) Passaggio di particelle cariche attraverso la materia - J. LINDHARD.

La lettura dei vari saggi, scritti tutti da allievi ed amici di BOHR specialisti dei vari argomenti trattati, è estremamente interessante. Alcuni dei saggi rappresentano contributi originali, come quelli di PAULI e di LANDAU, altri, la maggioranza hanno invece più il carattere di rassegna.

Non è evidentemente possibile qui illustrare ciascun saggio; è invece interessante discutere il volume nel suo complesso. Non vi è dubbio che in un certo senso esso fa il punto di una fase di sviluppo delle nostre idee teoriche. La descrizione dei fenomeni atomici e degli aspetti qualitativi di quelli nucleari e, con moltissime riserve, la descrizione del campo elettromagnetico in interazione con gli elettroni costituiscono un capitolo « classico » della fisica teorica. Per potere scrivere il capitolo seguente, per poter fare un modello ragionevole non già di un atomo, ma di una particella elementare nuove idee sono necessarie; ma uomini come NIELS BOHR, sono rari.

G. MORPURGO

K. BECHERT and C. GERTHSEN – *Atomphysik*. Due volumetti rispettivamente di 124 e 112 pagine; W. De Gruyter, Berlin, 1955.

In due volumetti di complessivamente 236 pagine gli autori hanno voluto dare una esposizione delle nozioni fondamentali di fisica atomica e nucleare.

Brevi descrizioni dei metodi sperimentali accompagnano i risultati e la discussione dei concetti teorici fondamentali.

Il primo volume parte dalla teoria cinetica dei gas; vi si descrivono metodi di misura di massa e carica di elettroni ed atomi, alcune macchine acceleratrici di ioni (betatrone e ciclotrone), alcuni rivelatori di particelle (contatori di Geiger, contatori a scintillazione, camera di Wilson) per concludere con l'esperienza di Rutherford sullo scattering delle particelle α, cenni sulla radioattività naturale e sui raggi X.

Il secondo volume contiene un discussione dei fenomeni di interazione fra radiazione e materia (effetto Compton, effetto fotoelettrico, creazione di coppie di elettroni, emissione e assorbimento di luce da parte di atomi); particolare cura è stata data alla descrizione delle esperienze che formano il punto di partenza della meccanica ondulatoria. La trattazione è chiusa da brevi accenni alle più recenti scoperte nel campo della fisica delle particelle elementari.

In conclusione, è un testo breve ma ricco di cognizioni e dati utili (fra i quali una aggiornata tabella di costanti fondamentali): penso particolarmente utile per studenti del terzo anno di fisica.

C. FRANZINETTI

G. OBERDORFER – *Die Maßsysteme in Physik und Technik*. Springer-Verlag, Wien, 1956.

Possiamo segnalare questo volumetto all'attenzione dei lettori, meno facile è raccomandarlo alla loro lettura.

La metrologia deve considerarsi il capitolo di partenza per una sistemazione logica, razionale della trattazione della fisica. Nella metrologia non si cercano delle novità fisiche; si prepara piuttosto la metodologia della descrizione dei fatti fisici allo scopo di dare forma più conveniente alla descrizione di essi.

Perciò molte riserve si devono fare all'opportunità dello studio del libro qui in esame; accanto ad alcune pagine degne

di nota per il contenuto e per la forma, ne abbiamo trovate parecchie che lasciano perplessi.

Ne ricordiamo qui una delle più caratteristiche, ma per nulla isolata: la pagina, anzi le pagine, ove la legge di Newton della gravitazione universale è enunciata per i *pesi* e non per le *masse* mutuamente agenti.

E. Perucca

R. Sproull – *Modern Physics. A Textbook for Engineers.* John Wiley & Sons, New York, 1956, pp. 491.

Il libro è stato scritto seguendo le tracce di un corso tenuto dall'Autore per diversi anni all'Università di Cornell (U.S.A.) e in industrie vicine, a studenti dei primi anni della facoltà di Ingegneria.

I primi cinque capitoli sono introduttivi: dopo alcuni elementi sulla fisica delle particelle elementari e degli atomi e sulla meccanica statistica, nei capitoli IV e V sono esposti con notevole chiarezza i principi fondamentali della meccanica quantistica, con quel tanto di matematica che basta per poter rendere il testo autosufficiente.

Vi è poi un capitolo sulla fisica delle molecole; i quattro seguenti (capitoli VIII-XI) sono dedicati a quella parte della fisica dello stato solido che più interessa l'ingegneria moderna, come le proprietà elettriche, termiche e magnetiche dei solidi ed i semiconduttori.

Il capitolo XII è dedicato alla fisica elettronica, e nell'ultimo capitolo viene ripresa la fisica nucleare con brevi accenni alla radioattività α, β e γ, alle reazioni nucleari ed al processo di fissione.

La chiarezza nell'esposizione e nell'organizzazione della materia è la dote principale che rende questo libro un testo di facile e proficuo studio.

L'intento di presentare la fisica moderna in modo quanto più possibile analitico, piuttosto che puramente descrittivo, è, secondo me, ben riuscito. L'Autore non si limita ad enunciare a parole il principio di indeterminazione od alcuni esempi di quantizzazione, ma usa le funzioni d'onda come normale strumento per l'interpretazione dei fenomeni, raggiungendo così lo scopo di togliere alla meccanica quantistica quel che di magico che essa ha per quasi tutti gli studenti di facoltà scientifiche che non siano fisica.

Un giusto rilievo viene dato all'esposizione dei mezzi di sperimentazione e viene messo bene in evidenza il significato fisico del formalismo matematico; sia nel testo che nei problemi al termine di ogni capitolo vi sono molti dati numerici, che, insieme con l'uso costante del sistema mks, renderanno questo libro bene accetto agli ingegneri.

Ad ogni capitolo vi è poi una buona bibliografia, utile per coordinare uno studio più approfondito di argomenti specifici.

Il libro presuppone semplicemente la conoscenza della fisica classica che viene insegnata nel primo biennio delle nostre facoltà di ingegneria; vorrei anzi aggiungere che gli argomenti ivi trattati ne dovrebbero costituire l'ormai necessario completamento.

F. Amman

U. Stille – *Messen und Rechnen in der Physik*, pp. VIII + 416. F. Wieweg & Sohn, Braunschweig, 1955.

La traduzione del sottotitolo: « le basi della introduzione delle grandezze fisiche e delle unità di misura » ci chiarisce il contenuto di questo libro. Le ragioni per cui esso è stato scritto possono invece essere ricavate dalla prefazione dell'Autore.

In essa si afferma che la scelta dell'una o dell'altra unità di misura o definizione di una grandezza fisica corrisponde a criteri di praticità. È quindi logico esaminare da vicino tutti i sistemi

fin qui usati per l'introduzione di unità di misura e, dopo averli studiati, coordinarli con formule e tabelle in modo che i risultati formulati in un qualsiasi sistema siano comodamente confrontabili tra di loro.

Non ci si limita però solo a questo, ma si forniscono i valori sperimentali delle costanti più importanti in tutti i campi della fisica. Questo programma è svolto in sette capitoli. Dopo una introduzione di carattere generale, si passano in rassegna tutte le parti della fisica: meccanica, termologia, elettricità, magnetismo. Il quinto capitolo è dedicato all'intricata questione delle unità fonometriche e fotometriche. Il sesto ai valori delle costanti fondamentali e degli standard.

Le relazioni dimensionali tra grandezze fisiche nei vari sistemi di unità, i valori dei coefficienti di conversione e tabelle numeriche di uso corrente sono concentrate nelle ultime sessanta pagine del libro. Infine estesi indici completano l'esposizione; nella bibliografia sono citati circa mille lavori.

Tutte le parti di questo libro dedicate alle unità di misura, all'esposizione dei dati numerici, alle tabelle di conversione ecc. sono ineccepibili. I numeri sono citati con minuzia, si può dire quasi con pignoleria. Non vi è costante fondamentale di cui non si dia una accurata cronistoria, accompagnata dall'estratto, in lingua originale, della decisione della Commissione Internazionale che ne ha sanzionato la definizione, o il valore numerico, adottato al presente.

U'unica critica è quella che sorge dalla lettura delle primissime pagine del libro. In esse infatti si comincia a stabilire una netta distinzione, introducendo di proposito due vocaboli diversi, tra la « grandezza fisica » e i valori numerici della grandezza stessa. Poichè dopo alcune pagine si dichiara esplicitamente che la misurabilità è una caratteristica essenziale delle grandezze fisiche, è probabile che l'Autore abbia introdotto due vocaboli distinti solamente per comodità di esposizione. Non risulta comunque abbastanza chiaro il fatto che una grandezza fisica coincide con ciò che si misura.

Questa critica non può naturalmente intaccare il valore dell'opera, necessario complemento di qualsiasi biblioteca di Istituto scientifico e fonte di informazione sicura per chi si interessi di metrologia.

G. CORTELLESSA

Direttore responsabile: G. POLVANI Tipografia Compositori - Bologna

Questo fascicolo è stato licenziato dai torchi il 27-VI-1956